AD-772 721

FEATURES OF THE CALCULATION OF
REINFORCED PLASTIC PARTS

Yu. M. Tarnopolskii, et al

Foreign Technology Division
Wright-Patterson Air Force Base, Ohio

12 November 1973

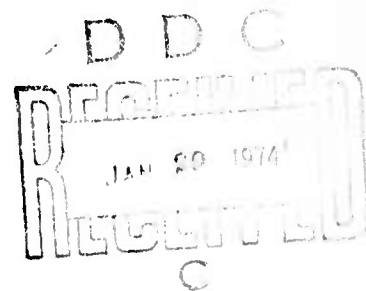# FOREIGN TECHNOLOGY DIVISION

FEATURES OF THE CALCULATION OF REINFORCED
PLASTIC. PARTS

by

Yu. M. Tarnopol'skiy, A. V. Roze

AD772721

DDC

JAN 29 1974

C

Approved for public release;
distribution unlimited.

DOCUMENT CONTROL DATA - R & D

(Security classification of title, body of abstract and indexing annotation must be entered when the overall report is classified)

1. ORIGINATING ACTIVITY *(Corporate author)*	2a. REPORT SECURITY CLASSIFICATION
Foreign Technology Division	Unclassified
Air Force Systems Command	2b. GROUP
U. S. Air Force	

3. REPORT TITLE

FEATURES OF THE CALCULATION OF REINFORCED PLASTIC PARTS

4. DESCRIPTIVE NOTES *(Type of report and inclusive dates)*

Translation

5. AUTHOR(S) *(First name, middle initial, last name)*

Yu. M. Tarnopol'skiy, A. V. Roze

6. REPORT DATE	7a. TOTAL NO. OF PAGES	7b. NO. OF REFS
1969	241 259	321

8a. CONTRACT OR GRANT NO.	9a. ORIGINATOR'S REPORT NUMBER(S)
b. PROJECT NO.	FTD-MT-24-384-73
c.	9b. OTHER REPORT NO(S) *(Any other numbers that may be assigned this report)*
d.	

10. DISTRIBUTION STATEMENT

Approved for public release;
distribution unlimited.

11. SUPPLEMENTARY NOTES	12. SPONSORING MILITARY ACTIVITY
	Foreign Technology Division
	Wright-Patterson AFB, Ohio

13. ABSTRACT

11

DD FORM 1 NOV 65 **.1473**

EDITED MACHINE TRANSLATION

FTD-MT-24-384-73   12 November 1973

FEATURES OF THE CALCULATION OF REINFORCED PLASTIC.
PARTS

By: Yu. M. Tarnopol'skiy, A. V. Roze

English pages: 241

Source: Osobennosti Rascheta Detaley iz Armirovannykh
         Plastikov, 1969, pp. 1-12, 66-274

Country of Origin: USSR

Requester: FTD/FAOO

This document is a SYSTRAN machine aided
translation, post-edited for technical accuracy
by: Robert Allen Potts

Approved for public release;
distribution unlimited.

All figures, graphs, tables, equations, etc.
merged into this translation were extracted
from the best quality copy available.

ib

FTD-MT-24-384-73

TABLE OF CONTENTS

U. S. BOARD ON GEOGRAPHIC NAMES TRANSLITERATION SYSTEM

Block	Italic	Transliteration	Block	Italic	Transliteration
А а	*А а*	A, a	Р р	*Р р*	R, r
Б б	*Б б*	B, b	С с	*С с*	S, s
В в	*В в*	V, v	Т т	*Т т*	T, t
Г г	*Г г*	G, g	У у	*У у*	U, u
Д д	*Д д*	D, d	Ф ф	*Ф ф*	F, f
Е е	*Е е*	Ye, ye; E, e*	Х х	*Х х*	Kh, kh
Ж ж	*Ж ж*	Zh, zh	Ц ц	*Ц ц*	Ts, ts
З з	*З з*	Z, z	Ч ч	*Ч ч*	Ch, ch
И и	*И и*	I, i	Ш ш	*Ш ш*	Sh, sh
Й й	*Й й*	Y, y	Щ щ	*Щ щ*	Shch, shch
К к	*К к*	K, k	Ъ ъ	*Ъ ъ*	"
Л л	*Л л*	L, l	Ы ы	*Ы ы*	Y, y
М м	*М м*	M, m	Ь ь	*Ь ь*	'
Н н	*Н н*	N, n	Э э	*Э э*	E, e
О о	*О о*	O, o	Ю ю	*Ю ю*	Yu, yu
П п	*П п*	P, p	Я я	*Я я*	Ya, ya

* ye initially, after vowels, and after ъ, ь; e elsewhere. When written as ё in Russian, transliterate as yё or ё. The use of diacritical marks is preferred, but such marks may be omitted when expediency dictates.

In the book are discussed the features of the structure, properties and regulation of the anisotropy of reinforced plastics (systems of the pliable matrix type - continuous reinforcing filaments). Primary attention is given to the negative features of these materials - weak shear and tensile-compressive strength perpendicular to the direction of reinforcing. Taking these features into account the traditional problems of the strength of materials and applied elasticity theory (rods, plate, thick-walled rings) are examined. Special attention is given to the mechanics of winding. There is estimated the error introduced by the application of solutions, constructed on the basis of the hypothesis of undeformable standards. The book contains vast experimental material, obtained during tests of oriented glass fiber-reinforced plastics with fibrous, laminated and three-dimensional cross-linked structure. Illustrations 162, Tables 40, References 321 titles.

PREFACE

Among the problems of contemporary technology the problem of
the creation of new structural materials with controlled physico-
mechanical characteristics occupies a special place. From this
viewpoint reinforced plastics are of great interest, properties
of which can be controlled in a sufficiently wide range of their
change.

The ordered and thoroughly substantiated theory of the strength
and deformation of anisotropic heterogeneous materials, which
considers the specific features of the mechanical characteristics
of material, in particular heterogeneity, strong anisotropy,
weak shear resistance, different tensile and compressive strength
and others, undoubtedly will aid the wide application of
reinforced plastics in the different areas of contemporary
technology.

The account of the specific features of the mechanical
properties of material can significantly change the traditional
approach to the calculation of some structural elements,
manufactured from reinforced plastics. The fact is that the
mechanical characteristics of plastics, reinforced by filaments,
as a rule, are such that the practical need appears for the
account of the effect of such stresses and deformations, which in
the traditional applied theories of calculation of structural

elements are considered secondary and negligible. As applied to reinforced plastics these stresses and deformations, in spite of their comparative smallness, can become the reason for structural failure.

The authors of this book on the basis of their theoretical and experimental data, taking into account the known results of other researchers, revealed some specific features of the mechanical properties of reinforced plastics and showed how these features change the traditional methods of calculation of strength and deformation of structural elements. In the book in detail there are investigated the questions connected with the weak resistance of these materials to shear, the interesting problems of the mechanics of filament winding are examined, the questions of strength and deformation of glass fiber-reinforced plastics are discussed in detail taking into account small irregularities of the reinforcing filament, the correct ways of transition from heterogeneous to quasi-homogeneous material are shown and others.

The questions examined in the book are illuminated so fully and thoroughly that the reader-theoretician will find the experimental material in it which will help him to correctly evaluate the existing theories of reinforced media and to outline the ways of construction of new more substantiated applied theories, and the reader-applier - those methods and ways by which he will know how to correctly calculate the series of elements of constructions, manufactured from reinforced plastics. The authors of the book did not answer all the questions connected with the problem of the construction of the mechanics of reinforced plastics, but the steps made by them in this area are very successful. The principles, which form the basis of the book, and also the results given in it are such that they will interest a wide circle of specialists, who are occupied with the theoretical and applied problems of the mechanics of reinforced media.

S. A. Ambartsumyan

INTRODUCTION

Contemporary technical progress considerably expanded the
circle of utilized structural materials. The anisotropic composite
materials and, first of all, reinforced plastics occupy a vi...e
place among them. At the basis of the creation of these materials
lies the idea of reinforcing. Attention to this idea is caused by
the tendency to combine lightness with strength and hardness in
the assigned directions. Anisotropic natural materials have already
long been used in technology; however, only the creation of
artificial reinforced materials opens the possibility of the wide
and purposeful control of the anisotropy of properties. This
makes it possible within known limits to coordinate the fields of
resistances and effective forces. At present two basic classes of
composite materials can be isolated matrix + particle and matrix +
+ continuous filaments. The materials of matrix + particle class
can be related to quasi-isotropic materials [227]. They are used
mainly for the manufacture of intricate-shape parts with low
strength properties. The materials reinforced by filaments are
structural anisotropic materials. The anisotropy of properties
is created in the process of the production of articles and is a
controllable value. These materials received the greatest
propagation during the creation of important constructions. The
prospect of materials, reinforced by filaments, is doubtless.
Strengthening by filaments has so many advantages that, apparently,
in the future it will make up the basis of producing strong

engineering materials [116]. The construction of compositions
is at present the subject of numerous investigations (see, for
example, [199] and other articles of the collection).

The leading place among materials of the pliable matrix +
+ continuous filament type is occupied by reinforced plastics:
glass fiber-reinforced plastics, asbestos fiber-reinforced plastics,
boron fiber-reinforced plastics, materials reinforced by carbon and
graphite fibers, and others. The idea of the creation of reinforced
plastics is extremely simple [107, 114]. They are materials,
the reinforcement of which provides strength and hardness of
composite, and polymer bonding agent - solidity of material and
pliability. This principle of construction of material makes it
possible to combine high strength and hardness, characteristic for
reinforcing filaments, with the technical properties, which are
valuable in polymer substance, and to control the anisotropy by
means of changing the orientation and mutual arrangement of the
reinforcing filaments.

In spite of the wide application of reinforced plastics,[1] up
to the sixties the empirical approach to the creation of the
materials themselves and constructions of them predominated.
Recently in connection with the numerous technical applications
the interest in the mechanics of composite materials, including
the mechanics of reinforced plastics, considerably increased.
Large investigations on the creation of the theory of reinforced
media were conducted by V. V. Bolotin, P. M. Ogibalov, G. N. Savin
and G. A. Van Fo Fy, Hashin and Rosen, Hill, Tsai and Azzi and
others. The strength of reinforced plastics and the development

---

[1]The industrial production of reinforced plastics rapidly
increases. For example, the production of glass fiber-reinforced
plastics in recent years in many countries of the world grew into
a large branch of industry. In the immediate future - the
creation of the industrial production of metals reinforced by
filaments. However, while the technology of the creation of rein-
forced plastics and their subsequent treatment is comparatively
simple, for metals reinforced by filaments the technical problems
are the main ones.

)

of criteria of limiting states for parts from these materials are
examined in the works of I. I. Gol'denblat, N. I. Malinin,
A. K. Malmeyster, J. Martin, Niederstadt, Noris, Yu. N. Rabotnov,
S. V. Serensen and coworkers, N. T. Smotrin and V. M. Chebanov
and others. To the development of methods of calculation of
parts from composite materials there are dedicated the works of
S. A. Ambartsumyan, V. L. Biderman, L. A. Galin, E. I. Grigolyuk,
V. I. Korolev, M. K. Smirnova, A. M. Skudra, G. A. Teters and
others.[1]   In J. Hugo's work [294] there are given the methods
of calculation of typical parts from isotropic plastics.

In literature, especially in chemical-technological, it is
accepted to emphasize the high specific strength and the rigidity
of composite materials and to keep quite about their negative
properties. However these materials inherit not only positive,
but also the negative properties of components; the knowledge of
negative properties is no less important for the correct
utilization of composite materials [224]. The basic features
of the materials reinforced by filaments, which it is necessary
to consider during the development of methods of calculation and
the evaluation of the supporting power of parts, are caused by
the pliable matrix (for example, polymer bonding agent), by the
features of the structure and combination of the properties of
components. Diagram 1 is an attempt to show that it engenders
these features, and also the ways of taking them into account
during the development of methods of calculation and evaluation
of the supporting power of constructions.

The strength and deformating properties of reinforced plastics
(the left side of Diagram 1) are not the deterministic value, and

---

[1]A detailed bibilography is given in the list of the used
literature, and also in the books of many of the enumerated
authors (for example in [5, 6, 23, 30, 112, 132, 153, 170, 302]).

essentially depend not only on the diagram of reinforcing, but also on technological, structural and operational factors. For the designation of substantiated safety factors the knowledge of the actual supporting power is necessary. Unlike the traditional materials, which in delivered state have certain preassigned properties, the strength characteristics of parts made of reinforced plastics are created in the process of molding and are mainly determined by the parameters of this process. As the experience of the manufacture and operation of different parts from glass fiber-reinforced plastics shows, in articles it is often not possible to realize the strength properties of materials, obtained during tests of standard samples [227]. This requires the optimization of the methods and procedures of obtaining parts. Thus, the presence of polymer bonding agent by virtue of the specific character of the properties of polymers makes the reinforced plastics extremely sensitive to the previous temperature and power history of the sample - to the technology of manufacture and condition of subsequent operation (temperature, character and the duration of loading).[1]

The load-carrying capacity of a number of materials reinforced by filaments is sufficiently studied in detail. For example, strength and deformation of reinforced plastics taking into account structural, technological and operational factors are examined in the books published recently (see, for example, [21, 153, 203, 268, 298]; detailed bibliography is given there). The calculated resistance of glass fiber-reinforced plastics of different structure is given in review sources [23, 227], in these works there is given a summary of the theories of limiting states

---

[1]The inelastic properties of polymer bonding agent require the complication of mechanical models of the material. In the book this question is not considered. The inelastic properties of the pliable matrix of composite materials are taken into account for example in [66, 67, 130, 171, 200], which contain vast bibliographies. The problems which appear in this area are formulated by A. A. Il'yushin and P. M. Ogibalov [103, 104].

for composite materials. The features of the materials, reinforced
by filaments, caused by their structure and the combination of
properties of components (the right side of Diagram 1) and the
questions engendered by these features are studied in less detail.
The examination of these questions comprises the basic content
of the book.

The composites, reinforced by filaments, are heterogeneous
structural anisotropic materials. However the existing elasticity
theory of anisotropic body, developed in S. G. Lekhnitskiy's
basic works [121-123], is developed basically for homogeneous
materials. The specific properties of composite materials
require an account of the real structure and circumspection
during the replacement of homogenous medium by quasi-homogeneous;
in any case the error introduced by such a replacement must be
evaluated. The theories of reinforced media developing in recent
years possess precisely such an advantage. The utilization
of these theories makes it possible, at least at the stage of
derivation of the fundamental equations, to consider the material
as a structurally heterogeneous medium.

The classical methods of calculation of typical constructions
are irreparably indifferent to the transverse mechanical
characteristics of the material. In the real ranges of change
of the properties of reinforced plastics this can lead to sub-
stantial errors, therefore it is necessary to turn to the refined
theories, which make it possible to feel the phenomena connected
with weak shear and transverse characteristics. For the materials
and constructions in question the engineering theories
(E. Reissner, S. A. Ambartsumyan, et al.), considering the indicated
features, acquire special interest. The book contains an account
of the negative features of materials reinforced by filaments,
caused by the structure and the combination of properties of
the components: by the substantial anisotropy of elastic and
strength properties, by weak resistance to interlayered shear

and compression perpendicular to the reinforcing filaments. On an example of comparatively uncomplicated, but principally important problems there is shown not only the importance, but also the need for the account of the noted features during the calculation of parts made of these materials. In every case in question there is given an estimate of the error introduced by the application of traditional methods of calculation and it is shown that in many procedurally important cases the introduced error is inadmissible.

The majority of the materials reinforced by filaments combine the high strengths in the direction of fibers with comparatively low rigidity. For the oriented glass fiber-reinforced plastics with the strength approximately equal to steel the elastic moduli in the direction of filaments are 4-7 times less.[1] The utilization of the high strength of reinforced plastics is connected with large deformations. At the same time the working structural deformations are comparatively small. From here comes increased interest in the refinement of methods of calculation for the rigidity and stability of parts from these materials (since precisely the rigidity is often definite for constructions of materials reinforced by filaments) and the possibility and advisability of elastic examination.[2] In the book the main attention is given to the

---

[1] Recently there appeared monodirectional compositions (reinforced by filaments of boron and graphite), whose elastic modulus in the direction of filaments exceeds $3 \cdot 10^5$ kgf/cm^2 [245, 260], i.e., is higher than for steel.

[2] Requirements for the assigned hardness lead to the fact that the material virtually works only in the initial, comparatively small section of dependence $\sigma \sim \epsilon$, in which the existing composite materials of the pliable matrix + continuous filament type with loading in the direction of reinforcing lead completely to linearly elastic (see, for example, [29, 91, 130] and others).

rigidity of the construction; strength was evaluated only from the viewpoint of the danger of failure as a result of interlayered shear and compression in the direction perpendicular to the reinforcing filaments.

Research of the materials reinforced by filaments is conducted, as a rule, on an idealized model, made up of straight and strictly parallel reinforcing elements routinely arranged in pliable matrix.[1] In actuality the macrostructure of all the types of materials in question is far from this model. The bendings of filaments - regular and random - are the unavoidable result of the existing technology of manufacture of the materials, reinforced by filaments, and parts made of them. Therefore special attention is given to departures from the idealized model of material and to the evaluation of the role of bending and subsequent tension of the reinforcing filaments on strength and deformating properties. The effect of small initial bendings is so great that the idealization of the materials in question, reinforced by filaments, as systems of direct reinforcing element is inadmissible for many problems.

The book contains vast experimental material, obtained basically during tests of glass fiber-reinforced plastics, reinforced by rove (AG-4S, LSB-F, 27-63S and others) and fabric of ordinary and three-dimensional braiding (VPS-7, SKT-11, EF-32-301 and others), with different anisotropy, being regulated because of the placement of filaments.

It is necessary to note that although the examination is conducted on an example of reinforced plastics and in elastic formulation, the investigated features are general for all materials

_____

[1]The statistical theory of elasticity of reinforced plastics, which considers the random character of the arrangement of the reinforcing filaments, is developed by S. D. Volkov and colleagues [73, 74, 205, 207] and others.

of the class in question. The increase of strength and rigidity
in the direction of filaments because of the application of
stronger and more rigid reinforcement is unavoidably accompanied
by relative intensification of negative properties. The elastic
statement of the problem does not deprive the obtained results of
practical interest, since often in constructions it is possible
to use only the "useful strength" of composite materials. Spreading
of the obtained results to the case where the pliable matrix is
linear-elastic-viscous can be realized on the basis of viscoelastic
analogy [84]. The investigated features of the materials reinforced
by filaments are basically determined by the pliable matrix,
which is more sensitive to the duration of loading. For this
very reason many reinforced plastics possess distinctly expressed
shear creep. The account of inelastic properties should lead to
intensification of the effect of the investigated features.

The authors worked on the book together. The basic work on
writing Chapters I and IV was accomplished by Yu. M. Tarnopol'skiy;
II and III Chapters were written by A. V. Rose. In the work are
used the results obtained by colleagues of the laboratory of
polymer constructions of the Institute of Mechanics of Polymers
of the Academy of Sciences of Latvian SSR G. G. Portnov,
R. E. Brivmanis, I. G. Zhigun, T. Ya. Kintsis, V. A. Polyakov,
V. V. Khitrov, R. P. Shlits, on whose works are given references
in the appropriate paragraphs. On the manuscript and illustrations
worked L. L. Volgina, S. A. Vanaga, G. A. Klyavinya. The authors
are sincerely grateful to all these comrades. All critical
observations and wishes about the questions touched upon in the
book will be received with great appreciation.

SECOND CHAPTER

RODS FROM MATERIALS WHICH WEAKLY RESIST SHEAR

§ 2.1.   TENSION-COMPRESSION AND SHEAR

2.1.1. The simplest cases. The simplest loading cases are
uniform tension and compression along the direction of reinforcing
x or in perpendicular direction (Fig. 2.1.1), and also pure shear
(Fig. 2.1.2). With loading at a certain angle to the direction
of reinforcing the problem
becomes somewhat com-
plicated, since normal
stresses σ_x and σ_z
cause also shears γ_{xz},
and tangential stresses
τ_{xz} - elongation or
shortening ε_x and ε_z
[23, 117, 123]. The
features of the structure

Fig. 2.1.1. Diagram of uniform ten-
sion (compression). a) along the
direction of reinforcing; b) perpen-
dicular to the direction of reinforc-
ing.

and properties of materials reinforced by filaments (see
Chap. 1) make it possible to disregard the changes of stresses
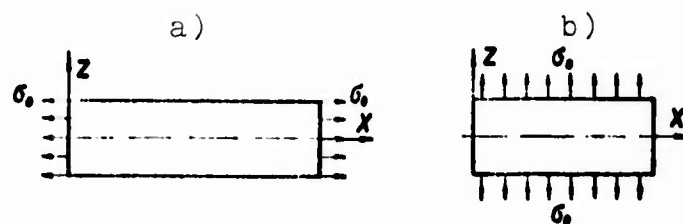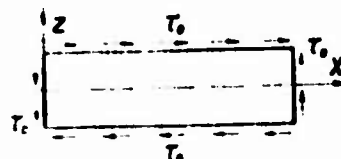and deformations in the thickness of the separate layer of

Fig. 2.1.2. Dia-
gram of pure shear.

reinforcement h' and the interlayer of bonding agent h"
(Fig. 2.1.3). This assumption can be preserved for a broad class
of problems, where the stressed state is changed sufficiently
slowly [41, 42, 148, 159]. In the assumption that the layers
and interlayers work together (without slippage), from the
examination of Fig. 2.1.4 follows

$$
\begin{aligned}
\varepsilon_{xi} = \varepsilon'_{xi} = \varepsilon''_{xi}; \quad & h\sigma_{xi} = h'\sigma'_{xi} + h''\sigma''_{xi}; \\
\tau_{xzi} = \tau'_{xzi} = \tau''_{xzi}; \quad & h\gamma_{xzi} = h'\gamma'_{xzi} + h''\gamma''_{xzi}; \\
\sigma_{zi} = \sigma'_{zi} = \sigma''_{zi}; \quad & h\varepsilon_{zi} = h'\varepsilon'_{zi} + h''\varepsilon''_{zi}.
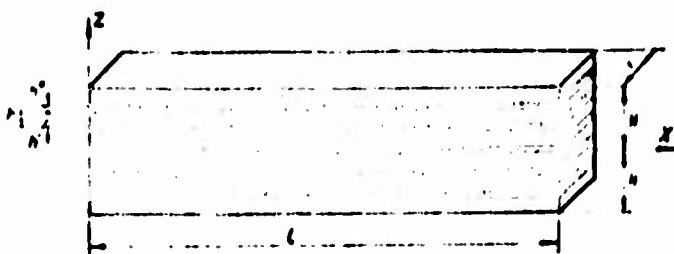\end{aligned}
\tag{2.1.1}
$$

Fig. 2.1.3. Laminated model of rod.

(values with one prime
pertain to layer, with
two they pertain to inter-
layer; the values without
prime pertain to composite
material, i.e., are
averaged along the layer
and interlayer lying   side by side). On the basis of Hooke law,
disregarding the Poisson effect, it is possible to write:

$$
\begin{aligned}
\sigma_x = E_x \varepsilon_x; \quad & \sigma'_x = E'_x \varepsilon'_x; \quad & \sigma''_x = E''_x \varepsilon''_x; \\
\sigma_z = E_z \varepsilon_z; \quad & \sigma'_z = E'_z \varepsilon'_z; \quad & \sigma''_z = E''_z \varepsilon''_z; \\
\tau_{xz} = G_{xz} \gamma_{xz}; \quad & \tau'_{xz} = G'_{xz} \gamma'_{xz}; \quad & \tau''_{xz} = G''_{xz} \gamma''_{xz}.
\end{aligned}
\tag{2.1.2}
$$

The joint solution of (2.1.1) and (2.1.2) makes it possible for the
accepted laminated model of material to express the elastic moduli
of the composite material by the parameters of the layer and
interlayer:

$$
\begin{aligned}
E_x &= E'_x \frac{h'}{h}\left(1 + \frac{E''_x h''}{E'_x h'}\right); \\
E_z &= E''_z \frac{h}{h''}\left(1 + \frac{E''_z h'}{E'_z h'}\right)^{-1}; \\
G_{xz} &= G'_{xz} \frac{h}{h''}\left(1 + \frac{G''_{xz} h'}{G'_{xz} h''}\right)^{-1}.
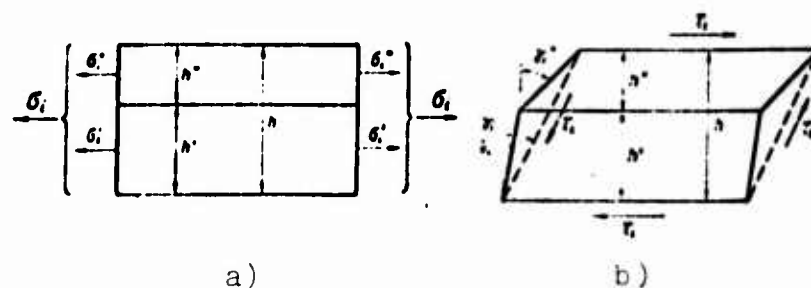\end{aligned}
\tag{2.1.3}
$$

Fig. 2.1.4. The elements of i-th layer and i-th interlayer lying side by side with loading by normal (a) and tangential (b) stresses.

Since the rigidity of reinforcement is substantially greater than the rigidity of bonding agent ($E'_x \gg E''_x$, $E'_z \gg E''_z$, $G'_{xz} \gg G''_{xz}$), the second terms of the expressions in parentheses can be disregarded. The rejection of these terms corresponds to the assumption that the layers work only on compression-tension, and the interlayers work only on shear. This assumption is widely used during the study of the mechanism of the transmission of forces in oriented glass fiber-reinforced plastics (see, for example, [227]).

With uniform tension-compression along the reinforcement (see Fig. 2.1.1) all the elements of the rod have identical deformation $\varepsilon_x = \varepsilon'_x = \varepsilon''_x = \sigma_0/E_x$, consequently, all the cross sections remain flat. The stresses σ'_x and σ''_x are determined by expressions (2.1.2), and the supporting power in this case - basically by the strength of the reinforcing filaments. With pure shear (see Fig. 2.1.2) there is achieved uniform stressed state $\tau_{xz} = \tau'_{xz} = \tau''_{xz} = \tau_0$, and the corresponding shearing strain is computed by (2.1.2). Since the stresses in the components of material are identical, the supporting power under conditions of pure shear is determined by the pliable matrix.

The stresses received by the matrix, which possesses low strength and rigidity (primarily tangential stresses, which cause interlayered shears, i.e., shears in the interlayer of

bonding agent, which is located between the filaments or layers of reinforcement),[1] are the most dangerous for constructions from materials reinforced by filaments. It is impossible to completely avoid interlayered shears by means of the corresponding placement of reinforcement at the present level of technology of reinforcing, at least near places of application of loads and attachment. Therefore there is a class of problems, in the examination of which the main attention must be given to the weak shear strength.

2.1.2. **The bending of cross sections with stretching.** In the diagram of loading, which differs from that depicted on Fig. 2.1.1, the cross sections near the places of loading are bent. There appear zones of edge effect, in which $\tau_{xz} \neq 0$ and $\sigma_x \neq$ const. In isotropic rods the edge effect of this type in accordance with the St. Venant principle attenuates very rapidly (see, for example, the investigations of S. P. Timoshenko [236], P. F. Papkovich [157], M. M. Filonenko-Borodich [249]). In anisotropic rods the extent of the zone of edge effect due to the weak shear strength can be substantially changed depending on the parameters $\beta = \sqrt{\dfrac{E_x}{G_{xz}}}$. Consequently, the purely geometric approach, common for isotropic or slightly anisotropic bodies, in many instances turns out to be insufficient and can lead to significant errors. Let us note that the estimation of the zone of edge effect is of interest not only during the calculation of constructions, but also during the development of the procedure of tests of substantially anisotropic materials. The heterogeneity of the stressed state, connected with conditions of attachment and loading of samples, strongly affects the results of tests of such

---

[1]The weak resistance of the matrix becomes apparent during the loading of unidirectional and laminated materials perpendicular to the reinforcing filaments (see Fig. 2.1.1b).

materials as, for example, oriented glass fiber-reinforced
plastics.

The loading of a rod by forces applied on the ends is
examined by A. S. Kosmodamianskiy [115]. There is practical
interest in the case where the rod is stretched by tangential
forces, applied on the sections of the lateral surface
(Fig. 2.1.5). The diagram of loading in question is realized,
for example, during the tensile test of samples made of reinforced
plastics.

The differential equation of the problem can be obtained
during the examination of equilibrium of the element of the layer
and interlayer (Fig. 2.1.6). After the substitution into the
equation of projections to longitudinal axis x

$$h \frac{d\sigma_{xi}}{dx} dx + (\tau_{x:i} - \tau_{x:,i-1}) dx = 0 \qquad (2.1.4)$$

of stresses expressed through displacements of layers u_i,

$$\sigma_{xi} = E_x \frac{du_i}{dx}; \ \tau_{x:i} = G_{x:} \frac{u_{i+1} - u_i}{h} . \qquad (2.1.5)$$
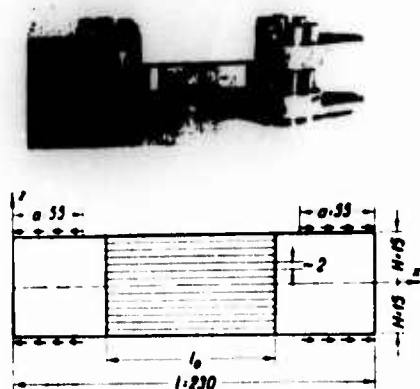

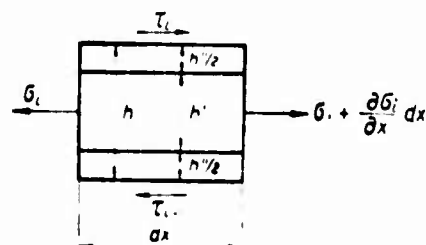Fig. 2.1.5. The sample in
grips and the diagram of
loading.

Fig. 2.1.6. The forces which
act on the element of the
laminated rod.

5

we obtain the system of differential-difference equations:

$$\beta^2 \frac{d^2u_i}{dx^2} + \frac{u_{i+1} - 2u_i + u_{i-1}}{h^2} = 0.$$ (2.1.6)

The second term of equation (2.1.6) can be considered as the second derivative of function u(x, z) with respect to variable z, written in finite differences with interval h. This makes it possible to replace system of equations (2.1.6) with the equation in partial derivatives

$$\frac{\partial^2 u}{\partial x^2} + \frac{1}{\beta^2} \cdot \frac{\partial^2 u}{\partial z^2} = 0.$$ (2.1.7)

Such replacement corresponds to transition from laminated medium to homogeneous. The error made in this case decreases with decrease of thickness h, i.e., with increase of the number of layers n.

Obviously, equation (2.1.7) can be obtained directly, substituting into the equation of equilibrium

$$\frac{\partial \sigma_x}{\partial x} + \frac{\partial \tau_{xz}}{\partial z} = 0$$ (2.1.8)

stresses expressed through displacements taking into account the adopted assumption about the constancy of displacement w:

$$\sigma_x = E_x \frac{\partial u}{\partial x}; \quad \tau_{xz} = G_{xz} \frac{\partial u}{\partial z}.$$ (2.1.9)

If tangential forces are distributed over the lateral surfaces of the rod z = ±H according to law

$$p = \tau|_{z=\pm H} = \pm p_m \cos \lambda_m x$$

(λ_m = mπ/l; m - integer), the corresponding solution of equation (2.1.7) has the form [221]

6

$$u = u_m \, \text{ch} \, \lambda_m \beta z \cos \lambda_m x. \tag{2.1.10}$$

In expression (2.1.10) $u_m = \dfrac{p_m}{\lambda_m \beta \, G \, \text{sh} \, x_m}$, $x_m = \lambda_m \beta H$.

For other cases of force distribution the solution is obtained in the form of series

$$u = \sum_{m=1}^{\infty} u_m \cos \lambda_m x. \tag{2.1.11}$$

where during determination of u_m the value of p_m is the general term of expansion of tangential load $p(x)$ into trigonometric Fourier series:

$$p(x) = \sum_{m=1}^{\infty} p_m \cos \lambda_m x. \tag{2.1.12}$$

In the case in question (Fig. 2.1.5), when the intensity of tangential forces along the length of section a is constant and equal to p_0,

$$p_m = -\frac{4p_0}{m\pi} \sin \lambda_m a. \tag{2.1.13}$$

If it is necessary to look over a large number of different laws of loading, less work consuming, in comparison with the numerical, is the method of the solution of Laplace equation (2.1.7), based on the method of electrolytic analogy; such an approach is used in [186].

The diagrams of displacements, which characterize the bending of cross sections, are given on Fig. 2.1.7, where $u_2 = u\dfrac{\pi^3 H E_x}{4 p_0 l^2}$ and $u_2^* = \lim\limits_{\kappa \to 0} u_2$ corresponds to the displacement of rods of infinite
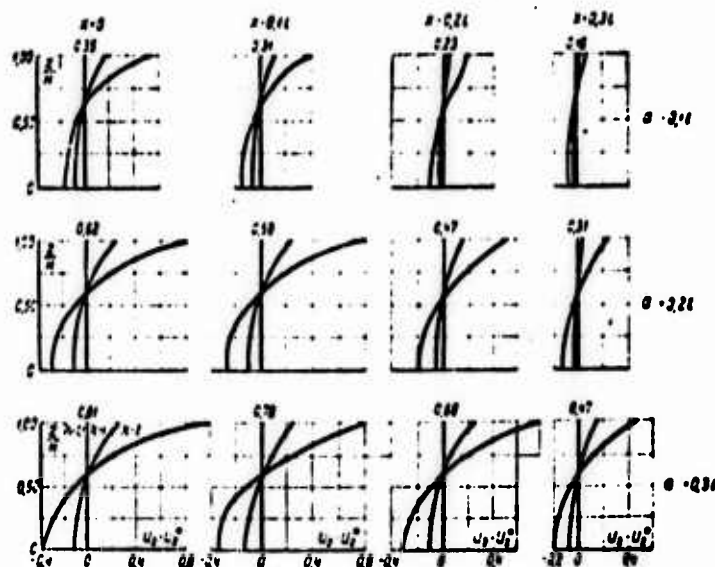
7

Fig. 2.1.7. The bending of cross sections with $\kappa = 0.1$; $\kappa = 1$ and $\kappa = 2$.

length or from material with infinite shear rigidity (i.e., u_2^* - displacement calculated on the basis of hypothesis of flat sections). As is evident, the bending of sections is substantial at large

values of parameter $\kappa = \pi\frac{H}{l}\beta$, characteristic for the materials reinforced by filaments, because of large values of $\beta = \sqrt{\dfrac{E_x}{G_{xz}}}$ (see Table 1.1.1) inherent to the latter. In this case there appears significant nonuniformity of the distribution of normal stresses σ_x, and also tangential τ_{xz}, the magnitude and the area of propagation of which can be very substantial. Consequently, the unsuccessful selection of the dimensions of the sample during tensile test can lead to incorrect estimations of strength and elastic modulus of material.

   2.1.3. The experimental evaluation of the bending of cross sections. The bending of cross sections with stretching is revealed experimentally during tests of samples of unidirectional glass fiber-reinforced plastics AG-4S [216] with special sensor-wires stuck on two sides (photograph of the sample in grips and the

8

diagram of its loading are given on Fig. 2.1.5). During the
stretching of samples, fastened along the planes, on which the
sensors are stuck (i.e., turned 90°), the readings of the latter
were identical:

$$u^* = \lim_{x \to 0} u = \frac{ap}{HE_x}\left(\frac{x}{l} - \frac{1}{2}\right).$$

Experimental results during stretching by the diagram 2.1.5,
obtained on samples with different length of wire-sensors l_0 (on
2 samples with l_0 = 60, 90 and 120 mm), and also theoretical curves
u/u^*, calculated according to (2.1.11) on the assumption that
tensile force N is realized by tangential forces evenly distributed
on the sections with length a (see Fig. 2.1.5), are represe
on Fig. 2.1.8. As is evident, the character of the arrangement
of experimental points and theoretical curves is identical. The
obtaining of more accurate quantitative coincidence is difficult
as a result of the impossibility of the exact determination of
the law of distribution of tangential forces p.
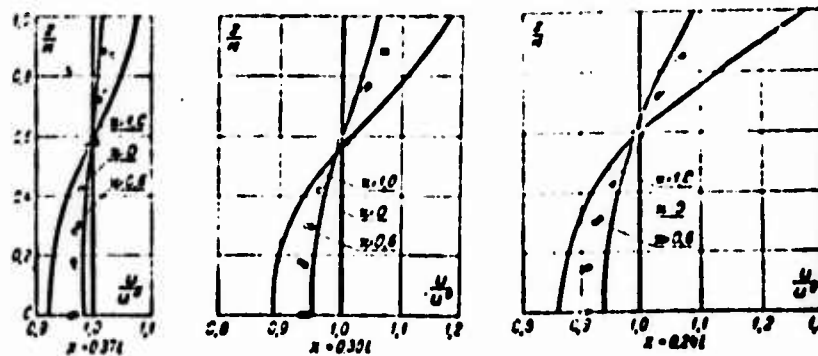

Fig. 2.1.8. The experimental evaluation
of the bending of cross sections.

2.1.4. The bending of radii during twisting of round rods.
The cross sections of noncircular or nonorthotropic rods warp
[23, 122]. Articles made of materials reinforced by filaments,
as a rule, possess orthotropy. With the twisting of round rods
from cylindrically orthotropic materials (axis of orthotropy

9

coincides with the axis of the rod) their cross sections remain planes. The edge effect is exhibited in the bending of radii near the places of application of torsional moment. The extent of these zones is determined by parameter $\beta_\theta = \sqrt{\dfrac{G_{\theta z}}{G_{\theta r}}}$, which for the materials reinforced by filaments can differ significantly from one (for isotropic rods $\beta_\theta = 1$).

The effect of anisotropy on the bending of radii is the simplest to trace on an example of a cylinder, fastened on the ends and loaded by concentrated torsional moment M (Fig. 2.1.9). The equation of twisting of orthotropic rod [122]

$$\frac{\partial^2 \Psi_\theta}{\partial r^2} + \frac{3}{r} \cdot \frac{\partial \Psi_\theta}{\partial r} + \beta^2_\theta \frac{\partial^2 \Psi_\theta}{\partial z^2} = 0 \qquad (2.1.14)$$

($\Psi_\theta = \dfrac{v}{r}$; v is the circular displacement) by the introduction of new variable $\zeta = \beta_{\theta z}$ can be reduced to the appropriate equation for isotropic rod:

$$\frac{\partial^2 \Psi_\theta}{\partial r^2} + \frac{3}{r} \cdot \frac{\partial \Psi_\theta}{\partial r} + \frac{\partial^2 \Psi_\theta}{\partial z^2} = 0. \qquad (2.1.15)$$

With this $\tau_{\theta z} = G_{\theta z} \dfrac{r}{r_\theta} \cdot \dfrac{\partial \Psi_\theta}{\partial \zeta}$, $\tau_{\theta r} = G_{\theta r} r \dfrac{\partial \Psi_\theta}{\partial r}$.

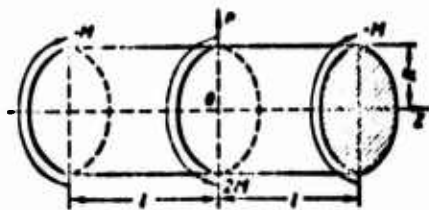Fig. 2.1.9. The diagram of twisting of rod.

The meaning of the introduction of new variable ζ is the fact that instead of a cylinder of orthotropic material there is introduced isotropic, whose length is transformed β_θ times

10

with respect to the initial anisotropic cylinder. The solution of equation (2.1.15) for the different cases of loading of isotropic bodies is examined in detail in [20], and for a number of problems with the aid of the Timpe method [318] there are obtained estimates of the zone of edge effect. In order to make use of these solutions, generally it is necessary in the appropriate manner to transform the zones of action of load and boundary conditions. For the problem in question of twisting by concentrated moment 2M (Fig. 2.1.9) this question loses significance if the rod can be considered infinitely long ($l = \infty$). In this case the length of the zone of edge effect is transformed β_θ times. Consequently, if in the isotropic rod it is possible to disregard stress level $\tau_{\theta r}$ and the nonlinearity of stresses $\tau_{\theta z}$ (i.e., bending of radii) at distance $\pi R/4$ from the place of application of the concentrated moment, then in the orthotropic rod the corresponding distance is equal to $\beta_\theta \frac{\pi R}{4}$ [223] (Fig. 2.1.10).
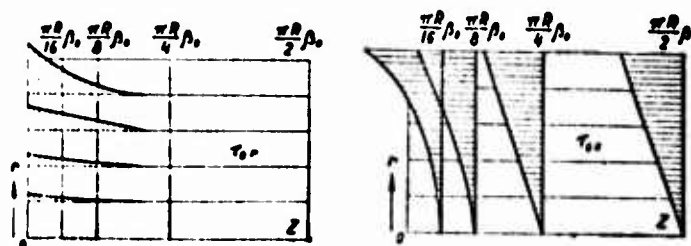
Fig. 2.1.10. The diagrams of tangential stresses $\tau_{\theta r}$ and $\tau_{\theta z}$.

During the solution of the problem of twisting of a cylinder of finite length with its loading by tangential forces on the sections of the side surface (such a diagram of loading and restraint is typical during torsion tests) the calculation formulas can be obtained in a similar manner, i.e., with utilization of the solution for isotropic case [20]. In this case the area of the edge effect is not determined through the coefficient of anisotropy in explicit form.

11

§ 2.2. TECHNICAL THEORY OF BENDING

2.2.1. Methods of the account of shears. The basic feature, subject to account during the construction of the technical theory of bending of constructions made of materials reinforced by filaments, is their weak shear strength. The classical theory of bending of solid rods,[1] constructed on the hypothesis of undeformable sections, was proposed by Bernoulli in 1705 [238]. The mechanical sense of this geometrically formulated hypothesis — cross sections remain planes and do not change their shape — consists of the fact that the negligible smallness of the effect of "secondary" stresses τ_{xz} and σ_z (x-axis is directed along the axis of the rod, z-axis — perpendicular to it in the plane of bending) on the displacements of points of the beam with the distribution of "main" stresses σ_x is postulated. The division of stresses into main and secondary appeared during the comparison of their relative values (see, for example, [175]):

$$\tau_{xz} \sim \frac{\overline{h}}{l}\sigma_x, \quad \sigma_z \sim \left(\frac{\overline{h}}{l}\right)^2\sigma_x; \qquad (2.2.1)$$

here $\overline{h}$, l are the transverse and longitudinal dimensions of the rod, respectively, i.e., its height and length; symbol $\sim$ means that the compared values have identical order. For anisotropic materials there is necessary the comparison not only of relative values of stresses, but also the corresponding resistances. Taking into account Hooke law on the basis of (2.2.1) it is possible to obtain the relationships between deformations:

$$\gamma_{xz} \sim \frac{E_x}{G_{xz}} \cdot \frac{\overline{h}}{l} \, \varepsilon_x, \quad \varepsilon_z \sim \frac{E_x}{E_z}\left(\frac{\overline{h}}{l}\right)^2 \varepsilon_x. \qquad (2.2.2)$$

---

[1] Effect of shear in thin-walled rods is examined in [140, 141].

12

from which it is clear that the hypothesis of undeformable cross
sections can be treated as the allotment of material with
infinite shear and transversal rigidity. Thus, within the
framework of the technical theory of bending, constructed on
Bernoulli's hypothesis, essentially there is examined the bending
of rods from transversally isotropic material with $G_{xz} = E_z =$
$= \frac{1}{\nu_{zx}} = \infty$.

For rods of isotropic material, for which moduli E_x and E_z
are equal, and shear modulus G_{xz} is close to them in value
($E_x = E_z \sim G_{xz}$), deformations γ_{xz} and ε_z become noticeable only
in very short beams, i.e., with large $\bar{h}/\bar{l}$. Therefore the bending
of cross sections, caused by stresses τ_{xz}, was noticed for the
first time by St. Venant in 1856 during the solution in the
refined statement of the problem about the transverse bending
of a cantilever of narrow rectangular cross section. Later a
number of problems of bending of such isotropic beam-strips under
some particular forms of load and conditions of restraint was
solved by Menage, Timpe (with the aid of polynomial functions of
stress), Rib'yer, Faylon, Bleykh (with the aid of trigonometric
series); for more detail see [129, 236, 238].

As S. P. Timoshenko indicates [238], the first expression
for deflection of the beam taking into account shear was given to
Poncelet as early as the beginning of the past century; he examined
a special case - cantilever loaded by force at the end. The
elementary derivation of the formula, which describes the effect
of stresses τ_{xz} on deflection, was given by Rankine [306] and
Grashof [288]. They proposed representing the total slope angle
of the axis of beam $w' = \frac{dw}{dx}$ as the sum of the slope angles
from the bending moment M (i.e., from normal stresses σ_x) and
shearing force Q (i.e., from tangential stresses τ_{xz}):

$$w' = w'_\sigma - w'_\tau \qquad (2.2.3)$$

13

(the process of summation is depicted schematically on Fig. 2.2.1). Actually the cross sections are bent as a result of the nonuniform distribution of stresses τ_{xz} along the height of the beam. The connection between the bending moment and the deflection component w_σ is kept the same as in the theory based on Bernoulli's hypothesis,

$$E_i I \ddot{w}_\sigma = -M = -\int_F z \sigma_i dF$$

(2.2.4)

(F and I - the area and the moment of inertia of the cross section), and the supplementary slope angle w_τ' is equated to the maximum shearing strain in the corresponding section $\gamma_{xz\ max}$.
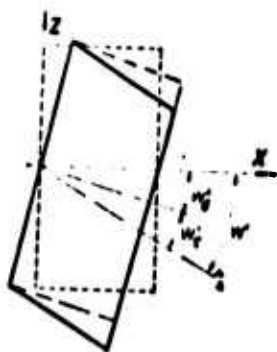
Fig. 2.2.1. Element of beam, ---·- before deformation w_σ'; -·-·- after rotation by bending moment; ———— after further shearing strain w_τ'.

A more accurate value of correction from the account of shear is obtained if instead of $\gamma_{xz\ max}$ we use the average (in an energy sense) deformation $\gamma_{xz\ cp}$, which is determined from the equality of the works of tangential stresses in this section and the shearing force Q on $\gamma_{xz\ cp}$:

$$\int_F \frac{\tau_{xz}^2}{2G_{xz}} dF = \frac{1}{2} Q \gamma_{xz\ cp} = \frac{1}{2} K_\tau Q^2.$$

(2.2.5)

This modified Rankine-Grashof approach in literature carries the name Timoshenko approach, in the works of whom it is the most developed in detail.

Turning angles $w'_\tau = \gamma_{xz\ max}$ or $w'_\tau = \gamma_{xz\ cp}$ are calculated on the assumption that the tangential stresses are distributed according to D. I. Zhuravskiy. For a beam with rectangular cross section, whose stress τ_{xz} along coordinate z is changed according to the law of quadratic parabola,

$$\gamma_{xz\ max} = 1{,}5\,\frac{Q}{FG_{xz}}; \quad \gamma_{xz\ cp} = 1{,}2\,\frac{q}{FG_{xz}}.$$

In general case

$$w'_\tau = K_\tau \frac{Q}{FG_{xz}}; \quad w''_\tau = -K_\tau \frac{q}{FG_{xz}}, \tag{2.2.6}$$

where q is transverse load; K_τ is the coefficient which depends on the shape of the cross section and the method of the account of shears (according to Rankine-Grashof or according to Timoshenko).

The differential equation of the elastic axis of the beam is obtained if we differentiate (2.2.3) with respect to coordinate x and place w''_σ and w''_τ into the obtained expression from (2.2.4) and (2.2.6):

$$w'' = -\frac{M}{E_xI} - \frac{K_\tau q}{G_{xz}F}$$

or taking into account that $d^2M/dx^2 = -q$ after double differentiation

$$w^{IV} = \frac{q}{E_xI} - \frac{K_\tau q''}{G_{xz}F} = \frac{1}{E_xI}(q - \beta^2 i^2 q''), \tag{2.2.7}$$

where $\beta^2 = \dfrac{E_x}{G_{xz}} \cdot i = \sqrt{\dfrac{I}{F}}$ - the moment of inertia of the section.

Equation (2.2.7) can be obtained with the aid of the geometric equations of the mechanics of continuum [27]. With the bending of beam by transverse load, as is known, the expressions for deformation components have the form:

15

$$e_x = \frac{\partial u}{\partial x} = \frac{M}{E_x I} z;$$

$$\gamma_{xz} = \frac{\partial u}{\partial z} + \frac{d\omega}{dx} = \frac{K_\tau Q}{G_{xz} F},$$

where bending moment M and shearing force Q are functions of coordinate x. We hence find the equation

$$\frac{\partial \gamma_{xz}}{\partial x} - \frac{\partial e_x}{\partial z} = \frac{\partial^2 \omega}{\partial x^2} = -\frac{M}{E_x I} + \frac{K_\tau}{G_{xz} F} \cdot \frac{\partial Q}{\partial x},$$

which coincides with (2.2.7) if one considers that $\partial Q/\partial x = -q$.

All the mentioned calculation methods of the account of shears, and also the experiments and the practice of operation show that in constructions of isotropic materials the shears are a secondary factor, the influence of which can be **disregarded virtually** in all real cases.

The bending of anisotropic beams taking into account shear (or the adequate problem of the bending of plates along a cylindrical surface) is examined in the works of S. G. Lekhnitskiy [123], S. A. Ambartsumyan [6], V. I. Korolev [112] and others. It is shown that the error of the theory of flat sections increases with an increase of ratios E_x/G_{xz} and E_x/E_z, to which this theory is indifferent. In the beams reinforced by filaments along x-axis (see Table 1.1.1),

$$\frac{E_x}{G_{xz}} \sim 10 \div 100, \quad \frac{E_x}{E_z} \sim 5 \div 10.$$

For these materials, as follows from (2.2.2), tangential stresses τ_{xz} in spite of their smallness (2.2.1), can cause very large deformations; the account of ε_z, as a rule, introduces substantially less correction [148]: $\varepsilon_z \ll \gamma_{xz}$. This is evident from expressions (2.2.2), if we consider that $G_{xz} \sim E_z$ and $\bar{h}/\bar{l} \ll 1$.

16

Generally speaking, the traditional (appearing in the examination of isotropic constructions) division of stresses into main and secondary, depending on their relative values, becomes meaningless in the case of anisotropic materials. For these materials comparatively small, it would seem secondary stresses, if they act in the directions of weak resistance (directions of low rigidity or strength), can become dangerous. For the materials reinforced by filaments primarily tangential stresses are dangerous, therefore the question concerning their possibly more accurate distribution, examined in this chapter, acquires practical interest.

2.2.2. Elastic line. Let us examine bending of a beam with length l, height 2H, composed of layers of reinforcement with thickness h' and interlayers of bonding agent with thickness h" (Fig. 2.1.3). Without limiting the generality of reasonings, we take the width of beam b equal to one. As shown by theoretical [236] and experimental [149] studies, the effect of the width can be disregarded if b < 2H. In another case, where b >> 2H, the problem in question changes to the problem of bending of a plate along the cylindrical surface. Its solution is analogous with the case of bending of a narrow beam with the difference that instead of flexural rigidity $E_x I$ it is necessary to introduce cylindrical rigidity $D_x = \dfrac{2H^3 E_x}{3(1-\nu_{xz}\nu_{zx})}$ [123, 151, 241].

The average shearing strain (Fig. 2.2.2)

$$\gamma_{x:i} = \frac{u_{i+1} - u_i + h\dfrac{d\omega}{dz}}{h}. \qquad (2.2.8)$$

It is expressed through longitudinal displacements of the middle of adjacent layers u_{i+1} and u_i, angle of rotation of section

17

$\theta = \frac{dw}{dx}$, which is identical for all layers and interlayers as a result of the adopted assumption $\varepsilon_z = \frac{dw}{dx} = 0$.

From the condition of equilibrium of the element of the i-th layer and adjacent contiguous interlayers (Fig. 2.2.3) in the projection to x-axis it follows (see also equation (2.1.4)) that

$$hd\sigma_{xi} + (\tau_{xzi} - \tau_{xz(i-1)})dx = 0. \qquad (2.2.9)$$
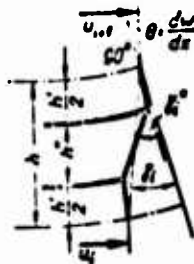
Fig. 2.2.2. The determination of shearing strains with bending.

Fig. 2.2.3. The stresses which act on the element of beam.
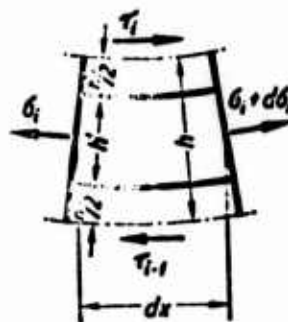
Transverse force Q in the section of the beam is equal to the sum of tangential stresses τ_{xz}, acting in layers and interlayers. Taking into account that Q is connected with transverse load q by dependence $\frac{dQ}{dx} = -q$, we have

$$q = -\frac{d}{dx}\sum_{i=1}^{n}\tau_{xzi}, \qquad (2.2.10)$$

where n is the number of layers.

18

The equations of equilibrium (2.2.9), (2.2.10) taking into account (2.2.8) and (2.1.2) can be rewritten in displacements:

$$\beta^2 \frac{d^2 u_i}{dx^2} + \frac{u_{i+1} - 2u_i + u_{i-1}}{h^2} = 0; \qquad (2.2.11)$$

$$q = -\frac{d}{dx}\left[\sum_{i=1}^{n} G_{xz}h\left(\frac{u_{i+1} - u_i}{h} + \frac{d\ddot{w}}{dx}\right)\right]. \qquad (2.2.12)$$

With a rather large number of layers n the finite differences and the sums which enter equations (2.2.11), (2.2.12) can be replaced by differentials and integrals respectively. In this case we obtain the system of equations of bending of uniform anisotropic beam:

$$\frac{\partial^2 u}{\partial x^2} + \frac{1}{\beta^2}\cdot\frac{\partial^2 u}{\partial z^2} = 0; \qquad (2.2.13)$$

$$2H\frac{d^2 \ddot{w}}{dx^2} + \int_{-H}^{H}\frac{d^2 u}{dx dz}\,dz = -\frac{q}{G_{xz}}. \qquad (2.2.14)$$

It is possible to arrive at these equations by variation (energy) means. Total energy $\ni$ of the system in question (beam with transverse load q) is composed of potential strain energy

$$\ni_1 = \frac{1}{2}\int_{0}^{l}\int_{-H}^{H}(\text{...})\,dx\,dz \qquad (2.2.15)$$

and potential energy of load

$$\ni_2 = -\int_{0}^{l} q\ddot{w}\,dx, \qquad (2.2.16)$$

where $q = \int_{-H}^{H} q_x dz$ - the total transverse load which acts on the rod.

The connection between the stresses and deformations in orthotropic body (x and z are the principal axes of orthotropy,) can be represented in the form

19

$$\sigma_x = \overline{E}_x e_x + \nu_{xz} \overline{E}_x e_z;$$

$$\sigma_z = \overline{E}_z e_z + \nu_{zx} \overline{E}_z e_x;$$

$$\tau_{xz} = G_{xz} \gamma_{xz}.$$

(2.2.17)
(2.2.18)
(2.2.19)

Here

$$\overline{E}_x = \frac{E_x}{1 - \nu_{zx}\nu_{xz}}; \quad \overline{E}_z = \frac{E_z}{1 - \nu_{zx}\nu_{xz}}$$

(first index in Poisson's ratio ν shows the direction of the reduction of dimensions with stretching in the direction designated by the second index).

Taking into account that

$$e_x = \frac{\partial u}{\partial x}; \quad e_z = \frac{\partial w}{\partial z}; \quad \gamma_{xz} = \frac{\partial u}{\partial z} + \frac{\partial w}{\partial x},$$

(2.2.20)

we express potential strain energy through displacements

$$\mathfrak{z}_i = \frac{1}{2} \int_0^l \int_{-h}^{h} \left[\overline{E}_x \left(\frac{\partial u}{\partial x} \right)^2 + \overline{E}_z \left(\frac{\partial w}{\partial z} \right)^2 + 2\nu_{xz} \overline{E}_z \frac{\partial u}{\partial x} \cdot \frac{\partial w}{\partial z} + G_{xz} \left(\frac{\partial u}{\partial z} + \frac{\partial w}{\partial x} \right)^2 \right] dx\, dz.$$

(2.2.21)

Following [43, 46], the weight of the terms entering integrand (2.2.21) can be evaluated using the approximate equalities

$$\frac{\partial}{\partial x} \sim \frac{1}{l}; \quad \frac{\partial}{\partial z} \sim \frac{1}{h},$$

where, as earlier, l and $\overline{h}$ - the characteristic dimensions of the rod along x and z axes. Then from the equations of equilibrium

$$\frac{\partial \sigma_x}{\partial x} + \frac{\partial \tau_{xz}}{\partial z} = 0$$

(2.2.22)

$$\frac{\partial \tau_{xz}}{\partial x} + \frac{\partial \sigma_z}{\partial z} = 0$$

(2.2.23)

we obtain the estimates already given in the preceding paragraph:

20

from equation (2.2.22) - $\tau_{xz} \sim \dfrac{\hbar}{l}\,\sigma_z$, and from equation (2.2.23) -

$\sigma_z \sim \dfrac{\hbar}{l}\,\tau_{xz} \sim \left(\dfrac{\hbar}{l}\right)^2\!\sigma_x$. By accepting stress σ_x from Hooke law as "standard" stress $\bar{\sigma}$

$$e_x = \frac{1}{E_x}\,\sigma_x - \frac{\nu_{zx}}{E_z}\,\sigma_z,\; e_z = \frac{1}{E_z}\,\sigma_z - \frac{\nu_{xz}}{E_x}\,\sigma_x,\; \gamma_{xz} = \frac{\tau}{G_{xz}}.$$

we obtain estimates for deformations:

$$e_x \sim \frac{1}{E_x}\,\bar{\sigma} - \frac{\nu_{zx}}{E_z}\left(\frac{\bar{h}}{l}\right)^2\!\bar{\sigma};$$

$$e_z \sim -\frac{\nu_{xz}}{E_x}\,\bar{\sigma} + \frac{1}{E_z}\left(\frac{\bar{h}}{l}\right)^2\!\bar{\sigma}; \qquad\qquad (2.2.24)$$

$$\gamma_{xz} \sim \frac{1}{G_{xz}}\cdot\frac{\bar{h}}{l}\,\bar{\sigma}$$

and potential strain energy

$$\mathfrak{I}_1 \sim \int_0^l \int_{-H}^{H} \frac{\bar{\sigma}^2}{2E_x}\left[1 - 2\nu_{zx}\left(\frac{\bar{h}}{l}\right)^2 + \frac{E_x}{E_z}\left(\frac{\bar{h}}{l}\right)^4 + \frac{E_x}{G_{xz}}\left(\frac{h}{l}\right)^2\right]dx\,dz. \qquad (2.2.25)$$

For the materials reinforced by filaments (see Table 1.1.1)

$$\frac{E_x}{E_{zz}} \gg \nu_{zx};\quad \frac{E_x}{G_{xz}} > \frac{E_x}{E_z}.$$

therefore the second and third terms in square brackets (2.2.25) can be disregarded. This formally corresponds to the assumption that $\dfrac{1}{E_z} = \nu_{zx} = 0$, i.e., to the allotment of material with infinite transversal rigidity. For isotropic materials E_x and G_{xz} are values of one order, which makes it possible to disregard also the last term in the square brackets of expression (2.2.25). This, obviously, is equivalent to the allotment of material with infinite shear rigidity. Having assumed $\dfrac{1}{G_{xz}} = 0$, let us turn to hypothesis of flat sections.

As is noted in [46], the method used makes it possible only on the average to evaluate the contribution of the different components of the stress-strain state. This method can turn out to be unsuitable during the study of local effects, i.e., in the zones located near the restraint of edges and the application of concentrated forces. By excluding these zones from detailed examination, on the basis of the obtained evaluations (assuming $\varepsilon_z = 0$) we will use the expression for total energy of the system

$$\Im = \Im_1 + \Im_2 = \frac{1}{2} \int_0^l \left\{ \int_{-H}^{H} \left[E_x \left(\frac{\partial u}{\partial x} \right)^2 + G_{xz} \left(\frac{\partial u}{\partial z} + \frac{\partial w}{\partial x} \right)^2 \right] dz - qw \right\} dx. \qquad (2.2.26)$$

According to Lagrange principle, the total energy in the position of equilibrium should reach the minimum value, which requires vanishing of the first variation $\delta\Im = 0$. The Euler-Ostrogradskiy equations correspond to this variational problem:

$$\frac{\partial L}{\partial u} - \frac{\partial}{\partial x} \cdot \frac{\partial L}{\partial \left(\frac{\partial u}{\partial x} \right)} - \frac{\partial}{\partial z} \cdot \frac{\partial L}{\partial \left(\frac{\partial u}{\partial z} \right)} = 0, \qquad (2.2.27)$$

$$\frac{\partial L}{\partial w} - \frac{\partial}{\partial x} \cdot \frac{\partial L}{\partial \left(\frac{\partial w}{\partial x} \right)} = 0, \qquad (2.2.28)$$

where L is the Lagrange function, i.e., integrand of dependence (2.2.26). Using this expression, from (2.2.27) we will obtain (2.2.13), and from (2.2.28) - (2.2.14).

2.2.3. The stress-strained state. In the absence of tangential load, when only transverse load q acts, the following conditions must be fulfilled:

$$\frac{\partial u}{\partial z} + \frac{dw}{dx} = 0 \quad \text{when} \quad z = \pm H. \qquad (2.2.29)$$

By direct substitution it is easy to check that the solution of equation (2.2.13), which satisfies condition (2.2.29), has the form

$$u_m = A_{1m} \, \text{sh} \, \lambda_m \beta z \cos \lambda_m x + A'_{1m} \, \text{sh} \, \lambda_m \beta z \sin \lambda_m x +$$
$$+ A_{2m} z x + A_{3m} z + A_{4m} x + A_{5m};$$

(2.2.30)

$$w_m = -A_{1m} \beta \, \text{sh} \, \varkappa_m \sin \lambda_m x + A'_{1m} \beta \, \text{ch} \, \varkappa_m \cos \lambda_m x -$$
$$- A_{2m} \frac{x^2}{2} - A_{3m} x + A_{6m};$$

(2.2.31)

$\varkappa_m = \lambda_m \beta H$, λ_m, A_m – constants. The terms, which contain coefficients A_{2m}, A_{3m}, A_{4m}, A_{5m} and A_{6m}, are the solution of homogeneous equation ($q = 0$), which corresponds to (2.2.14). The homogeneous solution describes the displacement of the rod as a rigid integral (terms A_{5m}, A_{6m}), tension-compression (term A_{4m}) and pure bending under the action of stresses σ_x, linearly distributed on the ends of the rod (terms with coefficients A_{2m}, A_{3m}).

If transverse load is distributed according to law

$$q = q_m \sin \lambda_m x,$$

(2.2.32)

where $\lambda_m = \frac{m\pi}{l}$; m – integer (the case where $q = q_m \cos \lambda_m x$ is analogously looked over), then from (2.2.14) it follows that

$$A_{1m} = -\frac{q_m}{\lambda_m E_x l \varphi_m \beta \, \text{ch} \, \varkappa_m}.$$

(2.2.33)

Here

$$\varphi_m = \frac{3(\varkappa_m - \text{th} \, \varkappa_m)}{\varkappa^3_m}; \quad \varkappa_m = m\varkappa; \quad \varkappa = \pi \frac{H}{l} \beta.$$

The terms which contain A_{1m}, A'_{1m} and are the solution of nonhomogeneous equation, describe the transverse bending of the rod. The solution in the case of arbitrary load can be obtained by expanding it into trigonometric Fourier series

$$q(x) = \sum_{m=1}^{\infty} q_m \sin \lambda_m x$$

(2.2.34)

and summarizing the solutions which correspond to fractional loads $q_m \sin \lambda_m x$.

23

Coefficients q_m are determined by formula

$$q_m = \frac{2}{l} \int_0^l q(x) \sin \lambda_m x \, dx.$$

For example, for evenly distributed load q_0 = const

$$q_m = \frac{4q_0}{m\pi} \quad (m = 1, 3, 5 \ldots);$$

in the case of concentrated force P, applied at point x',

$$q_m = \frac{2P}{l} \sin \lambda_m x' \quad (m = 1, 2, 3 \ldots).$$

In the examination only of bending, neglecting terms A_{4m}, A_{5m}, A_{6m} it is possible to present displacements u and w as the sum of components of transverse $u_п$, $w_п$ and pure bending $u_ч$, $w_ч$:

$$u = u_п + u_ч;$$
$$w = w_п + w_ч.$$

Correspondingly the total bending moment

$$M = M_п + M_ч = E_x \int_н^H z \frac{\partial u_п}{\partial x} \, dz + E_x \int_{-H}^H z \frac{\partial u_ч}{\partial x} \, dz.$$

Using (2.2.30), (2.2.31), we find the connection between the curvature of the beam w" = d^2w/dx^2 and bending moment:

$$E_x I w''_ч = -M_ч; \tag{2.2.35}$$
$$\varphi_m E_x I w''_п = -M_п. \tag{2.2.36}$$

In the case of pure bending the connection between the curvature and bending moment (2.2.35) is the same as in classical theory

24

(2.2.4). This was to be expected in view of the absence of
tangential stresses. With transverse bending (2.2.36) there appears
correction factor ϕ_m, which is a function of paratmer κ_m. It
depends on the degree of anisotropy of material β ($\beta^2 = \dfrac{E_x}{G_{xz}}$), the
relative height of beam $\dfrac{H}{l}$ and the rate of change of the load
along the length of beam (number of half-waves m, along length l).
With $\kappa_m \to 0$ (see Table 2.2.1), i.e., in the case of an infinitely
long beam (H/l = 0) or infinite shear rigidity of material
(β = 0), $\phi_m \to 1$ and the obtained dependences change to formulas
of the theory constructed on the hypothesis of flat sections
(2.2.4). The error of this theory increases with increase of
parameter κ_m. In this case the value of $\phi_m E_x I$, which can be
treated as the given flexural rigidity of the beam, decreases
(Table 2.2.1).

Table 2.2.1. The functions of the effect of
transverse shear.

x	$\frac{3(x - \text{th } x)}{x^3}$	$\frac{1}{1 - 0.4x^2}$	$1 - 0.4x^2$	$\frac{x^3}{3(x - \text{th } x)}$	$1 + 0.4x^2$
0	1,0000	1,0000	1,0000	1,0000	1,0000
0,02	0,9998	0,9998	0,9994	1,0002	1,0002
0,04	0,9994	0,9994	0,9994	1,0006	1,0006
0,06	0,9986	0,9986	0,9986	1,0014	1,0014
0,08	0,9974	0,9974	0,9974	1,0026	1,0026
0,10	0,9960	0,9960	0,9960	1,0040	1,0040
0,12	0,9942	0,9942	0,9942	1,0058	1,0058
0,14	0,9922	0,9922	0,9942	1,0078	1,0078
0,16	0,9899	0,9899	0,9898	1,0102	1,0102
0,18	0,9872	0,9872	0,9870	1,0130	1,0130
0,20	0,9842	0,9842	0,9810	1,0160	0,0160
0,25	0,9756	0,9756	0,9750	1,0250	1,0250
0,30	0,9652	0,9652	0,9640	1,0360	1,0360
0,35	0,9533	0,9533	0,9510	1,0490	1,0490
0,40	0,9398	0,9398	0,9360	1,0640	1,0640
0,45	0,9251	0,9251	0,9190	1,0809	1,0810
0,50	0,9092	0,9091	0,9000	1,0998	1,1000
0,55	0,8922	0,8921	0,8790	1,1208	1,1210
0,60	0,8743	0,8741	0,8560	1,1437	1,1440
0,65	0,8557	0,8554	0,8331	1,1686	1,1690
0,70	0,8364	0,8361	0,8040	1,1956	1,1960
0,75	0,8167	0,8163	0,7750	1,2244	1,2250
0,80	0,7966	0,7962	0,7440	1,2553	1,2560
0,85	0,7764	0,7758	0,7110	1,2879	1,2890
0,90	0,7560	0,7553	0,6760	1,3227	1,3240
0,95	0,7356	0,7348	0,6390	1,3594	1,3610
1,00	0,7152	0,7113	0,6000	1,3982	1,4000

25

Table 2.2.1.(Cont'd.).

x	$\dfrac{1/2(\mathrm{ch}\,x)}{x^2}$	$\dfrac{1}{1+0.4x^2}$	$1-0.4x^2$	$\dfrac{x^2}{1/2(\mathrm{ch}\,x)}$	$1+0.4x^2$
1.1	0.6751	0.6738	—	1.481	1.481
1.2	0.6369	0.6315	—	1.572	1.576
1.3	0.5985	0.5966	—	1.672	1.676
1.4	0.5627	0.5605	—	1.776	1.784
1.5	0.5288	0.5263	—	1.890	1.900
1.6	0.4968	0.4941	—	2.012	2.024
1.7	0.4669	0.4638	—	2.111	2.156
1.8	0.4389	0.4355	—	2.278	2.296
1.9	0.4128	0.4092	—	2.421	2.444
2.0	0.3885	0.3816	—	2.577	2.600
2.1	0.3659	0.3618	—	2.732	2.764
2.2	0.3449	0.3406	—	2.898	2.936
2.3	0.3254	0.3209	—	3.077	3.116
2.4	0.3074	0.3027	—	3.257	3.304
2.5	0.2906	0.2857	—	3.436	3.500
2.6	0.2750	0.2699	—	3.636	3.704
2.7	0.2605	0.2554	—	3.818	3.916
2.8	0.2470	0.2418	—	4.048	4.136
2.9	0.2344	0.2291	—	4.274	4.364
3.0	0.2228	0.2174	—	4.481	4.600
3.1	0.2119	0.2064	—	4.717	4.844
3.2	0.2017	0.1962	—	4.950	5.096
3.3	0.1922	0.1867	—	5.208	5.356
3.4	0.1834	0.1778	—	5.461	5.624
3.5	0.1751	0.1695	—	5.711	5.900
3.6	0.1673	0.1617	—	5.988	6.184
3.7	0.1600	0.1544	—	6.250	6.476
3.8	0.1531	0.1476	—	6.536	6.776
3.9	0.1467	0.1412	—	6.803	7.084
4.0	0.1406	0.1351	—	7.092	7.400
4.1	0.1350	0.1294	—	7.407	7.724
4.2	0.1294	0.1241	—	7.752	8.056
4.3	0.1245	0.1191	—	8.064	8.396
4.4	0.1198	0.1144	—	8.333	8.744
4.5	0.1152	0.1099	—	8.696	9.100
4.6	0.1110	0.1057	—	9.099	9.464
4.7	0.1069	0.1017	—	9.345	9.836
4.8	0.1031	0.0979	—	9.709	10.216
4.9	0.0994	0.0943	—	10.101	10.604
5.0	0.0965	0.0909	—	10.417	11.000
6.0	0.0694	0.0649	—	14.49	15.40
7.0	0.0525	0.0485	—	19.23	20.60
8.0	0.0410	0.0376	—	24.39	26.60
9.0	0.0329	0.0299	—	30.30	33.40
10.0	0.0270	0.0243	—	37.04	41.00

For the description of the stress-strained state it is necessary to determine the constants, which enter expressions (2.2.30), (2.2.31). A_{1m} is assigned by transverse load; the remaining constants A_m are determined from conditions on the ends of the beam. For a freely resting beam with $x = 0$ and $x = l$ $w = \sigma_x = 0$. These conditions are satisfied if we assume

$A^!_{1m} = A_{2m} = A_{3m} = A_{4m} = A_{5m} = A_{6m} = 0$. In the case of a restrained beam different methods of restraint of the supporting sections are possible (Fig. 2.2.4). Some versions of accomplishment of the rigid fixing are particular cases of condition

$$a_1 u|_{z=\pm z_0} + a_2 \frac{\partial u}{\partial z}\Big|_{z=z_1} + a_3 \frac{d\omega}{dx} = 0 \text{ при } x=0, \ x=l,$$

(при = when)

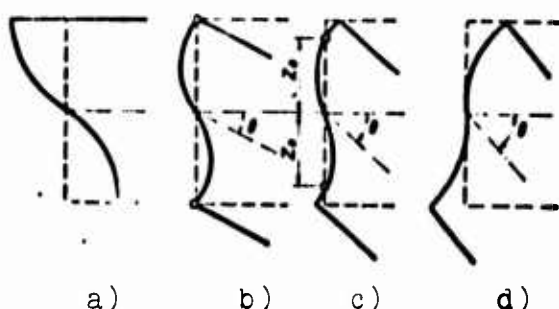where a_1, a_2, a_3, z_0, z_1 are constants.

Fig. 2.2.4. The versions of restraint of end sections. a) $\theta = dw/dx$; b) $u = 0$ when $z = \pm H$; c) $u = 0$ when $z = \pm z_0$; d) $\partial u/\partial z = 0$ when $z = 0$.

a) b) c) d)

When $a_1 = a_2 = 0$ and $a_3 \neq 0$ there is realized "rigid" fixing with restrained horizontal element of the axis of beam (Fig. 2.2.4a). With this $\partial u/\partial z = 0$ when $z = \pm H$. In the case $a_2 = a_3 = 0$, $a_1 \neq 0$ we have two restrained points at distance z_0 from the axis of beam (Fig. 2.2.4b and c). With decrease of value z_0 the pliability of restraint (slope angle θ) grows; $z_0 \to 0$ corresponds to the case where at the level of neutral axis there is fixed the vertical element of the end section (Fig. 2.2.4d): $\partial u/\partial z = 0$ when $z = 0$. With $a_1 = a_3 = 0$, $a_2 \neq 0$ the slope angle of the end section is fixed at height z_1. Thus, cases $a_2 = a_3 = z_0 = 0$ and $a_1 = a_3 = z_1 = 0$ are equally justified.

Differences in the methods of realization of fixing appear only in the theory which considers shear and increase with an increase in parameter κ_m. They can become substantial for beams made of materials reinforced by filaments.

27

The general condition ($a_1 \neq 0$, $a_2 \neq 0$, $a_3 \neq 0$) is satisfied if

$$m = 1, 3, 5 \ldots; \quad A_{4m} = A_{5m} = A_{6m} = 0;$$

$$-\frac{l}{2} A_{2m} = A_{3m} = \frac{q_m}{\lambda_m E_x I q_m} C_m;$$

$$C_m = \frac{a_1 \operatorname{sh} \lambda_m \beta z_0 + a_2 \lambda_m \beta \operatorname{ch} \lambda_m \beta z_1 - a_3 \lambda_m \beta \operatorname{ch} \varkappa_m}{\beta \operatorname{ch} \varkappa_m (a_1 z_0 + a_2 - a_3)}.$$

Thus, including the case of free support, when $C_m = 0$, the solution for the examined conditions of restraint of the beam can be presented in the form

and

$$u_m = -\frac{q_m}{\lambda_m E_x I q_m} \left[\frac{\operatorname{sh} \varkappa_m \frac{z}{H}}{\beta \operatorname{ch} \varkappa_m} \cos \lambda_m x - C_m z \left(1 - \frac{2x}{l} \right) \right] \tag{2.2.37}$$

$$\omega_m = \frac{q_m}{\lambda_m E_x I q_m} \left[\sin \lambda_m x - C_m x \left(1 - \frac{x}{l} \right) \right]. \tag{2.2.38}$$

2.2.4. The bending of cross sections.

The nonlinear term, which contains hyperbolic sine, enters the formula for determination of displacements (2.2.37). This indicates bending of the cross sections of the beam, which is more intense, the larger is parameter $\varkappa_m$. The direct measurement of the bending of cross sections during bending of the beam is done in [216]. It is measured during the bending of freely supported beams, loaded by two concentrated forces (Fig. 2.2.5). For the diagram in question from (2.2.37) taking into account (2.2.34) it follows that

$$u = \frac{4P z \beta H}{3\pi E_x I} \sum_{m=1,3,5\ldots}^{\infty} \frac{\cos \lambda_m x \sin \lambda_m l_2 \operatorname{sh} \varkappa_m \frac{z}{H}}{m (\varkappa_m - \operatorname{th} \varkappa_m) \operatorname{ch} \varkappa_m}. \tag{2.2.39}$$
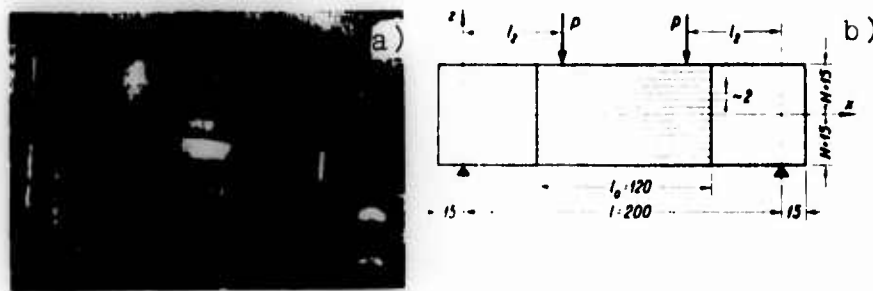
28

Fig. 2.2.5. Determination of the bending of
cross sections during bending, a) experimental
installation, b) loading diagram.

The result obtained on the basis of classical theory is expressed
by dependence

$$u^* = \lim_{x \to 0} u = \frac{P_1}{2E_x I} \, (l_2 l - l_2^2 - x^2).$$

(2.2.40)

The diagrams of longitudinal displacements for different values
of x and l_2 are given on Fig. 2.2.6, on which there are placed
the values of relative quantity $u_1 = u(3\pi^3 E_x I / 4 P \kappa^2 l^2 H)$. Straight
lines ($\kappa = 0$) are obtained by the classical theory and curved
correspond to values $\kappa = 2$.

The effect of bending of cross sections during bending is
investigated experimentally on samples with wire-sensors (see
§ 2.1.3). The dimensions of samples (with thickness 12 mm), the
diagram of restraint and loading is shown on Fig. 2.2.5.

The study of samples with different length of wire-sensors
(see Fig. 2.2.5) made it possible to determine longitudinal
displacements at different values of coordinate x. On Fig. 2.2.7
theoretical and experimental data are compared. As is evident,
tne character of the arrangement of calculated curves and
experimental points is identical, the latter lie in the expected
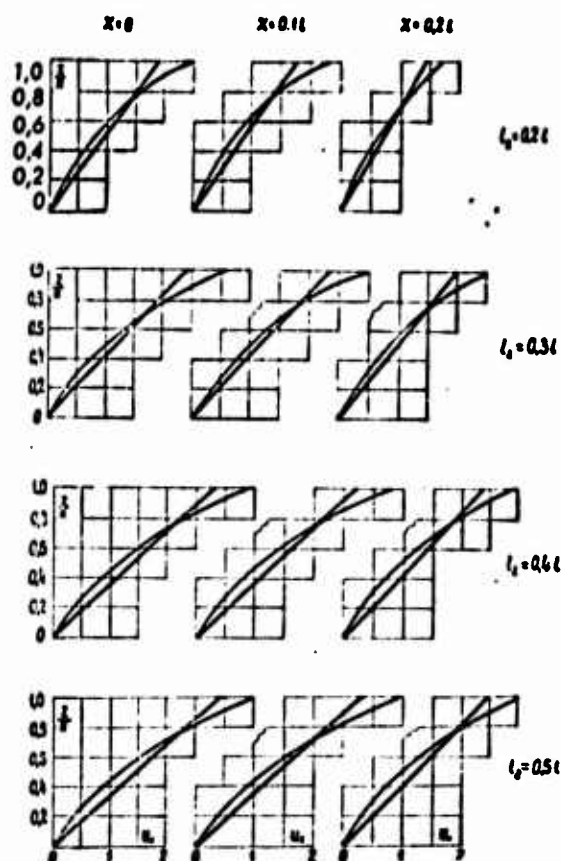region of parameter κ.

29

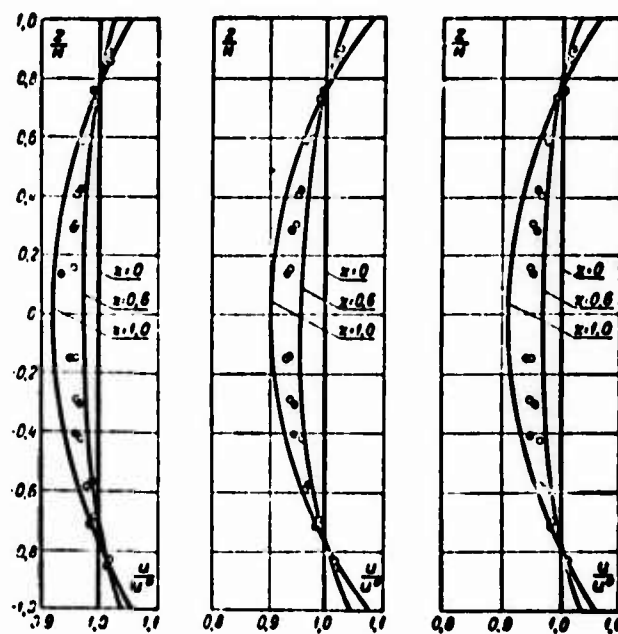Fig. 2.2.6. Diagrams of the longitudinal displacements of beam.

Fig. 2.2.7. The experimental evaluation of the bending of cross sections during bending ($l_2 = 0.2l$, $l_2 = 0.3l$, $l_2 = 0.5l$, $l_0 = 120$ mm).

30

2.2.5. The estimation of error of the replacement of laminated beam by homogeneous.

The bending equations (2.2.13), (2.2.14) do not consider the heterogeneity of material. The number of layers of reinforcement and interlayers of bonding agent is taken as i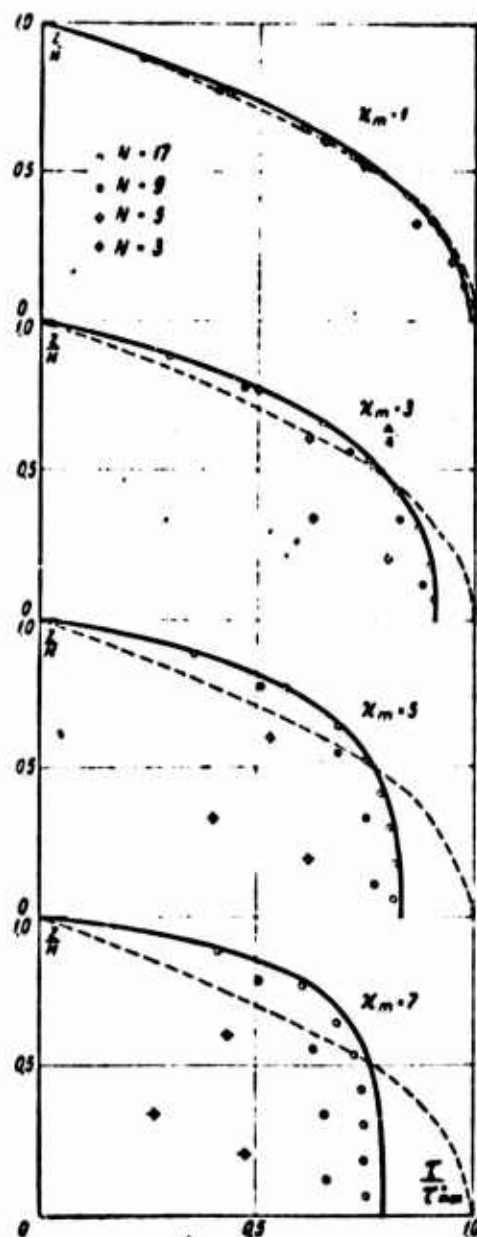nfinite. To evaluate the error, introduced by limit transition (transition from system of equations (2.2.11), (2.2.12) to (2.2.13), (2.2.14), by A. R. Rzhanitsin's method [182] there is solved the problem for a laminated (n = 3, 5, 9, 17) free beam, loaded by sinusoidal load $q = q_m \sin \lambda_m x$. The comparison of these solutions with the solution of (2.2.37), (2.2.38), corresponding to n = ∞, shows that for real constructions of reinforced materials, for which, as a rule n > 10, the error introduced by the replacement of laminated medium by homogeneous is insignificant. For the illustration of this conclusion there is given Fig. 2.2.8, on which solid lines designate the diagrams of tangential stresses, calculated on the basis of (2.2.37), (2.2.38) and points – the corresponding values of tangential stresses in the interlayers of composite beam (dotted line – diagrams of tangential stresses τ_{xz} according to D. I. Zhuravskiy).

Fig. 2.2.8. Estimation of error with the replacement of laminated beam by quasi-homogeneous. N is the number of layers.

V. L. Biderman [29] evaluated the error of the replacement of

31

laminated beam by homogeneous on the basis of the comparison of coefficients in the equations of elastic line of the beam. For homogeneous M_0 and laminated $M_{c\pi}$ beams respectively

$$M_0 = -E_i I_0 \frac{d^2 w}{dx^2}; \quad M_{c\pi} = -E_i I_{c\pi} \frac{d^2 w}{dx^2}.$$

where

$$I_0 = \frac{2}{3} H^3; \quad I_{c\pi} = \frac{2H}{n} \sum_{i=1}^{n} z_i^2;$$

z_i - the distance between the axis of beam and the axis of the i-th layer.

As calculation showed, even at $n > 5$ values I_0 and $I_{c\pi}$ differ by less than 5%.

Equations for quasi-homogeneous medium, obtained by V. V. Bolotin [37], make it possible to consider the flexural rigidity of reinforced layers, without resorting to the labor-consuming process of solving a large number of equations, corresponding to the number of layers. These equations in the case of a beam have the form

$$\frac{\partial^2 u}{\partial x^2} + \frac{1}{\beta^2} \cdot \frac{\partial^2 u}{\partial z^2} = 0; \tag{2.2.41}$$

$$-\frac{2H^3}{3} \cdot \frac{\beta^2}{n^2} \left(\frac{h'}{h}\right)^2 \frac{d^4 w}{dx^4} + 2H \frac{d^2 w}{dx^2} + \int_{-H}^{H} \frac{d^2 u}{dx dz} dz = -\frac{q}{G_{xz}}. \tag{2.2.42}$$

Equation (2.2.41) coincides with equation (2.2.13), and (2.2.42) differs from (2.1.14) by the first term, the value of which decreases with increase of the number of layers as $1/n^2$. By solving system (2.2.41), (2.2.42) similarly to that shown in § 2.2.3, we find that in the case of a free beam under load $q = q_m \sin \lambda_m x$ deflection is determined by formula

32

$$\omega_6 = \frac{\omega}{k_6}. \qquad (2.2.43)$$

where w is the deflection, calculated by formula (2.2.38);

$k_\sigma = 1 + \dfrac{\kappa_m}{3n^2}\left(\dfrac{h'}{h}\right)^2$ - the coefficient which considers the flexural

rigidity of the reinforcement layers. The numerical values of this coefficient, given in Table 2.2.2 (for $\dfrac{h'}{h} = 0.5$), make it possible to draw the conclusion that during the determination of deflections of the constructions made of reinforced materials the flexural effects in the reinforcement layers can be disregarded for a broad class of problems.

Table 2.2.2.   The values of coefficients

$k_\sigma = 1 + \dfrac{\kappa^2}{3n^2}\left(\dfrac{h'}{h}\right)^2$ when $\dfrac{h}{h'} = 0.5$.

A\n	1	2	1	3
3	1.0003	1.0370	1.0833	1.2312
5	1.0033	1.0133	1.0300	1.0833
10	1.0008	1.0033	1.0075	1.0209
20	1.0002	1.0008	1.0019	1.0052

2.2.6.   Estimation of error introduced by neglect of lateral deformation.   The equations corresponding to system (2.2.13), (2.2.14), but considering lateral deformation, can be obtained, by substituting in the equations of equilibrium (2.2.22), (2.2.23) the stresses of (2.2.17), (2.2.19), expressed through displacements:

$$\bar{E}_x \frac{\partial^2 u}{\partial x^2} + G_{xz} \frac{\partial^2 u}{\partial z^2} + (G_{xz} + \nu_{xz}\bar{E}_x)\frac{\partial^2 w}{\partial x \partial z} = 0; \qquad (2.2.44)$$

$$\bar{E}_z \frac{\partial^2 w}{\partial z^2} + G_{xz} \frac{\partial^2 w}{\partial x^2} + (G_{xz} + \nu_{xz}\bar{E}_z)\frac{\partial^2 u}{\partial x \partial z} = 0. \qquad (2.2.45)$$

Accepting that half of transverse load $q_m \sin \lambda_m x$ is applied
to the upper, and half - to the bottom surfaces of the beam,
in the absence of tangential load the boundary conditions have
the form

$$
\begin{aligned}
\tau_{zx} &= 0 && \text{при} \quad z = \pm H; \\
\sigma_z &= \frac{q_m}{2} \sin \lambda_m x && \text{при} \quad z = H; \\
\sigma_z &= -\frac{q_m}{2} \sin \lambda_m x && \text{при} \quad z = -H.
\end{aligned}
\tag{2.2.46}
$$

(при = when)

Examining a free beam, the displacement should be sought in
the class of functions which satisfy the appropriate boundary
conditions of freely supported beam ($\sigma_x = w = 0$ when $x = 0$, $x = l$):

$$
\begin{aligned}
w_m &= B_m \sin \lambda_m x \exp (s\lambda_m x); \\
u_m &= A_m \cos \lambda_m x \exp (s\lambda_m x).
\end{aligned}
\tag{2.2.47}
$$

Having substituted (2.2.47) into equations (2.2.44), (2.2.45),
we will obtain the system of homogeneous equations:

$$
\begin{cases}
A_m (G_{xz} s^2 - \overline{E}_x) + B_m s (G_{xz} + v_{xz} \overline{E}_x) = 0; \\
-A_m s (G_{xz} + v_{xz} \overline{E}_x) + B_m (\overline{E}_z s^2 - G_{xz}) = 0.
\end{cases}
\tag{2.2.48}
$$

which will have non-trivial solutions, when its determinant is
equal to zero

$$
\begin{vmatrix}
G_{xz} s^2 - \overline{E}_x & -s(G_{xz} + v_{xz} \overline{E}_x) \\
-s(G_{xz} + v_{xz} \overline{E}_x) & \overline{E}_z s^2 - G_{xz}
\end{vmatrix} = 0.
\tag{2.2.49}
$$

Equation (2.2.49) has four roots: $\pm\sqrt{a^2}$, $\pm\sqrt{b^2}$, where

$$
a^2 = \frac{\overline{\beta}^2}{2}\left(1 + \sqrt{1 - \frac{4\alpha^2}{\overline{\beta}^2}}\right), \quad b^2 = \frac{\overline{\beta}^2}{2}\left(1 - \sqrt{1 - \frac{4\alpha^2}{\overline{\beta}^2}}\right),
$$

$$
\overline{\beta}^2 = \frac{\overline{E}_x}{G_{xz}}\left(1 - 2v_{xz}\frac{G_{xz}}{\overline{E}_z} - v_{xz}^2\frac{\overline{E}_x}{\overline{E}_z}\right), \quad \alpha^2 = \frac{\overline{E}_x}{\overline{E}_z}.
$$

34

These roots for real anisotripic materials are real and different (for isotropic materials a = b), consequently, solutions of (2.2.47) taking into account the connection between coefficients A_m and B_m (2.2.48) can be presented in the form

$$u_m = (C_{1m}\,\text{sh}\,a\lambda_m z + C_{2m}\,\text{ch}\,a\lambda_m z + C_{3m}\,\text{sh}\,b\lambda_m z + C_{4m}\,\text{ch}\,b\lambda_m z)\cos\lambda_m x; \qquad (2.2.50)$$
$$w_m = (C_{2m}p_a\,\text{sh}\,\lambda_m z + C_{1m}p_a\,\text{ch}\,a\lambda_m z + C_{4m}p_b\,\text{sh}\,b\lambda_m z + C_{3m}p_b\,\text{ch}\,b\lambda_m z)\sin\lambda_m x.$$

where

$$p_a = \frac{\bar{E}_z - a^2 G_{xz}}{a(G_{xz} + \nu_{zx}\bar{E}_z)}; \quad p_b = \frac{\bar{E}_z - b^2 G_{xz}}{b(G_{xz} + \nu_{zx}\bar{E}_z)}.$$

By substituting (2.2.50) into boundary conditions (2.2.46), we find unknown constants C_{1m}, C_{2m}, C_{3m}, C_{4m}. Thus, there is determined expression

$$w_m = \frac{q_m\left[p_a(b+p_b)\dfrac{\text{ch}\,a\lambda_m z}{\text{ch}\,a\lambda_m H} - p_b(a+p_a)\dfrac{\text{ch}\,b\lambda_m z}{\text{ch}\,b\lambda_m H}\right]\sin\lambda_m x}{2\nu_{zx}\bar{E}_z[(ap_a - \nu_{zx})(b+p_b)\,\text{th}\,\lambda_m\,aH - (a+p_a)(bp_a - \nu_{zx})\,\text{th}\,b\lambda_m H]}. \qquad (2.2.51)$$

For materials reinforced by filaments $E_x \gg G_{xz}$ (see Table 1.1.1), therefore when $\nu_{zx} = 0$ it is possible to accept

$$a^2 = \frac{E_z}{G_{xz}} - \frac{G_{xz}}{E_z}, \quad b^2 = \frac{G_{xz}}{E_z}$$

and deflection when $z = \pm H$ taking into account that $\frac{H}{l} \ll 1$, to determine as

$$w_m = w^*_m\left(1 + 0.4\lambda_m^2 H^2\,\frac{E_x}{G_{xz}}\right)\left(1 + \frac{G_{xz}^2}{E_z E_x}\right). \qquad (2.2.52)$$

Here w^*_m is the deflection, determined according to classical theory; the expression in the first parenthesis is the multiplier, which characterizes the correction from shears, in the second - from lateral deformation. As is evident, the correction caused by

lateral deformation for the materials **reinforced by filaments is**
negligible, since $G_{xz} \ll E_x$ (see Table 1.1.1). This conclusion
agrees with that given in § 2.2.2 during the analysis of the weight
of components which enter the formula of potential strain energy.

§ 2.3. FLEXURAL RIGIDITY

**2.3.1. The comparative analysis of the methods of account of
shear.** The comparison of the methods of account of shear according
to Rankine-Grashof and Timoshenko (see § 2.1.1) with the refined
method given in § 2.1.2 can be the most visually performed on
an example of a free beam of rectangular cross section, loaded by
sinusoidal load $q = q_m \sin \lambda_m x$. In this case the deflection
according to Rankine-Grashof w_I, Timoshenko w_{II} and refined formula
(2.2.38) w is expressed through the deflection determined without
allowing for shear w^*, and the parameter $\kappa_m = m\pi\beta\frac{H}{l}$:

$$w_I = w^* (1 + 0.5\kappa_m^2); \qquad\qquad (2.3.1)$$

$$w_{II} = w^* (1 + 0.4\kappa_m^2); \qquad\qquad (2.3.2)$$

$$w = w^* \frac{\kappa_m^3}{3(\kappa_m - \text{th }\kappa_m)}. \qquad\qquad (2.3.3)$$

As can be seen from the expansion of functions $\dfrac{1}{\phi_m} = \dfrac{\kappa_m^3}{3(\kappa_m - \text{th }\kappa_m)}$
into Taylor series

$$\frac{1}{\phi_m} = 1 + 0.4\kappa_m^2 - 0.0019\kappa_m^4 + 0.00014\kappa_m^6 - \ldots \left(\kappa_m < \frac{\pi}{2}\right). \qquad (2.3.4)$$

Timoshenko's formula (2.3.2) gives the best approximation. Values
w and w_{II} are very close to one another over a wide range of
change of parameter κ_m (see Table 2.2.1).

If Timoshenko's formula is presented in the form

$$w = w^* \left(1 + K\frac{\kappa_m^2}{3}\right) \qquad\qquad (2.3.5)$$

36

and we consider coefficient K depending not only on the shape of
the cross section of the beam (see § 2.2.1), but also on parameter
κ_m,

$$K(\varkappa_m) = \frac{3}{\varkappa_m^2}\left(\frac{1}{\varphi_m} - 1\right).$$ (2.3.6)

then coincidence (2.3.3 and 2.3.5) will be complete. Consequently,
shear coefficient K depends on the relationship of elastic constants
and the relationship of cross and longitudinal dimensions.[1] Since
Timoshenko's approach assumes the value of K = 1.2 to be constant
for a beam of rectangular cross section, the error for this
approach can be characterized by how much function $K(\kappa_m)$ depends
on parameter κ_m. Elementary study shows that $K(\kappa_m)$ is the
monotonically decreasing function which is changed within
sufficiently narrow limits:

$$\lim_{\varkappa_m \to 0} K(\varkappa_m) = 1,2, \quad \lim_{\varkappa_m \to \infty} K(\varkappa_m) = 1.$$

When $\kappa_m < \frac{\pi}{2}$

$$K(\varkappa_m) = 1,2 - 0,0057\varkappa_m^2 + 0,00012\varkappa_m^4 - \ldots$$ (2.3.7)

This bears out the fact that formula (2.3.2) catches the principal
part of the correction from shear.

One should still note that as a result of the bending of
cross sections the deflection from normal stresses w_σ does not
identically coincide with the deflection determined without
allowing for shear w^*. Therefore into the formula of superposition
of deflections (2.2.7) it is necessary to introduce coefficient
K_σ:

_____

[1]The effect of the relationship of elastic constants on
coefficient K without allowing for the relationship of geometric
dimensions is examined in [278].

$$w'' = w''_\sigma + w''_\tau = -K_\sigma \frac{M}{E_x I} - K_\tau \frac{q}{G_{xz} F}.$$

This coefficient must be determined similarly to how K_τ of formula (2.2.5) is determined from equality of works

$$\frac{1}{2E_x} \int_F \sigma_x^2 dF = \frac{K_\sigma M^2}{2E_x I}. \tag{2.3.8}$$

Here $w''_\sigma = K_\sigma \frac{M}{E_x I}$ - the curvature of elastic line, caused by normal stresses. Taking into account that in the case in question the normal stresses are determined by formula

$$\sigma_x = \frac{\sigma^*_{max}}{\varkappa_m \varphi_m \operatorname{ch} \varkappa_m} \operatorname{sh} \varkappa_m \frac{z}{H}. \tag{2.3.9}$$

on the basis of (2.3.8) we have

$$K_\sigma = \frac{1}{2\varphi_m} \left(\frac{3 \operatorname{th}^2 \varkappa_m}{\varphi_m \varkappa_m^2} - 1 \right). \tag{2.3.10}$$

In the limiting case $\varkappa_m \to 0$, $K_\sigma \to 1$, consequently, we have the classical connection between curvature and the bending moment. With $\varkappa_m$, different from zero, i.e., taking into account shears,

$$w = w_\sigma + w_\tau = w^* \left(K_\sigma + K_\tau \frac{\varkappa_m^2}{3} \right). \tag{2.3.11}$$

As can be seen from comparison of (2.3.5) and (2.3.11)

$$K = \frac{3}{\varkappa_m^2} (K_\sigma - 1) + K_\tau, \tag{2.3.12}$$

whence

$$K_\tau = \frac{9}{2\varphi_m \varkappa_m^2} \left(1 - \frac{\operatorname{th}^2 \varkappa_m}{\varphi_m \varkappa_m^2} \right). \tag{2.3.13}$$

38

This value of K_τ can be obtained from equality (2.2.5) if one considers that the distribution of tangential stresses is determined by formula (2.4.1):

$$\tau = \frac{2}{q_n x_m^2} \tau^*_{max} \left(1 - \frac{ch\, x_m \frac{z}{H}}{ch\, x_m} \right).$$

2.3.2. Deflection, caused by shears. The effect of shear on deflection is convenient to investigate by parameter $\kappa = \pi\beta\frac{H}{l}$, which simultaneously considers the relationship of the geometric dimensions of the beam $\frac{H}{l}$ and the degree of anisotropy of material E_x/G_{xz}. With accuracy to multiplier π parameter κ can be treated as the relative height of the beam, given taking into account the degree of anisotropy. An increase in the relative height of the beam corresponds to decrease of the shear rigidity. Thus, beams of reinforced materials of the same geometric dimensions as isotropic, in comparison with the latter, work as the beams of greater height.

The effect of shears is analyzed on an example of free, restrained and cantilever beams,[1] loaded as shown in Figs. 2.3.1-2.3.3. In these figures are given the relationships of maximum deflections, calculated taking into account (w_{max}) and without allowing for (w^*_{max}) shears. In these figures results obtained from formula (2.2.38) taking into account (2.2.33) are given - on graphs they are noted by the numeral 3, and obtained from the diagrams of Rankine-Grashof (curves 1) and Timoshenko (curves 2). As in the case of sinusoidal load, the amount of deflection calculated according to Rankine-Grashof is high, and the results determined according to Timoshenko and formula (2.2.38) are very close. Therefore the Timoshenko approximation formulas can be used

---

[1]The cantilever is considered as half the symmetrically loaded free beam [26, 220]. The stricter solution for isotropic cantilever is given in [34].

39

in practical calculations. However, such formulas are known only for a limited number of cases of load distribution (see [239], and also [6, 112]).[1]
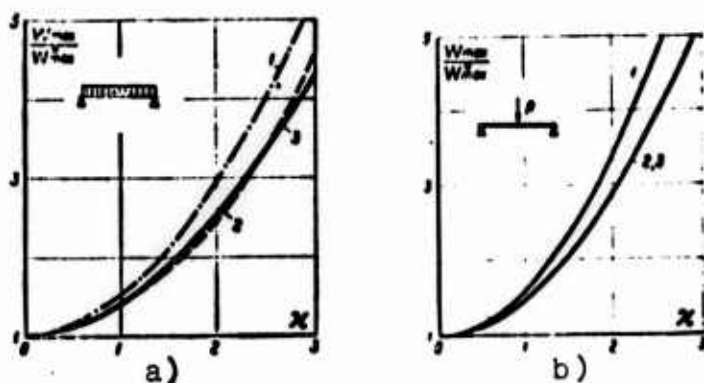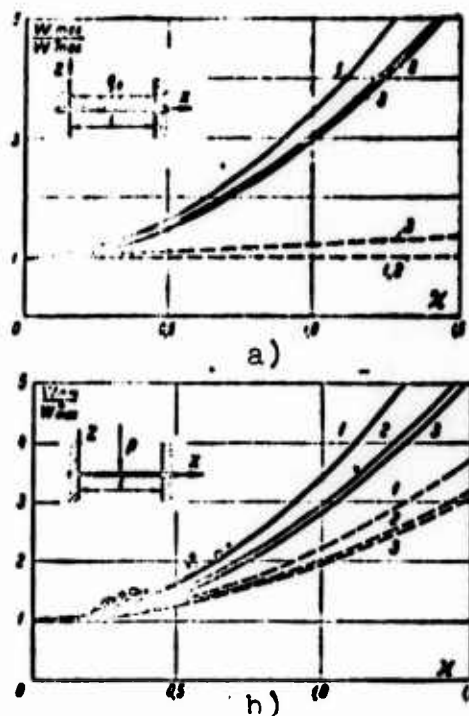

Fig. 2.3.1. The effect of shear on the deflection of free beams, loaded by evenly distributed load (a) and concentrated force halfway along the span (b).

Fig. 2.3.2. The effect of shears on the deflection of fixed beams, loaded by evenly distributed load (a) and by concentrated force in the span (b). ——— $\partial u/\partial z = 0$ (when $z = 0$). - - - $dw/dx = 0$.

---

[1]The number of problems, during the solution of which shears are considered, is extremely small. This is explained by the fact that before the appearance of materials reinforced by filaments the account of shear had purely academic interest.
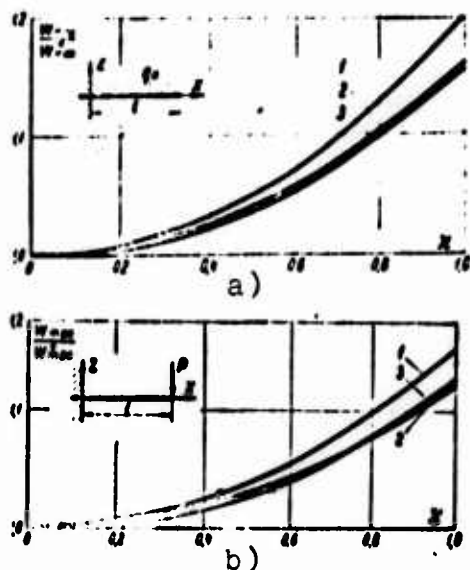
Fig. 2.3.3. The effect of shear on the deflection of cantilevers loaded by evenly distributed load (a) and by concentrated force at the end (b).

In more complex cases it is necessary to use formula (2.2.38), after expanding the load into series (2.2.33).

The series for determining the calculated values are frequently rapidly converging, which makes it possible to be limited to keeping only the first or their several first terms. Furthermore, there is the possibility of improving the convergence by separating from the total series the series whose sum is expressed in closed form [83]. For example, the deflection of evenly loaded (q_0 = const) beam with boundary conditions $w = dw/dx = 0$ with $x = 0$ and $x = l$ is determined by expression

$$w = \frac{1 q_0 l^4 x^3}{3 \pi^5 E_x I} \left\{ \sum_{m=1,3,5\ldots}^{\infty} \frac{\sin m \pi \frac{x}{l}}{m^2 (m \varkappa - \text{th } m \varkappa)} - \frac{\pi x}{l} \left(1 - \frac{x}{l} \right) \sum_{m=1,3,5\ldots}^{\infty} \frac{1}{m (m \varkappa - \text{th } m \varkappa)} \right\}.$$

By converting the first sum

$$\sum_{m=1,3,5\ldots}^{\infty} \frac{\sin m \pi \frac{x}{l}}{m^2 (m \varkappa - \text{th } m \varkappa)} = \frac{1}{\varkappa} \sum_{m=1,3,5\ldots}^{\infty} \frac{\sin m \pi \frac{x}{l}}{m^3} + \frac{1}{\varkappa} \sum_{m=1,3,5\ldots}^{\infty} \frac{\text{th } m \varkappa \sin m \pi \frac{x}{l}}{m (m \varkappa - \text{th } m \varkappa)}.$$

we will obtain

$$\sum_{m=1,3,5\ldots}^{\infty} \frac{\sin m\pi \frac{x}{l}}{m^3} = \frac{1}{2} \sum_{m=1,2,3\ldots}^{\infty} \frac{(1-\cos m\pi) \sin m\pi \frac{x}{l}}{m^3} =$$

$$= \frac{1}{2} \sum_{m=1,2,3\ldots}^{\infty} \frac{\sin m\pi \frac{x}{l}}{m^3} + \frac{1}{4} \sum_{m=1,2,3\ldots}^{\infty} \frac{\sin m\pi \left(1-\frac{x}{l}\right)}{m^3} -$$

$$- \frac{1}{4} \sum_{m=1,2,3\ldots}^{\infty} \frac{\sin m\pi \left(1+\frac{x}{l}\right)}{m^3} = \frac{\pi^3}{8} \cdot \frac{x}{l}\left(1-\frac{x}{l}\right).$$

In turn

$$\sum_{m=1,3,5\ldots}^{\infty} \frac{1}{m(m\varkappa - \text{th } m\varkappa)} = \frac{1}{\varkappa} \sum_{m=1,3,5\ldots}^{\infty} \frac{1}{m^2} + \frac{1}{\varkappa} \sum_{m=1,3,5\ldots}^{\infty} \frac{\text{th } m\varkappa}{m^2(m\varkappa - \text{th } m\varkappa)}.$$

Taking into account that $\sum_{m=1,3,5\ldots}^{\infty} \frac{1}{m^2} = \frac{\pi^2}{8}$, instead of the initial expression for deflection (sum) we obtain the sum with improved convergence:

$$w = \frac{4 l q l^4 \varkappa^2}{4\pi^5 E_x J}\left\{ \sum_{m=1,3,5\ldots}^{\infty} \frac{\text{th } m\varkappa \sin m\pi \frac{x}{l}}{m^3(m\varkappa - \text{th } m\varkappa)} - \frac{\pi x}{l}\left(1-\frac{x}{l}\right) \sum_{m=1,3,5\ldots}^{\infty} \frac{\text{th } m\varkappa}{m^2(m\varkappa - \text{th } m\varkappa)}\right\}.$$

As can be seen from Figs. 2.3.1-2.3.3 and Table 2.3.1, for free and, especially, fixed beams the effect of shears   must be taken into account with any practically important ratio $\frac{H}{l}$. At the same time, the effect of shear on the deflection of cantilever is substantial only for very short beams made of highly anisotropic material.

Figure 2.3.4 illustrates the dependence of deflection on conditions of restraint of the ends of fixed beams. The differences in deflections, caused by restraint (see Fig. 2.3.4), are increased with increase of parameter $\varkappa$. Consequently, if for isotropic beams with small $\varkappa$ the realization of the method of fixing has virtually no effect on deflection, then in beams of anisotropic material

42

with large κ this effect is already substantial - deflection to
a considerable degree depends on the realization of conditions of
the restraint of supporting sections, in other words, with an
increase of parameter κ the sensitivity to the method of
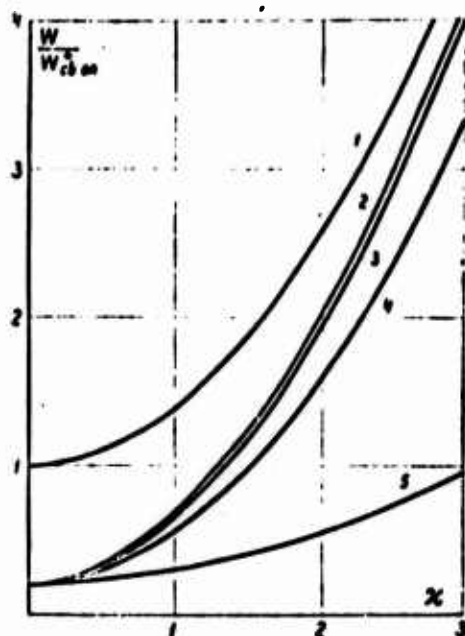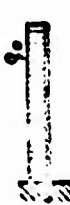restraint of the beam is increased.

Fig. 2.3.4. The effect of the
method of restraint of the beam
on deflection: 1 - free beam
($w^*_{\text{CB.on}}$ deflection without allow-
ing for shear); 2 - $\partial u/\partial z = 0$
when $z = 0$ (Fig. 2.2.4d); 3 - u =
= 0 when $z = \pm 0.5H$ (Fig. 2.2.4c);
4 - u = 0 when $z = H$ (Fig. 2.2.4b);
5 - dw/dx = 0 (Fig. 2.1.4a).

V. I. Biderman proposed the method which makes it possible
to determine the deflection of a fixed beam, using the solution
for the free beam (Fig. 2.3.5). The fixed beam is considered
as a section of a continuous beam. It is obvious that in view of
the symmetry in the restraint u = 0. As can be seen from the
figure, maximum deflection w_{max} of restrained, centrally loaded beam
with length l is two times more than maximum deflection w_{1max} of
centrally loaded, free beam with length $l/2$. Thus,

$$w_{max} = 2 w_{1\,max} = 2 w^*_{1\,max}\left[1 + C\,\frac{H^2}{\left(\frac{l}{2}\right)^2}\right] = w^*_{max}\left[1 + 4C\,\frac{H^2}{l^2}\right].$$

i.e., correction from shear in fixed beam exceeds the correction
for free beam 4 times.

43

Table 2.3.1. The effect of shears on the deflection of beams of materials reinforced by filaments.

Loading diagram	$\dfrac{W_{max}}{W^*_{max}}$	$\dfrac{l}{2H}$	$\dfrac{N}{N^*_{HP}}$					
			Glass fiber-reinforced plastic with three-dimensional cross-linked reinforcement $\beta^2 = 8\text{-}13$	Fiber-glass laminates $\beta^2 = 10\text{-}15$	Nonfabric glass fiber-reinforced plastics (packing 1:1) $\beta^2 = 15\text{-}20$	Unidirectional glass fiber-reinforced plastic $\beta^2 = 25\text{-}50$	Nonfabric boron fiber-reinforced plastics (packing 1:1) $\beta^2 < 40$	Unidirectional boron fiber-reinforced plastics $\beta^2 < 100$
	$1 + 0.162x^2$	5	1.13—1.21	1.16—1.21	1.21—1.32	1.30—1.50	$\leqslant 1.64$	$\leqslant 2.60$
		20	≈ 1.01	1.01—1.02	≈ 1.02	1.03—1.05	$\leqslant 1.04$	$\leqslant 1.10$
	$1 + 0.389x^3$	5	1.31—1.70	1.33—1.5	1.38—1.77	1.65—2.92	$\leqslant 2.54$	$\leqslant 4.84$
		20	1.02—1.03	1.02—1.04	1.01—1.05	1.06—1.12	$\leqslant 1.10$	$\leqslant 1.24$
	$\dfrac{1}{1 + 2.43x^3}$ $\left(\text{when } x=0,\ x=l\ \dfrac{dw}{dx}=0\right)$ $\left(\text{when } x=0,\ x=l\ \dfrac{\partial u}{\partial z}\Big\|_{z=0}=0\right)$	5	2.92—4.12	3.40—4.69	4.60—5.80	7.00—13.00	$\leqslant 10.60$	$\leqslant 24.98$
		20	1.12—1.19	1.15—1.23	1.23—1.30	1.23—1.75	$\leqslant 1.60$	$\leqslant 2.60$

Under these boundary conditions the tangential stresses do not affect the maximum deflection of the rod

44

Table 2.3.1. (Cont'd.).

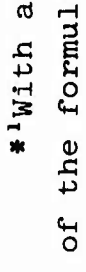| Diagram	Formula							
	$\dfrac{\operatorname{ch}\alpha l+\cos\cdot cl-2\left(\operatorname{ch}\dfrac{\alpha l}{2}\cos\dfrac{cl}{2}-\dfrac{0.2B^2}{|1-0.4B^4}\operatorname{sh}\dfrac{\alpha l}{2}\sin\dfrac{cl}{2}\right)}{(\operatorname{ch}\alpha l+\cos\alpha l)-2\operatorname{ch}\dfrac{\alpha l}{2}\cos\dfrac{cl}{2}}\times$ $\times\dfrac{\operatorname{ch}\alpha l+\cos cl}{\operatorname{ch}\alpha l+\cos cl}$ (in the middle of the span of the beam)	5	1.14—1.21	1.17—1.24	1.24—1.29	1.31—1.32	≤1.46	—∙¹
		20	Tangential stresses virtually do not affect the deflection of beam with given $\frac{l}{2H}$, i.e., the beam can be considered infinitely long					
	$1+\dfrac{N}{N^0{}_{\kappa p}}$	5	1.25—1.50	1.31—1.45	1.45—1.58	1.71—2.22	≤2.04	≤2.95
		20	1.20—1.30	1.24—1.33	1.33—1.42	1.50—1.79	≤1.69	≤2.13
	$\dfrac{N}{3(z-\operatorname{th}z\iota)+\dfrac{N}{N^0{}_{\kappa p}}}$	5	1.02—1.03	1.02—1.04	1.04—1.05	1.06—1.11	≤1.09	≤1.20
		20	1.02—1.03	1.02—1.03	1.03—1.04	1.04—1.08	≤1.07	≤1.16
	$1-\dfrac{N}{\dfrac{3(z-\operatorname{th}z\iota)}{z^3}-\dfrac{N}{N^0{}_{\kappa p}}}$	5	1.13—1.73	1.55—1.87	1.65—2.23	2.02—5.62	—4.18	—∙³
		20	1.02—3.10	2.31—3.89	3.60—8.23	—∙⁸	—∙³	—∙³
	$1+0.122 z^3$	5	1.03—1.04	1.04—1.05	1.05—1.07	1.08—1.16	≤1.13	≤1.33
		20	1.01—1.07	1.05—1.08	1.08—1.11	1.11—1.29	≤1.23	≤1.66
	$1+0.486 z^3$	5	1.10—1.16	1.12—1.18	1.18—1.24	1.30—1.60	≤1.48	≤2.20
		20	≈1.01	≈1.01	1.01—1.02	1.02—1.04	≤1.03	≤1.08
	$1+0.973 z^3$ $\left(x=0\xi,\ \dfrac{dz}{dx}=0\right)$	5	1.38—1.62	1.48—1.72	1.72—1.96	2.20—3.40	≤2.92	≤5.80
		20	1.02—1.04	1.03—1.05	1.05—1.06	1.08—1.15	≤1.12	≤1.30
	$1+2.19 z^3$ $\left(x=0\xi,\ \dfrac{\partial u}{\partial z}\Big|_{z=0}=0\right)$	5	1.77—2.25	1.96—2.41	1.44—2.92	2.21—5.80	≤4.84	≤10.60
		20	1.05—1.08	1.06—1.09	1.02—1.12	1.15—1.30	≤1.24	≤1.60
		5	2.83—3.61	3.16—4.21	1.24—5.32	6.30—11.81	≤9.65	≤22.62
		20	1.11—1.18	1.14—1.20	1.20—1.27	1.31—1.68	≤1.51	≤2.35

45

Table 2.3.1. (Cont'd.).

$\frac{(1+0.4B^2)\,1-0.2B^2\,\mathrm{sh}\,al-}{-(1-0.4B^2)\,1+0.2B^2\,\sin al}$ $\times \frac{\mathrm{ch}\,al+\cos al}{\mathrm{sh}\,al-\sin al}$ (in the middle of the span of the beam)	5		1.30—1.46	1.37—1.51	1.31—1.65	1.77—2.23	≤2.16	— ²
	20		1.20—1.31	1.24—1.35	1.35—1.46	1.56—2.00	≤1.87	— ²
$\dfrac{0.985\left(1+\dfrac{N}{N^\circ_{\mathrm{кр}}}\right)}{3(z-\mathrm{th}\,z)}+\dfrac{N}{N^\circ_{\mathrm{кр}}}$	5		1.23—1.37	1.29—1.83	1.13—1.55	1.58—2.18	— 2.60	⩾ 2.50
			1.17—1.27	1.21—1.31	1.31—1.39	1.17—1.75	— 1.66	⩾ 2.00
	20		1.00—1.01	1.01—1.02	1.02—1.03	1.01—1.09	— 1.07	⩾ 1.18
			1.00—1.01	1.00—1.01	1.01—1.03	1.03—1.06	— 1.05	⩾ 1.13
$\dfrac{0.985\left(1-\dfrac{N}{N^\circ_{\mathrm{кр}}}\right)}{3(z+\mathrm{th}\,z)}-\dfrac{N}{N^\circ_{\mathrm{кр}}}$	5		1.41—1.71	1.52—1.88	1.84—2.18	2.58—5.51	— 4.11	— ³
			1.89—3.04	2.26—3.82	3.82 8.08	— ³	— ³	— ³
	20		1.01—1.03	1.02—1.03	1.03—1.05	1.06—1.14	— 1.11	⩾ 1.31
			1.03—1.05	1.04—1.06	1.06—1.09	1.12—1.26	— 1.20	⩾ 1.63
$1+2.12\beta^2\dfrac{H^2}{R^2}$	$\dfrac{R}{2H}=5$		1.17—1.28	1.21—1.32	1.32—1.42	1.53—2.06	— 1.85	⩾ 3.11
	$\dfrac{R}{2H}=20$		1.01—1.02	1.01—1.02	1.02—1.03	1.03—1.07	— 1.05	⩾ 1.13

*[1]With assigned $k_0/E_x = 0.01$ the limiting value $\beta^2 = 57.7$ (limit of applicability of the formula).

*[2]With assigned $K/E_x = 0.01$ the limiting value $\beta^2 = 57.7$ (limit of applicability of the formula).

**[3]Rod loses stability with $N/N^*_{\mathrm{кр}}$ less than that given in the table.

46

Fig. 2.3.5. Diagram of
determination of the
deflection of fixed beam.
KEY: (1) Point of inflec-
tion.
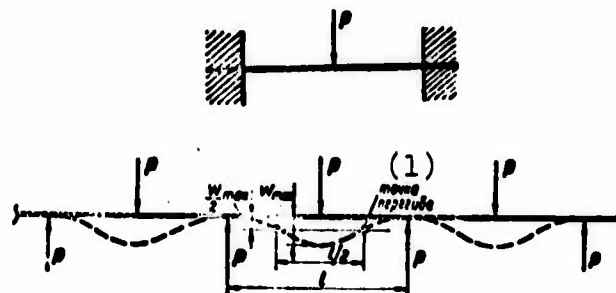
2.3.3. **Experimental estimation.** At fixed value of β, i.e.,
for this material, the value of correction factors which consider
shear depends only on relative height H/l. For the case of load-
ing by concentrated force halfway along the span this dependence,
constructed from parameter $2H/l$, is shown on Fig. 2.3.6 (axis of
abscissa - solution without
allowing for shears). For
the isotropic materials,
which have $\beta < \sqrt{3}$, the effect
of shears on deflection of
even short beams is
insignificant. For oriented
glass fiber-reinforced
plastics the values of β lie
within 3-8, consequently,
during the calculation of
beams made of this material
for rigidity the account of
shears is necessary for all
practically important design
concepts. Shears during

Fig. 2.3.6. The effect of rela-
tive height $2H/l$ and the degree
of anisotropy β on deflection
from shear $-\cdot-\cdot-$ $dw/dx = 0$
when $x = 0$, $x = l$;
$- - - \frac{\partial u}{\partial z}\big|_{z=0} = 0$ when $x = 0$, $x =$
$= l$.

the calculation of beams from boron-epoxy plastics, for which β
reaches 10, play an even larger role. Figure 2.3.6 also gives
the results of experiments on unidirectional glass fiber-reinforced
plastics AG-4S ($\beta = 4.8$), 27-63S ($\beta = 3.5$) and glass laminate
ST on epoxy bonding agent ($\beta = 4.0$) [222]. The theoretical and
experimental curves have identical character (see also [149,
256, 275, 300]).

47

Fixed beams and cantilevers [220] of **unidirectional glass** fiber-reinforced plastics 27-63S and glass laminate EF 32-301 with different **packing of the reinforcing layers (for example,** by packing 1:3 it is implied that the ratio of the number of layers, packed basically along the axis of the beam, to the number of layers packed with weft along this axis is equal to 1:3) are experimentally investigated. The characteristics of materials and samples are given in Table 2.3.2; Young's modulus E_x and shear modulus G_{xz} were determined on the same samples by the methods described below. The results of tests are given on Figs. 2.3.2, 2.3.3. They confirm the conclusion made in § 2.3.2 about the substantial effect of shear strain on the deflection of beams with both ends restrained and about the negligible effect of shears on the deflection of cantilever beams.

Table 2.3.2. The characteristics of samples and materials of beams.

Material	Packing of reinforcement	Quantity of samples	$b \times 2H$, mm	$E_x (\cdot 10^6)$, kgf/cm^2	$G_{xz} (\cdot 10^6)$ kgf/cm^2	β	Designation on Figs. 2.3.2, 2.3.3.
27-63S	1: 0	6	15×19	1.3	0.31	3.7	×
EF 32-301	1: 1	4	15×12	2.1	0.19	3.5	+
The same	1: 3	4	15×12	2.2	0.20	3.3	□
" "	1: 5	4	15×12	2.2	0.27	2.9	◇
" "	1: 10	4	15×12	2.0	0.21	3.1	●
	0: 1	4	15×12	1.8	0.23	2.8	○

The low shear strength forces the reexamination of the procedure for **bending test of materials reinforced by filaments.** ГОСТ 4648-63 [ГОСТ = GOST = All Union State Standard] recommends determining Young's modulus by formula

48

$$E_f = \frac{Pl^3}{48 I w_{max}},$$ (2.3.14)

where w_{max} is the deflection of free beam ($2H/l = 0.1$) under force applied halfway along the span. The Young's modulus determined in this way is ficticious, since it includes also the effect of shears. On the basis of (2.2.38) it is possible to obtain the relationship E_f, E_x and G_{xz}:

$$\frac{1}{E_f} = \frac{1}{E_x} + \frac{1.2}{G_{xz}}\left(\frac{2H}{l}\right)^2.$$ (2.3.15)

The distinction of ficticious module E_f from real E_x is greater, the shorter the tested beam and the higher the degree of anisotropy of materials ($\beta^2 = E_x/G_{xz}$). For the materials reinforced with filaments, as a result of their low shear rigidity the determination of Young's modulus from formula (2.3.14) when testing samples, recommended by GOST 4648-63 ($2H/l = 0.1$), leads to incorrect estimations, which places in doubt the numerous data available in literature on the moduli of oriented glass fiber-reinforced plastics while bending (as shown in [269], the aforesaid is also related to tests of wooden beams, which have $3 \le \beta \le 7$). According to standard ASTM 790-63 [271] the ratio $2H/l$ is brought to 1/16, but in the case of highly anisotropic materials this does not guarantee freedom from systematic error (Fig. 2.3.7, borrowed from [275]).

Thus, bending tests must be conducted only on very long beams; during the examination of results obtained on short beams it is
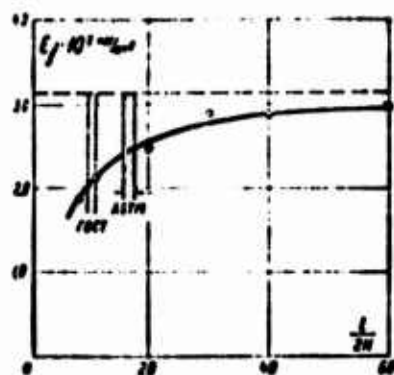

Fig. 2.3.7. The error of determination of Young's modulus of oriented glass fiber-reinforced plastics by formula (2.3.14). - - - pure bending. Designation: кгс/мм^2 = = kgf/mm^2.

49

necessary to consider shear. This is possible if we test samples
with different $2H/l$. Dependence (2.3.15) in coordinates $(2H/l)^2$,
$1/E_f$ has the form of a straight line, the slope angle tangent
to the horizontal axis of which is equal to $1.2/G_{xz}$; this straight
line intersects the axis of ordinates at point $1/E_x$. Having
a number of values of E_f, found for this material at different
ratios $2H/l$, this straight line can be constructed experimentally.
The examined approach reveals the possibility not only of determin-
ing E_x, but also indirectly determining the value of G_{xz} - modulus,
determination of which from direct experiments is quite difficult.
An example of the construction of dependence (2.3.15) is given
on Fig. 2.3.8. On this figure are plotted the results of testing
beams of glass laminate EF 32-301. The straight line is drawn
with the aid of the least squares method.

Fig. 2.3.8. The determina-
tion of moduli E_x and G_{xz}
by bending tests.
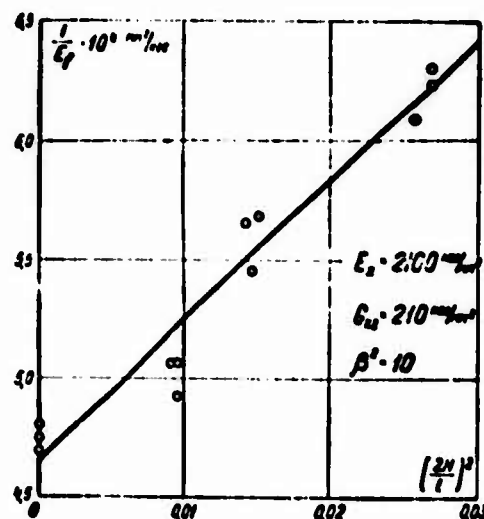
2.3.4. **The effect of the length of the ends, which protrude
beyond supports, on deflection.** The precise support of a beam
by its ends is virtually impracticable. When determining
deflection under force P, applied halfway along the span, there
is actually measured the value of $f = w_2 - w_1$, which represents
the difference between deflections at points 2 and 1 of a beam with
length $L = l + 2l_1$ loaded by forces $P = P/2$ (Fig. 2.3.9). For

50
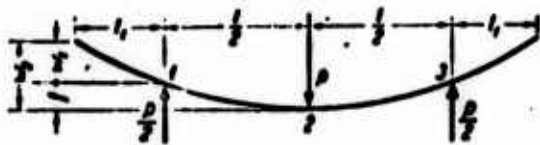
Fig. 2.3.9. The calculation diagram to evaluate the effect of ends of the beam, which protrude beyond supports.

the loading diagram in question on the basis of (2.2.38) taking into account free ends [217] the expression for deflection can be written in the form

$$f\left(\frac{L}{l}\right) = \frac{8P\varkappa^2 l^3}{3\pi^5 E_x J} \sum_{m=1,3,5,\ldots}^{\infty} \frac{\sin^4 m\pi \frac{l}{4l}}{m\left(m\varkappa\frac{l}{L} - \text{th } m\varkappa\frac{l}{L}\right)}. \tag{2.3.16}$$

If in formula (2.3.16) we perform the approximate replacement of

$$\frac{m^3\varkappa^3 l^3}{3L^3\left(m\varkappa\frac{l}{L} - \text{th } m\varkappa\frac{l}{L}\right)} \approx 1 + 0.4 m^2\varkappa^2 \frac{l^3}{L^3}$$

(see Table 2.2.1), then we will obtain the expression for deflection, which does not depend on ratio l/L:

where

$$f = w^*_{max}(S_1 + 0.4\varkappa_m^2 S_2),$$

$$w^*_{max} = \frac{Pl^3}{48E_x J};$$

$$S_1 = \frac{384 L^3}{\pi^4 l^3} \sum_{m=1,3,5,\ldots}^{\infty} \frac{\sin^4 \frac{m\pi l}{4L}}{m^4} = 1;$$

$$S_2 = \frac{384 L}{\pi^4 l} \sum_{m=1,3,5,\ldots}^{\infty} \frac{\sin^4 \frac{m\pi l}{4L}}{m^2} = \frac{12}{\pi^2}.$$

The calculation of the sum of (2.3.16) on a BESM-2 with accuracy to 0.3% showed that at values $\kappa \leq 3$ (this parameter value is limiting for actual constructions from oriented glass fiber-reinforced plastics) the deflection f virtually does not

51

depend on the ratio of the overall length of the beam to its working length L/l:

$$0.99 < \frac{f\left(\frac{L}{l}\right)}{f(1)} < 1 \text{ when } \frac{L}{l} = 1 \div 10;$$

$f(1)$ - deflection for the case where ratio $L/l = 1$.

The effect of ends which protrude beyond supports can be estimated also by the formulas obtained by V. L. Biderman [29] on the basis of the energy method. Expressions for maximum deflection respectively not taking into account and taking into account free ends have the form

$$w_{max} = w^*_{max}(1 + 0.486\varkappa^2 - 0.00697\varkappa^3); \qquad (2.3.17)$$
$$w_{max}' = w^*_{max}(1 + 0.486\varkappa^2 - 0.01032\varkappa^3); \qquad (2.3.18)$$

in these expressions w_{max} - the maximum deflection calculated according to Bernoulli's theory. When $\varkappa \leq 3$ the results calculated by formulas (2.3.17) and (2.3.18) differ by less than 2.2%, i.e., the effect of the projecting ends is negligible (analogous conclusion is also obtained in [148, 251]). At large values of $\varkappa$ formulas (2.3.17), (2.3.18) are inapplicable, since they give the negative values of deflections; from formula (2.3.16) it follows that in limiting case $\varkappa \to \infty$, when the deflection is determined only by shearing strain, it does not depend on the length of the ends projecting beyond supports.

The experimental data, obtained during tests of beams of oriented glass fiber-reinforced plastics, attest to the negligible smallness of the effect of the ends which protrude beyond supports on the deflection. Work [217] gives the results of experiments on three materials: unidirectional glass fiber-reinforced plastics AG-4S, 27-63S and glass laminate on epoxy-phenol

bonding agent. With constant height 2H and working length l the length of free ends l_1 was changed. The results of tests on determination of relative deflection in the center of the beam $f(L/l)/f^*$ depending on L/l and their statistical interpretation are given in Table 2.3.3. Dispersion analysis shows that at the 5% confidence level the results of experiments do not contradict the theoretical conclusion about the independence of deflection f from relationship L/l.

Table 2.3.3.   The effect of the ends of the beam projecting beyond supports on its deflection.

Material and dimensions of cross section	$\frac{l_1 + l + l_1}{l}$, mm	L/l	Quantity of samples	$\frac{f_{min}}{f^*} - \frac{f_{max}}{f^*}$	f_{cp}/f^*	Mean square deviation	Coefficient of variation
Glass laminate 15×17	5+150+ 5	1,07	7	1,126–1,313	1,201	0,0586	4,87
	15+150+15	1,20	7	1,100–1,325	1,223	0,0835	6,82
	25+150+25	1,34	7	1,191–1,313	1,261	0,0495	3,93
	35+150+35	1,47	6	1,131–1,423	1,286	0,1251	9,72
AF-4S 8×11	5+100+ 5	1,10	3	1,313–1,348	1,319	0,0110	3,26
	25+100+25	1,50	5	1,208–1,119	1,286	0,0807	6,27
	80+100+80	2,60	1	1,290–1,160	1,313	0,0792	5,80
27-63S 8×11	5+ 80+ 5	1,12	10	1,031–1,196	1,130	0,0197	4,47
	15+ 80+15	1,38	10	0,901–1,351	1,112	0,1418	12,94
	25+ 80+25	1,62	9	1,023–1,480	1,310	0,1510	11,50
	35+ 80+35	1,88	9	0,972–1,565	1,251	0,7820	14,52

2.3.5. Beams with bent and prestressed reinforcement.

Earlier (§ 1.4) it was shown that the tensioning and bending of the reinforcement mainly affect Young's modulus E_x, barely changing the value of the modulus of interlayer shear G_{xz}. As applied to the problems of bending this means that with tensioning (or bending) of fibers there is changed the component of deflection, caused by normal stresses w_σ, and deflection from shear w_τ remains constant. Consequently, total deflection $w = w_\sigma + w_\tau$ does not vary in proportion to increase or decrease of Young's

53

modulus of material. For example, for the case of a free,
centrally loaded beam the relationship of maximum deflections for
material with loose $w_{max}(0)$ and tightened reinforcement $w_{max}(N)$ is
equal to (see formula (2.3.1)):

$$\frac{w_{max}(0)}{w_{max}(N)} = \frac{E_x(N)}{E_x(0)} \cdot \frac{1 + 1{,}2 \frac{E_x(0)}{G_{xz}} \left(\frac{2H}{l}\right)^2}{1 + 1{,}2 \frac{E_x(N)}{G_{xz}} \left(\frac{2H}{l}\right)^2}. \qquad (2.3.19)$$

As can be seen from this formula and the graph constructed by it
(Fig. 2.3.10), the nonlinearity of function $w(0)/w(N)$ grows with
increase of the relative height of beam H/l and decrease of the
shear rigidity of the material G_{xz}.
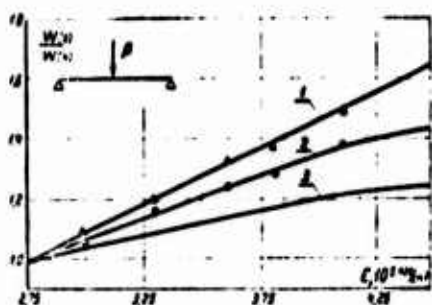
Fig. 2.3.10. Dependence of $\frac{w_{(0)}}{w_N}$ on E_x:
1 – $2H/l$ = 1/20; 2 – $2H/l$ = 1/10; 3 –
$2H/l$ = 1/5 (G_{xz} = 0.14·10^5 kgf/cm^2)

In the case of bent reinforcement on the basis of formulas
(1.3.8) and (1.3.13) we obtain the relationship between the deflec-
tions of beam with straight $w(0)$ and bent reinforcement $w(f_{\sim})$ with
degree of bending $f_{\sim}$:

$$\frac{w(0)}{w(l_{\sim})} = \frac{1 - \dfrac{1{,}2 \left(\frac{2H}{l}\right)^2 \frac{l_{\sim}^2}{2} \beta^1(N)}{1 + 1{,}2 \left(\frac{2H}{l}\right)^2 \beta^2(N)}}{1 - \frac{l_{\sim}^2}{2} \beta^2(N)}. \qquad (2.3.20)$$

The experimental data on the effect of bending and tensioning
of reinforcement on the flexural rigidity are presented in

Table 2.3.4 [72, 100]. They are obtained during tests of unidirectional, laminated and three-dimensional cross-linked materials. The given data attest to the substantial effect of the state of reinforcement on flexural rigidity. The maximum rigidity for unidirectional materials is reached with comparatively small tightening force, which does not exceed 20% of the breaking stress of the strip. The rigidity of woven materials in the investigated range grows continuously with increase of the tightening force of the reinforcement. The last line of Table 2.3.3 and Fig. 2.3.11 characterize the correction from shears with bending; the tensioning of reinforcement substantially increases the correction from shear both for unidirectional (AG-4S) and for orthotropic materials (SKT-11).

Table 2.3.4. The effect of bending and tensioning of reinforcement on flexural rigidity.*

$\frac{2H}{l}$	Relationship of deflections	Unidirectional AG-4S							SKT-11			Three-dimensional cross-linked material		
		prescribed bending of reinforcement, f		straight unstressed reinforcement	Prestressed reinforcement, in portions of strength of material									
		0.157	0.078		0.1	0.2	0.3	0.4	0	0.25	0.5	0	0.25	0.30
$\frac{1}{20}$	$\frac{w}{w_0}$	1.29	1.07	1.00	0.81	0.84	0.86	0.91	1.00	0.815	0.670	1.00	0.855	0.845
$\frac{1}{10}$	$\frac{w}{w_0}$	1.14	1.02	1.00	0.85	0.90	0.92	1.02	1.00	0.885	0.820	1.00	0.860	0.830
	$\frac{w}{w_0}$	1.25	1.33	1.40	1.49	1.50	1.50	1.58	1.29	1.40	1.57	1.07	1.04	1.06

*Data given in the table are obtained according to the results of testing 8-10 samples; $\overline{w}$ is deflection when $2H/l = 1/10$.

Fig. 2.3.11. The effect of shear on deflection: 1 - prestressed fibers (β = 5.31); 2 - straightened fibers (β = 5.05); 3 - fibers with technological bending (β = = 4.32).
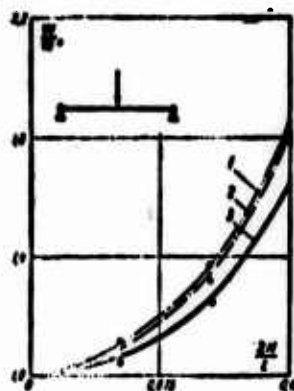
Thus, small initial bendings lead to a drop of rigidity. The introduction of tensioning of reinforcement increases the flexural rigidity in the classical sense, i.e., decreases w_σ, but simultaneously increases the correction from shear. The presence of bent or, on the contrary, prestressed reinforcement does not qualitatively change the picture of deformation of rods made of materials reinforced by filaments, and does not diminish the need for the account of shear effect with bending.

2.3.6. Beams on elastic support. With the presence of elastic support its reaction can be treated as a supplementary transverse load, proportional to deflection (bed coefficient k_0). The total transverse load is equal to $q - k_0 w$, and differential equations of bending (2.2.13), (2.2.14) take the form [225]:

$$\frac{\partial^2 u}{\partial x^2} + \frac{1}{\beta^2} \cdot \frac{\partial^2 u}{\partial z^2} = 0;$$

$$2H\frac{d^2 w}{dx^2} + \int_{-H}^{H} \frac{\partial^2 u}{\partial x \partial z}\, dz = -\frac{q - k_0 w}{G_{xz}}. \qquad (2.3.21)$$

Deflection of the free beam under sinusoidal load $q = q_m \sin \lambda_m x$ ($\lambda_m = \frac{m\pi}{l}$; m is whole number)

$$w_m = \frac{\omega^\bullet_m}{q_m + \frac{k_0}{\lambda_m E_x I}}; \qquad (2.3.22)$$

56

$$w_m^* = \frac{q_m}{\lambda_m^4 E_x I}$$ - deflection of the beam not allowing for shears

and elastic support.

By introducing shears by Timoshenko's diagram, with the presence of elastic support instead of equation (2.2.7) we obtain

$$\frac{d^4\omega}{dx^4} - \frac{Kk_0}{FG_{xz}} \cdot \frac{d^2\omega}{dx^2} + \frac{k_0\omega}{E_x I} = \frac{q}{E_x I} - \frac{K}{FG_{xz}} \cdot \frac{d^2q}{dx^2}. \qquad (2.3.23)$$

For a beam of rectangular cross section, when $F = 2H$, $I = \frac{2}{3}H^3$, $K = 1.2$, equation (2.3.23) assumes the form

$$\frac{d^4\omega}{dx^4} - 0.8B^2 a_0^2 \frac{d^2\omega}{dx^2} + 4a_0^2\omega = \frac{q}{E_x I} - \frac{0.2B^2}{a_0^2 E_x I} \cdot \frac{d^2q}{dx^2}, \qquad (2.3.24)$$

where $\alpha_0 = \frac{k_0}{4E_x I}$; $B = \bar{2}\alpha_0 \beta H$ (this equation is used in the work of V. I. Korolev [112]).

For two of the most widespread particular cases of loading (evenly distributed load and concentrated force applied halfway along the span) the expressions for deflection halfway along the beams are given in Table 2.3.5. The graphs constructed according to the formulas in this table are shown on Figs. 2.3.12 and 2.3.13. The results obtained from Timoshenko's diagram are close to results obtained by (2.3.22); for the case of evenly distributed load this difference <2% when L > 0.6 and <5% when L < 0.6; for the case of concentrated force the difference <10% when B/L < 8 and <5% when B/L < 4. In this case of sinusoidal load the solution of equation (2.3.24) leads to (2.3.22), where ϕ_m is replaced by its approximate value $\frac{1}{1+0.4\kappa_m}$ (see Table 2.2.1).

As can be seen from Fig. 2.3.12, on which the relationships of deflections calculated taking into account (w) and without taking into account (w*) shear are shown, the effect of this factor is substantial for all beams loaded by concentrated force,

57

Table 2.3.5. Deflection of a beam on elastic support (in the middle of the span).

	Beam of finite length	Infinitely long beam
Infinitely long beam		

According to formula (2.3.22)

$$-\frac{q}{k_0}\cdot\frac{4\beta^4}{\pi}\sum_{m=1,3,5,\ldots}^{\infty}(-1)^{\frac{m-1}{2}}\cdot\frac{1}{m(3\pi^2x^2-3m\pi\,\mathrm{th}\,m\pi x+\beta^4)}$$

Infinitely long beam: $-\dfrac{q}{k_0}$

Beam of finite length:
$$-\frac{P a_0}{2k_0}\cdot\frac{1|\sqrt{2}}{\pi}\cdot\frac{\beta^4}{L}\sum_{m=1,3,5,\ldots}^{\infty}\frac{1}{3m^2x^2-3m\pi\,\mathrm{th}\,m\pi x+\beta^4}$$

Infinitely long beam:
$$-\frac{P a_0}{k_0}\cdot\frac{1|\sqrt{2}}{\pi}\cdot\beta^4\times\int_0^{\infty}\frac{d(m\pi x)}{3m^2x^2-3m\pi\,\mathrm{th}\,m\pi x+\beta^4}$$

When $G_{33}\to\infty$

$$-\frac{q}{k_0}\cdot\frac{4}{\pi}\sum_{m=1,3,5,\ldots}^{\infty}(-1)^{\frac{m-1}{2}}\cdot\frac{1}{2}\cdot\frac{L^4}{m^4+4^4}$$

Infinitely long beam: $-\dfrac{q}{k_0}$

Beam of finite length:
$$-\frac{P a_0}{2k_0}\cdot\frac{4|\sqrt{2}}{\pi}\sum_{m=1,3,5,\ldots}^{\infty}\frac{L^4}{m^4+L^4}$$

Infinitely long beam: $-\dfrac{P a_0}{2k_0}$

According to Timoshenko's diagram

$$-\frac{q}{k_0}\left[1-\frac{2\left(\mathrm{ch}\frac{\alpha l}{2}\cos\frac{cl}{2}-\frac{0.2B^4}{1-0.04B^4}\,\mathrm{sh}\frac{\alpha l}{2}\sin\frac{cl}{2}\right)}{\mathrm{ch}\,\alpha l+\cos cl}\right]$$

Infinitely long beam: $-\dfrac{q}{k_0}$

Beam of finite length:
$$\frac{P a_0}{2k_0}\cdot\frac{(1+0.4B^3)(1-0.2B^4)\,\mathrm{ch}\,\alpha l-(1-0.4B^4)(1+0.2B^4)\sin cl}{(1-0.04B^4)(\mathrm{ch}\,\alpha l+\cos cl)}$$

Infinitely long beam: $\dfrac{P a_0}{2k_0}\cdot\dfrac{1+0.4B^4}{\sqrt{1+0.2B^4}}$

When $G_{33}\to\infty$

$$-\frac{q}{k}\left(1-\frac{2\,\mathrm{ch}\frac{\alpha_0 l}{2}\cos\frac{\alpha_0 l}{2}}{\mathrm{ch}\,\alpha_0 l+\cos\alpha_0 l}\right)$$

Infinitely long beam: $-\dfrac{q}{k_0}$

Beam of finite length:
$$-\frac{P a_0}{2k_0}\cdot\frac{\mathrm{ch}\,\alpha_0 l-\sin\alpha_0 l}{\mathrm{ch}\,\alpha_0 l+\cos\alpha_0 l}$$

Infinitely long beam: $-\dfrac{P a_0}{2k_0}$

In the table $a=a_0\sqrt[4]{1+0.2B^4}$; $c=a_0\sqrt[4]{1-0.2B^4}$; $a_0^4=\dfrac{k_0}{4E_xI}$; $B=\sqrt[4]{2a_0\beta H}$.

58

Fig. 2.3.12. The effect of shears on deflection. a) evenly distributed load; b) concentrated force half-way along the span $L = \sqrt{2}\,\dfrac{l\alpha_0}{\pi}$.
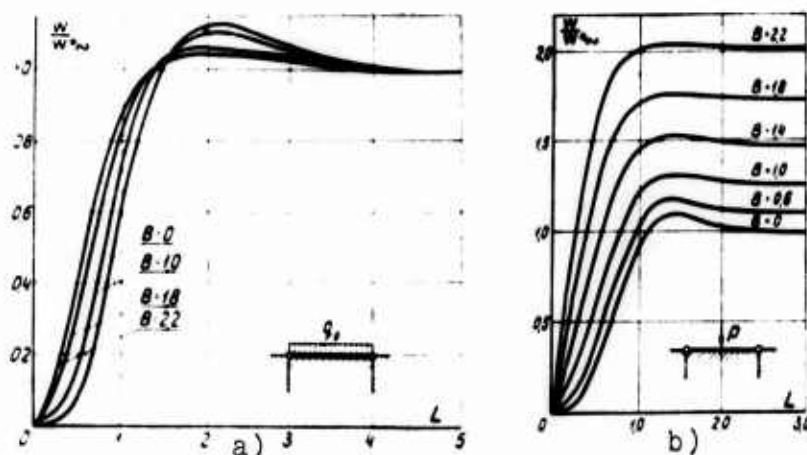
Fig. 2.3.13. The effect of the length of beam on deflection. a) evenly distributed load; b) concentrated force halfway along the span, w_{∞}^{*} - deflection in the center of infinitely long beam.

and also for short beams under evenly distributed load. The dependence of deflection in the middle of the beam, referred to deflection of infinitely long beam, on the reduced length at different values of reduced height is depicted on Fig. 2.3.13. For the majority of the values of parameter B the beams can be

considered virtually infinitely long, if reduced length L > 3.

The need for the account of shears during bending of the beam on elastic support appears, for example, during the calculation of short fixed shells [120], the receptacles of electrical machines on plastic housings [210, 250] and in a number of other problems. The restraint of lams (Fig. 2.3.14a, b) is a cantilever beam-strip on an elastic base with elastic support in the span. The refined solution of the problem taking shears into account in this case made it possible to decrease the dimensions of the supporting section, and the account of shears led to lowering of the moment in the supporting section by 20-25%.
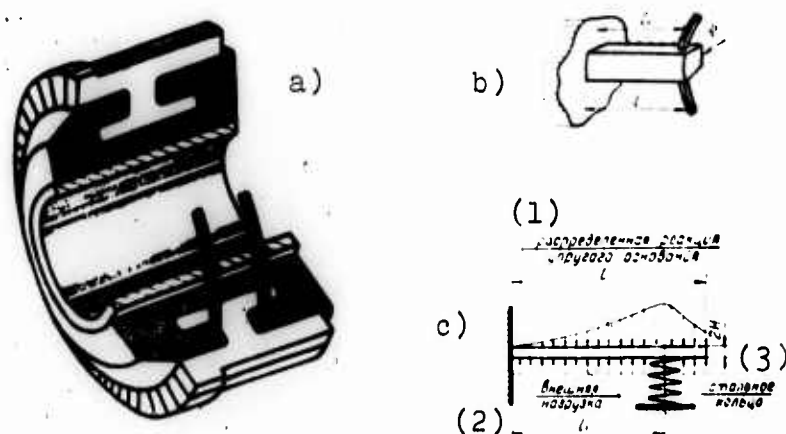
Fig. 2.3.14. The restraint of lams of receptacle in plastic housing. a) cutaway of receptacle; b) reinforced ring projection; c) calculation diagram.
KEY: (1) Distributed reaction of elastic support;
(2) External load; (3) Steel ring.

2.3.7. **The effect of shears on the extent of the edge effect for cylindrical shells.** Cylindrical shell (see, for example, [239]) can be represented as a system of strips, isolated from one another by planes passing through the axis of the cylinder. In the case of axisymmetric deformation each strip is under the same conditions as a beam on an elastic support with bed coefficient $k_0 = \frac{2HE}{R}$, where 2H and R are the thickness and

60

radius of the shell, and E_θ - Young's modulus in circular direction. In this case the flexural rigidity of the strip

$$D = \frac{2H^3 E_x}{3(1-\nu_{\theta x}\nu_{x\theta})}$$ (E_x = Young's modulus in axial direction; $\nu_{\theta x}$, $\nu_{x\theta}$ - corresponding Poisson ratios). Thus, results obtained in the examination of beams on an elastic support can be used during the study of cylindrical axisymmetrically loaded shells, in particular for determining the zones of edge effect. In this case by the zone of edge effect there is meant the area in which the heterogeneity of the stressed state, i.e., the phenomena of bending, cannot be disregarded. The deflection of the shell under uniform pressure q near the restraint of edges is changed wavelike with decreasing wave amplitude, approaching value $w_\infty = q_0/k_0$ (Fig. 2.3.15). Bending stresses (normal σ_x and tangential τ_{xz}) analogously attenuate.

It is accepted to estimate the extent of the zone of edge effect depending on the prescribed accuracy according to coordinate $x = s_0$ (Fig. 2.3.15), with which relative bending $\tilde{w} = w - w_\infty$ or bending stresses reverse sign (see, for example, [7, 169, 172]), or at distance s (Fig. 2.3.15), for which with prescribed p-percent accuracy (in [228, 247] five-percent accuracy is accepted) the stressed state of shells can be considered moment-less. The expression for estimating the zone of edge effect for elastic orthotropic axisymmetrically loaded cylindrical shells, obtained on the basis of
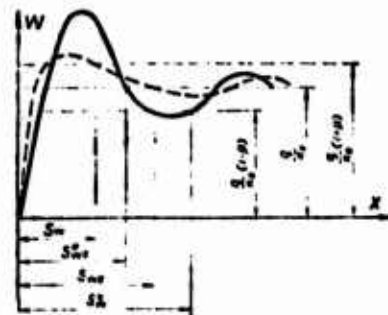

Fig. 2.3.15. Change of the deflection in the zone of edge effect, ——— not allowing for shears; - - - taking into account shears.

the Kirchhoff-Love hypothesis by S. A. Ambartsumyan, has the form

$$s^* = \frac{c\sqrt{2RH}}{\sqrt[4]{\frac{3E_\theta}{E_x}(1-\nu_{x\theta}\nu_{\theta x})}};$$

(2.3.25)

61

here 2H is the thickness of shell; R is the radius of shell; E_x, E_θ are elastic moduli in axial and circular directions; $\nu_{x\theta}$, $\nu_{\theta x}$ - Poisson ratios (first index shows the direction of transverse contraction, the second - the direction of force); c is a constant which depends on the prescribed accuracy of estimation of the extent of the zone of edge effect (with first approach $c = \pi$, when evaluating with five-percent accuracy $c = 3.33$).

The effect of shears on the extent of the zone of edge effect is investigated in detail in [228],[1] in which equation (2.3.24) is used. The estimation is accomplished on deflections and tangential stresses. More exact determination of the zone of propagation of tangential stresses is necessary for establishment of the length of the section of strengthening and the "winding" diagram of the thickened places of shells made of glass fiber-reinforced plastics. As can be seen from Fig. 2.3.16, when evaluating according to coordinate s_{0w} (**according to deflections**) or $s_{0\tau}$ (according to tangential stresses) the account of shear leads to an increase in the zone of edge effect. When evaluating according to distances s_w and s_τ (Fig. 2.3.17) the length of the zone of edge effect, determined taking into account shear, is less than the corresponding length determined with the utilization of hypothesis of straight normals (with the exception of estimation of s_w for the case of free support). In this case, with certain values of B there are observed skips, caused by the accepted accuracy of estimation of the edge effect; the reason for the emergence of skips is clear from Fig. 2.3.18.

---

[1]In [112] it is noted that the low shear rigidity contributes to the damping of edge effects; however, this question in the indicated work was not investigated in detail. The account of shears during the study of the behavior of thick-walled restrained cylinders of glass fiber-reinforced plastics is contained in V. T. Tomashevskiy's works [242, 243]. The error introduced by the hypothesis of straight normals during the calculation of the deflection of shells loaded by ring pressure is estimated by V. V. Vasil'yev [68, 69]. In [169, 172] to evaluate the edge effect during tests of pipes made of glass fiber-reinforced plastics expression (2.3.25) is used.
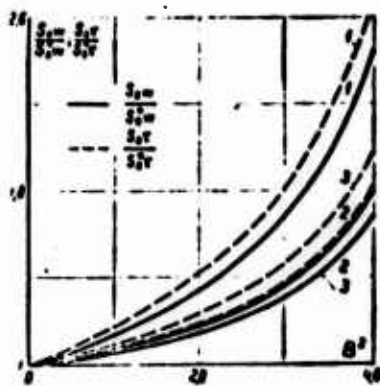
Fig. 2.3.16.   Fig. 2.3.17.

Fig. 2.3.16. The effect of shears on the extent of
the zone of edge effect: 1 - rigid fixing (dw/dx = 0);
2 - pliable fixing ($\partial u/\partial z$ = 0 when z = 0); 3 - hinged
support.
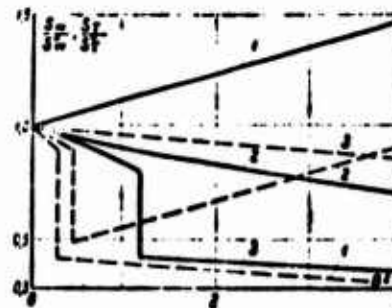
Fig. 2.3.17. The effect of shears on the extent of the
zone of edge effect (p = 0.05): 1 - rigid fixing
(dw/dx = 0); 2 - pliable fixing ($\partial u/\partial z$ = 0 with z = 0);
3 - hinged support, ———— with respect to deflections;
- - - stresses.

Fig. 2.3.18. The zone
boundaries of edge effect
S_1, S_2 and S_3 when
evaluating with prescribed
accuracy (B_1 < B_2 < B_3)
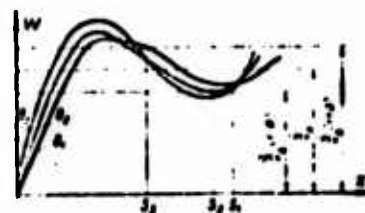
The need for the account of shears is determined by
parameter

$$B^2 = \sqrt{3}\,\frac{H}{R}\sqrt[4]{\frac{E_x E_\theta}{G_{x z}^2(1 - \nu_{x\theta}\nu_{\theta x})}}.$$

and also by the accepted diagram of support and the required
accuracy of estimation of stresses and deformations. Conducted
analysis [228] showed that in the majority of practically interest-
ing cases for estimation of the zone of edge effects it is possible
not to consider shears.

63

§ 2.4. BENDING STRENGTH

2.4.1. The effect of shear on stress distribution. The results obtained in the preceding paragraph attest to the fact that the determination of the deflections of beams of materials, which weakly resist shear, according to the formulas obtained on the basis of the hypothesis of flat sections can lead to inadmissible errors. The error introduced by neglecting the shears during the determination of stresses requires analogous estimation. Taking into account that within the framework of the assumption $\varepsilon_z = 0$, $\sigma_x = E_x \frac{\partial u}{\partial x}$, $\tau_{xz} = G_{xz}\left(\frac{\partial u}{\partial z} + \frac{\partial w}{\partial x}\right)$ (subsequently stresses σ_x and τ_{xz} and moduli E_x and G_{xz} are written without subscripts x and z), on the basis of (2.2.37), (2.2.38) we obtain the following expressions for determining normal σ_m and tangential τ_m stresses in the case of sinusoidal load $q = q_m \sin \lambda_m x$:
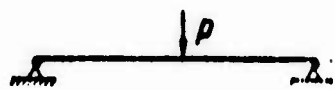
$$\sigma_m = \frac{q_m}{\lambda_m^3 / \varphi_m}\left(\frac{\lambda_m \operatorname{sh} \varkappa_m \frac{z}{H}}{\beta \operatorname{ch} \varkappa_m} \sin \lambda_m x - \frac{2C_m z}{l}\right);$$

$$\tau_m = \frac{q_m}{\beta^2 \lambda_m^3 / \varphi_m}\left(1 - \frac{\operatorname{ch} \varkappa_m \frac{z}{H}}{\operatorname{ch} \varkappa_m}\right)\cos \lambda_m x. \qquad (2.4.1)$$

For the three most widespread load cases the expressions for the stresses in free beams ($C_m = 0$), obtained on the basis of (2.4.1), are given in Table 2.4.1 in conjunction with the formulas derived on the basis of the hypothesis of flat sections. They are the limiting case where $\varkappa_m \to 0$.

The diagrams of normal stresses for the case of a sinusoidal load are presented on Fig. 2.4.1. As is evident, the deviation from linearity of the distribution of normal stresses σ is greater, the larger the value of $\varkappa_m = m\varkappa$. With increase of $\varkappa_m$ there is observed an increase in the degree of deviation of the law of distribution of tangential stresses from parabolic (Fig. 2.2.8).

64

Table 2.4.1. Bending stress distribution.

	$q = q_m' \sin m\pi \frac{x}{l}$ (arch load)	$q_0 = const$	P
σ	$\frac{3q'l^2}{2\pi^3/l^2 m^3} \cdot \frac{m^3 x^3}{3(mx - \th\, mx)} \cdot \frac{\sh mx \frac{z}{H}}{\ch mx} \times$ $\times \sin m\pi \frac{x}{l}$	$-\frac{3q_0 l^2}{4H^2} \cdot \frac{8x^2}{3\pi^2} \sum_{m=1,3,5\ldots}^{\infty}$ $\frac{\sin m\pi \frac{x}{l}}{m(mx - \th\, mx)} \cdot \frac{\sh mx \frac{z}{H}}{\ch mx}$	$-\frac{3Pl}{4H^2} \cdot \frac{4x^2}{3\pi^2} \sum_{m=1,3,5\ldots}$ $\frac{(-1)^{\frac{m-1}{2}} \sin m\pi \frac{x}{l}}{mx - \th\, mx} \cdot \frac{\sh mx \frac{z}{H}}{\ch mx}$
τ	$\frac{3q'l}{4\pi H m} \cdot \frac{2mx}{3(mx - \th\, mx)} \times$ $\times \left(1 - \frac{\ch mx \frac{z}{H}}{\ch mx}\right) \cos m\pi \frac{x}{l}$	$-\frac{3q_0 l}{4H} \cdot \frac{8x}{3\pi^2} \sum_{m=1,3,5\ldots}^{\infty}$ $\frac{\cos m\pi \frac{x}{l}}{m(mx - \th\, mx)} \left(1 - \frac{\ch mx \frac{z}{H}}{\ch mx}\right)$	$-\frac{3P}{8H} \cdot \frac{8x}{3\pi} \sum_{m=1,3,5\ldots}$ $\frac{(-1)^{\frac{m-1}{2}} \cos m\pi \frac{x}{l}}{mx - \th\, mx} \left(1 - \frac{\ch mx \frac{z}{H}}{\ch mx}\right)$
σ^*	$\frac{3q'l^2}{2\pi^3/l^2 m^3} \cdot \frac{z}{H} \cdot \sin m\pi \frac{x}{l}$	$-\frac{3q_0 l^2}{4H^2} \cdot \frac{x}{l}\left(1 - \frac{x}{l}\right)\frac{z}{H}$	$\frac{3Pl}{4H^2} \cdot \frac{z}{H} \cdot \frac{x}{l}$
τ^*	$\frac{3q'l}{4\pi H m}\left(1 - \frac{z^2}{H^2}\right)\cos m\pi \frac{x}{l}$	$-\frac{3q_0 l}{8H}\left(1 - 2\frac{x}{l}\right)\left(1 - \frac{z^2}{H^2}\right)$	$\frac{3P}{8H}\left(1 - \frac{z^2}{H^2}\right)$

*Expressions marked with an asterisk correspond to $\kappa \to 0$.
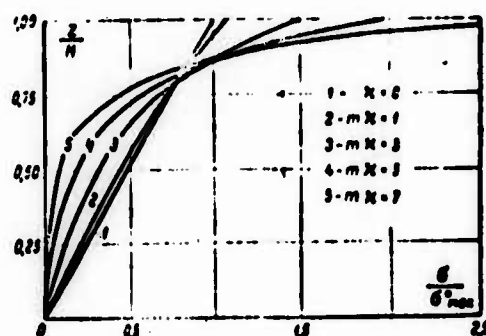
Fig. 2.4.1. The effect of shears on the diagrams of normal bending stresses ($q = q_m \sin \lambda_m x$).

During the investigation of the questions of strength the values of maximum stresses are of the greatest interest. The dependences of relationships $\sigma_{max}/\sigma^*_{max}$ and τ_{max}/τ^*_{max} on parameter κ for the three methods of loading are presented on Fig. 2.4.2. The maximum normal stresses are calculated with $x = 0.5l$ and $z = \pm H$, tangential are calculated with $x = 0$ and $z = 0$. (In

65

the case of concentrated load the corresponding series with
$z = \pm H$, $x = 0.5l$ diverges, therefore σ_{max} and σ^*_{max} of the extreme
fibers are compared with $x = 0.4l$.) As can be seen from the graph
(Fig. 2.4.2), the effect of shear on the maximum amounts of stress
is substantial only with
sufficiently large κ, i.e., for
short beams of essentially
anisotropic materials. For
example, with the permissible
error of calculation 10% for the
examined cases the deviation of
the law of distribution of
normal stresses from   linear
and tangential from parabolic can
be disregarded if $\kappa < 1.2$. This
makes it possible during the
calculation of stresses to use
elementary formulas of the strength
of materials.

Fig. 2.4.2. The effect of
shears on maximum stresses.

The deviations of the distribution of σ from linear law and
τ from parabolic can be judged by the expansions of stresses into
Taylor series according to parameter κ $\left(\kappa < \dfrac{\pi}{2}\right)$:

$$\frac{\sigma}{\sigma^*_{max}} = \frac{z}{H} + \varkappa^2\left(\frac{z^3}{6H^3} - \frac{z}{10H}\right) + \varkappa^4\left(\frac{z^5}{120H^5} - \frac{z^3}{60H^3} + \frac{9z}{1400H}\right) + \ldots; \qquad (2.4.2)$$

$$\frac{\tau}{\tau^*_{max}} = \left(1 - \frac{z^2}{H^2}\right) - \frac{\varkappa^2}{60}\left(1 - \frac{6z^2}{H^2} + \frac{5z^4}{H^4}\right) +$$
$$+ \frac{\varkappa^4}{12600}\left(11 - \frac{81z^2}{H^2} + \frac{105z^4}{H^4} - \frac{35z^6}{H^6}\right) + \ldots;$$

$$\lim_{x \to \infty} \tau = \begin{cases} \dfrac{Q}{2H} & \text{при } -H < z < H; \\ 0 & \text{при } z = \pm H; \end{cases}$$

$$\lim_{x \to \infty} \sigma = \begin{cases} 0 & \text{при } -H < z < H; \\ \infty & \text{при } z = \pm H. \end{cases}$$

[при = when]

66

For maximum stresses

$$\frac{\sigma_{max}}{\sigma'_{max}} = 1 + \frac{1}{15}\varkappa^2 - \frac{1}{525}\varkappa^4 + \dots;$$

$$\frac{\tau_{max}}{\tau'_{max}} = 1 - \frac{1}{60}\varkappa^2 + \frac{11}{12600}\varkappa^4 - \dots$$

(2.4.3)

By comparing series (2.4.3) with the appropriate series for deflection (2.3.4), we see that the effect of shears on stress is substantially less than for deflection.

Near the ends of the beam the stress distribution can noticeably differ from the classical, obtained on the basis of the hypothesis of flat sections. At these places there are observed the greatest differences in the results obtained during the application of different theories, which consider shear. For example, according to the formula given in S. G. Lekhnitskiy's work [123] the stresses in a free evenly loaded beam are defined as

$$\sigma_2 = -\frac{3q_0 l}{4H^2}\left[\frac{x}{l}\left(1 - \frac{x}{l}\right)\frac{z}{H} + 0.00676\varkappa^2\left(\frac{5z^3}{H^3} - \frac{3z}{H}\right)\right];$$

(2.4.4)

$$\tau_2 = -\frac{3q_0 l}{4H}\left(1 - \frac{2x}{l}\right)\left(1 - \frac{z^2}{H^2}\right).$$

The stress diagrams, calculated by (2.4.4) and corresponding to formulas in Table 2.4.1, are given on Fig. 2.4.3. As is evident, near the supports appears noticeable divergence of diagrams, which is the result of the fact that formulas (2.4.4) are derived under the condition of the integral satisfaction of the boundary conditions ($\sigma = 0$) on the ends of the beam.

The addend of expression (2.4.4) is stress σ^*, determined by Bernoulli's elementary bending theory. The augend σ^{**} – the corrective correction, which does not depend on coordinate x and

67
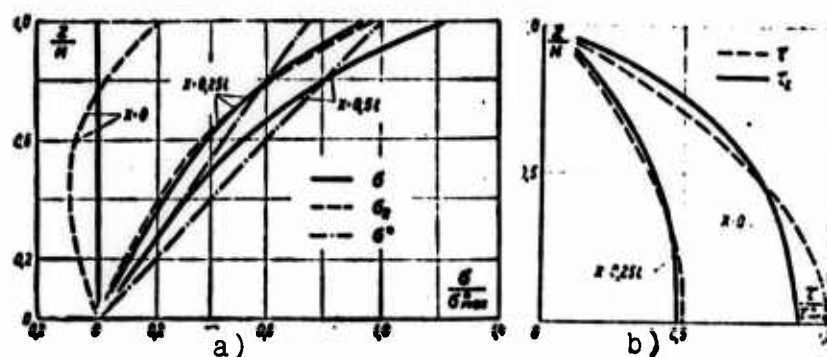
Fig. 2.4.3. Diagrams of normal (a) and
tangential (b) stresses in the sections of
evenly loaded beams. - - - κ = 2; ———— κ =
= 0.

therefore does not disappear on the ends (with x = 0 $\sigma^{**} = \sigma_2$).
Relation

$$\frac{\sigma^{**}_{max}}{\sigma^*_{max}} = 0.0541 \varkappa^2, \qquad (2.4.5)$$

characterizing discrepancy with boundary conditions σ = 0 when
x = 0, is increased with an increase of parameter κ. It is small
for isotropic beams, which have $\beta^2 \leq 3$, but it becomes substantial
for beams of highly anisotropic materials, when as a result
of large β parameter κ is great even for long beams.

2.4.2. **Expansion of the area of failure from shear.** With
bending of rods of isotropic materials the relationship of the
maximum tangential τ_{max} and normal stresses σ_{max} is of order
$2H/l$, and strengths with respect to normal Π_σ and tangential Π_τ
stresses are close to one another (see, for example, [247]).
Therefore, the calculation, as a rule, is performed by normal
stresses. For the materials in question Π_σ and Π_τ differ by
an order and more (experimental data are given earlier in
Table 1.1.1). Due to the low shear strength of material the
tangential stresses, in spite of their relative smallness, can
substantially affect the strength and character of bending fracture
[92, 274]).

68

The maximum normal and tangential stresses increase in proportion to the growth of load.[1] In axes σ_{max}-τ_{max} (Fig. 2.4.4) the course of loading is described by a ray, outgoing from the origin of coordinates. One ought to emphasize that this ray does not depict the path of loading in the usual sense of theories of strength and plasticity, since σ_{max} and τ_{max} are reached at different points of the beam (σ_{max} when $z = \pm H$, τ_{max} when $z = 0$).

The slope of the ray depends on the type of effective load, relationship $2H/l$ and parameter β. On Fig. 2.4.4 rays are constructed for three types of loading with $2H/l = 0.2$

Fig. 2.4.4. The diagrams of the growth of maximum normal and tangential stresses with an increase in the load. $\Pi \equiv \Pi_\sigma$, $T \equiv \Pi_\tau$.

and 0.05 for materials with infinite shear rigidity ($\beta = 0$) and materials of the oriented glass fiber-reinforced plastics type ($\beta = 4$). The effect of parameters β on the slope of the ray for small $2H/l$ is insignificant: with $2H/l = 0.05$ the rays for $\beta = 0$ and $\beta = 4$ virtually coincide, since in this case $\kappa < 0.5$ and, as can be seen from Fig. 2.4.2, at such values of κ the correction introduced by taking into account shear is negligible.

The disposition of limiting straight lines Π_σ and Π_τ, known for this material, on the graph (Fig. 2.2.4) makes it possible to judge the expected form of failure. In the case depicted on Fig. 2.4.4 there is expected the failure of beams with $2H/l = 0.2$, loaded by transverse load $q = q' \sin \pi\frac{x}{l}$ and $q_0 = $ const, from
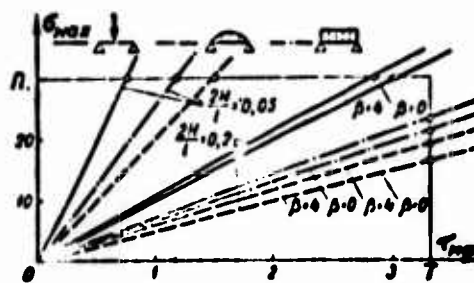
_____

[1]This is confirmed for glass fiber-reinforced plastics if we disregard some nonlinearity of deformation diagrams.

shear, since the four lower rays corresponding to these types of loadings intersect boundary Π_τ.

For isotropic material Π_σ and Π_τ - values of one order. Consequently, the boundary of failure with respect to tangential stresses is moved far to the right and failure from shear is virtually impossible. For oriented glass fiber-reinforced plastics $\Pi_\tau/\Pi_\sigma = 0.05$-$0.10$ (see Table 1.1.1), and rather long beams can be destroyed from shear, therefore experimental research on this phenomenon acquires practical interest. Research on the failure from shear when bending a beam of reinforced plastics under conditions of elevated temperatures has special importance. The strength of polymer bonding agent is substantially lowered with rise of temperature. It is obvious that an increase of testing temperature expands the area of failure of glass fiber-reinforced plastics from shear when bending.

2.4.3. The effect of ends, which protrude beyond supports, on the bending strength. In § 2.3.3 it was shown that the effect of ends, protruding beyond supports, on deflection is insignificant. The effect of ends on strength is investigated on the samples of three different materials. The results of the test are given in Table 2.4.2. Dispersion analysis shows that the obtained results at the 5% confidence level do not contradict the assumption about the independence of breaking load from the length of the ends, which protrude beyond the support. However this question, especially in the case where the length of the ends, which protrude beyond the support, is comparatively small, needs further study.

2.4.4. Experimental study. The effect of relationships $2H/l$ and Π_τ/Π_σ on the type of bending failure is studied on three series domestic glass fiber-reinforced plastics - AG-4S, 27-63S and EF32-301 [217] with different packing of filaments in two mutually perpendicular directions. The relationship of the

70

Table 2.4.2. The effect of the ends of the beam projecting beyond the support on the bending strength.

Material	$b \times 2H$, mm	l, mm	l_1, mm	Breaking load, kgf	Coefficient of variation
27-63S 1:3	10×12	50	10 30 90	710 779 678	5.6 6.2 4.1
		100	10 70	550 517	4.1 6.3
27-63S 1:0	10×19.4	100	10 40 100	1501 1515 1570	2.7 5.6 2.3
		180	10 50	955 945	0.5 0.7
AG-4S 1:1	10×17.4	50	10 30 90	713 717 655	7.0 6.5 1.1
		100	10 70	492 460	8.1 8.6

number of longitudinal and transverse layers for the tested materials is shown in Table 2.4.3. The samples are tested by the scheme of a free beam loaded halfway along the span by concentrated force P. The speed of movement of the punch 10 mm/min. Figure 2.4.5 gives the characteristic oscillogram with the recording of force P and the displacement under force w.

The results of tests are given in Table 2.4.3. All the samples, with the exception of those shown in the last part of the table, were bent in the plane perpendicular to the layers. In the table above the line are given the values of the greatest normal stresses in kg/mm^2, calculated by formula $\sigma_{max} = \dfrac{3Pl}{8bH^2}$ (P corresponds to point D on Fig. 2.4.5). Alongside in parentheses are given the normal stresses, which correspond to the origin of failure (point C on Fig. 2.4.5). Under the line are given the

71

Table 2.4.3. Experimental data on the bending strength.

Material of sample (packing)	Distance between supports, mm							
	50		100		150		200	
AG-4S								
1:5	17.9(17.9)/1.74	c 4.4	25.8(22.8)/1.29	·H 6.6	21.5(23.4)/0.84	H 4.4	21.2(21.2)/0.60	H 6.4
1:3	21.8(21.8)/2.18	c 4.7	26.3(25.4)/1.31	H 3.3	26.1(22.2)/0.84	H 4.0	25.8(25.8)/0.64	H 1.0
1:1	21.0(21.0)/2.05	c 6.1	29.1(21.4)/1.5	c 9.7	31.3(29.5)/1.03	H 9.8	31.6(30.9)/0.81	H 7.5
3:1	25.1(25.1)/2.43	c 9.7	40.4(40.1)/1.94	H—c 5.6	41.7(40.9)/1.38	H 2.9	45.0(45.0)/1.12	H 3.4
5:1	22.5(22.5)/2.19	c 7.9	35.0(35.0)/1.70	c 2.6	43.0(43.0)/1.43	H. 7.2	49.4(49.4)/1.18	H 1.0
10:1	25.4(25.4)/2.63	c 5.8	40.8(40.8)/2.13	c 1.9	53.4((17.5)/1.75	H—c 9.9	51.3(49.2)/1.38	H 3.2
27-63S								
1:3	28.6(28.6)/2.83	c 9.9	31.6(31.6)/1.63	c-H 4.5	32.5(30.3)/1.12	H 2.2	29.3(29.3)/0.76	H 3.3
1:1	46.3(46.3)/4.53	c 8.2	63.8(50.8)/3.10	c 4.7	60.3(60.3)/1.99	H 5.8	59.7(54.5)/1.43	H 3.2
3:1	43.2(43.2)/4.24	c 10.1	71.3(71.3)/3.55	c 2.7	70.0(70.0)/2.38	H—c 2.5	69.3(62.8)/1.73	H 10.4
5:1	47.8(47.8)/5.28	c 4.2	75.7(75.7)/4.15	c 3.8	75.4(75.4)/2.80	c 0.5	84.0(84.0)/2.66	H 5.3
10:1	58.3(58.3)/6.30	c 2.3	64.4(55.4))/3.26	H—c 8.3	64.6(64.6)/2.38	H 7.2	69.5(68.2)/1.95	H 6.2
EF32-301								
1:0	34.7(34.7)/4.15	c 2.4	35.2(33.8)/2.10	H 4.2	35.1(31.9)/1.37	H 3.0	35.5(35.5)/1.06	H 3.5
1:10	28.5(28.5)/3.50	c 2.3	36.1(34.2)/2.21	H 4.7	34.8(33.4)/1.44	H 4.7	37.2(37.2)/1.14	H 3.5
1:3	31.6(31.6)/3.85	c 3.6	37.4(34.0)/2.27	H 3.1	36.0(33.2)/1.47	H 3.6	37.5(36.1)/1.14	H 1.7
1:5	38.5(36.5)/4.69	c 2.3	40.7(35.6)/2.47	H 1.9	38.8(36.1)/1.57	H 5.3	39.7(39.7)/1.21	H 3.1

Table 2.4.3. (Cont'd.).

Bending in the plane of layers

AG-4S 1:1	31.7(30.7) 3.04	н 4.2	30.8(3..) 1.54	н 2.1	33.3(2..2) 1.75	н 3.8	31.5(31.2) 0.74	н 1.6
AG-4S 3:1	43.8(23.5) 4.36	н-с 0.2	46.1(46.1) 2.50	н 1.9	45.8(43.3) 1.58	н 1.2	42.8(42.8) 1.07	н 1.6
27-63S 3:1	61.2(62.2) 6.30	н-с 7.7	66.5(62.4) 3.32	н 2.8	63.3(60.5) 2.17	н 8.9	69.7(67.5) 1.74	н 6.2

Note: c - destruction occurred as a result of shear along a plane, close to neutral; н - material failed from normal stresses.

Fig. 2.4.5. Characteristic oscillogram during bending test.
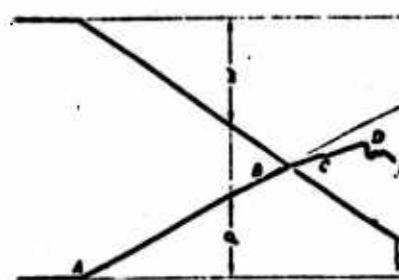
values of the greatest tangential stresses (in kg/mm^2), calculated by formula $\tau_{max} = \frac{3P}{8bH}$. To the right of these values is given the coefficient of variation (in %), letters "c" and "н" designate the form of fracture.

As can be seen from Table 2.4.3, the range of failure from shear encompasses the area of relationships $\frac{2H}{l} = \frac{1}{5} - \frac{1}{15}$. Only when $\frac{2H}{l} = \frac{1}{20}$ are all samples destroyed by normal stresses. The characteristic types of failure are shown on Fig. 2.4.6. Failure from shear occurs approximately at the level of neutral line, as a rule, along the plane of the joint between layers (Fig. 2.4.6a). Sometimes it occurs virtually simultaneously along all joint planes between layers (Fig. 2.4.6b). With bending in the plane of layers the tangential stresses do not act along joint surfaces, therefore these samples even with large relationship

73

$\frac{2H}{l}$ do not fail from shear (Fig. 2.4.6c). Failure from normal stresses (Fig. 2.4.6d) for materials AG-4S and 27-63S, as a rule, is observed in the stretched zone, and for material EF32-301 in the compressed zone.
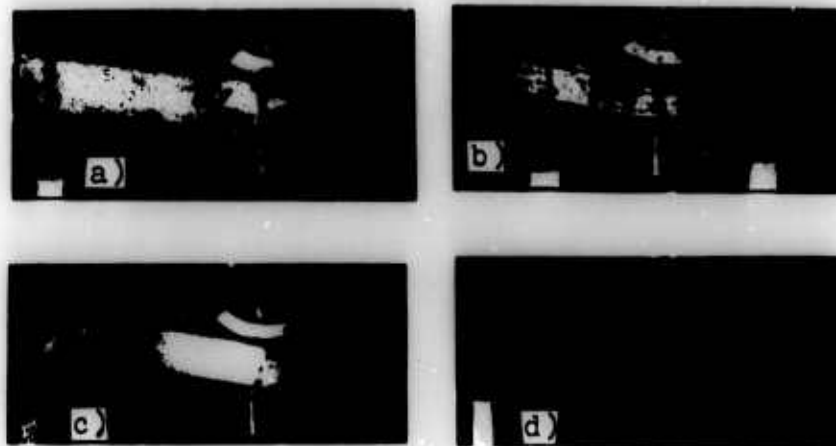
Fig. 2.4.6. The characteristic types of bending failure: a) EF-32-301; b-d) 27-63S.

For illustration of the effect of the ratio of the height of the beam to the span and the arrangement of layers of reinforcement in the material to the character of failure Fig. 2.4.7 depicts the results obtained during the test of inspection materials (see Table 2.4.3); the light points correspond to failure from normal stresses, dark from tangential stresses. As can be seen from the figure, transition from one type of failure to another occurs with relationship $\frac{2H}{l}$, characteristic for this material. Sufficiently long beams fail when σ_{max} reaches the boundaries $\Pi_\sigma \sim$ const. Figure 2.4.7 and Table 2.4.3 show that with bending, as also with stretching, the ultimate strength Π_σ virtually linearly increases with increase of the number of filaments, packed in the direction of the effective forces. With failure from shear constancy of Π_τ is not observed - it is increased with increase of relationship $\frac{2H}{l}$. The analogous conclusion follows from the results of [274] (Fig. 2.4.8). This can be partially explained by the local failures of separate glass fibers before the total loss of supporting

power, since large normal stresses correspond to smaller values of $\frac{2H}{l}$. It is possible to consider this phenomenon formally when using a diagram of the type of Fig. 2.4.4, if instead of vertical boundary Π_τ we constructed the curve which corresponds to the test results.

a)

b)

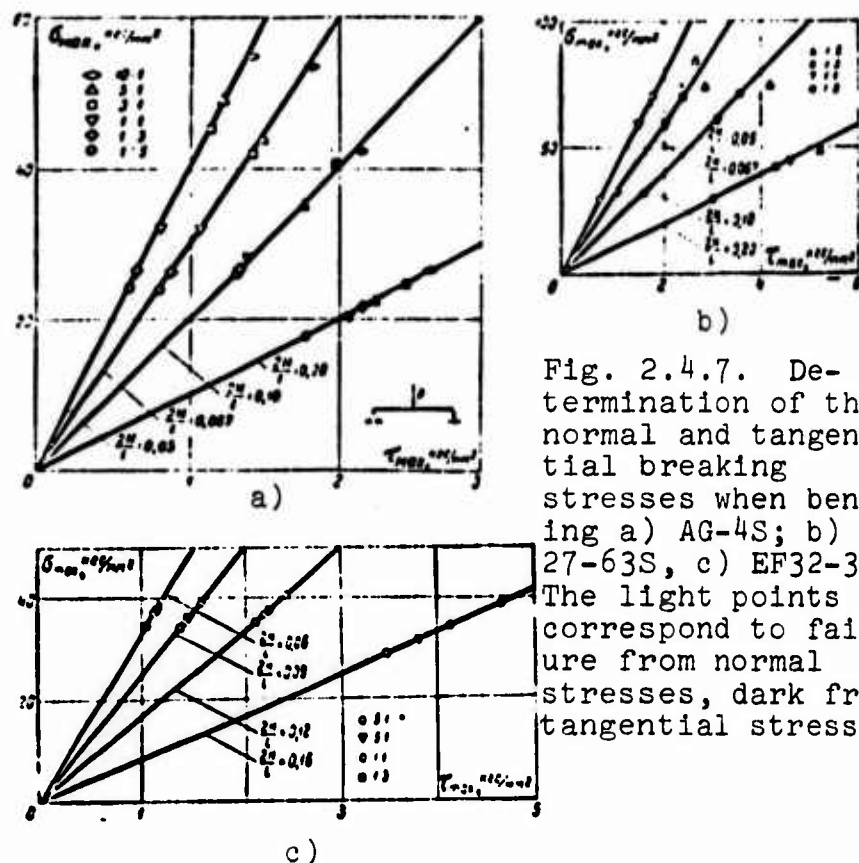Fig. 2.4.7. Determination of the normal and tangential breaking stresses when bending a) AG-4S; b) 27-63S, c) EF32-301. The light points correspond to failure from normal stresses, dark from tangential stresses.

c)

Fig. 2.4.8. The maximum bending stresses Π during failure depending on span/height ratio [274]: 1 - unidirectional glass fiber-reinforced plastics; 2 - packing 1:1; 3 - glass laminate.

75
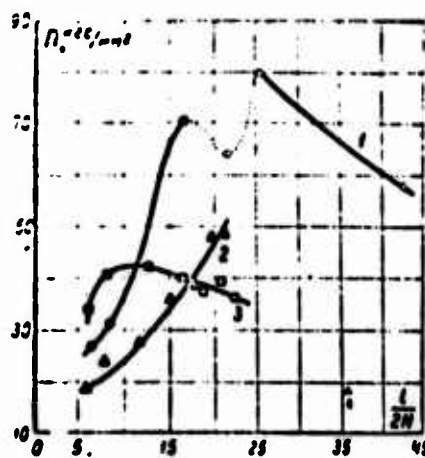
The main reason for the expansion of the area of failure from shear is the smallness of the ratio of ultimate strength with respect to tangential stresses Π_τ to strength with respect to normal stresses Π_σ. For the investigated materials Π_τ/Π_σ was changed within from 0.03 to 0.12 (as can be seen from Fig. 2.4.8, these limits can be still wider). The anisotropy of elastic properties barely influences the type of failure. Transition from one type of failure to another occurs with the relationship $\frac{2H}{l}$ characteristic for this material, which for the majority of the investigated cases proved to be less than that recommended by GOST 4648-63 ($2H/l = 0.1$). This places doubt upon the numerous data available in literature on the flexural strength of oriented glass fiber-reinforced plastics, especially during tests under conditions of elevated temperatures (see, for example, [147]). During the determination of bending strength it is necessary to indicate the type of failure, since otherwise the results are virtually incomparable.

2.4.5. **The effect of tensioning of fibers.** The introduction of tensioning of fibers leads to the growth of strength with respect to normal stresses and to the noticeable growth of shear strength, in comparison with Π_0 and T_0, for materials with straightened, but unstressed fibers. Typical data for material AG-4S are presented on Fig. 2.4.9. Relationship Π/T somewhat drops with rise of the degree of tautness. The zone of failure from shear (Fig. 2.4.10) is changed insignificantly. When testing rods of woven materials the strength grows in the entire investigated range of change of forces.

When evaluating the rigidity according to the ultimate load for prestressed short beams the obtained results prove to be significantly higher than shown in Table 2.3.3. This is explained by the fact that without exception all the beams of the indicated dimensions are destroyed from shear, and the shear strength (Fig. 2.4.9) increases with increase of the tensioning force.

This, apparently, is consisted in the error of Goldfein [287],[1] who obtained overstated data on the effect of stretching force on the strength and flexural rigidity. The estimation with respect to ultimate load is possible only with sufficiently large ratios of span and height.
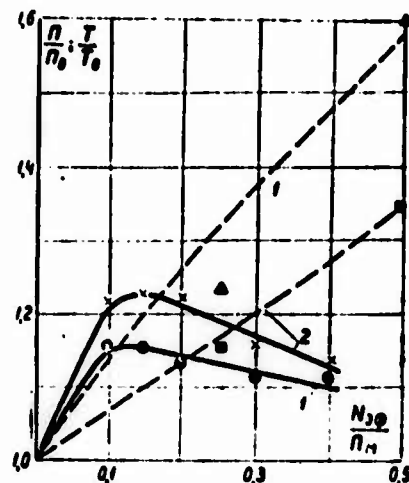
Fig. 2.4.9. The effect of tensile force on the bending strength: 1 - growth with respect to normal stresses (● - AG-4S, ▲ - SKT-11); 2 - growth of strength with respect to tangential stresses (× - AG-4S, ■ - SKT-11).

Fig. 2.4.10. The character of failure of beams of unidirectional material AG-4S depending on the tensioning of fibers. ● - samples with straightened, but unstressed fibers; × - prestressed samples.

---
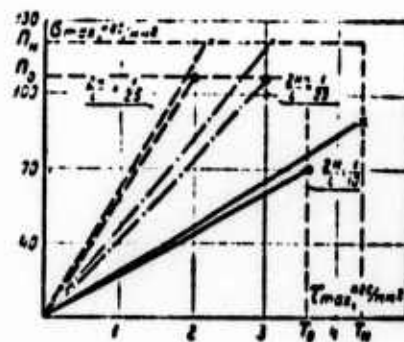
[1]The effect of the force of pretensioning of reinforcement on the rigidity and strength of oriented glass fiber-reinforced plastics, apparently, was investigated for the first time by Goldfein [287], however, the processing of experimental results by him was performed without allowing for the weak resistance of these materials to shear, which led to overstated estimations of the effect of tensioning on the properties of material.

§ 2.5. STABILITY AND LONGITUDINAL-
TRANSVERSE BENDING

2.5.1. The account of shear in problems of the stability of rods.

Shears in the problem of stability of a straight rod were taken into account for the first time by Engesser in 1891 [282] according to the diagram, which is accepted to call Timoshenko's diagram (see § 2.2.1). Taking into account that the bending moment, caused by longitudinal stretching (+) or compressive (-) force N, is equal to M = -Nω, Engesser derived an equation of stability of a centrally compressed rod:

$$\left(1+\frac{KN}{FG_{x:}}\right)\frac{d^2\omega}{dx^2}+\frac{N}{E_x I}\,\omega=0, \tag{2.5.1}$$

whence for the case of a rectangular cross section the value of critical force is obtained [183]:

$$N_{\text{кр}\,m}=\frac{N^*_{\text{кр}\,m}}{1+0.1\varkappa_m^2}; \tag{2.5.2}$$

$N^*_{\text{кр}\,m}$ - Eulerian critical force, i.e., the critical force calculated without allowing for shear, which corresponds to case $\varkappa_m = 0$. Let us note that if shears are introduced according to Rankine-Grashof's diagram (§ 2.2.1) [237], then in the second term of the denominator of expression (2.5.2) instead of multiplier 0.4 it is necessary to substitute multiplier 0.5.

Formulas for determining the critical forces in round and rectangular plates, close to Timoshenko's diagram, i.e., derived on the basis of the postulate about the fact that shears do not change the picture of distribution of tangential stresses (for a beam this means that they can be determined according to D. I. Zhuravskiy), are given in [6, 14, 112, 136, 137, 162, 163] and others. Stricter solutions are obtained in [39, 43, 49, 93].

In book [317] (see also [193]) there is given the equation of stability, modified (according to the terminology of the authors of book [317]) in comparison with (2.5.1):

$$\left(1 - \frac{KN}{FG_{xz}}\right)^{-1}\frac{d^2w}{dx^2} + \frac{N}{E_xI}\, w = 0.$$
(2.5.3)

It can be obtained from the system of equations of transverse vibrations of a stretched rod, given in [181], taking into account shearing strain, if we change from the equations of dynamics to the static case.   In the case of rectangular cross section from (2.5.3) follows the expression for critical force:

$$N_{\text{кр }m} = N^*{}_{\text{кр }m}\frac{\sqrt{1 + 1.6\varkappa_m^2} - 1}{0.8\varkappa_m^2}.$$
(2.5.4)

Experimentally the stability of rods of materials reinforced by filaments is extremely insufficiently studied. The results obtained in [154] during tests of free rods of circular cross section of three brands of glass fiber-reinforced plastics are depicted on Fig. 2.5.1. Experimental points attest to the noticeable effect of shears on the value of critical force in the investigated range of flexibility of rods. However, due to the unsuccessful construction of the supporting unit of the fixture for testing rods for stability there is obtained a large scattering of values of $N_{\text{кр}}$, which does not make it possible to decipher the experimental data with sufficient accuracy. In the article of L. V. Bayev and N. G. Torshenov[1] an attempt is made at the experimental estimation of the effect of shears on the value of critical force for circular rods whose diameter is 8 mm, length l for the cases of support: hinge-hinge and hinge-fixing. As can be seen from the given table, the experimentally measured

---

[1]L. V. Bayev, N. G. Torshenov. The Stability of Rods of Glass Fiber-Reinforced Plastics. - Mechanics of Polymers, 1968, 5.

value of critical force $N_{кр э}$ is close to the critical force determined taking into account shears $N_{кр}$, and it can be noticeably lower than Eulerian critical force $N^*_{кр}$

Hinge-hinge

l, мм	160	120	106	82	72	62	54
$N_{э р}^*$, кгс	330	500	720	1160	1470	1880	2460
$N^*_{кр}$, кгс	340	533	775	1295	1680	2270	2990
$N_{кр}$, кгс	331	510	728	1171	1460	1915	2400

Hinge-fixing

152	117	92,5	72
675	1038	1560	2142
710	1148	1745	2680
687	1070	1562	2250

[кгс = kgf]
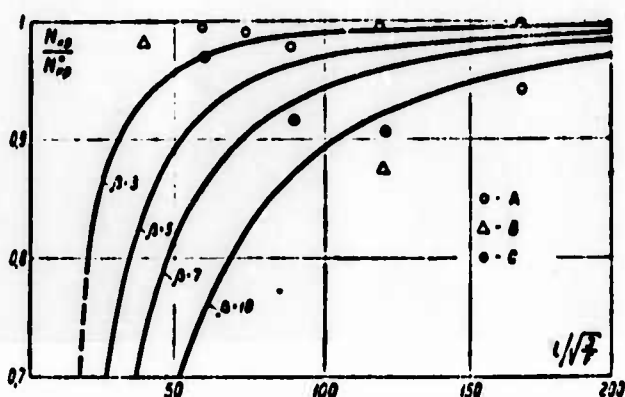
Fig. 2.5.1. The effect of shears on the value of critical force [154]. - - - calculated curves; 0, ●, Δ are experimental points obtained during tests of glass fiber-reinforced plastics with different structure (A and C are glass laminates reinforced by fabric of different weave, B is unidirectional material). KEY: (1) Structure.

(1) Структура	A	B	C
$E_x(\cdot 10^3)$, кгс/см²	2,93	3,16	2,62

2.5.2. **The effect of shears on the amount of critical force of compressed rods.** As was shown in § 2.2, the basic correction during the refinement of the technical theory of bending is introduced by the account of shears, therefore their effect on the amount of critical force is investigated under the assumption about the negligible smallness of lateral deformation ($\varepsilon_{\cdot} = 0$) and the compressibility of the axis of the rod ($\sigma_{кр} \ll E_x$). In this case, assuming that the loss of stability occurs in plane xz, from system of equations (2.2.13), (2.2.14) we obtain the system of equations of stability [188]:

$$\frac{\partial^2 u}{\partial x^2} + \frac{1}{\beta^2} \cdot \frac{\partial^2 u}{\partial z^2} = 0; \qquad (2.5.5)$$

$$(2HG_{xz} + N)\frac{d^2 w}{dx^2} + \dot{G}_x \int_{-H}^{H} \frac{\partial^2 u}{\partial x \partial z}\, dz = 0. \qquad (2.5.6)$$

If we make use of known solution of (2.2.30), (2.2.31), equation (2.5.5), equation (2.5.6) can be given the form

$$A_{1m}\beta\lambda_m^2 \, \mathrm{ch}\, \varkappa_m (\lambda_m^2 E_x / \varphi_m + N) \sin \lambda_m x -$$
$$- A'_{1m}\beta\lambda_m^2 \, \mathrm{ch}\, \varkappa_m (\lambda_m^2 E_x / \varphi_m + N) \cos \lambda_m x - A_{2m} N = 0. \qquad (2.5.7)$$

Equation (2.5.7) will be satisfied if $A_{2m} = 0$ and

$$N = -\lambda_m^2 E_x / \varphi_m.$$

Critical values of parameter $\lambda_{\text{кр } m}$ are determined from the boundary conditions which form the system of homogeneous equations. These values (or equations for their determination) under some usually examined boundary conditions are given in Table 2.5.1.

Table 2.5.1. Values of $\lambda_{m\ \text{кр}}$ for different methods of restraint of the rod ends.

Boundary conditions	Method of restraint of rod			
	With one restrained end	Hinge-supported	With one restrained, the other – hinge-supported end	With restrained ends
$x=0$	$w=0;$ $\frac{\partial w}{\partial x}=0$	$w=0;$ $\frac{\partial u}{\partial z}=0$	$w=0;$ $\frac{\partial w}{\partial x}=0$	$w=0;$ $\frac{\partial w}{\partial x}=0$
$x=l$	$\frac{\partial u}{\partial z}=0;$ $\frac{\partial u}{\partial z}+\frac{\partial w}{\partial x}=0$	$w=0;$ $\frac{\partial u}{\partial x}=0$	$w=0;$ $\frac{\partial u}{\partial x}=0$	$w=0;$ $\frac{\partial w}{\partial x}=0$
	$\lambda=\frac{a\pi}{2l}$ $(a=1,2,3\ldots)$	$\lambda=\frac{a\pi}{l}$ $(a=1,2,3\ldots)$	$\lambda l = \mathrm{tg}\,\lambda l$	$\lambda=\frac{2a\pi}{l}$ $(a=1,2,3\ldots)$

The expressions for critical force $N_{\text{кр } m}$ and for critical stress $\sigma_{\text{кр } m} = N_{\text{кр } m}/2H$ for the cases of support of ends examined in Table 2.5.1, when shears do not affect the value of $\lambda_{\text{кр } m}$ (Table 2.5.1), can be presented in the form

$$N_{\text{кр } m} = \varphi_m N_{\text{кр } m}^{*}, \quad \sigma_{\text{кр } m} = \varphi_m \sigma_{\text{кр } m}^{*}; \qquad (2.5.8)$$

$N_{\text{кр } m}^{*} = -\lambda_{\text{кр } m}^{2} E_2 I, \quad \sigma_{\text{кр } m}^{*} = \dfrac{N_{\text{кр } m}^{*}}{2H}$ - the critical forces and stresses, calculated without allowing for shears, φ_m - the coefficient which determines the correction from shear. The solutions by formulas given in [239, 282 and 317] give the appropriate correction factors (see § 2.5.1):

$$\varphi_{m\,\text{I}} = \frac{1}{1+0,5\varkappa_m^2}; \quad \varphi_{m\,\text{II}} = \frac{1}{1+0,4\varkappa_m^2}; \quad \varphi_{m\,\text{III}} = \frac{\sqrt{1+1,6\varkappa_m^2}-1}{0,8\varkappa_m^2}.$$

The accuracy of these diagrams can be evaluated by comparing the Taylor series for coefficients $\varphi_{m\text{I}}$, $\varphi_{m\text{II}}$, $\varphi_{m\text{III}}$:

$$\varphi_m = 1 - 0,4\varkappa_m^2 + 0,1619\varkappa_m^4 - 0,0656\varkappa_m^6 + \ldots \qquad (2.5.9)$$

$$\varphi_{m\,\text{I}} = 1 - 0,5\varkappa_m^2 + 0,2500\varkappa_m^4 - 0,125\varkappa_m^6 + \ldots \qquad (2.5.10)$$

$$\varphi_{m\,\text{II}} = 1 - 0,4\varkappa_m^2 + 0,1600\varkappa_m^4 - 0,0640\varkappa_m^6 + \ldots \qquad (2.5.11)$$

$$\varphi_{m\,\text{III}} = 1 - 0,4\varkappa_m^2 + 0,3200\varkappa_m^4 - 0,3200\varkappa_m^6 + \ldots \qquad (2.5.12)$$

This makes it possible to establish that coefficient $\varphi_{m\text{I}}$ is understated, $\varphi_{m\text{III}}$ - overstated, and $\varphi_{m\text{II}}$ is a sufficiently broad range of change of parameter $\varkappa_m$ is very close to φ_m (see also Table 2.2.1).

As can be seen from formulas (2.5.9-2.5.12), coefficients φ_m and thereby relation $\sigma_{\text{кр } m}/\sigma_{\text{кр } m}^{*}$ decrease with increase of parameter $\beta\frac{H}{l}$ faster, the larger $\lambda_{\text{кр } m}$ is, i.e., the more rigid the restraint of ends of the rod (Table 2.5.2). With increase of $\beta\frac{H}{l}$ the effect of the method of restraint of ends weakens.

82

(Fig. 2.5.2). When $\kappa_m = 0$, which corresponds to infinitely long rod ($H/l = 0$) or to material with infinite shear rigidity ($\beta = 0$), $\phi_m = 1$, consequently $\sigma_{\kappa p} = \sigma_{\kappa p}^*$.
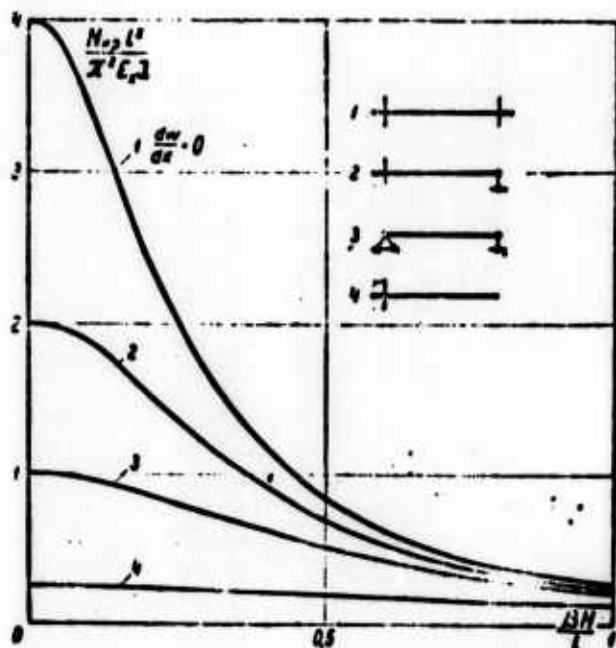
Fig. 2.5.2. The effect of shears on critical force under varied conditions of restraint of ends of the rod.

2.5.3. **Ways of increase of the critical force. Limiting cases.** Critical stress $\sigma_{\kappa p}$ can be increased in two ways: by increasing the shear modulus G_{xz} or $\sigma_{\kappa p\ m}^*$, i.e., Young's modulus E_x, relation $\frac{H}{l}$ or the rigidity of restraint of ends. The effectiveness of one method or other can be investigated by examining the partial derivatives:

$$\frac{\partial \sigma_{\kappa p\ m}}{\partial \sigma_{\kappa p\ m}^*} = \frac{3\,\mathrm{th}^2\,\varkappa_m}{2\varkappa_m^2} - \frac{\varphi_m}{2};\qquad (2.5.13)$$

$$\frac{\partial \sigma_{\kappa p\ m}}{\partial G_{xz}} = 1 - \frac{3\,\mathrm{th}\,\varkappa_m}{2\varkappa_m} + \frac{1}{2\,\mathrm{ch}^2\,\varkappa_m};\qquad (2.5.14)$$

The graphs of these functions are presented on Fig. 2.5.3. With $\kappa_m = 0\,\frac{\partial \sigma_{\kappa p\ m}}{\partial \sigma_{\kappa p\ m}^*} = 1$, $\frac{\partial \sigma_{\kappa p\ m}}{\partial G_{xz}} = 0$ with $\kappa_m = \infty$, on the contrary, $\frac{\partial \sigma_{\kappa p\ m}}{\partial \sigma_{\kappa p}^*} = 0$, $\frac{\partial \sigma_{\kappa p\ m}}{\partial G_{xz}} = 1$. Consequently, increase of $\sigma_{\kappa p\ m}^*$ is

83

Table 2.5.2. The effect of shears on the amount of critical force for rods of materials reinforced by filaments.

$$\frac{N^{*}_{\text{кр}}}{N_{\text{кр}}}$$

Loading diagram	Formula	x	$\lambda_{\text{кр}}$	$\frac{l}{H}$	Glass fiber-reinforced plastics with three-dimensional cross-linked structure $\beta'=8-13$	Glass laminates $\beta'=10-15$	Nonfabric glass fiber-reinforced plastics (packing 1:1) $\beta'=15-20$	Unidirectional glass fiber-reinforced plastics $\beta'=25-50$	Nonfabric glass fiber-reinforced plastics (packing 1:1) $\beta'\leq40$	Unidirectional glass fiber-reinforced plastics $\beta'\leq100$
	$\dfrac{3(x-\mathrm{th}\,x)}{x^2}$	$\lambda_{\text{кр}}\,\beta\dfrac{H}{l}$	$m\dfrac{\pi}{2}\ (m=1,2,3\ldots)$	5	0.93−0.89	0.91−0.87	0.87−0.84	0.80−0.67	≤0.72	≤0.51
				20	≈1,00	≈0.99	≈0.99	0.93−0.97	≤0.98	≤0.94
			$m\pi\ (m=1,2,3\ldots)$	5	0.76−0.66	0.72−0.63	0.63−0.56	0.51−0.34	≤0.39	≤0.21
				20	0.98−0.97	0.98−0.96	0.96−0.95	0.91−0.89	≤0.91	≤0.80
			$\lambda_{\text{кр}}=\mathrm{tg}\,\lambda_{\text{кр}}$ $(\lambda_{\min}=4.4934)$	5	0.61−0.49	0.56−0.46	0.46−0.39	0.34−0.20	≤0.24	≤0.12
				20	0.96−0.94	0.95−0.93	0.93−0.91	0.89−0.80	≤0.83	≤0.67
			$2m\pi\ (m=1,2,3\ldots)$	5	0.45−0.33	0.39−0.30	0.30−0.25	0.21−0.12	≤0.14	≤0.06
				20	0.93−0.89	0.91−0.87	0.87−0.84	0.60−0.67	≤0.72	≤0.51

84

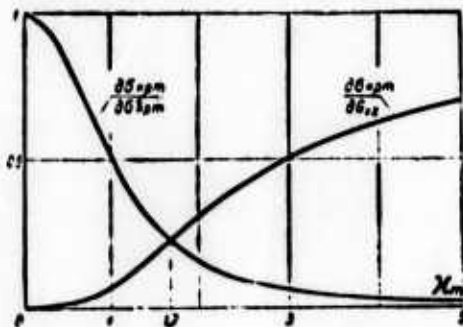effective only with small κ_m. With large κ_m (order 1-2), characteristic for rods of materials reinforced by filaments, an increase of $\sigma^*_{\text{кр }m}$ without a simultaneous increase of the shear modulus G_{xz} becomes ineffective. With still larger κ_m the change of $\sigma^*_{\text{кр }m}$ virtually no longer affects the critical stress $\sigma_{\text{кр }m}$, which when $E_x \to \infty$ or $H/l \to \infty$ approaches not infinity, as follows from Euler formula $(\sigma^*_{\text{кр }m} = \frac{\lambda_{\text{кр }m}{}^2 H^2 E_x}{3})$, but toward a finite quantity equal to shear modulus G_{xz}:

Fig. 2.5.3. The effectiveness of increase of G_{xz} and $\sigma^*_{\text{кр }m}$.

$$\lim_{\kappa_m \to \infty} \sigma_{\text{кр }m} = G_{xz}. \tag{2.5.15}$$

(The obtained result is qualitatively analogous to results of [56, 93].)

The conducted analysis is related not only to the problems of stability, but generally to the question concerning increase of the total (taking into account shear) flexural rigidity, which is directly proportional to critical force. For greater clarity it is possible to use Timoshenko's diagram, with the aid of which, as follows from § 2.2, the basic correction from shear is caught. The replacement of coefficient ϕ_m in formula (2.5.9) by coefficient ϕ_{mI} corresponds to the transition to this diagram. Hence follows

$$\frac{1}{\sigma_{\text{кр}m}} = \frac{1}{\sigma^*_{\text{кр}m}} + \frac{1.2}{G_{xz}}.$$

As is evident, total flexural pliability $1/\sigma_{\text{кр }m}$ consists of flexural pliability of the classical sense $1/\sigma^*_{\text{кр }m}$ and shear

pliability $1.2/G_{xz}$. Obviously it is more effective to decrease the large component. For isotropic materials always $1/\sigma^*_{\text{кр m}} \gg \gg 1/G_{xz}$ (according to Bernoulli's theory, $1/G_{xz} = 0$); however, for materials reinforced by filaments cases are possible where $1/\sigma^*_{\text{кр m}} < 1.2/G_{xz}$ (this takes place when $\kappa_m > 1.7$; see Fig. 2.5.3).

A model, composed of coaxial absolutely rigid rods, hinge connected with rigidity G_{xz} (Fig. 2.5.4), corresponds to the examined limiting case (2.5.15). With such a form of the loss of stability it is theoretically impossible to predict which of the equal forms (see, for example, Fig. 2.5.5a, b), adjacent to the initial form (Fig. 2.5.5c), the rod takes when the stress reaches its critical value $\sigma_{\text{кр m}} = G_{xz}$.
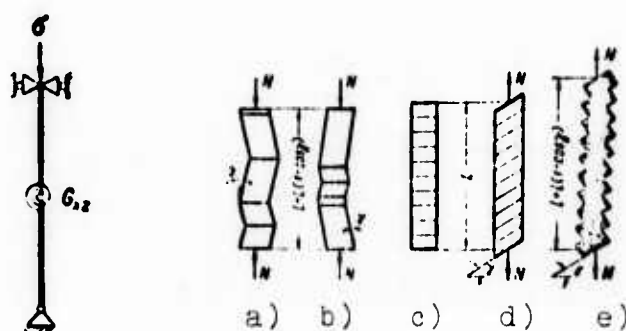
Fig. 2.5.4.   Fig. 2.5.5.

Fig. 2.5.4.   Model of the shear form of loss of stability.
Fig. 2.5.5.   The possible shear forms of the loss of stability during compression (a, b) and tension (d, e).

Result $\sigma_{\text{кр m}} = G_{xz}$ when $E_x \to \infty$ can be obtained also by the energy method, taking into account that in this case the potential strain energy of the rod is determined only by shears $\Im_1 = = 0.5\gamma_{xz}{}^2 G_{xz} Fl$ (F - the cross-sectional area of the rod, γ_{xz} - angle of shear). The corresponding change of potential of external force $N = F\sigma$, with this $\Im_2 = F\sigma l (1 - \cos \gamma_{xz}) \approx F\sigma l \frac{\gamma_{xz}^2}{2}$. From equality $\Im_1 = \Im_2$ follows equality $\sigma_{\text{кр m}} = G_{xz}$.

86

During the action of tensile force the shear form of loss of stability of the solid rod is impossible, since with the observance of conditions of continuity of deformations a potential of external forces less than with the initial form cannot exist (Fig. 2.5.5c, d). Such a loss of stability is possible with the expansion of a spring [248], each coil of which can slip relative to the adjacent coils (Fig. 2.5.5e). In this case for $\Im_1$ and $\Im_2$ we obtain the same expressions as for a compressed solid rod, and therefore, the same final result $\sigma_{\text{кр m}} = G_{\text{усл}}$ (here $G_{\text{усл}}$ - the conventional shear modulus, which corresponds to the shear modulus of an equivalent solid rod).

From equation (2.5.4) it follows that when $E_x \to \infty$ or $H/l \to \infty$ $\sigma_{\text{кр m}} \to G_{xz}/K$, i.e., according to Timoshenko's diagram (and also according to Rankine-Grashof), in the examined limiting case the critical stress must depend on the shape of cross section (coefficient K). However, as follows from the derivative of formula $\sigma_{\text{кр}} = G_{xz}$ by the energy method, the shape of cross section when $E_x \to \infty$ or $\frac{H}{l} \to \infty$ does not affect the value of critical stress.

The disagreement of results is caused by the fact that in the approaches of Rankine-Grashof and Timoshenko the distribution of tangential stresses over the section of the rod is accepted as not depending on the relationship of geometric dimensions (H/l) and the elastic characteristics of material (E_x/G_{xz}), i.e., on parameter κ_m. However, as can be seen from Fig. 2.2.8, with increase of κ_m the law of distribution $f(z)$ increasingly differs from parabolic (a rod of rectangular cross section is examined). Coefficient K (see the method of its determination in § 2.2.1) is the function of parameter κ_m, but this is not considered in the indicated diagrams, according to which it is accepted as constant. For a rod of rectangular cross section in the limiting case ($\kappa_m = 0$; shears are absent) K = 1.2 (according to Timoshenko) or K = 1.5 (according to Rankine-Grashof). In another limiting case ($\kappa_m \to \infty$) the tangential stresses are distributed over the section of the rod evenly, regardless of the shape of its cross section, consequently, K = 1.

87

Formula (2.5.4) in the limiting case ($\kappa_m \to \infty$) gives result $\lim\limits_{\kappa_m \to \infty} \sigma_{\kappa p} m = \infty$, qualitatively different from formula (2.5.15). Furthermore, from equation (2.5.3) it follows that for a rod under tension the shear form of the loss of stability is possible when $\sigma = G_{xz}/K$ [106].

The nonconformity of these derivations to the results obtained earlier is due to the inconsistency of the account of the force factors, which act in the section of the rod. Equations of equilibrium for an oblique-angled element (Fig. 2.2.1) are composed the same as for rectangular [317].

As a result of the intense decrease of critical force, caused by shear, difficulties appear during the tests of materials of the type of oriented glass fiber-reinforced plastics for compression, since even very short samples ($l/2H = 5-10$) lose stability. A sample made of glass laminate on epoxy bonding agent ($l/2H = 7.5$) loses stability if the compressive stress reaches values of the same order as the shear modulus, which qualitatively agrees with (2.5.15) (Fig. 2.5.6). The limiting relative height of the rod, at which failure of material begins earlier than the loss of stability, is determined by inequality

$$\sigma_{kp} < \Pi_\sigma^-,$$

whence, by using Timoshenko's formula (2.5.2), for a beam with hinge-mounted ends we obtain

$$\frac{2H}{l} > \frac{2\sqrt{3}}{\pi\beta}\left(\frac{G_{xz}}{\Pi_\sigma^-} - 1.2\right)^{-0.5}.$$

The given analysis shows that the calculation for stability of rods of materials reinforced by filaments must be performed taking into account shears. For constructions made of such

88

materials cases are possible where an increase in the shear modulus
is more effective than an increase in Young's modulus of the
relative thickness or rigidity of restraint.

Fig. 2.5.6. Sample 2H × l = 8 ×
× 60 mm^2 with loss of stability.

2.5.4. **Longitudinal-transverse bending.** The simultaneous
account of longitudinal forces N (we will consider them positive
when they stretch the bent rod) and transverse load q leads to
the system of equations which describes longitudinal-transverse
bending:

$$\frac{\partial^2 u}{\partial x^2} + \frac{1}{\beta^2} \cdot \frac{\partial^2 u}{\partial z^2} = 0; \qquad (2.5.16)$$

$$(2HG_{xz} + N)\frac{d^2 w}{dx^2} + G_{xz} \int_{-H}^{H} \frac{\partial^2 u}{\partial x \partial z} dz = -q. \qquad (2.5.17)$$

The course of solutions of system of equations (2.5.16),
(2.5.17) is completely analogous to that given in § 2.2.3. Thus,
instead of (2.2.37), (2.2.28) we have

$$u_m = -\frac{q_m}{\lambda_m^2(N + \lambda_m^2 E_x I)}\left[\frac{\text{sh}\,\varkappa_m \frac{z}{H}}{\beta\,\text{ch}\,\varkappa_m} \cos\lambda_m x - C_m z\left(1 - \frac{2x}{l}\right)\right]; \qquad (2.5.18)$$

$$w_m = -\frac{q_m}{\lambda_m^2(N + \lambda_m^2 E_x I)}\left[\sin\lambda_m - C_m x\left(1 - \frac{x}{l}\right)\right]. \qquad (2.5.19)$$

89

In the case of sinusoidal load ($q = q_m \sin \lambda_m x$) the expression for deflection assumes the form

$$w_m = \frac{w^*_m}{\dfrac{N}{N^*_{\text{кр } m}} + \varphi_m} \qquad (2.5.20)$$

or with small κ_m

$$w_m \approx w^*_m \left(1 + 0.4\kappa_m^2 - \frac{N}{N^*_{\text{кр } m}} \right)$$

(w^*_m - deflection according to Bernoulli when $N = 0$; $N^*_{\text{кр } m}$ - Eulerian critical force).

As can be seen from (2.5.20), the tensile force decreases the deflection. For compensation of the component of deflection, caused by shears, it is required to apply the tensile force

$$N_1 = N^*_{\text{кр}}(1 - \varphi_m). \qquad (2.5.21)$$

With not very large κ_m, when the approximate replacement of $\phi_m = 1 - 0.4\kappa_m^2$ is permissible (see Table 2.2.1),

$$N_1 = 0.133\kappa_m^4. \qquad (2.5.22)$$

In the case of compressive force the deflection is increased and, as one ought to expect, when $N = N_{\text{кр } m} = \phi_m N^*_{\text{кр } m}$ becomes infinite, i.e., the rod loses stability.

The effect of the longitudinal force and shear on the deflection is illustrated by Fig. 2.5.7 and Table 2.3.1, on which there is given relation w_{max}/w^*_{max} with different relations $N/N_{\text{кр}}$ for beams loaded with evenly distributed load and by force applied halfway along the span. As is evident, relation w_{max}/w^*_{max} insignificantly depends on the type of transverse load, therefore formula (2.5.20) can be recommended to evaluate the effect of axial forces also in the case of loads different from sinusoidal. When $\kappa_m \to 0$ and $\phi_m \to 1$ formula (2.5.20) turns into known approximation formula [239].
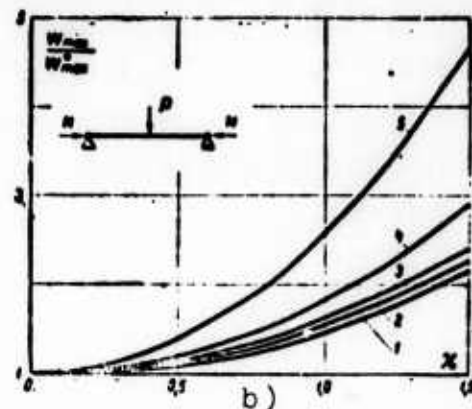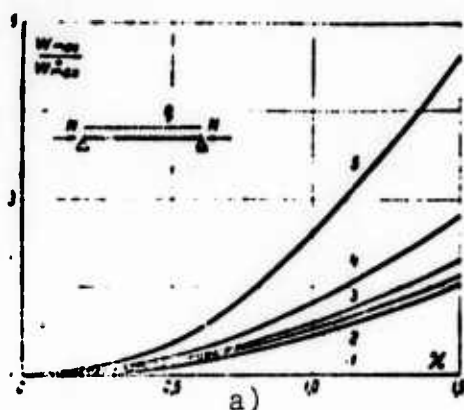
90

Fig. 2.5.7. The effect of shears on deflection of flattened beams. a) evenly distributed load; b) concentrated force halfway along the span. KEY: (1) Curve.

(1)

Кривая	1	2	3	4	5
$\dfrac{N}{N_{вр}}$	0,1	0,2	0,3	0,5	0,75

If the calculation is performed on prescribed deformation, then the low shear rigidity of reinforced plastics with prescribed relation $N_{кр}/N$ sharply limits the permissible transverse load. Relation q_0/q_0^* (asterisk notes the permissible transverse load for a beam with infinite shear rigidity) turns out to be inversely proportional to the ratio of deflection w_{max}/w_{max}^*:

$$\frac{q_0}{q^*_0} = \frac{w^*_{max}}{w_{max}}. \qquad (2.5.23)$$

Relation $\dfrac{q_0}{q^*_0} = f(x, \dfrac{N'}{N_{кр}})$ is shown on Fig. 2.5.8. From the presented

data it is evident that the permissible transverse load can be decreased several times. Thus, the account of shears is necessary during the calculation of critical force and the calculation of deflections for all practically important constructive uses of flattened beams made of reinforced plastics. Utilization in these problems of the hypothesis of flat sections can lead to inadmissible errors.

Fig. 2.5.8. The effect of shears on the value of permissible load at prescribed deflection of free evenly loaded beams. KEY: (1) Curve.

(1)

Кривая	1	2	3	4	5
$\dfrac{N}{N^*_{кр}}$	0,1	0,2	0,3	0,4	0,5
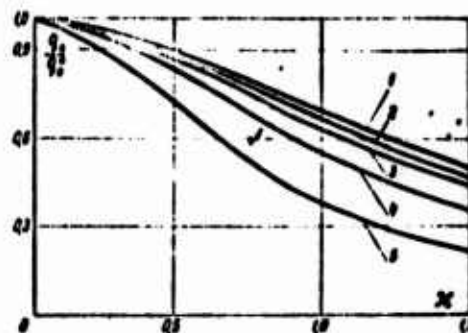
2.5.5. Longitudinal-transverse bending of beams on an elastic support.

With the presence of a linear elastic support, the reaction of which is proportional to deflection w, the equations which describe longitudinal-transverse bending have the form

$$\frac{\partial^2 u}{\partial x^2} + \frac{1}{\beta^2} \cdot \frac{\partial^2 u}{\partial z^2} = 0; \tag{2.5.24}$$

$$(2HG_{xz} + N)\frac{d^2 w}{dx^2} - k_0 w + G_{xz}\int_{-H}^{H} \frac{\partial^2 u}{\partial x \partial z}\, dz = -q \tag{2.5.25}$$

(k_0 - bed coefficient). The solution of system (2.5.24), (2.5.25) (method of solution is analogous to that given in § 2.2) for the case of free support leads to the following dependences for displacements:

$$u_m = -\frac{q_m}{\lambda_m^4 E_x I\left(\varphi_m + \dfrac{N}{\lambda_m^2 E_x I} + \dfrac{k_0}{\lambda_m^4 E_x I}\right)} \cdot \frac{\operatorname{sh}\varkappa_m \dfrac{z}{H}}{\beta \operatorname{ch}\varkappa_m}\cos\lambda_m x; \tag{2.5.26}$$

$$w_m = \frac{q_m}{\lambda_m^4 E_x I\left(\varphi_m + \dfrac{N}{\lambda_m^2 E_x I} + \dfrac{k_0}{\lambda_m^4 E_x I}\right)}\sin\lambda_m x; \quad \lambda_m = \frac{m\pi}{l}. \tag{2.5.27}$$

As can be seen from formulas (2.5.26), (2.5.27), the displacements become infinite (this attests to the loss of stability) when longitudinal force N reaches critical value:

$$N_{кр}{}^{(h)} = -\lambda_m^2 E_x I\left(\varphi_m + \frac{k_0}{\lambda_m^4 E_x I}\right). \tag{2.5.28}$$

As is evident, the critical force increases with increase of rigidity of elastic base (coefficient k_0). The relationship between dimensionless quantities $\bar{N}_{кр\ m} = N_{кр\ m} l^2 / \pi^2 E_x I$ and $\bar{k}_0 = k_0 l^4 / \pi^4 E_x I$ is linear:

$$\bar{N}_{кр\ m} = m^2\varphi_m + \frac{\bar{k}_0}{m^2}.$$

This relationship at different values of the parameter $\varkappa = \pi\beta\frac{H}{l}$ is represented on Fig. 2.5.9. The inclination of straight line $\bar{N}_{кр\ m} = f(\bar{k}_0)$ does not depend on shears. The latter affect only the location of the point of intersection of the straight line with the axis of ordinates. When $k_0 = 0$ the minimum value of critical force corresponds to one half-wave (m = 1); however, with increase

92

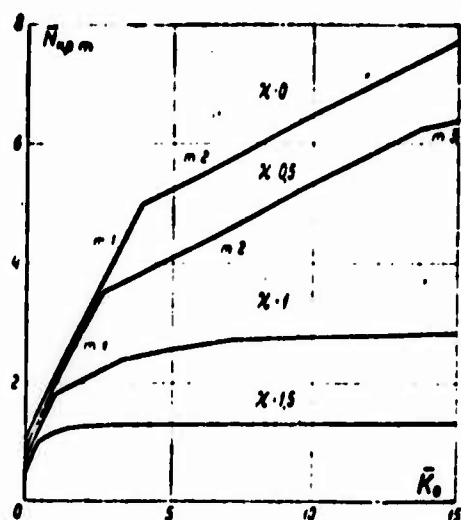of k_0 the number of half-waves, at which the minimum of critical force is reached, is increased.[1]

Fig. 2.5.9. Change of the critical force depending on the rigidity of elastic support at different values of parameter κ, which considers the effect of shears.

The transition from m half-waves to m + 1 half-wave is determined from condition:

$$\lambda_m{}^2 \varphi_m + \frac{k_0}{\lambda_m{}^2 E_x I} = \lambda_{m+1}{}^2 \varphi_{m+1} + \frac{k_0}{\lambda_{m+1}{}^2 E_x I}, \qquad (2.5.29)$$

whence

$$\bar{k}_0 = m^2 (m+1)^2 \frac{(m+1)^2 \varphi_{m+1} - m^2 \varphi_m}{(m+1)^2 - m^2}, \qquad (2.5.30)$$

or for values of κ_m, at which the approximate replacement of $\phi_m \simeq (1 + 0.4\kappa_m)^{-1}$ is permissible (see Table 2.2.1),

$$\bar{k}_0 = \bar{k}^*_0 \varphi_m \varphi_{m+1}. \qquad (2.5.31)$$

With $\kappa_m \to 0$ and $\phi_m \to \phi_{m+1} \to 1$ formula (2.5.30) changes to the formula not taking into account shears [76]:

---

[1]Analogous results are obtained in work of B. L. Pelekh, G. A. Teters, R. V. Mel'nik "The Stability of Glass Fiber-Reinforced Plastic Plates, Connected with an Elastic Support," Mechanics of Polymers, 1968, 6, 1082.

$$\lim_{x \to 0} \bar{k}_0 = \bar{k}^*_0 = m^2(m+1)^2. \qquad (2.5.32)$$

As can be seen from Fig. 2.5.9, the effect of shears is manifested in the fact that the boundaries of transition from the less number of waves to greater are shifted toward smaller values of parameter $\bar{k}_0$. This effect can be judged from Fig. 2.5.10, on which there are shown the zones which correspond to m = 1-4 half-waves, depending on parameters κ and $\bar{k}_0$.
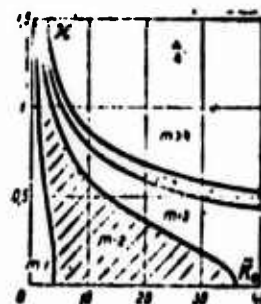
Fig. 2.5.10. The areas which correspond to loss of stability with number of half-waves m = = 1-4.

The obtained results can be used for determining the upper critical forces of cylindrical shells. If we examine the axisymmetric problem of a round cylindrical shell with Young's modulus along generatrix E_x and in circumferential direction E_θ, then

$$k_0 = \frac{2HE_\theta}{R^2}; \quad \bar{k}_0 = \frac{3E_\theta l^2}{x_m^2 G_{\theta x} R^2}.$$

where

$$x_m^2 = \frac{m^2 \pi^2 E_x H^2}{G_{\theta x} l^2 (1 - v_{x\theta} v_{\theta x})}$$

(for isotropic shell $\bar{k}_0 = \frac{3(1-v^2) l^2}{\pi^2 H^2 R^2}$). Consequently, the critical axial pressure

$$P_{1.p} = \frac{m^2 \pi^2 E_x H^2}{3 l^2} + f_m \frac{E_\theta l^2}{m^2 R^2}.$$

94

§ 2.6. FLEXURAL VIBRATIONS

2.6.1. The account of shears in problems of flexural vibrations.

Shears in the problem of transverse vibrations of a beam were introduced for the first time by S. P. Timoshenko [240]:

$$\frac{\partial^4 w}{\partial x^4} + \frac{\varrho}{E_x} \cdot \frac{F}{I} \cdot \frac{\partial^2 w}{\partial t^2} - K\frac{\varrho}{G_{xz}} \cdot \frac{\partial^4 w}{\partial x \partial t^2} - \frac{\varrho}{E_x} \cdot \frac{\partial^4 w}{\partial x \partial t^4} +$$
$$+ K\frac{\varrho}{G_{xz}} \cdot \frac{\varrho}{E_x} \cdot \frac{\partial^4 w}{\partial t^4} = 0. \qquad (2.6.1)$$

here ρ - material density, K - the coefficient which depends on the shape of the cross section and the method of the account of shears (see § 2.2.1). The last two terms of equation (2.6.1) consider the rotary inertia of the section. Disregarding it, i.e., taking into account only shears, instead of (2.6.1) we obtain

$$\frac{\partial^4 w}{\partial x^2} + \frac{\varrho}{E_x} \cdot \frac{E}{I} \cdot \frac{\partial^2 w}{\partial t^2} - K\frac{\varrho}{G_{xz}} \cdot \frac{\partial^4 w}{\partial x^2 \partial t^2} = 0, \qquad (2.6.2)$$

which follows from (2.2.7), if in it on the basis of the d'Alembert principle we replace the transverse load by inertia term

$$q = \varrho F \frac{\partial^2 w}{\partial t^2}.$$

In the case of a free beam[1] from equation (2.6.1) follows the equation of frequencies

$$\left(\frac{\omega_m}{\omega^*_m}\right)^4 - \frac{1}{K\beta^2 i^4 \lambda_m^4}[1 - i^2\lambda_m^2(1 + K\beta^2)]\left(\frac{\omega_m}{\omega^*_m}\right)^2 + \frac{1}{K\beta^2 i^4 \lambda_m^4} = 0, \qquad (2.6.3)$$

---

[1] In [192] it is proposed to use formula (2.6.4) for determining natural beam frequencies with different conditions of restraint of ends.

where $\omega^*_m = \lambda_m^2 i \sqrt{\dfrac{E_x}{\varrho}}$ — m angular frequency, determined without allowing for shear and rotary inertia; $i = \sqrt{\dfrac{I}{F}}$ – the radius of inertia of the cross section of the beam; $\lambda_m = m\pi/l$, m – integer. The roots of equation (2.6.3) are determined by expression [181]:

$$\left(\frac{\omega_m}{\omega^*_m}\right)^2 = \frac{1 + i^2\lambda_m^2(1 + K\beta^2)}{2K\beta^2 i^2\lambda_m^4}\left\{1 \pm \sqrt{1 - \frac{4K\beta^2 i^2\lambda_m^4}{[1 + i^2\lambda_m^2(1 + K\beta^2)]^2}}\right\}. \qquad (2.6.4)$$

Frequencies ω_{0m} correspond to predominantly flexural [48] vibrations (sign "+" in expression (2.6.4)). Taking into account rotary inertia one additional series of frequencies appears ω_{1m} (sign "−" in expression (2.6.4)). Taking into account the smallness of the augend under the square root in formula (2.6.4), we have

$$\omega_{0m}^2 = \frac{\omega^{*2}_m}{1 + i^2\lambda_m^2(1 + K\beta^2)}; \qquad (2.6.5)$$

$$\omega_{1m}^2 = \frac{\omega^{*4}_m}{K\beta^2 i^4\lambda_m^4} - \omega_{0m}^2. \qquad (2.6.6)$$

Without taking into account rotary inertia we have only one series of frequencies ω_m, which corresponds to ω_{0m}:

$$\omega_m^2 = \frac{\omega^{*2}_m}{1 + K\beta^2 i^2\lambda_m^2}. \qquad (2.6.7)$$

In S. P. Timoshenko's work [240] there are given formulas taking into account rotary inertia and shears:

$$\omega_{0m} = \omega^*_m[1 - 0{,}5i^2\lambda_m^2(1 + K\beta^2)] \qquad (2.6.8)$$

and taking into account only shears:

$$\omega_m = \omega^*(1 - 0{,}5K\beta^2 i^2\lambda_m^2). \qquad (2.6.9)$$

Formula (2.6.8) follows from (2.6.5), and (2.6.9) – from (2.6.7),

if one assumes that parameters λ_m (lowest frequencies) and β (isotropic materials) are small.

The examined approaches obtained their development in the theory of vibration of plates and shells (see detailed bibliography in [2, 98, 138, 142, 155, 156, 160]). As applied to constructions made of anisotropic materials a series of problems taking into account shears has been solved by S. A. Ambartsumyan [6], V. I. Korolev [112] and others (see review [142]). V. V. Bolotin and coauthors developed the theory of vibrations of constructions made of reinforced materials [38, 43, 52, 270], on the basis of which there is solved a series of problems, which makes it possible to consider the flexural effects in the reinforcing layers.

2.6.2. Basic dependences. The equations of vibrations of the beam can be obtained from equations (2.2.13), (2.2.14) by the addition of inertia terms to them:

$$\frac{\partial^2 u}{\partial x^2} + \frac{1}{\beta^2} \cdot \frac{\partial^2 u}{\partial z^2} = \frac{\varrho}{E_x} \cdot \frac{\partial^2 u}{\partial t^2};$$
(2.6.10)

$$2H\frac{\partial^2 w}{\partial x^2} + \int_{-H}^{H} \frac{\partial^2 u}{\partial x \partial z}\, dz = 2H \frac{\varrho}{G_{xz}} \cdot \frac{\partial^2 w}{\partial t^2}.$$
(2.6.11)

These equations can be obtained on the basis of the Hamilton principle (see, for example, [52]), according to which the proper motion of the system is such that it imparts steady-state value to integral

$$I = \int_{t_0}^{t_1} (T_1 - \Im_1 - \Im_2)\, dt$$

(at the ends of interval (t_0, t_1) the expression is not varied). Expressions for potential strain energy $\Im_1$ and potential energy

97

of external load Θ_2 are obtained earlier in § 2.2. The kinetic energy of the system T is determined by expression

$$T = \int\limits_{-H}^{H} \int\limits_{0}^{l} \left[\left(\frac{\partial u}{\partial t} \right)^2 + \left(\frac{\partial w}{\partial t} \right)^2 \right] dx \, dz.$$

By presenting displacements u, w in the form of periodic functions of time

$$u = U(x, z) \sin(\omega t + \delta);$$
$$w = W(x) \sin(\omega t + \delta),$$

from (2.6.10), (2.6.11) we obtain the system of equations for the amplitudes of vibrations U, W:

$$\frac{\partial^2 U}{\partial x^2} + \frac{\varrho \omega^2}{E_x} U + \frac{1}{\beta^2} \cdot \frac{\partial^2 U}{\partial z^2} = 0; \tag{2.6.12}$$

$$2H \left(\frac{d^2 W}{\partial x^2} + \frac{\varrho \omega^2}{G_{xz}} W \right) + \int\limits_{-H}^{H} \frac{\partial^2 U}{\partial x \partial z} \, dz = 0. \tag{2.6.13}$$

Conditions of free beam

$$W - \frac{\partial U}{\partial x} = 0 \quad \text{при } x = 0, \ x = l;$$

$$\frac{\partial U}{\partial z} + \frac{dW}{\partial x} = 0 \quad \text{при } z = \pm H$$

[при = when]

will be satisfied if (see § 2.2.3)

$$U_m = -\frac{A_m}{\beta \operatorname{ch} \varkappa_m} \operatorname{sh} \mu_m \beta z \cdot \cos \lambda_m x; \tag{2.6.14}$$

$$W_m = A_m \sin \lambda_m x,$$

where $\mu_m^2 = \lambda_m^2 - \frac{\varrho \omega_m^2}{E_x}$, $\varkappa_m = \mu_m \beta H$. In this case equation (2.6.12) is satisfied identically, and from (2.6.13) follows the equation for

98

determining the circular frequency:

$$\omega_m{}^2 = \omega^{*2}{}_m \frac{\mu_m{}^2}{\lambda_m{}^2} \varphi_m,$$ (2.6.15)

where

$$\varphi_m = \frac{3(x_m - \text{th } x_m)}{x_m{}^3}.$$

2.6.3. The effect of shears and rotary inertia. If we disregard the forces of inertia in the direction of the axis of the rod, i.e., rotary inertia and bending of cross sections, then equation (2.6.10) will not have a right side. Hence it follows that $\mu_m = \lambda_m$ and correction from shear for the square of circular frequency is the same as obtained earlier (see § 2.5) for critical force:

$$\omega_m{}^2 = \omega^{*2}{}_m \varphi_m.$$ (2.6.16)

Taking into account the rotary inertia and bending of cross sections, it is necessary to solve transcendental equation (2.6.15). The circular frequencies are determined by expression

$$\omega_m{}^2 = \omega^{*2}{}_m \frac{\lambda_m{}^2 \beta^2 H^2 - \overline{x_m}{}^2}{3\lambda_m{}^4 H^4 \beta^2}.$$ (2.6.17)

where $\overline{\kappa}_m$ are the roots of equation:

$$\text{th } x_m = \frac{x_m{}^3}{\lambda_m{}^2 H^2} - (\beta^2 - 1) x_m.$$ (2.6.18)

Equation (2.6.18) with fixed m has (see Fig. 2.6.1) one real positive root $\overline{\kappa}_{0m}$, which corresponds predominantly to flexural vibrations, and infinitely many imaginary roots. Consequently, the account of inertia of bending of sections instead of the averaged value (rotary inertia) leads to the appearance of an infinite multitude of series of frequencies. Formally equation (2.6.3) follows from equation (2.6.15), if in the latter we

99

Fig. 2.6.1. For determination of the roots of equation (2.6.18).
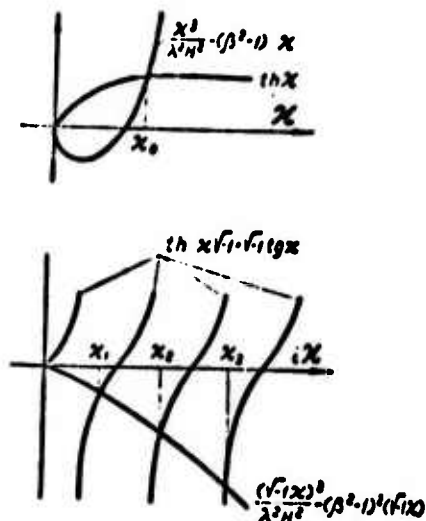
replace function ϕ_m by its approximate expression $\dfrac{1}{1+0.4\kappa_m^2}$ (see Table 2.2.1) taking into account that for the beam in question of unit width and with height 2H the radius of inertia $i = \sqrt{3H}$. The determination of frequencies ω_{0m} by formula (2.6.5) instead of the more accurate (2.6.17) leads to error <6%, if $2H/l \le 0.1$, $m < 10$, $\beta^2 \le 60$.

The imaginary roots of equation (2.6.18), taking into account that for materials reinforced by filaments $\beta^2 \gg 1$, can be determined with sufficient accuracy by expression

$$\overline{x}_{nm} = (2n-1)\frac{\pi}{2}\sqrt{-1}.$$

Consequently, m frequency of n series

$$\omega_{nm} = \sqrt{3}\frac{H}{l}\omega^*\sqrt{m^2 + \frac{(2n-1)^2\beta^2}{4\beta^2 H^2}}.\qquad (2.6.19)$$

The comparison of values of natural frequencies for beams with relative height $2H/l = 0.1$, calculated according to the given formulas, is given in Table 2.6.1, from which it is clear that

100

Table 2.6.1. The effect of shears on the
natural vibration frequency of beams.

m	$\beta = \dfrac{l}{r_{ii}}$	(1) ω_{0m}/ω^*_m с учетом инерции вращения		(2) ω_{0m}/ω^*_m без учета инерции вращения		ω_{1m}/ω^*_m		$\dfrac{\omega_{2m}}{\omega^*_m}$	$\dfrac{\omega_{3m}}{\omega^*_m}$
		(3) по (2.6.?)	(3) по (2.6.8)	(3) по (2.6.?)	(3) по (2.6.9)	(3) по (2.6.6)	(3) по (2.6.19)	(3) по (2.6.19)	
1	2.6	0.983	0.983	0.987	0.987	70.15	68.78	205.66	312.20
	20	0.911	0.807	0.911	0.901	27.28	27.00	74.61	124.79
	60	0.791	0.700	0.792	0.701	18.08	18.02	44.12	72.06
2	2.6	0.938	0.932	0.951	0.949	20.85	17.95	51.62	85.72
	20	0.745	0.589	0.717	0.606	8.23	8.27	10.30	31.31
	60	0.542	<0	0.511	<0	6.55	6.56	12.09	18.64
3	2.6	0.875	0.818	0.900	0.885	8.61	8.43	23.09	38.15
	20	0.593	0.075	0.579	0.113	4.55	4.58	9.01	14.19
	60	0.395	<0	0.398	<0	3.96	4.00	6.00	9.22
5	2.0	0.735	0.578	0.779	0.680	3.53	3.52	8.50	13.88
	20	0.405	<0	0.410	<0	2.32	2.41	3.69	5.40
	60	0.250	<0	0.251	<0	2.25	2.28	2.79	3.61
10	2.6	0.478	<0	0.527	<0	1.18	1.30	2.32	3.59
	20	0.216	<0	0.219	<0	1.09	1.13	1.33	1.66
	60	0.128	<0	0.129	<0	1.04	1.10	1.18	1.31

KEY: (1) Taking into account rotary inertia;
(2) Not taking into account rotary inertia;
(3) By.

Timoshenko's formulas (2.6.8), (2.6.9) even during the
determination of frequencies of the lowest tones give perceptible
error at large values of parameters β^2, characteristic for the
materials reinforced by filaments. For these materials the shears
strongly lower the values of natural frequencies, therefore
disregarding them can lead to incorrect estimations of Young's
modulus, determined according to the frequency of flexural
vibrations. When determining frequencies ω_{0m} for these materials
the correction, introduced by the account of rotary inertia,
is substantially less than the correction from shears, which
makes it possible with sufficient accuracy for practical
calculations to use formula (2.6.16).

2.6.4. The effect of elastic support and longitudinal force.[1]

The equations of vibrations of the beam on an elastic support, the

---

[1]The effect of longitudinal force on the vibrations of cylin-
drical coil springs, considering them as a bar with low shear
rigidity, was investigated in detail by V. I. Biderman [181].

mass of which can be disregarded with the presence of longitudinal tensile (+N) or compressive (-N) force are obtained from system of equations (2.5.24), (2.5.25), if to them we add the inertia terms:

$$\frac{\partial^2 u}{\partial x^2} + \frac{1}{\beta^2} \cdot \frac{\partial^2 u}{\partial z^2} = \frac{\varrho}{E_x} \cdot \frac{\partial^2 u}{\partial^2 t} ; \tag{2.6.20}$$

$$\left(\frac{N}{2HG_{xz}}\right)\frac{\partial^2 w}{\partial x^2} - \frac{k_0 w}{2HG_{xz}} + \frac{1}{2H}\int_{-H}^{H}\frac{\partial^2 u}{\partial x \partial z}\,dz = \frac{\varrho}{G_{xz}} \cdot \frac{\partial^2 w}{\partial t^2} . \tag{2.6.21}$$

By solving this system for the case of a beam with freely resting ends, similar to the solution of system of equations (2.6.10), (2.6.11), we come to the transcendental equation

$$\omega_{n}^{2} = \omega^{*}_{m}\left(\varphi_m \frac{\mu_m^2}{\lambda_m^2} + \psi_m\right). \tag{2.6.22}$$

where

$$\psi_m = \frac{1}{\lambda^2 E_x I}\left(\frac{k_0}{\lambda_m^2} + N\right).$$

Circular frequencies are determined by expression (2.6.13), in which $\bar{\kappa}_m$ - the roots of equation

$$\operatorname{th}\varkappa_m = \frac{\varkappa_m^3}{\lambda_m^2 H^2} - \varkappa_m\left(\beta^2 - 1 - \frac{k_0}{2HG_{xz}\lambda_m^2} - \frac{N}{2HG_{xz}}\right). \tag{2.6.23}$$

If in the equation of frequencies (2.6.22) we perform the approximate replacement

$$\varphi_m \approx \frac{1}{1 + 0.4\varkappa_m^2} ,$$

then it is converted into biquadratic equation

$$\left(\frac{\omega_m}{\omega^*_m}\right)^4 - \frac{3}{0.4\beta^2\lambda_m^2 H^2}\left[1 + \frac{\lambda_m^2 H^2}{3}(1 + 1.2\beta^2 + 0.4\lambda_m^2 H^2\beta^2\psi_m)\right] \times$$
$$\times\left(\frac{\omega_m}{\omega^*_m}\right)^2 + 1 + \psi_m + 0.4\lambda_m^2 H^2\beta^2\psi_m = 0. \tag{2.6.24}$$

102

By disregarding the rotary inertia, the correction from which for materials reinforced by filaments is an order less than the correction from shear, we have

$$\omega_m{}^2 = \omega^*{}_m(\varphi_m + \psi_m). \tag{2.6.25}$$

After the approximate replacement of

$$\varphi_m \approx \frac{1}{1 + 0.4 \varkappa_m{}^2}$$

for small values of $\varkappa_m{}^2$ formula (2.6.25) can be simplified:

$$\omega_m = \omega^*{}_m(1 - 0.2 H^2 \beta^2 \lambda_m{}^2 + 0.5 \psi_m + 0.1 \psi_m H^2 \beta^2 \lambda_m{}^2). \tag{2.6.26}$$

If we disregard shear ($G_{xz} \to \infty$), then formula (2.6.25) changes to the known formula obtained on the basis of the hypothesis of flat sections [240]:

$$\omega^2 = \omega^{*2}\left(1 + \frac{k_0}{\lambda_m{}^4 E_x I} + \frac{N}{\lambda_m{}^2 E_x I}\right). \tag{2.6.27}$$

In another limiting case ($E_x \to \infty$) the natural vibration frequency approaches not infinity, as follows from classical formula (2.6.27), but a finite quantity, equal to

$$\omega^2 = \frac{\lambda_m{}^2 G_{xz}}{\varrho}\left(1 + \frac{k_0}{2 H G_{xz} \lambda_m{}^2} + \frac{N}{2 H G_{xz}}\right). \tag{2.6.28}$$

From formula (2.6.28) follows

$$\lim_{E_x \to \infty} \omega^2 = \frac{\lambda_m{}^2 G_{xz}}{1.2 \varrho}. \tag{2.6.29}$$

i.e., the error of the approximate solution is the same as in the problem of stability of the rod (§ 2.5).

With an increase of the rigidity of elastic support the
vibration frequency, as can be seen from formula (2.6.25), is
increased. The longitudinal tensile force +N has analogous
effect. In the case of compressive force the vibration frequency
decreases and vanishes when

$$N \longrightarrow N_{\text{кр}\,m} \qquad\qquad (2.6.30)$$

where $N_{\text{кр}\,m} = -\varphi_m N^{\bullet}_{\text{кр}\,m} + \frac{k_0}{\lambda_m^2}$ - the critical force, calculated taking
into account the elastic support (§ 2.5).

§ 2.7. CURVED BARS

2.7.1. Introduced observations. Recently winding has become
one of the principal methods of manufacture of important con-
structions for materials reinforced by filaments. In this case
there is created material which possesses curvilinear anisotropy
[123]. The strong effect of the winding parameters (tensioning
force, number of turns, conditions of polymerization and others)
on the properties of the material in the article required the
development of corresponding methods of tests of the wound articles
and materials. It is recognized (see, for example, [266] and
others) that the most acceptable are samples which have the shape
of a ring or its part - segment. During the manufacture of ring-
shape samples the technology of winding is comparatively easily
reproduced. The testing technique of these samples is quite
simple. However, in the majority of cases the results of tests
of rings and segments are processed, as a rule, according to
formulas of classic strength of materials. Depending on the
relative thickness of the sample and the degree of anisotropy of
material the utilization of these formulas can lead to high errors.
Two dangers are possible. For comparatively thin samples geometric
nonlinearity is developed. With an increase of relative thickness

the weak shear strength begins to play an increasingly greater role.[1]   This is illustrated well by the experimental data presented in Fig. 2.7.1. From the figure one can see that the Young "apparent modulus" of oriented glass fiber-reinforced plastic, determined by the formula of strength of materials, depends substantially on the relative thickness of the sample. Let us note that the error is intensified by dis-regarding the "reptation" of samples from supports.
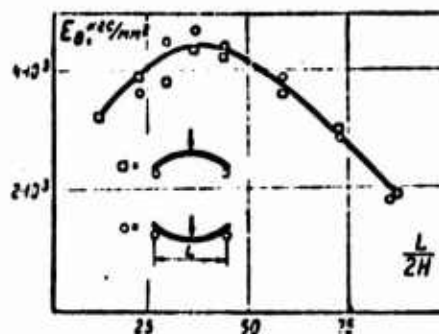

Fig. 2.7.1. The experimental values of Young's modulus of glass fiber-reinforced plastic, determined sample-segment tests. The calculated curve is constructed by the formula which does not consider the effect of shear and slipping on supports.

The account of non-linearity is given in [226]; the effect of shear when testing such samples (and also in the work of similar constructions) can be taken into account as is done for straight rods (§ 2.3). The corresponding equations of bending are derived for a uniform curved beam, which possesses cylindrical orthotropy. The effect of heterogeneity - the effects of bending in the layers of reinforcement - is examined in the works of V. V. Bolotin and his coworkers [38, 43, 53, 118]).

2.7.2. Equation of bending. The rod is related to coordinate system θ, z (Fig. 2.7.2); the corresponding displace-ments are designated by u, w. The curved beam is limited by circular arcs of radii a and b and radial planes $\theta = 0$ and $\theta = \theta_0$. The cross section is a rectangle of unit width, with height $2H = b - a$. The axis of cylindrical orthotropy of material is

----

[1]The weak shear strength presents an even larger danger during endurance tests of rings, when shear creep of materials reinforced by filaments is sharply manifested.
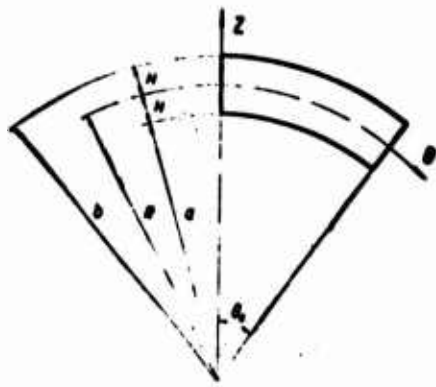
Fig. 2.7.2. Diagram of curved bar.

located at point 0. Considering the height of the rod sufficiently low, in order to disregard the change of radius along it (2H << R), and, as for straight rods (§ 2.2), assuming ε_z = 0 (effect of ε_z estimated in [180]), we represent Hooke law and the connection between deformations and displacements in the form

$$\sigma_\theta = E_\theta \varepsilon_\theta; \quad \tau_{\theta z} = G_{\theta z} \gamma_{\theta z}; \tag{2.7.1}$$

$$\varepsilon_\theta = \frac{1}{R}\left(\frac{\partial u}{\partial \theta} + \omega\right); \quad \gamma_{\theta z} = \frac{\partial u}{\partial z} + \frac{1}{R}\left(\frac{d\omega}{d\theta} - u\right). \tag{2.7.2}$$

The potential energy of deformation $\Im_1$ can be expressed through displacements:

$$\Im_1 = \int_0^{\theta_0} \int_{-H}^{H} \frac{1}{2} \left(\varepsilon_\theta \sigma_\theta + \gamma_{\theta z} \tau_{\theta z}\right) R d\theta dz =$$

$$= \int_0^{\theta_0} \int_{-H}^{H} \frac{1}{2R} \left[E_\theta \left(\frac{\partial u}{\partial \theta} + \omega\right)^2 + G_{\theta z} \left(R\frac{\partial u}{\partial z} + \frac{d\omega}{d\theta} - u\right)^2\right] d\theta dz. \tag{2.7.3}$$

The potential energy of normal load q

$$\Im_2 = - \int_0^\theta q \omega R d\theta, \tag{2.7.4}$$

$q = \int_{-H}^{H} q_z dz$ — total normal load. By composing the expression for

total energy $\Im = \Im_1 + \Im_2$, analogous to § 2.2.2, and solving variational problem $\delta \Im = 0$, we obtain the equation of bending of curved beam:

106

$$\beta^2 \frac{\partial^2 u}{\partial \Theta^2} + R^2 \frac{\partial^2 u}{\partial z^2} + (1+\beta^2)\frac{dw}{d\Theta} - u = 0; \qquad (2.7.5)$$

$$2H\left(\frac{d^2 w}{d\Theta^2} - \beta^2 w\right) + \int\limits_{-H}^{H}\left[R\,\frac{\partial^2 u}{\partial \Theta \partial z} - (1+\beta^2)\frac{\partial u}{\partial \Theta}\right]dz = -\frac{qR^2}{G_{\Theta z}}\,. \qquad (2.7.6)$$

where

$$\beta^2 = \frac{E_\Theta}{G_{\Theta z}}:$$

By introducing curvilinear coordinate x = Rθ instead of angular
coordinate θ, instead of (2.7.5), (2.7.6) we obtain system of
equations

$$\frac{\partial^2 u}{\partial x^2} + \frac{1}{\beta^2}\cdot\frac{\partial^2 u}{\partial z^2} + \frac{1+\beta^2}{\beta^2 R^4}\cdot\frac{dw}{dx} - \frac{1}{\beta^2 R^2}u = 0;$$

$$2H\frac{d^2 w}{dx^2} + \int\limits_{-H}^{H}\frac{\partial^2 u}{\partial x \partial z}\,dz - \frac{2H\beta^2}{R^2}\,w - \frac{1+\beta^2}{R}\int\limits_{-H}^{H}\frac{\partial u}{\partial x}\,dz = -\frac{q}{G_{xz}}\,.$$

which, as is easy to establish, changes to the system of
equations of a straight rod (2.2.13), (2.2.14), when the radius
of curvature R → ∞.

2.7.3. **Bending of circular ring.** The effect of shear during
bending of rods with circular axis is investigated on an example
of a solid ring, loaded by two concentrated forces, applied at
diametrically opposite points. Any transverse load q(θ) can be
represented in the form of Fourier series:

$$q(\Theta) = q_0 + \sum_{m=1}^{\infty} q_m \cos m\Theta, \qquad (2.7.7)$$

where

$$q_m = \frac{2}{\pi}\int\limits_{0}^{\pi} q(\Theta)\cos m\Theta d\Theta.$$

In the case in question (Fig. 2.7.3)

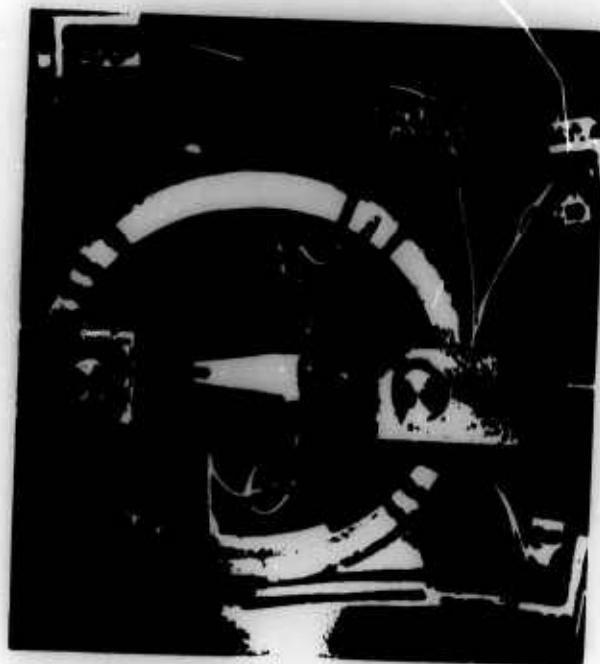$$q_m = \frac{2P}{\pi R} \quad (m = 0, 2, 4\ldots).$$

107

Fig. 2.7.3. The calculation diagram and attachment for loading and measuring deformations. (Failure from shear is distinctly evident - discontinuity of black lines, applied to the sample before loading.)

Since the ring the closed, the solution of system of equations (2.7.5), (2.7.6) should be searched for in the class of functions which satisfy the condition of periodicity on coordinate θ (period 2π):

$$u(\theta, z) = \sum_{m=2, 4, 6 \ldots}^{\infty} u_m(z) \sin m\theta; \qquad (2.7.8)$$

$$w(\theta) = w_0 + \sum_{m=2, 4, 6 \ldots}^{\infty} w_m \cos m\theta. \qquad (2.7.9)$$

As is easy to check by direct substitution, to the term of expansion of load $q_0 = 2P/\pi R$ corresponds the solution of

$$u_0 = 0; \quad w_0 = \frac{q_0 R^2}{2 H E_\theta}. \qquad (2.7.10)$$

With this particular load q_0 = const the deformation of the

108

ring is axisymmetric (shear is absent), and therefore formula
(2.7.10) coincides with the known formula of the strength
of materials [239].

For finding expressions u_m, w_m ($m = 2, 4, 6, \ldots$) system
of equations (2.7.5), (2.7.6) should be converted into system
of ordinary differential equations by substitution of expressions
(2.7.7)-(2.7.9) in (2.7.5), (2.7.6):

$$\frac{d^2 u_m}{dz^2} - \mu_m^2 u_m = \frac{m(1+\beta^2)}{R^2} w_m; \qquad (2.7.11)$$

$$-2H(m^2+\beta^2) w_m + m \int_{-H}^{H} \left[R \frac{\partial u}{\partial z} - (1+\beta^2) u \right] dz = \frac{q_m R^2}{G_{\Theta z}}. \qquad (2.7.12)$$

where

$$\mu_m^2 = \frac{1+m^2\beta^2}{R^2}.$$

The solution of equation (2.7.11) is

$$u_m = C_{1m} \operatorname{sh} \mu_m z + C_{2m} \operatorname{ch} \mu_m z - \frac{1+\beta^2}{1+\beta^2 m^2} m w_m. \qquad (2.7.13)$$

Constants C_m are determined from the condition that tangential
load on the surfaces of ring $z = \pm H$ is absent:

$$R \frac{\partial u}{\partial z} + \frac{dw}{d\Theta} - u = 0.$$

Substitution of expressions (2.7.8), (2.7.9) into this condition
with $z = \pm H$ gives

$$R \frac{d u_m}{dz} - u_m - m w_m = 0,$$

whence

$$C_{1m} = R \mu_m C_{2m}; \quad C_{2m} = \frac{(m^2-1) w_m}{m(1+m^2\beta^2) \operatorname{ch} \varkappa_m}; \quad \varkappa_m = \mu_m H. \qquad (2.7.14)$$

109

Further, from (2.7.12) we find

$$w_m = \frac{q_m R^4}{(m^2-1)^2 E_\theta I \varphi_m} \, . \tag{2.7.15}$$

where, as in § 2.2, $I = \dfrac{2H^3}{3}$ - the moment of inertia of the section

$$\varphi_m = \frac{3(\varkappa_m - \text{th}\, \varkappa_m)}{\varkappa_m^3} \, .$$

Thus, the deflection of points of the ring, loaded by two concentrated forces (Fig. 2.7.3), is equal to

$$w = \frac{PR}{\pi H E_\theta} + \frac{2PR^3}{\pi E_\theta I} \sum_{m=2,4,6\ldots}^{\infty} \frac{\cos m\theta}{(m^2-1)^2 \varphi_m} \, . \tag{2.7.16}$$

2.7.4. Experimental study. During tests of rings by the diagram of Fig. 2.7.3 there are measured the normal displacements of points of vertical $w(0) = w(\pi)$ and horizontal $w(\pm\frac{\pi}{2})$ diameters. After the replacement of parameter ϕ_m in formula (2.7.16) by its approximate value $\dfrac{1}{1+0.4\kappa_m^2}$ (see Table 2.2.1), the expressions for these displacements have the form

$$w(0) = \frac{2PR^3}{\pi E_\theta I} \left[\frac{H^2}{3R^2} + \sum_{m=2,4,6\ldots}^{\infty} \frac{1+0.1\frac{H^2}{R^2}(1+m^2\beta^2)}{(m^2-1)^2} \right] ; \tag{2.7.17}$$

$$w\left(\frac{\pi}{2}\right) = \frac{2PR^3}{\pi E_\theta I} \left[\frac{H^2}{3R^2} + \sum_{m=2,4,6\ldots}^{\infty} (-1)^{?} \frac{1+0.1\frac{H^2}{R^2}(1+m^2\beta^2)}{(m^2-1)^2} \right] . \tag{2.7.18}$$

By disregarding the stretching of the axis of ring, i.e., by rejecting terms which contain H^2/R^2 without factor θ^2, considering that [83]

110

$$\sum_{m=2,4,6,\ldots}^{\infty} \frac{1}{(m^2-1)^2} = \frac{\pi^2}{16} - \frac{1}{2}; \qquad \sum_{m=2,4,6,\ldots}^{\infty} \frac{m^2}{(m^2-1)^2} = \frac{\pi^2}{16};$$

$$\sum_{m=2,4,6,\ldots}^{\infty} \frac{(-1)^{\frac{m}{2}}}{(m^2-1)^2} = -\frac{1}{2} + \frac{\pi}{8}; \qquad \sum_{m=2,4,6,\ldots}^{\infty} \frac{(-1)^{\frac{m}{2}} m^2}{(m^2-1)^2} = -\frac{\pi}{8}.$$

instead of (2.7.17), (2.7.18) we will obtain Timoshenko formulas [239]:

$$w(0) = \frac{PR^3}{E_\theta I}\left(\frac{\pi}{8} - \frac{1}{\pi} + \frac{\pi}{20}\beta^2\frac{H^2}{R^2}\right) = w^*(0)\left(1 + 2{,}11\beta^2\frac{H^2}{R^2}\right); \qquad (2.7.19)$$

$$w\left(\frac{\pi}{2}\right) = -\frac{PR^3}{E_\theta I}\left(\frac{1}{\pi} - \frac{1}{4} + 0{,}1\beta^2\frac{H^2}{R^2}\right) = w^*\left(\frac{\pi}{2}\right)\left(1 + 1{,}46\beta^2\frac{H^2}{R^2}\right). \qquad (2.7.20)$$

The comparison of experimental and theoretical results is given on Fig. 2.7.4 [226]. As is evident, the coincidence of results is quite good. The overstated values of experimental results with small $\frac{2H}{R}$ can be explained by the extensibility of the axis of the ring.

The determination of Young's modulus E_θ of the materials reinforced by filaments, according to the test results of rings (analogous to that conducted during testing of beams, see § 2.3) according to the diagram presented on Fig. 2.7.3 can lead to substantial errors if we do not consider shears, i.e., determine Young's modulus according to formulas [239]:

$$E_f(0) = 0{,}149\frac{PR^3}{2I w(0)}; \qquad (2.7.21)$$

$$E_f\left(\frac{\pi}{2}\right) = 0{,}137\frac{PR^3}{2I w\left(\frac{\pi}{2}\right)}. \qquad (2.7.22)$$

The values of Young's modulus obtained in this case are ficticious. The connection between E_f and E_θ can be obtained by comparing formulas (2.7.21), (2.7.22) with formulas (2.7.19), (2.7.20):

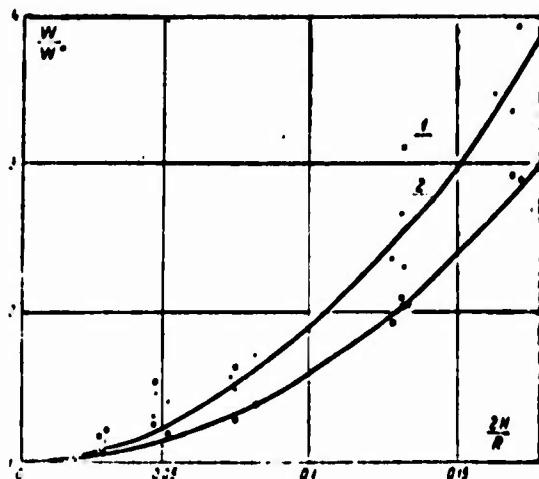Fig. 2.7.4.   Fig. 2.7.5.

Fig. 2.7.4.   The effect of shears on the normal displacements of
points of vertical (×, curve 1) and horizontal ($\bullet$, curve 2) dia-
meters of rings of material JSB-F ($E_\theta = 3.6 \cdot 10^5$ kgf/cm^2, $G_{\theta z} =$
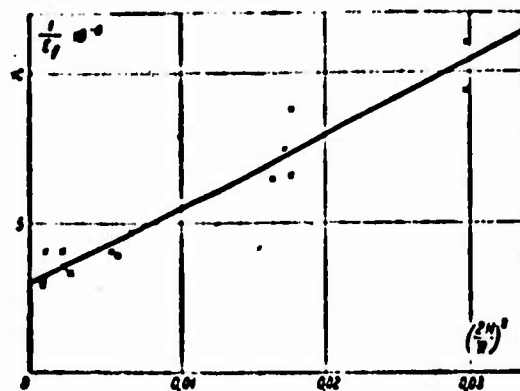$= 2.2 \cdot 10^3$ kgf/cm^2).

Fig. 2.7.5.   The   determination of   moduli E_θ and $G_{r\theta}$ when testing
rings of different relative thickness.

$$\frac{1}{E_f(0)} = \frac{1}{E_\theta} + \frac{0{,}503}{G_{\theta z}}\left(\frac{2H}{R}\right)^2 ; \qquad (2.7.23)$$

$$\frac{1}{E_f\left(\frac{\pi}{2}\right)} = \frac{1}{E_\theta} + \frac{0{,}365}{G_{\theta z}}\left(\frac{2H}{R}\right)^2 . \qquad (2.7.24)$$

Formulas (2.7.23), (2.7.24) have the same structure as (2.3.15).
Consequently, the values of moduli E_θ and $G_{\theta z}$ can be determined
by testing rings with different relationships $\frac{2H}{R}$ and plotting

results in coordinate system $\left(\frac{2H}{R}\right)^2$, $\frac{1}{E_f}$ (Fig. 2.7.5), analogous

to system of coordinates on Fig. 2.3.8.   With loading of rings by
nonaxisymmetric load it is necessary, as when testing beams, to
consider the possibility of failure from shears. For determining
the relative thickness $\frac{2H}{R}$, with which there is accomplished the
transition from failure from normal stresses to failure from

112

tangential stresses, similar to that done in the case of straight rods, let us disregard the deviation of the diagram of bending stresses from linear and tangential stresses from parabolic. Then maximum normal stresses[1]

$$\sigma_{max} = \frac{3M_{max}}{2H^3} = \frac{3PR}{2\pi H^2}; \quad \tau_{max} = \frac{3P}{8H}.$$

Consequently, the type of failure is changed with

$$\frac{2H}{R} = 2.55 \frac{\Pi_\tau}{\Pi_\sigma}.$$

whereas for straight beams this occurs when

$$\frac{2H}{l} = 2 \frac{\Pi_\tau}{\Pi_\sigma}.$$

For the examined materials $\frac{\Pi_\tau}{\Pi_\sigma}$ = 0.03-0.12, consequently, critical relationship $\frac{2H}{R}$ = 0.0765-0.306.

2.7.5. **The effect of shears on the value of critical pressure.** By considering the ring thin and its thickness constant ($\varepsilon_z = 0$), the equations of stability in the case of hydrostatic pressure p can be obtained by substituting in (2.7.6) q = $= \frac{P}{R}\left(\frac{d^2w}{d\theta^2} + w\right)$ [50]:

$$\beta^2 \frac{\partial^2 u}{\partial x^2} + R^2 \frac{\partial^2 u}{\partial z^2} - u + (\beta^2 + 1) \frac{dw}{d\theta} = 0; \qquad (2.7.25)$$

_____

[1]When loading before the failure of thin rings from normal stresses it is necessary to consider the geometric nonlinearity. Generally this diagram of loading is hardly suitable for determining Π_σ [226].

113

$$(2HG_{\theta z} - R)\frac{d^2w}{d\theta^2} - (2HE_\theta + pR)w +$$

$$+ G_{\theta z}\int_{-H}^{H}\left[R\frac{\partial^2 u}{\partial\theta\partial z} - (\beta^2 + 1)\frac{\partial u}{\partial\theta}\right]dz = 0. \qquad (2.7.26)$$

The solution of equation (2.7.25) is known (see 2.7.13). Equation (2.7.26) will be satisfied when

$$p = (m^2 - 1)\frac{E_\theta I}{R^3}\varphi_m.$$

Thus, critical pressure

$$p_{\text{кр}} = p^*_{\text{кр}}\varphi_m, \qquad (2.7.27)$$

where $p^*_{\text{кр}} = \dfrac{(m^2 - 1)E_\theta I}{R^3}$ - critical pressure, determined not taking into account shears. By coefficient ϕ_m there is determined the correction from shear and the compressibility of the axis of ring. In the case of essentially anisotropic materials $\beta^2 \gg 1$, therefore $\kappa_m \simeq m\frac{H}{R}\beta$ and the correction according to formula (2.7.27) is analogous to the correction from shear for critical force of compressed straight rod (§ 2.5).

2.7.6. Free flexural vibrations of the ring in its plane. The equations of vibrations of the ring can be obtained by addition of the following corresponding inertia term (ρ - material density) to the equations of bending (2.7.5), (2.7.6):

$$\beta^2\frac{\partial^2 u}{\partial\theta^2} + R^2\frac{\partial^2 u}{\partial z^2} - u + (\beta^2 + 1)\frac{\partial w}{\partial\theta} = \varrho\frac{R^2}{G_{\theta z}}\cdot\frac{\partial^2 u}{\partial t^2}; \qquad (2.7.28)$$

$$2H\left(\frac{\partial^2 w}{\partial\theta^2} - \beta^2 w\right) + \int_{-H}^{H}\left[R\frac{\partial^2 u}{\partial\theta\partial z} - (\beta^2 + 1)\frac{\partial u}{\partial\theta}\right]dz = 2H\varrho\frac{R^2}{G_{\theta z}}\cdot\frac{\partial^2 w}{\partial t^2}. \qquad (2.7.29)$$

The solution of system (2.7.28), (2.7.29) must be periodic with respect to coordinate θ with period 2π, since the ring is closed,

114

and periodic with respect to time, since the oscillating process is examined. Accepting

$$u = U_m(z) \sin m\Theta \sin (\omega t + \delta);$$
$$w = W_m \cos m\Theta \sin (\omega t + \delta). \tag{2.7.30}$$

from equation (2.7.28) we obtain ordinary differential equation

$$\frac{dU_m}{dz} - \mu_m^2 U_m = \frac{m(1 + \beta^2)}{R^2} W_m. \tag{2.7.31}$$

in which enters parameter

$$\mu_m^2 = \frac{1}{R}(1 + m^2\beta^2 - i^2\beta^2\overline{\omega}_m^2),$$

containing unknown value - the circular frequency of oscillations (here $\overline{\omega}_m = \omega_m \frac{R}{i}\sqrt{\frac{E_\Theta}{\rho}}$ — dimensionless frequency; $i = \frac{H^2}{3R^2}$). The solution of equation (2.7.31) is known (see (2.7.13)). After the substitution of expression (2.7.30) taking into account (2.7.13) into equation (2.7.29) we will obtain the equation for determining the circular frequency

$$-\beta^2 i^4\overline{\omega}_m^4 + i^2(\beta^2 + 1)(m^2 + 1) - (m^2 - 1)^2 +$$
$$+ \frac{m^2(m^2 - \overline{i\omega}_m^2 - 1)^2}{m^2 - i^2\omega_m^2} \cdot \frac{\mathrm{th}\, \varkappa_m}{\varkappa_m} = 0. \tag{2.7.32}$$

For thin rings, when it is possible to disregard the terms which contain powers of small parameter i higher than the second, from (2.7.32) follows the known formula for vibration frequency, determined not taking into account the shears:

$$\omega^{*2} = \frac{E_\Theta I}{2II_\rho R^4} \cdot \frac{m^2(m^2 - 1)^2}{m^2 + 1}. \tag{2.7.33}$$

If we also disregard inertia in circular direction, i.e., reject the right side of equation (2.7.28), then parameter μ_m will not

115

contain ω_m and instead of (2.7.33) we will obtain

$$\omega_1^{*2} = \frac{E_\theta I}{2H\varrho R^4}(m^2-1)^2.$$

(2.7.34)

As is evident, the difference between frequencies ω^* and ω_1^* is decreased with an increase in wave number m. The frequency of the basic tone (when m = 2), determined by formula (2.7.33), is 10% lower than this frequency determined by formula (2.7.34):

$$\omega^* = \frac{2}{\sqrt{5}}\omega_1^*.$$

By disregarding inertia in circular direction, but taking into account shears, we will obtain the formula analogous to formula (2.7.21) for determining critical pressure:

$$\omega^2 = \omega_1^{*2}\varphi_m.$$

(2.7.35)

The structure of formula (2.7.35) is analogous to the structure of formula (2.6.16), by which is determined the frequency of flexural vibrations of beams. Therefore the results of § 2.6.3 and 2.6.4 can be directly used for analysis of the effect of shears on the vibrations of a ring in its plane.

THIRD CHAPTER

PLATES WEAKLY RESISTING SHEAR

§ 3.1.   REFINEMENT OF THE CLASSICAL
THEORY

3.1.1. Brief review. The problems of bending of plates in
strict setting are three-dimensional problems of the theory of
elasticity, the direct solution of which even in the simplest cases
is very complicated.   Therefore the majority of the problems of
bending of plates is solved within the Kirchoff-Love classical
theory, which assumes only three strain tensor components - ε_x,
ε_y and γ_{xy} to be nonzero (plane xy is parallel to the middle plane
of the plate).   This makes it possible to bring the initial three-
dimensional problem to a two-dimensional, which naturally is
solved much more easily.

The Kirchoff-Love hypothesis, called also the hypothesis of
conservation of normal element [86], postulates that the normals
to the middle plane of the plate with deformation retain their
length and are not bent.   This hypothesis contains two assumptions -
about the negligible smallness of lateral deformation ε_z and
shearing strains γ_{xz} and γ_{yz}.   By emphasizing the last property,
the Kirchoff-Love hypothesis is occasionally referred to as the
hypothesis of straight normals.   The question concerning the
replacement of Kirchoff-Love hypothesis by less strong hypotheses
recently attracted the attention of many researchers (see, for

117

example, [71, 82, 124, 133-135, 144-146, 161, 165, 177-179, 254, 255, 261, 286, 297, 303]). The approach proposed by Reissner [307-309] is the most widely used. In this theory, besides basic (precisely in the classical sense) stresses σ_x, σ_y and τ_{xy}, there is also considered the effect of "secondary" stresses τ_{xz}, τ_{yz}, σ_z, the law of distribution of which is determined from the assumption of linear change of stresses σ_x, σ_y, τ_{xy} along the thickness of the plate. As shown by A. L. Gol'denveyzer [87], the Reissner theory can be easily generalized in the case of applying other laws of distribution $\psi(z)$ of stresses σ_x, σ_y and τ_{xy} different from linear. The refined relationships of the Reissner type theory differ from classical (according to Kirchoff-Love) by the terms that contain multiplier $\bar{h}^2$ - square of the relative thickness of the plate. Furthermore, these terms contain numerical coefficients, which, as shown in [87], depending on the selection of function $\psi(z)$ can vary within very wide limits.

The theory of anisotropic plates, which makes it possible to consider "secondary" stresses τ_{xz}, τ_{yz} and σ_z, is developed in detail by S. A. Ambartsumyan and his coworkers. The basic results of the carried out cycle of investigations [8-10, 13, 15, 16] are generalized in books [5, 6]. In the theory of S. A. Ambartsumyan, unlike the theory of Reissner, there is already postulated not law $\psi(z)$, but law $f(z)$ of distribution of tangential stresses τ_{xz}, τ_{yz} according to thickness of the plate. The proposed theory makes it possible to examine any law $f(z)$ of their distribution. However, the solution of the majority of problems is constructed on the reasonable (according to S. A. Ambartsumyan's terminology) selection of function $f(z)$. As approximating function there is selected quadratic parabola. As will be shown subsequently, precisely the parabolic law of distribution of tangential stresses is of the greatest practical interest. The assumption about the parabolic law of distribution of stresses τ_{xz} and τ_{yz} is used also by V. I. Korolev, in whose book [112] there is solved the cycle

118

of problems which are of practical interest for calculating plates and shells of laminated reinforced plastics.

Since $E_z > G_{\alpha z}$ (α = x, y), the basic correction to the classical theory will be given by the account of shears (see § 2.2.6). Quite many investigations are devoted to the theory of plates and shells with small shear rigidity (see, for example, [1, 63, 197, 203, 204, 229, 230-233]).[1] In all these works, which differ among themselves by the approach to determination of the stress-strain state, close results are obtained for the deflections and "basic" stresses σ_x, σ_y, τ_{xy}. As S. A. Ambartsumyan showed [5], when determining these values it is possible to be sufficiently freely directed by the law of distribution f(z) of stresses τ_{xz}, τ_{yz}, which, according to classical theory, are considered secondary. However, for materials reinforced by filaments (with low interlayer strength), the so-called secondary stresses can be the reason for failure. This forces relating them to the number of basic stresses, the more precise determination of which acquires practical interest.

Thus, the application of refined technical theories, constructed on the postulation of the law of distribution of shear stresses, to materials reinforced by filaments, requires the estimation of error introduced by such an approach. In this chapter on an example of the simplest problems, which are solved in the refined formulation, i.e., without postulation of law f(z), there are estimated the limits of applicability of the mentioned theories of bending of plates, which consider shears, to the materials reinforced by filaments. In this case on the basis of the analysis done in § 2.2.5, the material is considered as homogeneous; the effects of bending in rigid layers [36, 37, 40-43, 45] are not considered.

---

[1] The weak shear strength is manifested in the examination of problems of stress concentration around the openings in plates and shells of reinforced plastics [22, 45, 66].

The examined approaches are based on the different assumptions relative to the character of the stress-strain state of the plate. Such approaches, in spite of some inconsistency, in view of their simplicity during sufficient experimental check give practically applicable results faster than stricter theories (which in no way diminishes the value of the latter), which give the possibility in principle to obtain as exact a solution as desired of the initial three-dimensional problem of bending of the plate. The works of I. N. Veku, I. I. Vorovich, B. G. Galerkin, A. L. Gol'denveyzer, N. A. Kil'chevskiy, S. G. Lekhnitskiy, A. I. Lur'ye, Kh. M. Mushtari, V. V. Novozhilov, P. F. Papkovich, V. K. Prokopov, E. Reissner, K. Friedrichs, et al. are dedicated to the exact solution (for detailed review see [77-81, 88, 89, 108, 109, 119, 128]).

3.1.2. **The application of the refined theories to materials reinforced by filaments.** The classical theory, which disregards shearing strains γ_{xz}, γ_{yz} and lateral deformation ϵ_z, in essence examines plates from hypothetical transversally isotropic material with infinite moduli of interlayer shear ($G_{\alpha z} = \infty$) and Young modulus in transversal direction ($E_z = \infty$). Error of classical theory, obviously, is greater, the greater real plate differs from hypothetical ($E_z = G_{\alpha z} = \infty$), i.e., the smaller the actual moduli $G_{\alpha z}$ and E_z in comparison with E_α.

The available, although to be sure scarce, experimental data obtained during bending tests of plates of glass fiber-reinforced plastics and processed according to formulas, which do not consider transverse shears, attest to the fact that the measured values of deflections considerably exceed the calculated. As an example Fig. 3.1.2 shows the dependence of deflection in the center of the annular plate (Fig. 3.1.1) on the degree of orthotropy α, characterized by the relationship of elastic moduli in radial E_r and circular E_θ directions [94]. This relationship was changed

because of the number of reinforcing fibers, stacked in the indicated directions in the process of manufacture of plates.
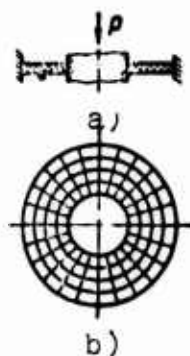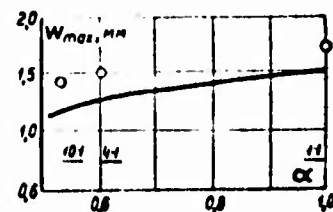

Fig. 3.1.1. Annular plate of glass fiber-reinforced plastic. Diagrams of loading (a) and packing (b) of reinforcing fibers.

Fig. 3.1.2. The effect of the packing of fibers on the rigidity of annular plate. ——— is calculated curve (not taking into account shears); O are experimental points for packing 10:1 (α = 0.53), 4:1 (α = 0.60), 1:1 (α = 1.00).

$a = \dfrac{E_\theta}{E_r}$.

The presented experimental data (Fig. 3.1.3) attest to the possibilities, which open the rational packing of reinforcing for the creation of constructions of the greatest rigidity and strength. In the considered example the strength of cover with packing 10:1 is 22% higher, and deflections 25% less than for a plate with packing 1:1 [206].

For polymer materials reinforced by glass and boron fibers $\dfrac{G_{\alpha z}}{E_\alpha} \approx 0.01\text{-}0.1$, $\dfrac{E_z}{E_\alpha} \approx 0.1\text{-}0.2$ (see Table 1.1.1). Consequently, the calculation of plates of such materials according to Kirchoff-Love theory, which is indifferent to the terms which have multiplier of type $E_\alpha/G_{\alpha z}$, E_α/E_z, can lead to inadmissible errors; plates of anisotropic materials of the type in question work as plates of greater thickness (in comparison with isotropic plates

of the same dimensions), therefore for them the deficiencies of the Kirchoff-Love theory appear very strongly. In the problems examined in the Third Chapter there is considered only the correction from transverse shears γ_{xz} and γ_{yz}. It, as a rule, substantially exceeds the corrections from the account of transverse deformation ε_z and flexural effects of the reinforcement. This is distinctly evident on Figs. 3.1.4, 3.1.5, borrowed from [54].
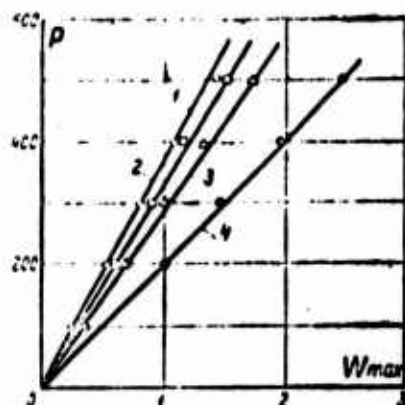

Fig. 3.1.3. The dependence of maximum deflection on the packing of reinforcement. The ratio of the number of radial layers to circular: 1 - 10:1; 2 - 4:1; 3 - 1:1; 4 - with chaotic packing of fibers.

Fig. 3.1.4. The effect of different factors on the deflection of a square plate (a × a × × 2H) under sinusoidal load [54]; n = 5, E'/E" = 20, h'/(h' + h") = 0.7 (axis of abscissa - deflection according to Kirchoff-Love: 1, 2 - deflection of the upper and lower faces of the plate, calculated taking into account γ_{xz}, γ_{yz}, ε_z and flexural effects in the reinforcement; 3 - deflection not taking into account ε_z; 4 - deflection taking into account only γ_{xz} and γ_{yz}).
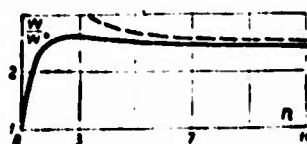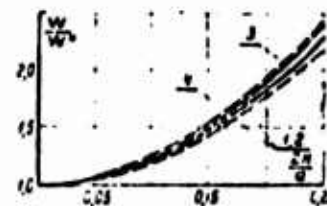

Fig. 3.1.5. The effect of flexural effects in the reinforcement on the deflection of n-layer plate [54]. ——— is the deflection calculated taking into account flexural effects; --- is not taking into account flexural effects.

122

§ 3.2. RECTANGULAR PLATES

3.2.1. Basic dependences. The orthotropic plate, referred to coordinate axes x, y, z (Fig. 3.2.1), so that its middle plane, which is simultaneously the plane of elastic symmetry,
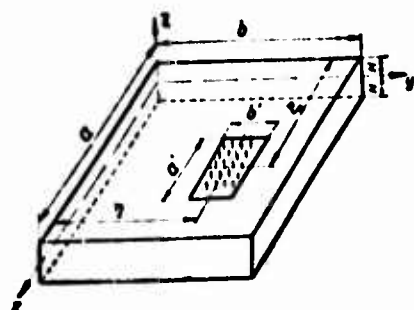

Fig. 3.2.1. The diagram of loading of orthotropic plate.

coincides with plane xy, and planes xz and yz are parallel to the two remaining planes of elastic symmetry.[1] If we disregard the change of the thickness of plate 2H ($\varepsilon_z = 0$), then Hooke law in the case in question has the form

$$\sigma_x - \bar{E}_x \epsilon_x + \bar{E}_x \nu_{yx}\epsilon_y; \quad \sigma_y - \bar{E}_y \epsilon_y + \bar{E}_x \nu_{xy}\epsilon_x;$$

$$\tau_{xy} - G_{xy}\gamma_{xy}, \quad \tau_{xz} - G_{xz}\gamma_{xz}; \quad \tau_{yz} - G_{yz}\gamma_{yz}.$$

(3.2.1)

where

$$\bar{E}_x = \frac{E_x}{1 - \nu_{xy}\nu_{yx}}; \quad \bar{E}_y = \frac{E_y}{1 - \nu_{xy}\nu_{yx}}.$$

Accordingly the potential strain energy

$$\vartheta_1 = \int_S l_1 dS,$$

(3.2.2)

where S is the area of the middle surface of plate,

$$l_1 = \frac{1}{2} \int_{-H}^{H} (\epsilon_x\sigma_x + \epsilon_y\sigma_y + \tau_{xy}\gamma_{xy} + \tau_{xz}\gamma_{xz} + \tau_{yz}\gamma_{yz}) dz =$$

$$= \frac{1}{2} \int_{-H}^{H} \left[\bar{E}_x \left(\frac{\partial u}{\partial x}\right)^2 + \bar{E}_y \left(\frac{\partial v}{\partial y}\right)^2 + 2\nu_{xy}\bar{E}_x \frac{\partial u}{\partial x} \cdot \frac{\partial v}{\partial y} + G_{xy}\left(\frac{\partial u}{\partial y} + \frac{\partial v}{\partial x}\right)^2 + \right.$$

$$\left. + G_{xz}\left(\frac{\partial w}{\partial x} + \frac{\partial u}{\partial z}\right)^2 + G_{yz}\left(\frac{\partial w}{\partial y} + \frac{\partial v}{\partial z}\right)^2 \right] dz.$$

---

[1]The rectangular orthotropic plate, loaded at an angle to the axes of elastic symmetry, is examined by L. I. Balabukh [25].

Potential energy of transverse load $q(x, y)$

$$\mathfrak{I}_2 = \int_S L_2 dS, \tag{3.2.3}$$

where

$$L_2 = -q\mathfrak{w}.$$

Since the total potential energy $\mathfrak{I} = \mathfrak{I}_1 + \mathfrak{I}_2$ in the case of equilibrium must have minimum value, it must be $\delta\mathfrak{I} = 0$. The Ostrogradskiy-Euler equations correspond to this variational problem (see, for example, [43]):

$$\frac{\partial L}{\partial u} - \frac{\partial}{\partial x} \cdot \frac{\partial L}{\partial\left(\frac{\partial u}{\partial x}\right)} - \frac{\partial}{\partial y} \cdot \frac{\partial L}{\partial\left(\frac{\partial u}{\partial y}\right)} - \frac{\partial}{\partial z} \cdot \frac{\partial L}{\partial\left(\frac{\partial u}{\partial z}\right)} = 0;$$

$$\frac{\partial L}{\partial v} - \frac{\partial}{\partial x} \cdot \frac{\partial L}{\partial\left(\frac{\partial v}{\partial x}\right)} - \frac{\partial}{\partial y} \cdot \frac{\partial L}{\partial\left(\frac{\partial v}{\partial y}\right)} - \frac{\partial}{\partial z} \cdot \frac{\partial L}{\partial\left(\frac{\partial v}{\partial z}\right)} = 0; \tag{3.2.4}$$

$$\frac{\partial L}{\partial \mathfrak{w}} - \frac{\partial}{\partial x} \cdot \frac{\partial L}{\partial\left(\frac{\partial \mathfrak{w}}{\partial x}\right)} - \frac{\partial}{\partial y} \cdot \frac{\partial L}{\partial\left(\frac{\partial \mathfrak{w}}{\partial y}\right)} = 0.$$

After substitution of integrand $L = L_1 + L_2$ of total energy of system $\mathfrak{I}$ in (3.2.4) there are obtained the equations of bending [185]:

$$E_x \frac{\partial^2 u}{\partial x^2} + G_{xy} \frac{\partial^2 u}{\partial y^2} + G_{xz} \frac{\partial^2 u}{\partial z^2} + (G_{xy} + E_x \nu_{yx}) \frac{\partial^2 v}{\partial x \partial y} = 0; \tag{3.2.5}$$

$$E_y \frac{\partial^2 v}{\partial y^2} + G_{xy} \frac{\partial^2 v}{\partial x^2} + G_{yz} \frac{\partial^2 v}{\partial z^2} + (G_{xy} + E_x \nu_{xy}) \frac{\partial^2 u}{\partial x \partial y} = 0; \tag{3.2.6}$$

$$2HG_{xz} \frac{\partial^2 \mathfrak{w}}{\partial x^2} + 2HG_{yz} \frac{\partial^2 \mathfrak{w}}{\partial y^2} + \int_{-H}^{H} \left(G_{xz} \frac{\partial^2 u}{\partial x \partial z} + G_{yz} \frac{\partial^2 v}{\partial y \partial z} \right) dz = -q. \tag{3.2.7}$$

which are simplified Lamé equations for orthotropic body:

124

$$a_{xx}\frac{\partial^2 u}{\partial x^2} + G_{xy}\frac{\partial^2 u}{\partial y^2} + G_{xz}\frac{\partial^2 u}{\partial z^2} + (G_{xy}+a_{xy})\frac{\partial^2 v}{\partial x\partial y} +$$

$$+ (G_{xz}+a_{xz})\frac{\partial^2 w}{\partial x\partial z} = 0;$$

$$a_{yy}\frac{\partial^2 v}{\partial y^2} + G_{xy}\frac{\partial^2 v}{\partial x^2} + G_{yz}\frac{\partial^2 v}{\partial z^2} + (G_{xy}+a_{xy})\frac{\partial^2 u}{\partial x\partial y} +$$

$$+ (G_{yz}+a_{yz})\frac{\partial^2 w}{\partial y\partial z} = 0;$$

$$a_{zz}\frac{\partial^2 w}{\partial z^2} + G_{xz}\frac{\partial^2 w}{\partial x^2} + G_{yz}\frac{\partial^2 w}{\partial y^2} + (G_{xz}+a_{xz})\frac{\partial^2 u}{\partial x\partial z} +$$

$$+ (G_{yz}+a_{yz})\frac{\partial^2 v}{\partial y\partial z} = 0,$$

where

$$a_{xx}=\frac{E_x}{B}(1-v_{yz}v_{zy});\quad a_{yy}=\frac{E_y}{B}(1-v_{zx}v_{xz});\quad a_{zz}=\frac{E_z}{B}(1-v_{xy}v_{yx});$$

$$a_{xy}=a_{yx}=\frac{E_x}{B}(v_{xy}+v_{xz}v_{zy})=\frac{E_y}{B}(v_y+v_{yz}v_{zx});$$

$$a_{yz}=a_{zy}=\frac{E_y}{B}(v_{yz}+v_{yx}v_{xz})=\frac{E_z}{B}(v_{zy}+v_{zx}v_{xy});$$

$$a_{xz}=a_{zx}=\frac{E_z}{B}(v_{zx}+v_{zy}v_{yx})=\frac{E_x}{B}(v_{xz}+v_{xy}v_{yz});$$

$$B = 1 - v_{xy}v_{yx} - v_{yz}v_{zy} - v_{zx}v_{xz} - v_{xy}v_{yz}v_{zx} - v_{yx}v_{zy}v_{xz}.$$

in this case where the hypothesis about absolutely transversal rigidity of the body is applicable ($1/E_z = v_{zx} = v_{zy} = 0$).

3.2.2.   Freely supported plate under sinusoidal load.   The system of initial equations (3.2.5)-(3.2.7) can be converted into a system of simple differential equations, if

$$q(x, y) = q_{max}\sin\lambda_m x\sin\lambda_n y. \tag{3.2.8}$$

and displacements $u(x, y, z)$, $v(x, y, z)$, $w(x, y)$ are sought in the form

$$u = u_{mn}(z)\cos\lambda_m x\sin\lambda_n y;$$
$$v = v_{mn}(z)\sin\lambda_m x\cos\lambda_n y; \tag{3.2.9}$$
$$w = w_{mn}\sin\lambda_m x\sin\lambda_n y.$$

125

Here $\lambda_m = \frac{m\pi}{a}$; $\lambda_n = \frac{n\pi}{b}$ $(m, n = 1, 2, 3 \ldots)$; w_{mn} is an unknown constant;

$u_{mn}(z)$, $v_{mn}(z)$ - unknown functions of variable z. In this case at the edges of the plate (Fig. 3.2.1) x = 0, x = a, y = 0, y = b the conditions of free support are automatically satisfied

$$w = 0; \quad \sigma_x = E_x \frac{\partial u}{\partial x} + E_x \nu_{xy} \frac{\partial v}{\partial y} = 0;$$

$$\sigma_y = E_y \frac{\partial v}{\partial y} + E_x \nu_{xy} \frac{\partial u}{\partial x} = 0.$$

Substitution of (3.2.9) in equations (3.2.5), (3.2.6) converts them into a system of two ordinary differential equations:

$$\begin{cases} \dfrac{\partial^2 u_{mn}}{\partial z^2} = A_{1mn} u_{mn} + A_{2mn} v_{mn}; \\[2mm] \dfrac{\partial^2 v_{mn}}{\partial z^2} = A_{3mn} u_{mn} + A_{4mn} v_{mn}; \end{cases}$$

$$A_{1mn} = \frac{1}{G_{xz}} (E_x \lambda_m^2 + G_{xy} \lambda_n^2); \quad A_{2mn} = \frac{1}{G_{xz}} (G_{xy} + \nu_{xy} E_x) \lambda_m \lambda_n; \qquad (3.2.10)$$

$$A_{3mn} = A_{2mn} \frac{G_{xz}}{G_{yz}}; \quad A_{4mn} = \frac{1}{G_{yz}} (E_y \lambda_n^2 + G_{xy} \lambda_m^2).$$

Characteristic equation of system (3.2.10)

$$s_i - (A_{1mn} + A_{4mn}) s^2 + A_{1mn} A_{4mn} - A_{2mn} A_{3mn} = 0 \qquad (3.2.11)$$

(for real materials, reinforced by fibers, which have $A_{1mn}A_{4mn} -$
$- A_{2mn}A_{3mn} > 0$) has four real roots: $\pm s_1$ and $\pm s_2$, where

$$S_1^2 - A_{1mn} \frac{1+p_{mn}}{2} + A_{4mn} \frac{1-p_{mn}}{2};$$

$$S_2^2 - A_{1mn} \frac{1-p_{mn}}{2} + A_{4mn} \frac{1+p_{mn}}{2};$$

$$p_{mn} = \sqrt{1+C_{mn}^2}; \quad C_{mn} = \frac{2G_{xz} A_{2mn}}{G_{yz} (A_{1mn} - A_{4mn})}.$$

126

In the case of absence of tangential load on the surfaces of the plate $(z = \pm H)$

$$\frac{\partial u}{\partial z} + \frac{\partial w}{\partial x} = 0; \quad \frac{\partial v}{\partial z} + \frac{\partial w}{\partial y} = 0$$

the solution of system of equations (3.2.10) will have the form

$$u_{mn} = C_{1mn} \operatorname{sh} s_1 z + C_{2mn} \operatorname{sh} s_2 z;$$
$$v_{mn} = C_{3mn} \operatorname{sh} s_1 z + C_{4mn} \operatorname{sh} s_2 z,$$

(3.2.12)

and constants C_{mn} will be determined by dependences:

$$C_{1mn} = -\frac{\lambda_m}{2s_1 \operatorname{ch} s_1 H}(1 + \gamma_{mn})w_{mn};$$

$$C_{3mn} = C_{1mn}\frac{c_{mn}G_{xz}}{(p_{mn}+1)G_{yz}};$$

$$C_{2mn} = -\frac{\lambda_m}{2s_2 \operatorname{ch} s_2 H}(1 - \gamma_{mn})w_{mn};$$

$$C_{4mn} = C_{2mn}\frac{c_{mn}G_{xz}}{(p_{mn}-1)G_{yz}};$$

$$\gamma_{mn} = \frac{1}{p_{mn}}\left(1 + \frac{G_{yz}\lambda_m}{G_{xz}\lambda_n}c_{mn}\right).$$

The unknown constant w_{mn} is found from equation (3.2.7) after substitution of (3.2.8), (3.2.9) in it taking into account (3.2.12):

$$w_{mn} = \frac{q_{mn}}{B_{mn}}.$$

(3.2.13)

In equation (3.2.13)

$$B_{mn} = 2HG_{xz}\lambda_m^2\left\{\left(1 + \frac{G_{xz}\lambda_n^2}{G_{xz}\lambda_m^2}\right) - \frac{1+\gamma_{mn}}{2}\left[1 + \frac{\lambda_m c_{mn}}{\lambda_n(p_{mn}+1)}\right]\frac{\operatorname{th} s_1 H}{s_1 H} - \frac{1-\gamma_{mn}}{2}\left[1 + \frac{\lambda_m c_{mn}}{\lambda_n(p_{mn}-1)}\right]\frac{\operatorname{th} s_2 H}{s_2 H}\right\}.$$

127

Thus the solution is obtained of the problem of bending of the plate without a priori postulation of the law of distribution of transverse shears f(z) along the thickness of the plate. The analysis of this solution (estimation of the effect of shears) and its comparison with the solutions obtained on the basis of the postulation of law f(z) can be the most visually accomplished on an example of a transversally isotropic plate.

3.2.3. The effect of shears on deflection and stresses.

In the case of transversal isotropy of material (planes of istropy are parallel to the middle plane of the plate), when

$$
\bar{E}_x = \bar{E}_y = E = \frac{E}{1-\nu^2}; \quad \nu_{xy} = \nu_{yx} = \nu;
$$

$$
G_{xy} = \frac{E}{2(1+\nu)}; \quad G_{xz} = G_{yz} \quad G_1;
$$

$$
A_{1mn} = \beta^2\left(\lambda_m^2 + \lambda_n^2 \frac{1-\nu}{2}\right); \quad A_{2mn} = A_{3mn} = \beta^2 \lambda_m \lambda_n \frac{1+\nu}{2};
$$

$$
A_{4mn} = \beta^2\left(\lambda_n^2 + \lambda_m^2 \frac{1-\nu}{2}\right); \quad c_{mn} = \frac{2\lambda_m \lambda_n}{\lambda_m^2 - \lambda_n^2};
$$

$$
p_{mn} = \frac{\lambda_m^2 + \lambda_n^2}{\lambda_m^2 - \lambda_n^2}; \quad s_1^2 = \frac{\varkappa_{mn}^2}{H^2}; \quad s_2^2 = \frac{\varkappa_{mn}^2}{H^2} \cdot \frac{1-\nu}{2}; \quad \gamma_{mn} = 1;
$$

$$
C_{1mn} = -\frac{\lambda_m H}{\varkappa_{mn} \operatorname{ch} \varkappa_{mn}}; \quad C_{2mn} = C_{3mn} = 0; \quad C_{4mn} = C_{1mn} \frac{\lambda_n}{\lambda_m};
$$

$$
B_{mn} = E_x I (\lambda_m^2 + \lambda_n^2)^2 q_{mn},
$$

(3.2.14)

the expressions for displacements (3.2.12), (3.2.13) are substantially simplified:

$$
u_{mn} = -\frac{\lambda_m H \operatorname{sh} \varkappa_{mn} \frac{z}{H}}{\varkappa_{mn} \operatorname{ch} \varkappa_{mn}} w_{mn};
$$

$$
v_{mn} = -\frac{\lambda_n H \operatorname{sh} \varkappa_{mn} \cdot \frac{z}{H}}{\varkappa_{mn} \operatorname{ch} \varkappa_{mn}} w_{mn};
$$

(3.2.15)

$$
w_{mn} = w^*_{mn} q_{mn}^{-1},
$$

where $\varkappa_{mn}^2 = (\lambda_m^2 + \lambda_n^2) H^2 \beta^2$; $\beta^2 = \frac{E}{G_1}$; $q_{mn} = \frac{3(\varkappa_{mn} - \operatorname{th} \varkappa_{mn})}{\varkappa_{mn}^3}$; $w^*_{mn} = \frac{q_{mn}(\lambda_m^2 + \lambda_n^2)}{16D}$

deflection, found without taking into account shears; $D = \frac{2EH^3}{3(1-\nu^2)}$ — flexural rigidity of the plate.

The law of distribution of tangential stresses τ_{xz} and τ_{yz} along the thickness of the plate $f^{(0)}(z)$ (Table 3.2.1) is the same as in the beam bent by sinusoidal load (§ 2.2). In S. A. Ambartsumyan's works [5, 6] there are examined laws $f^{(1)}(z)$, $f^{(2)}(z)$, $f^{(3)}(z)$, given in Table 3.2.1 , where expressions are also written out for other calculated values when m = n = 1, a = b. It is easy to check that when $\kappa_{mn} \to 0$ the refined expressions change to classical.

Table 3.2.1. Deflections and stresses with different laws of distribution of transverse shears along the thickness of the plate.

$f(z)$	$\frac{w}{w^*}$	$\frac{\sigma}{\sigma^*}$	$p = \frac{\tau_{max}}{\sigma_{max}}$
$f^{(0)} = \dfrac{\operatorname{ch} \varkappa_{11} \cdot \frac{z}{H}}{\operatorname{ch} \varkappa_{11}}$	$\dfrac{\varkappa_{11}^3}{3(\varkappa_{11} - \operatorname{th} \varkappa_{11})}$	$\dfrac{H \operatorname{sh} \varkappa_{11} \frac{z}{H}}{\varkappa_{11} z_i \operatorname{ch} \varkappa_{11}}$	$B \dfrac{\operatorname{ch} \varkappa_{11} - 1}{\operatorname{sh} \varkappa_{11}}$
$f^{(1)} = 1 - \dfrac{z^2}{H^2}$	$1 + 0.1\varkappa_{11}^2$	$1 - 0.1\varkappa_{11}^2 + 0.167\varkappa_{11}^2 \cdot \dfrac{z^2}{H^2}$	$\dfrac{B\varkappa_{11}}{2.4 + 0.134\varkappa_{11}^2}$
$f^{(2)} = 1 - \dfrac{z^4}{H^4}$	$1 + 0.381\varkappa_{11}^2$	$1 - 0.035\varkappa_{11}^2 + 0.083\varkappa_{11}^2 \dfrac{z^2}{H^2}$	$\dfrac{B\varkappa_{11}}{2.4 + 0.115\varkappa_{11}^2}$
$f^{(3)} = \text{const}$	$1 + 0.333\varkappa_{11}^2$	1	$\dfrac{B\varkappa_{11}}{3}$

In the table $B = \frac{E(1+\nu)}{2G_1(1-\nu)}$. The asterisk designates the values calculated without taking into account transverse shears.

Figure 3.2.2 gives graphs w/w^* and $\sigma_{max}/\sigma^*_{max}$, characterizing the amount of correction to the classical theory, introduced by the account of shear for the area of practically important values of parameter $\kappa_{11} = \pi\sqrt{2}\beta\frac{H}{a}$. As can be seen from the given graphs, this correction is most essential when determining deflections.

The disagreement between results, obtained without postulation of law $f(z)$ (we find law $f^{(0)}(z)$ in the course of solution) and with its postulation in the form $f^{(1)}$, $f^{(2)}$, $f^{(3)}$, is illustrated by graphs $w/w^{(0)}$, $\sigma_{max}/\sigma_{max}^{(0)}$, $\tau_{max}/\tau_{max}^{(0)}$, provided on Fig. 3.2.3; the diagrams of tangential and normal stresses along the thickness of the plate are given on Figs. 3.2.4 and 3.2.5. From these results it follows that $f^{(0)}$ is satisfactorily approximated by law $f^{(1)}$, whereas the arbitrary selection of law $f^{(2)}$ or $f^{(3)}$ leads to substantial error during determination of τ_{max} and p. Generally speaking, with

Fig. 3.2.2. The effect of shears on deflection and stresses σ_x and σ_y. 1-3 - laws investigated by S. A. Ambartsumyan [5]; 0 - solution without postulation of shears.

replacement of $f(z)$ by a parabola the error can be significant (see [87]); however, for a sufficiently broad class of problems it is small and the utilization of such an approach can be fruitful.
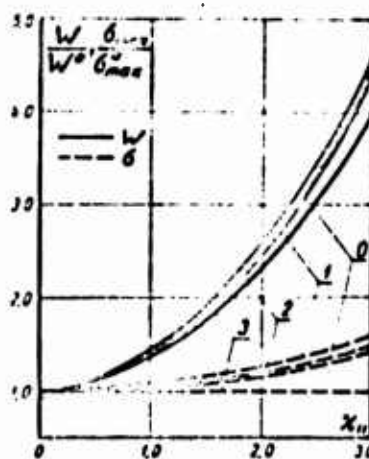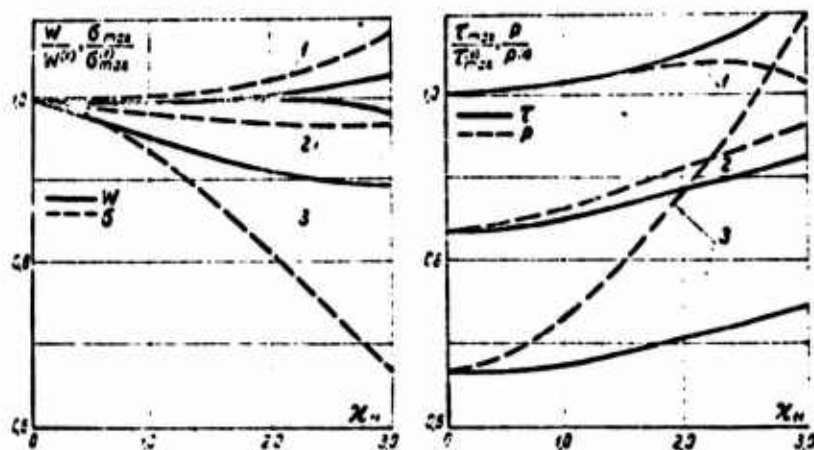

Fig. 3.2.3. The effect of the taken law $f(z)$ on deflection, maximum normal and tangential stresses and relationship $p = \sigma_{max}/\tau_{max}$. 1-3 - laws investigated by S. A. Ambartsumyan [5].
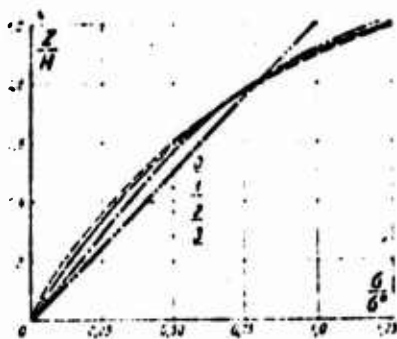
130

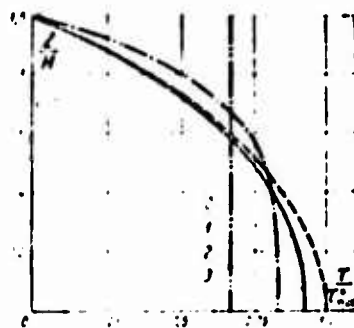Fig. 3.2.4. Diagrams of normal stresses σ_x and σ_y along the thickness of the plate.

Fig. 3.2.5. Diagrams of tangential stresses τ_{xz} and τ_{yz} along the thickness of the plate.

3.2.4. **Deflection of orthotropic plate.** In the case of a square plate (a × a), reinforced identically in two mutually perpendicular directions x and y, $E_x = E_y = E$, $\nu_{xy} = \nu_{yx} = \nu$, $G_{xz} = G_{yz} = G_1$ and the roots of characteristic equations (3.2.11) are determined by expression

$$s_{1,2}^2 = \frac{x_0}{4}\left[(n^2 + m^2)(1-\mu) \pm \sqrt{4n^2m^2(\nu+\mu)^2 + (n^2+m^2)(1-\mu)^2}\right];$$

$$x_0^2 = 2\pi^2\beta^2\frac{H^2}{a^2}; \quad \mu = \frac{G_{xy}(1-\nu^2)}{E}.$$

The general term of expansion q_{mn} of transverse load $q(x, y)$ into double trigonometric Fourier series

$$q(x, y) = \sum_{m=1}^{\infty} \sum_{n=1}^{\infty} q_{mn} \sin \lambda_m x \sin \lambda_n y$$

is determined by formula

$$q_{mn} = \int_0^a \int_0^b q(x, y) \sin \lambda_m x \sin \lambda_n y \, dx \, dy.$$

For the case of load evenly distributed along the area of a rectangle with the center at point (ξ, η) and sides a' and b'

131

(Fig. 3.2.1) with intensity q = P/a'b', where P is the total load,

$$q_{mn} = \frac{16P}{\pi^2 mna'b'}\sin\lambda_m\xi \sin\lambda_n\eta \sin\lambda_m \frac{a'}{2}\sin\lambda_n \frac{b'}{2}$$
$$(m, n = 1, 2, 3 \ldots).$$

Hence for even load along the entire area of the plate, when ξ = 0.5 a, η = 0.5 b, a' = a, b' = b

$$q_{mn} = \frac{16q}{\pi^2 mn} \quad (m, n = 1, 3, 5 \ldots).$$

For concentrated force P, applied at the point with coordinates ξ, η,

$$q_{mn} = \frac{4P}{ab}\sin\lambda_m\xi \sin\lambda_n\eta.$$

If force P is evenly distributed over the area of the circle of radius c' with the center at point (ξ, η), then

$$q_{mn} = \frac{8P\sin\lambda_m\xi\sin\lambda_n\eta}{abc'\sqrt{\lambda_m{}^2+\lambda_n{}^2}} J_1(c'\sqrt{\lambda_m{}^2+\lambda_n{}^2}),$$

where J_1 is the Bessel function of the first order. The deflection at the point with coordinates (x, y) is determined by formula

$$w = \frac{3a^2(1-\nu^2)}{2\pi^4 H^3 E}S. \tag{3.2.16}$$

The form of multiplier S depends on the assumptions forming the basis of the calculation scheme. If we disregard transverse shears [123], then

$$S = \sum_{m=1}^{\infty} \sum_{n=1}^{\infty} \frac{q_{mn}\sin\lambda_m x \cdot \sin\lambda_n y}{m^4 + n^4 + 2m^2n^2(\nu + 2\mu)} \tag{3.2.17}$$

If we consider transverse shears and accept that along the

thickness of the plate they are distributed according to the law
of quadratic parabola [5], then

$$S_1 = \frac{1}{5} \sum_{m=1}^{\infty} \sum_{n=1}^{\infty} \frac{5 + \varkappa_1(1+\mu)(n^2+m^2) + 0.2\varkappa_{11}[\mu(m^4+n^4)+m^2n^2(1-2\mu\nu-\nu^2)]}{m^4+n^4+2m^2n^2(\nu+2\mu) + \varkappa_{11}(m^2+n^2)[\mu(m^4+n^4)+m^2n^2(1-2\mu\nu-\nu^2)]} \times$$
$$\times q_{m,n} \sin \lambda_m x \sin \lambda_n y \qquad (3.2.18)$$

(formulas given in [112] coincide with expression S_1). Without
being given the law of their distribution (according to formula
3.2.13), we obtain [218]

$$S_2 = \frac{\varkappa_1^2}{3} \sum_{m=1}^{\infty} \sum_{n=1}^{\infty} \frac{q_{m,n} \sin \lambda_m x \sin \lambda_n y}{(n^2+m^2)\left(2\frac{\operatorname{th} s_2}{s_2} - \frac{\operatorname{th} s_1}{s_1}\right) + \frac{4n^2m^2(\nu+\mu)+(n^2-m^2)^2(1-\mu)}{[4n^2m^2(\nu+\mu)^2+(n^2-m^2)^2(1-\mu)]}\left(\frac{\operatorname{th} s_2}{s_2} - \frac{\operatorname{th} s_1}{s_1}\right)} \qquad (3.2.19)$$

As is easy to check, when $\kappa_1 \to 0$ $S_1 \to S_2 \to S^*$, i.e., refined
solutions (3.2.18), (3.2.19) coincide with classical (3.2.17), if
the plate is infinitely thin or has infinite shear rigidity in
the transverse planes. It should be noted that when a' → 0, b' →
→ 0, i.e., in the case of concentrated force, the expression for
deflection w at the point of application of force, calculated
by formulas (3.2.18) or (3.2.19), diverges, since the sum of

$\sum\limits_{m=1}^{\infty} \sum\limits_{n=1}^{\infty} \frac{1}{m^2+n^2}$ does not have a limit [83] (the physical unreality of

such a result shows the groundlessness of the assumption about
the fact that the force is applied at the point). The expression
for S^* converges everywhere. The quickness of convergence of
series S_2 is represented by Table 3.2.2, in which the values
are given for particular sums of S_2 in fractions of the addend,
if we are restricted to terms in which $m \le r$ and $n \le r$. The
results given in the table are calculated for $\nu = 0.1$, $\mu = 0.1$,

133

Table 3.2.2. For estimation of the convergence of series for determining the deflections.

	$x_{11} = 1.0$				$a' = 0.20a$		
r	$a'=0.04a$	$a'=0.10a$	$a=0.20a$	$a'=a$	x_{11} 0.1	$x_{11}=1.0$	$x_{11}=2.0$
1	1.000	1.000	1.000	1.000	1.000	1.000	1.000
3	1.162	1.182	1.138	0.601	1.062	1.138	1.214
5	1.235	1.259	1.183	0.660	1.072	1.183	1.333
7	1.282	1.303	1.197	0.640	1.074	1.197	1.368
9	1.315	1.329	1.200	0.649	1.074	1.200	1.374
11	1.310	1.346	1.199	0.644	1.074	1.999	1.371
13	1.300	1.356	1.196	0.647	1.074	1.196	1.365
15	1.376	1.361	1.194	0.645	1.074	1.194	1.360
17	1.390	1.364	1.193	0.646	1.074	1.193	1.358
19	1.401	1.364	1.193	0.646	1.074	1.193	1.357

$x = y = \xi = \eta = 0.5a$. The correction from shear, calculated by formula (3.2.18), for case $\xi = \eta = 0.5a$, $a' = b' = 0.2a$ is
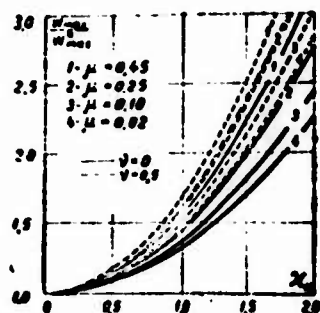

Fig. 3.2.6. The effect of shears on the deflection of centrally loaded plates.

illustrated by Fig. 3.2.6, on which there are given graphs $w_2/w^* = S_2/S^*$ at different values of Poisson ratio ν and parameter μ. For the comparison of results obtained by formulas (3.2.18) and (3.2.19) Fig. 3.2.6 also gives curve $w_1/w^* = S_1/S^*$ (designated ——·——), constructed for the case $\nu = 0.5$, $\mu = 0.25$. As is evident, it differs little from the corresponding curve w_2/w^*, which attests to the good approximation which the selection of function $f(z)$ in the form of quadratic parabola gives.

3.2.5. Experimental estimation. The experimental study (in the range of loads at which deviation from linear elasticity was not observed) of the effect of transverse shears on deflection is conducted on freely supported square ($a \times a$) plates made of

134

glass fiber-reinforced plastics equally reinforced in two directions (packing 1:1) [218].[1] The device for the loading of plates and measurement of deflections in the center of the plate is shown on Fig. 3.2.7. The necessary characteristics of the material of the investigated plates are given in Table 3.2.3 (elastic constants are determined according to the methods in § 2.3). As can be seen from Fig. 3.2.8, the results on determining the deflection in the center of the plate w_{max} satisfactorily agree with the calculated curves constructed by formula (3.2.19). The amounts of deflections of the points located on the diagonals of the plate (plates No. 5 and 6, Table 3.2.3) at distance d from the center are given on Fig. 3.2.9. As is evident, they can be calculated with sufficient accuracy by formula (3.2.19).
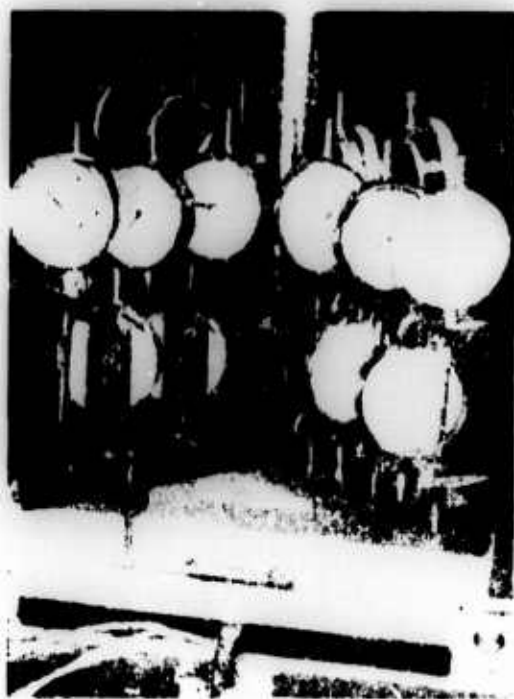

Fig. 3.2.7. Device for bending and measurement of deflections of free rectangular plate.

---

[1]The experimental check of the dependences, which consider transverse shears, is virtually absent. An exception is [273, 314]. In [314] the increase of deflection as a result of shear is investigated on round metal plates; in [273] the diagram of tangential stresses, calculated by Reissner, is compared with the experimental results obtained by the photoelastic method.
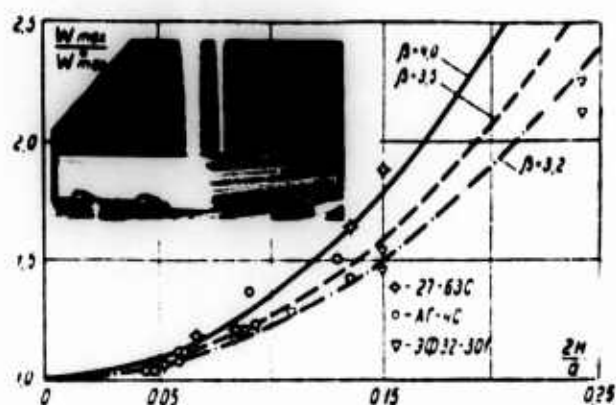
135

Fig. 3.2.8. The effect of degree of anisotropy β and $\frac{2H}{a}$ on deflection, caused by shears. In the upper corner is shown failure from shear.

Table 3.2.3. Parameters of the investigated plates and breaking load.

No. of plate	Material	a, mm	$2H$, mm	$E_x = E_y$, 10^3 kgf/mm^2	ν_{xy}	G_{xy}, 10^3 kgf/mm^2	$G^*_{xz} = G_{yz}$, 10^3 kgf/mm^2	Breaking load, kgf
1	AG-4S		10.7	2.1	0.11	0.28	0.13	980
2	AG-4S		11.8					1200
3	27-63S	80, 130,	10.3	2.7	0.13	0.32	0.23	1830
4	27-63S	180, 230	10.8					1580
5	EF 32-301		19.4	2.1	0.13	0.12	0.21	2300
6	EF 32-301		19.4					2600

Fig. 3.2.9. The comparison of experimental and calculation data. ——— deflection calculated taking into account shears by (3.2.19); - - - deflection not taking into account shears (3.2.17). KEY: (1) Plate.

136
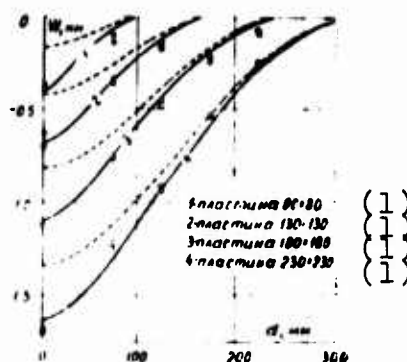
Plates $80 \times 80\,\text{mm}^2$ were brought to failure. In this case, besides the failure from normal stresses (Fig. 3.2.10) there was also observed failure from interlayer shears (Fig. 3.2.8). Therefore, as in § 2.4, strength calculation is necessary not only with respect to stresses σ_x, σ_y and τ_{xy}, but also with respect to tangential stresses τ_{xz} and τ_{yz}.

Fig. 3.2.10. The character of failure of plates: a) top view; b) bottom view.
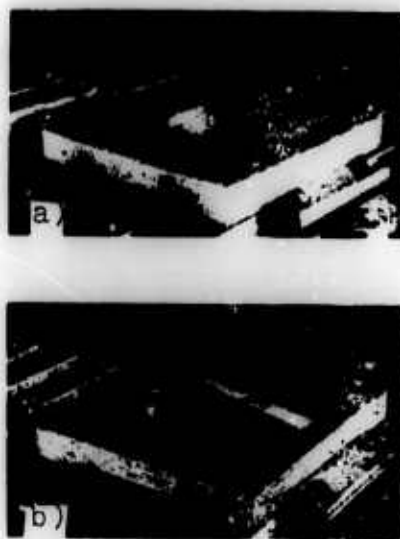
§ 3.3. ROUND PLATES

3.3.1. Basic dependences. A round plate with thickness 2H and radius R (axis of cylindrical orthotropy of material coincides with the axis of the plate) is examined in the system of cylindrical coordinates (r, θ, z) (Fig. 3.3.1); the corresponding elastic displacements are designated u, v, w. If, as in the case of rectangular plates, we disregard lateral deformation, i.e., assume $\varepsilon_z = 0$,[1] which is formally equivalent to $1/E_z = \nu_{zr} = \nu_{z\theta} = 0$ (ν_{zr} and $\nu_{z\theta}$ - Poisson ratios, which characterize abbreviation in direction z when stretching ir direction r or θ), then Hooke law takes the form

[1] In [95] without utilization of hypothesis $\varepsilon_z = 0$ there is examined the particular case of anisotropy and loading.
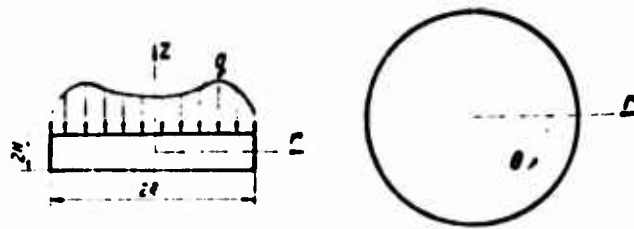
137

Fig. 3.3.1. Diagram of transverse loading of a round plate.

$$\sigma_r = \bar{E}_r \varepsilon_r + \nu_{r\theta} \bar{E}_r \varepsilon_\theta; \quad \sigma_\theta \quad \bar{E}_\theta \varepsilon_\theta + \nu_{r\theta} \bar{E}_r \varepsilon_r;$$
$$\tau_{r\theta} \quad G_{r\theta} \gamma_{r\theta}; \quad \tau_{rz} \quad G_{rz} \gamma_{rz}; \quad \tau_{\theta z} \quad G_{\theta z} \gamma_{\theta z}; \tag{3.3.1}$$
$$\bar{E}_r = \frac{E_r}{1 - \nu_{r\theta} \nu_{\theta r}}; \quad \bar{E}_\theta \quad \frac{E_\theta}{1 - \nu_{r\theta} \nu_{\theta r}}.$$

Proceeding as is shown during the derivation of equations of bending of rectangular plate (3.2.1), and taking into account that

$$\varepsilon_r = \frac{\partial u}{\partial r}; \quad \varepsilon_\theta = \frac{1}{r} \cdot \frac{\partial v}{\partial \theta} + \frac{u}{r}; \quad \varepsilon_z = \frac{\partial w}{\partial z} = 0;$$
$$\gamma_{r\theta} = \frac{1}{r} \cdot \frac{\partial u}{\partial \theta} + \frac{\partial v}{\partial r} - \frac{v}{r}; \quad \gamma_{\theta z} = \frac{\partial v}{\partial z} + \frac{1}{r} \cdot \frac{\partial w}{\partial \theta}; \tag{3.3.2}$$
$$\gamma_{rz} = \frac{\partial u}{\partial z} + \frac{\partial w}{\partial r}.$$

we obtain the system of equations for a round plate [187]:

$$\left\{ \begin{array}{l}
\bar{E}_r \dfrac{\partial^2 u}{\partial r^2} + G_{r\theta} \dfrac{1}{r^2} \cdot \dfrac{\partial^2 u}{\partial \theta^2} + G_{rz} \dfrac{\partial^2 u}{\partial z^2} + \bar{E}_r \dfrac{1}{r} \cdot \dfrac{\partial u}{\partial r} - \bar{E}_\theta \dfrac{u}{r^2} + \\[2mm]
\quad + (\nu_{r\theta} \bar{E}_r + G_{r\theta}) \dfrac{1}{r} \cdot \dfrac{\partial^2 v}{\partial \theta \partial r} - (\bar{E}_\theta + G_{r\theta}) \dfrac{1}{r^2} \cdot \dfrac{\partial v}{\partial \theta} = 0; \\[4mm]
G_{r\theta} \dfrac{\partial^2 v}{\partial r^2} + \bar{E}_\theta \dfrac{1}{r^2} \cdot \dfrac{\partial^2 v}{\partial \theta^2} + G_{\theta z} \dfrac{\partial^2 v}{\partial z^2} + G_{r\theta} \dfrac{1}{r} \cdot \dfrac{\partial v}{\partial r} - G_{r\theta} \dfrac{v}{r^2} + \\[2mm]
\quad + (\nu_{r\theta} \bar{E}_r + G_{r\theta}) \dfrac{1}{r} \cdot \dfrac{\partial^2 u}{\partial r \partial \theta} + (\bar{E}_\theta + G_{r\theta}) \dfrac{1}{r^2} \cdot \dfrac{\partial u}{\partial \theta} = 0; \\[4mm]
2H \left(G_{rz} \dfrac{\partial^2 w}{\partial r^2} + G_{rz} \dfrac{1}{r} \cdot \dfrac{\partial w}{\partial r} + G_{\theta z} \dfrac{1}{r^2} \cdot \dfrac{\partial^2 w}{\partial \theta^2} \right) + \\[2mm]
\quad + \displaystyle\int_{-H}^{H} \left(G_{rz} \dfrac{\partial^2 u}{\partial r \partial z} + G_{rz} \dfrac{1}{r} \cdot \dfrac{\partial u}{\partial z} + G_{\theta z} \dfrac{1}{r^2} \cdot \dfrac{\partial^2 v}{\partial \theta \partial z} \right) dz = -q,
\end{array} \right. \tag{3.3.3}$$

138

which is the simplified Lamé equations for cylindrically orthotropic body:

$$a_{rr}\left(\frac{\partial^2 u}{\partial r^2} + \frac{1}{r}\cdot\frac{\partial u}{\partial r}\right) + (a_{r\theta} + G_{r\theta})\frac{1}{r}\cdot\frac{\partial^2 v}{\partial r\partial\theta} + (a_{rz} + G_{rz})\frac{\partial^2 w}{\partial r\partial z} +$$
$$+ (a_{rz} - a_{r\theta})\frac{1}{r}\cdot\frac{\partial w}{\partial z} - (a_{\theta\theta} + G_{r\theta})\frac{1}{r^2}\cdot\frac{\partial v}{\partial\theta} + G_{rz}\frac{\partial^2 u}{\partial z^2} +$$
$$+ G_{r\theta}\frac{1}{r^2}\cdot\frac{\partial^2 u}{\partial\theta^2} - a_{\theta\theta}\frac{1}{r^2}u = 0;$$

$$(G_{r\theta} + a_{\theta\theta})\frac{1}{r^2}\cdot\frac{\partial u}{\partial\theta} + G_{r\theta}\frac{1}{r}\cdot\frac{\partial v}{\partial r} - G_{r\theta}\frac{1}{r^2}v + (G_{r\theta} + a_{r\theta})\frac{1}{r}\cdot\frac{\partial^2 u}{\partial r\partial\theta} +$$
$$+ G_{r\theta}\frac{\partial^2 v}{\partial r^2} + G_{\theta z}\frac{\partial^2 v}{\partial z^2} + ((G_{\theta z} + a_{z\theta}))\frac{1}{r}\cdot\frac{\partial^2 w}{\partial z\partial\theta} + a_{\theta\theta}\frac{1}{r^2}\cdot\frac{\partial^2 v}{\partial\theta^2} = 0;$$

$$G_{rz}\frac{\partial^2 w}{\partial r^2} + (G_{rz} + a_{rz})\frac{\partial^2 u}{\partial r\partial z} + G_{rz}\frac{1}{r}\cdot\frac{\partial w}{\partial r} + (G_{rz} + a_{z\theta})\frac{1}{r}\cdot\frac{\partial u}{\partial z} +$$
$$+ (G_{\theta z} + a_{z\theta})\frac{1}{r}\cdot\frac{\partial^2 v}{\partial z\partial\theta} + G_{\theta z}\frac{1}{r^2}\cdot\frac{\partial^2 w}{\partial\theta^2} + a_{zz}\frac{\partial^2 w}{\partial z^2} = 0.$$

Here

$$a_{rr}=\frac{E_r}{B}(1-v_{\theta z}v_{z\theta}); \quad a_{\theta\theta}=\frac{E_\theta}{B}(1-v_{zr}v_{rz});$$

$$a_{zz}=\frac{E_z}{B}(1-v_{r\theta}v_{\theta r});$$

$$a_{r\theta}=a_{\theta r}+\frac{E_r}{B}(v_{r\theta}+v_{rz}v_{z\theta})=\frac{E_\theta}{B}(v_{\theta r}+v_{\theta z}v_{zr});$$

$$a_{rz}=a_{zr}=\frac{E_z}{B}(v_{zr}+v_{z\theta}v_{\theta r})=\frac{E_r}{B}(v_{rz}+v_{r\theta}v_{\theta z});$$

$$a_{\theta z}=a_{z\theta}=\frac{E_\theta}{B}(v_{\theta z}+v_{\theta r}v_{rz})=\frac{E_z}{B}(v_{z\theta}+v_{zr}v_{r\theta});$$

$$B=1-v_{r\theta}v_{\theta r}-v_{rz}v_{zr}-v_{\theta z}v_{z\theta}-v_{r\theta}v_{z r}v_{z\theta}-v_{\theta z}v_{zr}v_{r\theta}$$

in the case where it is possible to accept the hypothesis about absolutely transversal rigidity of the material.

During the solution of axisymmetric problem, when $v = \partial u/\partial\theta = \partial w/\partial\theta = 0$, system (3.3.3) is simplified:

$$\frac{\partial^2 u}{\partial r^2} + \frac{1}{r}\cdot\frac{\partial u}{\partial r} - a^2\frac{u}{r^2} + \frac{1}{\beta^2}\cdot\frac{\partial^2 u}{\partial z^2} = 0; \qquad (3.3.4)$$

139

$$2H\left(\frac{d^2\cdot}{dr^2}\cdot\frac{1}{r}\cdot\frac{d\cdot}{dr}\right)\cdot\int_{H}^{H}\left(\frac{\partial^2 u}{\partial r\partial z}\cdot\frac{1}{r}\cdot\frac{\partial u}{\partial z}\right)dz\quad\frac{q}{G_{rz}}\qquad (3.3.5)$$

where

$$\beta^2\cdot\frac{E_r}{G_{rz}};\quad a^2\cdot\frac{E_w}{E_r}.$$

The course of the solution of system (3.3.4), (3.3.5) is analogous to that given earlier (§ 2.2); in the problem in question instead of trigonometric functions Bessel functions appear in the solution.

By direct substitution it is easy to check that the solution of equation (3.3.4) is

$$u\quad AJ_\alpha(\lambda r)\,\mathrm{sh}\,\lambda\beta z+A_1 J_\alpha(\lambda r)\,\mathrm{ch}\,\lambda\beta z+A_2 Y_\alpha(\lambda r)\,\mathrm{sh}\,\lambda\beta z+$$
$$+A_3 Y_\alpha(\lambda r)\,\mathrm{ch}\,\lambda\beta z+Br^a z+B_1 r^a+B_2 r^{-a}z+B_3 r^{-a}, \qquad (3.3.6)$$

where A, B, λ are constants; J_α, I_α – Bessel function of the first and second type of order α.

In the case of a solid plate in its center (r = 0) u = 0, whence $A_2 = A_3 = B_2 = B_3 = 0$. If the flat surfaces of plate z $\pm$ H are free from tangential stresses, i.e., $\partial u/\partial z + dw/dr = 0$ when z = $\pm$H, then also $A_1 = 0$. Consequently,

$$u(r,z) = AJ_\alpha(\lambda r)\,\mathrm{sh}\,\lambda\beta z+Br^a z+B_1 r^a; \qquad (3.3.7)$$

$$w(r) = -A\beta\,\mathrm{ch}\,\varkappa F_\alpha(\lambda r)-B\frac{r^{a+1}}{a+1}+C. \qquad (3.3.8)$$

where $\varkappa=\lambda\beta H$, $F_\alpha(\lambda r)=\int J_\alpha(\lambda r)d(\lambda r)$. constants A, B, C, λ are determined by restraint conditions of the edges of the plate. Equation (3.3.5) taking into account the expression for displacements (3.3.7), (3.3.8) takes the form

$$|q\rangle\lambda\beta H\,\mathrm{ch}\,\varkappa\Phi_\alpha(\lambda r)\quad q. \qquad (3.3.9)$$

where $D = \dfrac{2\overline{E}_r H^3}{3(1 - v_{r\theta} v_{\theta r})}$ — the flexural rigidity of the plate;

$$q = \frac{3(x - \operatorname{th} x)}{x^3}; \quad \Phi_\alpha = \frac{1+\alpha}{2\alpha} J_{\alpha-1}(\lambda r) + \frac{1-\alpha}{2\alpha} J_{\alpha+1}(\lambda r).$$

Thus, as in the case of bending of beams (§ 2.2), in solutions (3.3.7), (3.3.8) there are terms which correspond to transverse bending (terms with coefficient A) and terms which satisfy homogeneous system of equations (3.3.4), (3.3.5), which correspond to tension-compression and to pure bending of the plate (terms with coefficients B, B_1, C).

3.3.2. The effect of shears. In the case of transverse load

$$q = q_m \Phi_\alpha(\lambda_m r). \tag{3.3.10}$$

where λ_m — roots of equation $\Phi_\alpha(\lambda R) = 0$, from (3.3.9) follows

$$A_m = \frac{q_m}{q_m \beta \operatorname{ch} x_m \lambda_m^4 D}. \tag{3.3.11}$$

For fulfillment of conditions $w = 0$ when $r = R$ there must be

$$C_m = B_m \frac{R^{\alpha+1}}{\alpha+1}.$$

where B_m are constants, the expressions for which under varied conditions of restraint of the edges of plate are given in Table 3.3.1.

For plates with cylindrical orthotropy of type $E_\theta = E_r$, i.e., when $\alpha = 1$ (with axisymmetric deformation this case does not differ from the case of transversal isotropy),

$$F_1(\lambda r) = -J_0(\lambda r); \quad \Phi_\alpha(\lambda r) = J_0(\lambda r).$$

141

Table 3.3.1. The effect of shears on the deflection of round transversally isotropic plates.

Form of restraint of the edge of plate	$\dfrac{B_m}{A_m}$	Relationships $\dfrac{w_{max}}{w^0_{max}}$ for transversally isotropic plates*			
		according to S. P. Timoshenko [24]	according to S. A. Ambartsumyan [9]	according to V. I. Korolev [112]	obtained in this work
Free support $M = 0$	$-\dfrac{\lambda_{m}{}^{2}q_{m}\beta\,\mathrm{ch}\,x_{m}}{(\alpha+\nu)R^{\alpha-1}}\psi_{\alpha}(\lambda_{m}R)$	$1+1.6\beta^2\dfrac{H^2}{R^2}$ (I)	$1+1.28\beta^2\dfrac{H^2}{R^2}$ (III)	$1+1.28\beta^2\dfrac{H^2}{R^2}$ (VI)	$\dfrac{64}{5R^2}\sum_{m=1}^{\infty}\dfrac{1}{\lambda_{m}{}^{5}}\left[\dfrac{2}{\lambda_{m}R q_{m}J_{1}(\lambda_{m}R)}+1\right]$ (VIII)
Restraint $\dfrac{d\varpi}{dr}=0$	$-\dfrac{\lambda_{m}\beta\,\mathrm{ch}\,x_{m}}{R^{\alpha}}J_{\alpha}(\lambda_{m}R)$	—	— (IV)	—	$\dfrac{64}{R^4}\sum_{m=1}^{\infty}\dfrac{1}{\lambda_{m}{}^{4}q_{m}}\left[\dfrac{2}{\lambda_{m}RJ_{1}(\lambda_{m}R)}-1\right]$ (XI)
$\dfrac{\partial u}{\partial z}\Big|_{z=0}=0$	$-\dfrac{\lambda_{m}\beta}{R\alpha}J_{\alpha}(\lambda_{m}R)$	$1+8\beta^3\dfrac{H^2}{R^2}$ (II)	$1+8\beta^2\dfrac{H^2}{R^2}$ (V)	$1+6.4\beta^2\dfrac{H^2}{R^2}$ (VII)	$\dfrac{64}{R^4}\sum_{m=1}^{\infty}\dfrac{1}{\lambda_{m}{}^{4}}\left[\dfrac{2}{\lambda_{m}RJ_{1}(\lambda_{m}R)}-\mathrm{ch}\,x_{m}\dfrac{1}{\dots}\right]$ (X)

*Expressions for deflections not taking into account shears have the form: in the case of free support $\varpi^0_{max}=\dfrac{5qR^4}{64D}$; in the case of restraint $\varpi^0_{max}=\dfrac{qR^4}{64D}$; $\psi_{\alpha}(\lambda_r)=\dfrac{\nu+\alpha}{2\alpha}J_{\alpha-1}(\lambda_r)+\dfrac{\nu-\alpha}{2\alpha}J_{\alpha+1}(\lambda_r)$.

142

and the problem of transverse bending with arbitrary load can be solved by expansion of $q(r)$ into Fourier-Bessel series

$$q(r) = \sum_{m=1}^{\infty} q_m J_0(\lambda_m r).$$ (3.3.12)

where the general term of expansions q_m is determined by formula

$$q_m = \frac{2}{J_1^2(\lambda_m R)} \int_0^R r q(r) J_0(\lambda_m r)\, dr.$$

In the case of evenly distributed load (with intensity q_0)
$q_m = \dfrac{2q_0}{\lambda_m R J_1(\lambda_m R)}$ and deflection is determined by expression

$$w = \sum_{m=1}^{\infty} \left[\frac{2q_0 J_0(\lambda_m r)}{\lambda_m^3 q_m D R J_1(\lambda_m R)} - B_m \frac{r^2}{2} + C_m \right].$$ (3.3.13)

Corresponding solutions for deflection are given by S. P. Timoshenko [241], S. A. Ambartsumyan [6], V. I. Korolev [112].

The expressions, obtained by different methods for deflections in the center of the plate w_{max}, pertaining to deflection w_{max}^* (here as usual * designates the values obtained with taking into account shears, i.e., where $G_{rz} \to \infty$), are given in Table 3.3.1.

As is easy to check, when $\beta\frac{H}{R} \to 0$ $w_{max} \to w_{max}^*$, i.e., all the solutions taking into account shears convert to solutions obtained on the basis of the hypothesis of straight normals, when the plate is infinitely thin or its material possesses infinite shear rigidity.

Graphs w_{max}/w_{max}^* (Fig. 3.3.2), constructed by formulas I-X of Table 3.3.1, depending on relative thickness 2H/R and the degree of anisotropy of material $\beta = \sqrt{\dfrac{E_r}{G_{rz}}}$ make it possible to determine the correction from shear and to estimate the error introduced by
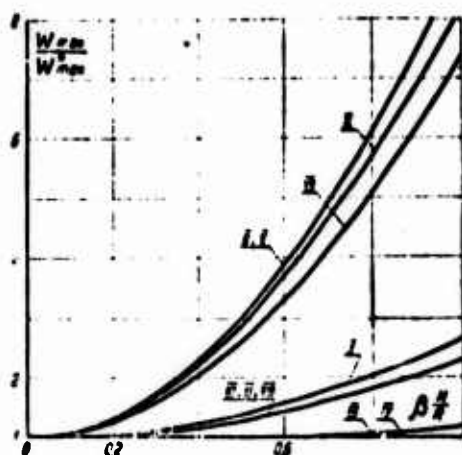
Fig. 3.3.2. The effect of shears on deflection of free (I, III, VI, VIII), pliably restrained ($\frac{du}{dz}\big|_{z=0} = 0$ when $r = R$; II, V, VII, IX) and rigidity restrained ($\frac{dw}{dr} = 0$ when $r = R$; IV, IX) evenly loaded round plates.

a priori postulation of the law $f(z)$ of distribution of tangential stresses τ along the thickness of the plate (see § 3.1.1). The practical coincidence of curves III, VI and VIII, and also the relative closeness (with not too large values $\beta\frac{H}{R}$) of curves IV and IX indicates that during the determination of deflections the parabolic law $f^0(z)$, accepted in [6], is a good approximation of the law found from the solution of system of equations (3.3.4), (3.3.5).

The data given on Fig. 3.3.2 attests to the fact that in the examined really possible range of changes of parameter $\beta\frac{H}{R}$ the shears strongly affect deflection even for a free plate. The effect of shears in the case of a restrained plate, when the vertical element of the edge of the plate ($\frac{\partial u}{\partial z}\big|_{z=0} = 0$ when $r = R$) is fixed, is very substantial. However, in case of the restraint of the horizontal element of the middle plane ($\frac{dw}{dr} = 0$ with $r = R$) the effect of shears can be disregarded. The large disagreements between the two cases of realization of fixing attest to the fact that deflection, determined in the experiment, highly depends on the realization of conditions of restraint (see Fig. 2.3.4). In this case the sensitivity to variations of boundary conditions is increased with increase of the anisotropy of material β.

Deflection due to shears for square (a × a) plates of material of uniform strength ($E_x = E_y$) with the same relative thickness $\frac{2H}{a} = \frac{2H}{2R}$ can be both more and less than the deflection due to shears for a round transversally isotropic plate. As can be seen from Fig. 3.3.3, this depends on the value of shear modulus in the plane of the plate G_{xy}
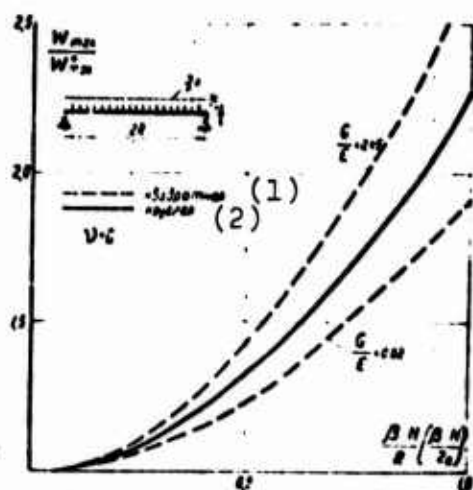

Fig. 3.3.3. The effect of shears on deflection of square (a × a × × 2H) and round (2R × 2H) plates. KEY: (1) Square; (2) Round.

In Table 3.3.2 $v = v_{...}, \; r = \frac{r}{R}, \; a = \frac{E_0}{E_r};$

$$A' = \frac{qR^2(4+v)}{2(9-a^2)}; \; a' = \frac{a+v}{3+v}; \; a'_1 \frac{a^2+3v}{3+v}; \; 1' = \frac{P(1+v)}{2\pi(1-a^2)}; \; a'' = \frac{a+v}{1+v};$$

$$a'_1 = \frac{a+v}{1+v}; \; B = \frac{2qH^2}{5} \cdot \frac{E_r}{E_z} \cdot \frac{a^2}{a^2-1}(v_{rz}-v_{\theta z});$$

$$C = \left[\frac{5(a^2+v^2)}{5(a^2-v^2)+a^2(9-a^2)v} \right] a^2; \; \eta \frac{v_{\theta z}(a^2+v)+v_{rz}(v-1)}{(a-v)(v_1-v_{\theta})};$$
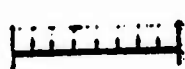
$$\chi = 2 \frac{H^2}{R^2} \cdot \frac{E_r}{G_{rz}}, \; \text{if } \frac{dw}{dr} = 0 \text{ when } r = R;$$

$$\chi = -0.5 \frac{H^2}{R^2} \cdot \frac{E_r}{G_{rz}}, \; \text{if } \frac{dw}{dz}\Big|_{r=R} = 0 \text{ when } r = R.$$

3.3.3. The stressed state of cylindrical orthotropic plates.

The distribution of stresses in round solid or annular plates depends significantly on the parameter of anisotropy $\alpha = \sqrt{E_\theta / E_r}$. So, in the solid plate of radius R, compressed by evenly distributed radial load with intensity N [123],

145

Table 3.3.2. Stresses and bending moments in cylindrically orthotropic round plates.

Схема опира-ния и нагру-жения (1)				
τ_{rz}	$-\dfrac{3q}{8H^3}r(H^2-z^2)$			$-\dfrac{3P}{8\pi H^3}\cdot\dfrac{1}{r}(H^2-z^2)$
σ_z	$-\dfrac{3q}{2H^3}\left[\dfrac{H^3}{3}-\dfrac{z}{2}\left(H^2-\dfrac{z^2}{3}\right)\right]$			0 при $r>0$ (2)
M_r°	$A'(x^a + x^2)$	$A'(a'x^a - x^2)$	$A''(x^a-1)$	$A''(a''x^a-1)$
M_θ°	$A'(ax^a-1-a'_1x^2)$	$A'(aa'x^a-1-a'_1x^2)$	$A''(ux^a-1-a''_1)$	$A''(aa''x^a-1-a''_1)$
M_r^τ	0	$-\dfrac{qR^2a^2}{10(a-\nu)}\chi x^a$	0	$-\dfrac{Pa^2}{10\pi(a-\nu)}\chi x^a$
M_θ^τ	0	$-\dfrac{qR^2a^3}{10(a-\nu)}\chi x^a$	0	$-\dfrac{Pa^3}{10\pi(a-\nu)}\chi x^a$
M_r^t	$B(1-x^{a-1})$	$B(1-\eta x^{a-1})$	0	0
M_θ^t	$B(1-ax^{a-1})$	$B(1-a\eta x^{a-1})$	0	0
x_r°	$\left(\dfrac{2}{a+1}\right)^{\frac{1}{a-1}}$	$C\left[\dfrac{2(3+\nu)}{(a-1)(a+\nu)}\right]^{\frac{1}{a-3}}$	(3)	
x_θ°	$\left[\dfrac{2(a^2+3\nu)}{a(a-1)(3+\nu)}\right]^{\frac{1}{a-3}}$	$C\left[\dfrac{2(a^2+3\nu)}{a(a-1)(a+\nu)}\right]^{\frac{1}{a-3}}$		

(3) Функции $M_r(x)$ и $M_\theta(x)$ являются монотонными

KEY: (1) Diagram of support and loading; (2) When; (3) Functions $M_r(x)$ and $M_\theta(x)$ are monotonic.

$$\sigma_r = N\left(\dfrac{r}{R}\right)^{a-1}; \quad \sigma_\theta = N\left(\dfrac{r}{R}\right)^{a-1}. \tag{3.3.14}$$

Consequently, the stressed state in the plate is uniform only when $\alpha = 1$. When $\alpha > 1$ the stresses decrease in proportion to approach to the center (when $r = 0$ $\sigma_r = \sigma_\theta = 0$), while when $\alpha < 1$, on the contrary, they grow unlimitedly. A similar pattern is observed during transverse bending - the bending moments,

both radial $M_r = \int_H^H z\sigma_r dz$ and circular $M_\theta = \int_H^H z\sigma_\theta dz$ in the center

of evenly loaded (q = const) plate are equal to zero when $\alpha > 1$, are nonzero, but are finite when $\alpha = 1$ and become infinite when $\alpha < 1$ [112]. It should be noted that case $\alpha < 1$ is hypothetical,

146

since it is virtually impossible to manufacture a plate (for example, by reinforcing with filaments) of constant thickness with anisotropy $E_\theta < E_r$.

The bending moments also depend on the tangential stresses in transverse planes τ_{rz} (with axisymmetric bending $\tau_{\theta z} = 0$) and normal stresses σ_z. According to S. A. Ambratsumyan's theory [6], these stresses in evenly ($\sigma_z = -q$ when $z = -H$, $\sigma_z = 0$ when $z = H$) and centrally loaded plates are determined by the formulas given in Table 3.3.2. The bending moment (radial M, or circular M_θ) in any section can be represented as the sum of

$$M = M^* + M^\tau + M^z. \tag{3.3.15}$$

where M* is the moment determined according to classical theory, i.e., not taking into account τ_{rz} and σ_z, and M^τ and M^z are corrections, which consider stresses τ_{rz} and σ_z. For freely resting and restrained plates, loaded by evenly distributed load with intensity q_0 or concentrated force P in the center, M*, M^τ and M^z are determined by the formulas given in Table 3.3.2. Analysis [164] shows that correction M^z, just as in beams (see § 2.2.6), is negligible. The effect of shears grows with increase of parameter χ (see Table 3.3.2), i.e., with increase of relative thickness H/R and degree of anisotropy β. With a change of parameter χ the relationships are changed between the radial and circular bending moments in the center of the plate and at its edge $M_r(0)$, $M_r(R)$, $M_\theta(0)$, $M_\theta(R)$. The qualitative change of the relationships between moments occurs at values of parameter χ equal to:

$$\chi_1 = -\frac{5(a - v_{,a})}{a^2(a+3)}; \quad \chi_2 = \frac{1+v}{a+1}\chi_0; \quad \chi_3 = \frac{v_{,a}}{a}\chi_0; \quad \chi_4 = \frac{v_{,a}-1}{a-1}\chi_0;$$

$$\chi'_1 = -\frac{5(a^2 - v^2)}{a^2(a^2-1)}; \quad \chi'_2 = \frac{1}{a^2}\chi'_0; \quad \chi'_3 = \frac{a-1}{a+v}\chi'_0;$$

$$\chi'_4 = \frac{(a-1)(a^2+v)}{(a+v)a^2(a+1)}\chi'_0; \quad \chi'_5 = \frac{v(a-1)}{a^2(a+v)}\chi'_0; \quad \chi'_6 = \frac{a-2-v}{a+v}\chi'_0.$$

$$\chi'_7 = \frac{\alpha v - \alpha^2 - 2v}{\alpha^3(\alpha+v)}\chi'_6; \quad \chi'_8 = \frac{v - \alpha^3}{\alpha^2(\alpha+v)}\chi'_7.$$

Diagram 4.   Change of the relation-
ships between bending moments in
restrained centrally loaded plates
depending on parameter χ.

Diagram 5.   Change of the relation-
ships between bending moments in
restrained evenly loaded plates
depending on parameter χ.

The form of these relationships with given χ can be
established by Diagrams 4 and 5. Thus, for instance, when
$\chi'_4 < \chi < \chi'_5$ from the first line of Diagram 4 it is evident
that $M_r(0) > |M_r(R)|$; from the following lines it follows that
$M_\theta(0) > |M_\theta(R)|$, $|M_r(R)| > |M_\theta(R)|$, $M_\theta'(R) > 0$, $M_r(R) < 0$.

Graphs on Figs. 3.3.4 and 3.3.5 illustrate the change of
bending moments ($\overline{M} = \frac{64D}{5q_0R^4}M$) along the radius r depending on
parameters $\alpha \geq 1$ and χ. As is evident, with increase of α points
x^3 (see also Table 3.3.2) and x^0, which correspond to extrema and
zero values of functions M_r and M_θ, are displaced toward larger
values of the coordinate.

It should be noted that in the case of free support the
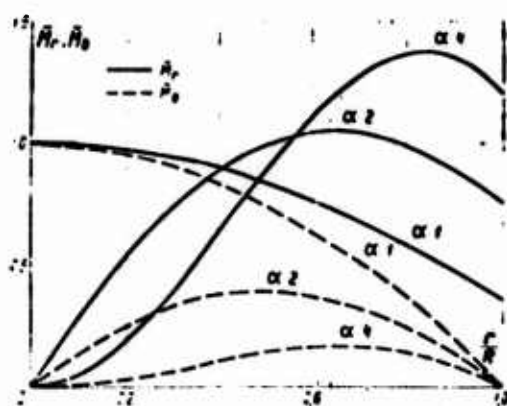shears (parameter χ) do not affect the distribution and the

148

Fig. 3.3.4. Change of the bending moments along the radius of free round plates depending on the degree of anisotropy α ($\nu'\theta = 0.4$).
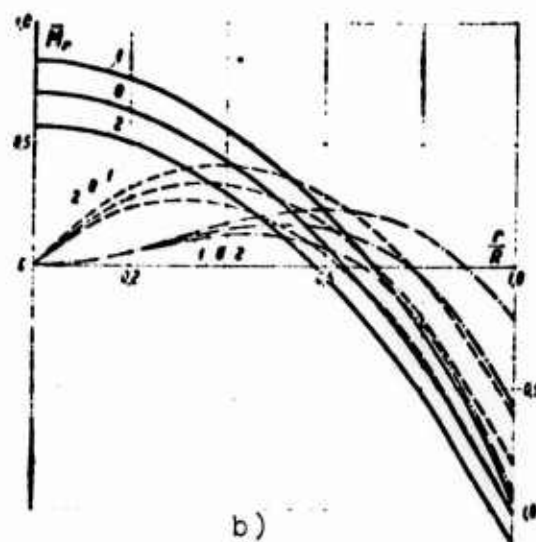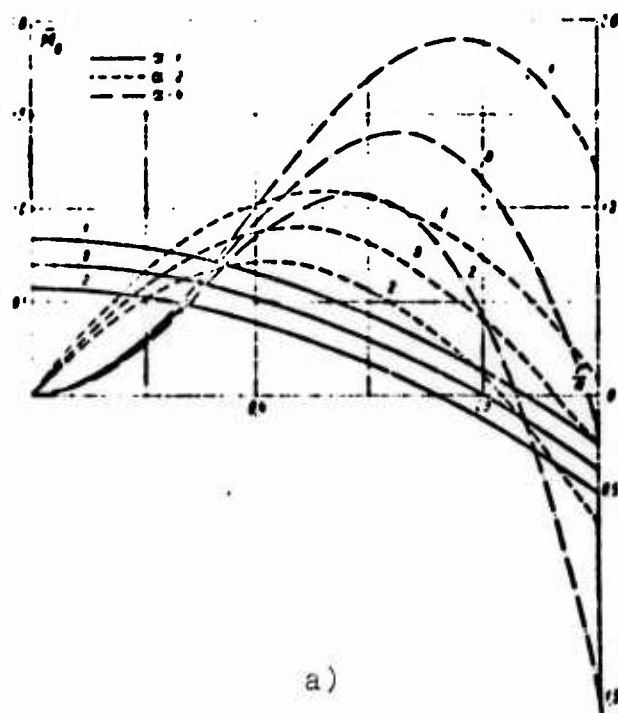
Fig. 3.3.5. Change of circular (a) and radial (b) bending moments along the radius of restrained round plates. $0 - \chi = 0$; $1 - \chi = -0.1$; $2 - \chi = 0.1$.

amount of bending moments; in the case of restrained edge the effect of shears is considered by coefficient C (see Table 3.3.2): coordinates x^3 and x^0 are changed C times, and moments at points $x^3 - C^2$ times in comparison with the corresponding values, calculated taking into account the hypothesis of straight normals.

149

The effect of shears shows up not only on the distribution of bending moments - consequently, and the stresses σ_r and σ_θ - along tne radius. Stresses τ_{rz} can significantly change the diagrams of distribution of σ_r and σ_θ along the thickness of the plate. According to S. A. Ambartsumyan's theory, these stresses along coordinate z are changed according to the law of cubic parabola

$$\sigma = az^3 + bz + c \tag{3.3.16}$$

(as is shown, the classical theory gives the linear law of distribution of these stresses, whereupon $\sigma = 0$ when $z = 0$). The basic correction to the classical solution is introduced by the account of shears. The effect of σ_z is considered constant c. By practically important cases it does not exceed 3% [164]. Disregarding σ_z, for evenly loaded plates we obtain

$$a = -\frac{15}{4H^3}\tilde{M}; \quad b = \frac{3}{4H^3}(2M - 3\tilde{M}); \quad c = 0. \tag{3.3.17}$$

When determining the radial deformations $\tilde{M}_r = \frac{q_0 H^2 a^2(1+\nu)E_z}{30(a^2-\nu^2)G_{rz}}$; when determining peripheral stresses $\tilde{M}_\theta = \tilde{M}_r \frac{a^2+\nu}{1+\nu}$. Thus, stresses σ_r and σ_θ can be expressed by the appropriate bending moments and supplementary correction, which is considered by parameters $\tilde{M}_r$, $\tilde{M}_\theta$:

$$\sigma = \frac{3M}{2H^3}\left[1 - \frac{3\tilde{M}}{2M}\left(1 - \frac{5z^2}{3H^2}\right)\right]. \tag{3.3.18}$$

The comparison of the maximum stresses max σ with their corresponding values in the center of isotropic plate, determined according to classical theory max σ^*, is given on Figs. 3.3.6, 3.3.7. Curves 1 correspond to calculation not taking into account shears (but taking into account anisotropy E_θ/E_r), and 2 and 3 - to the case where $H^2E_r/R^2G_{rz} = 0.5$. As can be seen from Figs. 3.3.4,

3.3.5, the maximum bending moments in terms of absolute value can appear when $x = 0$, $x = x^3$ or $x = 1$. Taking this into account max σ_r and max σ_θ for the cases of free and pliably restrained ($\partial u/\partial z = 0$ when $x = 1$, $z = 0$) plates are determined when $x = x_*$. and in the case of rigid fixing ($dw/dr = 0$ when $x = 1$) – when $x = 1$.

Fig. 3.3.6. The effect of anisotropy on the maximum normal stresses in free plates ($\nu_{r\theta} = 0.4$). 1 – $\chi = 0$; 2 – $\chi = 0.1$.
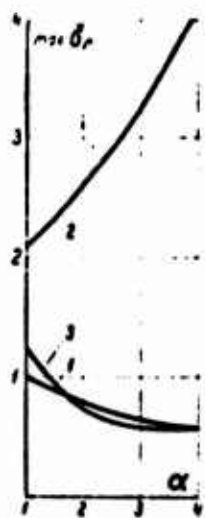

Fig. 3.3.7.

Fig. 3.3.8.

Fig. 3.3.7. The effect of anisotropy on the maximum radial stresses for restrained plates. 1 – not taking into account shears; 2 – $dw/dr = 0$ when $r = R$; 3 – $\partial u/\partial z \big|_{z=0} = 0$ when $r = R$.

Fig. 3.3.8. The effect of anisotropy on the maximum peripheral stresses for restrained plates. Designations are the same as on Fig. 3.3.7.

151

It should be noted that cases are theoretically possible where the stresses σ_r and σ_θ reach extreme values inside the plate, and not when $z = \pm H$, as follows from classical theory. This phenomenon is illustrated by Fig. 3.3.9, on which the change of the character of diagrams of normal stresses is shown depending on parameter $\tilde{M}$, with the aid of which shears are considered (3.3.17).
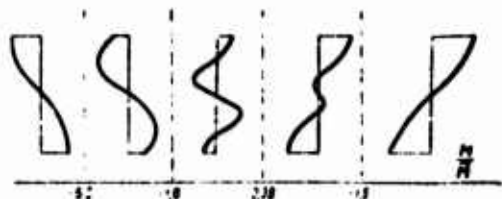

Fig. 3.3.9. The effect of shears on the diagrams of normal stresses σ_r.

§ 3.4. THE EFFECT OF SHEARS ON THE MAGNITUDE OF CRITICAL FORCES AND NATURAL VIBRATION FREQUENCY

3.4.1. The stability of rectangular plates. The equations of stability of a rectangular orthotropic plate, compressed along axes x and y by evenly distributed forces with intensity N_x and N_y (Fig. 3.4.1), can be obtained from system of equations (3.2.5), (3.2.7), if we replace q by ficticious load q =
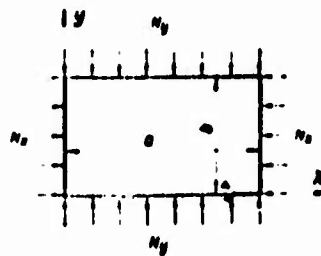
$$= -N_x\frac{d^2w}{dx^2} + N_y\frac{d^2w}{dy^2}$$ (see, for example, [43]). Consequently,

$$\bar{E}_x\frac{\partial^2 u}{\partial x^2} + G_{xy}\frac{\partial^2 u}{\partial y^2} + G_{xz}\frac{\partial^2 u}{\partial z^2} +$$

$$+ (G_{xy} - \nu_{xy}E_x)\frac{\partial^2 v}{\partial x\partial y} = 0;$$ (3.4.1)

$$\bar{E}_y\frac{\partial^2 v}{\partial y^2} + G_{xy}\frac{\partial^2 v}{\partial x^2} + G_{yz}\frac{\partial^2 v}{\partial z^2} + (G_{xy} + \nu_{xy}E_x)\frac{\partial^2 u}{\partial x\partial z} = 0;$$ (3.4.2)

$$(2HG_{xz} - N_x)\frac{\partial^2 w}{\partial x^2} + (2HG_{yz} - N_y)\frac{\partial^2 w}{\partial y^2} +$$

$$+ \int_H^H \left(G_{xz}\frac{\partial^2 u}{\partial x\partial z} + G_{yz}\frac{\partial^2 v}{\partial y\partial z} \right) dz = 0.$$ (3.4.3)

152

Fig. 3.4.1. Diagram of evenly
compressed rectangular plate.

For the case of free support the solutions of equations
(3.4.1), (3.4.2) are given in § 3.2. By substituting them in
(3.4.3), we find the critical values N_x and N_y. The value of the
critical load depends on many independent geometric and physical
quantities, therefore in the most general case the complete
analysis of the behavior of critical load depending on the
indicated factors is difficult. If the plate is transversally
isotropic (§ 3.2.2) and the relationship between compressive
forces N_x and N_y is kept constant ($N_x = N$, $N_y = cN$), then

$$N_{\text{кр } mn} = \frac{(\lambda_m^2 + \lambda_n^2)^2}{\lambda_m^2 + c\lambda_n^2}\, \varphi_{mn} D. \qquad (3.4.4)$$

If we disregard shears, then $\varkappa_{mn}^2 = (\lambda_m^2 + \lambda_n^2)\beta^2 H = 0,\ \varphi_{mn} = \frac{3(\varkappa_{mn} - \text{th}\,\varkappa_{mn})}{\varkappa_{mn}^3} = 1$

and formula (3.4.4) changes into the formula obtained on the
basis of Kirchoff-Love hypothesis [123]. In the case of
compression only in direction x ($N_y = 0$) from (3.4.4) follows

$$N_{\text{кр } mn} = \varphi_{mn} N^*_{\text{кр } mn} \qquad (3.4.5)$$

$N^*_{\text{кр } mn} = \dfrac{(\lambda_m^2 + \lambda_n^2)^2}{\lambda_m^2} D$ - critical load determined not taking

into account shears [123]. Consequently, in this case the connec-
tion between the critical load, determined taking into account
shears $N_{\text{кр } mn}$ and not taking into account shears $N^*_{\text{кр } mn}$, is the
same as in the case of rods (formula (2.5.8)). The solution,

which considers transverse shears, but which a priori assumes that they are distributed according to the law of quadratic parabola, leads to formula [6, 14]:

$$N_{\text{кр } mn} = \frac{N^{*}_{\text{кр } mn}}{1 + 0.4\varkappa_{mn}^{2}} \cdot$$

Consequently, the accuracy of approximation of the actual law of distribution of transverse shears f(0) (see Table 3.2.1) by quadratic parabola is equal to the accuracy of approximation of function ϕ_{mn} by function $\dfrac{1}{1+0.4\kappa_{mn}^{2}}$. The error introduced by such replacement can be judged from Table 2.2.1. The decrease of critical load depending on parameter $h^{*} = 0.4\pi^{2}\,\dfrac{H^{2}}{b^{2}}\,\beta^{2}$ is characterized by stability curves depicted on Fig. 3.4.2, borrowed from S. A. Ambartsumyan's book [6]. As is evident, shears substantially lower the critical load for plates of ma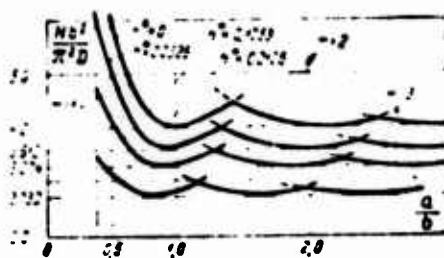terials reinforced by filaments, for which large values of β^{2} are characteristic (see Table 1.1.1). The noted feature is frequently overlooked (see, for example, source [125], in which the stability of plates of glass fiber-reinforced plastics is examined).

Fig. 3.4.2. Stability curves for different values of parameters [6].

During the action of complex contour loads, for example concentrated forces, on the plate the problem of stability is conveniently solved by using the energy criterion proposed by N. A. Alfutov and L. I. Balabukh [3], which does not contain initial (subcritical) stresses. The determination of these stresses in the case of complex loads presents significant difficulties.

154

Following the line of reasoning of the authors of the mentioned work [3], the criteron proposed by them can be spread also to anisotropic plates. In the case of orthotropy the critical values of external loads, applied to the outline of the plate in its plane, can be found from equation

$$\mathfrak{Z}_1 + H \iint \left[\sigma_{x0}{}^+ \left(\frac{\partial w}{\partial x}\right)^2 + \sigma_{y0}{}^+ \left(\frac{\partial w}{\partial y}\right)^2 + 2\tau_{xy0}{}^+ \frac{\partial w}{\partial x}\frac{\partial w}{\partial y} \right] dxdy -$$
$$- 2H \iint \left[\frac{1}{E_x} \sigma_{x0}{}^+ \sigma_{x1} + \frac{1}{E_y} \sigma_{y0}{}^+ \sigma_{y1} + \right.$$
$$\left. + \frac{1}{2}\left(\frac{1}{G_{xy}} - \frac{2\nu_{yx}}{E_x}\right)(\sigma_{x0}{}^+ \sigma_{y1} + \sigma_{y0}{}^+ \sigma_{x1}) \right] dxdy = 0. \qquad (3.4.6)$$

Here integrals are taken along the area of the middle plane; $\mathfrak{Z}_1$ - the potential energy of the bending of the plate; $\sigma_{x0}{}^+$, $\sigma_{y0}{}^+$, $\tau_{xy0}{}^+$ - the system of statically possible initial stresses, i.e., stresses which satisfy the equation of equilibrium of two-dimensional problem and conditions on the sections of the boundary where external loads are prescribed; $\sigma_{x1} = \dfrac{\partial^2 \phi_1}{\partial u^2}$; $\sigma_{y1} = \dfrac{\partial^2 \phi_1}{\partial x^2}$ - secondary stresses in the middle plane of the plate, which appear at the moment of loss of stability and are determined by the function of stresses ϕ_1, which satisfies the Karman equation of orthotropic plate

$$\frac{1}{E_y}\frac{\partial^4 \phi_1}{\partial x^4} + \left(\frac{1}{G_{xy}} - \frac{2\nu_{yx}}{E_x}\right)\frac{\partial^4 \phi_1}{\partial x^2 \partial y^2} + \frac{1}{E_x}\frac{\partial^4 \phi_1}{\partial y^4} = \left(\frac{\partial^2 w}{\partial x \partial y}\right)^2 - \frac{\partial^2 w}{\partial x^2}\frac{\partial^2 w}{\partial y^2}.$$

and boundary conditions $\phi_1 = \dfrac{\partial \phi_1}{\partial n} = 0$ on the contour, normal to which is n.

The effect of transverse shears shows up on the amount of potential energy of bending $\mathfrak{Z}_1$. If deflection w of free rectangular plate is predetermined in the form (3.2.9), then in the case of transversal isotropy from formula (3.2.2) taking into account (3.2.15) it follows that $\mathfrak{Z}_1 = \mathfrak{Z}_1^* \phi_{mn}$, where

155

$\ni_1^* = \frac{ab}{2}Dw_{mn}^2(\lambda_m^2 + \lambda_n^2)^2$ - the potential energy of bending,
determined not taking into account transverse shears. In the case
where all external forces, and also the integral terms of
expression (3.4.6) (for example, as in the case of loading by
concentrated forces, examined in [3]) are proportional to one
parameter N, the critical value of the latter is determined by
formula $N_{кр} = N_{кр}^* \phi_{mn}$, i.e., the correction from transverse
shears, as in the case of plates evenly loaded in the middle plane,
is determined by multiplier ϕ_{mn}.

3.4.2. Flexural vibrations of rectangular plates. Using
the estimations obtained in the examination of flexural vibrations
of beams (§ 2.6), let us examine the effect of shears on the natural
vibration frequency of plates without taking into account inertia
in the directions parallel to the middle plane and the compress-
ibility of normals ($\varepsilon_z = 0$). Under these assumptions the system
of equations of free vibrations can be obtained from system
of equations (3.2.5)-(3.2.7), by replacing in it, taking into
account the d'Alembert principle, the transverse load by inertia
term

$$q = -2H\rho\frac{\partial^2 w}{\partial t^2} .$$

By representing the displacements in the form of periodic functions
of time

$$u = U(x, y, z) \sin(\omega t + \delta);$$
$$v = V(x, y, z) \sin(\omega t + \delta);$$
$$w = W(x, y) \sin(\omega t + \delta).$$

from (3.2.5)-(3.2.7) we will obtain the system of equations for
amplitudes of vibrations U, V, W:

156

$$\bar{E}_x \frac{\partial^2 U}{\partial x^2} + G_{xy} \frac{\partial^2 U}{\partial y^2} + G_{xz} \frac{\partial^2 U}{\partial z^2} + (G_{xy} + \nu_{xy}\bar{E}_x) \frac{\partial^2 V}{\partial x \partial y} = 0; \qquad (3.4.7)$$

$$\bar{E}_y \frac{\partial^2 V}{\partial y^2} + G_{xy} \frac{\partial^2 V}{\partial x^2} + G_{yz} \frac{\partial^2 V}{\partial z^2} + (G_{xy} + \nu_{xy}\bar{E}_x) \frac{\partial^2 U}{\partial x \partial y} = 0; \qquad (3.4.8)$$

$$2H G_{xz} \frac{\partial^2 W}{\partial x^2} + 2H G_{yz} \frac{\partial^2 W}{\partial y^2} + \int_{H}^{H} \left(G_{xz} \frac{\partial^2 U}{\partial x \partial z} + G_{yz} \frac{\partial^2 V}{\partial x \partial z} \right) dz =$$
$$= -2H\rho\omega^2 W. \qquad (3.4.9)$$

The solution of system of equations (3.4.7), (3.4.8) for the case
of a free plate is known. Values of natural frequencies ω are
clearly determined by equation (3.4.9). Upon consideration of the
inertia in directions x and y the right sides of equations (3.4.7),
(3.4.8) are equal to $\rho\omega^2 U$ and $\rho\omega^2 V$ respectively. This leads
to the need for the solution of transcendental equations (see
§ 2.6.3), i.e., to considerable complication of the problem.

For clarity let us give the estimation of the effect of
shears on an example of a transversally isotropic plate. Using
results of § 3.2.2, from (3.4.7)-(3.4.9) we find

$$\omega_{mn}^2 = \omega_{mn}^{*2} \varphi_{mn}; \qquad (3.4.10)$$

ω_{mn}^{*} - the frequency determined not taking into account transverse
shears [123]:

$$\omega_{mn}^{*} = (\lambda_m^2 + \lambda_n^2) H \sqrt{\frac{E}{\rho}} \qquad (3.4.11)$$

Approximate replacement (see Table 2.2.1)

$$\varphi_m = \frac{3(x_{mn} - \text{th} \, x_{mn})}{x_{mn}^3} \approx \frac{1}{1 + 0.4 x_{mn}^2} \qquad (3.4.12)$$

turns (3.4.10) into the expression obtained by the postulation
of the parabolic law of distribution f(z) of tangential stresses

157

τ_{xz} and τ_{yz} [6, 14]. Consequently, in this case the error introduced by postulation $f(z)$ is the same as in the case of vibration of a rod (§ 2.6).

3.4.3. The stability of a round plate.

During the compression of a round plate by evenly distributed load N_r (Fig. 3.4.3) the equations of stability with axisymmetric buckling can be obtained by substitution of ficticious transverse load

$$q = N_r\left(\frac{d^2w}{\partial r^2} + \frac{1}{r}\cdot\frac{dw}{dr}\right) \quad [187]:$$

$$\frac{\partial^2 u}{\partial r^2} + \frac{1}{r}\cdot\frac{\partial u}{\partial r} - u^2\frac{u}{r} + \frac{1}{\beta^2}\cdot\frac{\partial^2 u}{\partial z^2} = 0; \qquad (3.4.13)$$

$$(2HG_{1,} - N_r)\left(\frac{d^2 w}{dr^2} + \frac{1}{r}\cdot\frac{dw}{dr}\right) + G_{1,}\int_H^H\left(\frac{\partial^2 u}{\partial r\partial z} + \frac{1}{r}\cdot\frac{\partial u}{\partial z}\right)dz = 0. \qquad (3.4.14)$$

It should be noted that such an approach is strict only in the case of $\alpha = 1$ ($E_\theta = E_r$), when the initial stressed state caused by compressive stresses N_r is uniform. In the case $\alpha \neq 1$ the initial stressed state is changed depending on coordinate r - distance from the center of the plate (see (3.3.14)).[1] For values of α, close to one, the stressed state is close to uniform, therefore system of equations (3.4.13), (3.4.14), at least for the

Fig. 3.4.3. Diagram of compressed round plate.

qualitative evaluation of the magnitude of critical forces, can be used also with $\alpha \neq 1$. The error introduced by the assumption about
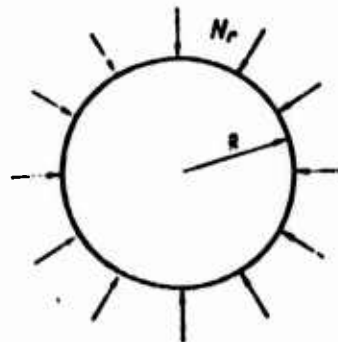
---

[1]N. A. Alfutov and L. I. Balabukh proposed the method [3], which makes it possible to solve such a problem without determination of the subcritical stressed state. The stability of transversally isotropic round plate is investigated by A. P. Melkonyan, A. A. Khachatryan [137] and A. Sh. Petoyan [163].

158

the homogeneity of the initial stressed state with $\alpha \neq 1$ can be estimated by Fig. 3.4.4, on which solid lines depict curves $N_{кр} = f(\alpha)$, obtained taking into account the heterogeneity of stressed state [305, 320] (not taking into account shears), and broken lines - not taking into account heterogeneity (also not taking into account shears).
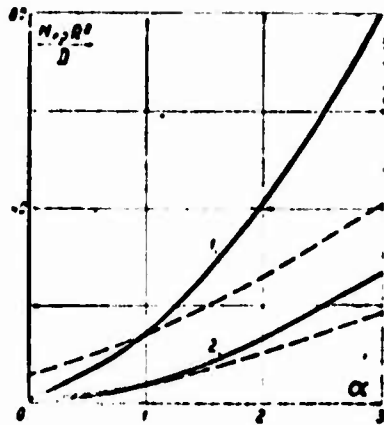

Fig. 3.4.4. The effect of heterogeneity of subcritical stressed state on the magnitude of critical force of round cylindrically orthotropic plates ($\nu_{r\theta} = 0.3$): 1 - restrained plate; 2 - free plate.

Using solution (3.3.7), equation (3.4.13), from (3.4.14) we obtain

$$A\Phi_{z}(\lambda_m r)D\lambda_m^2\beta\,\text{ch}\,\varkappa \left(q_m - \frac{N_r}{\lambda_m^2 D}\right) - BN_r(u+1)r^{n-1} = 0. \qquad (3.4.15)$$

This equation will be fulfilled if $B = 0$ and

$$N_r = \lambda_m^2 D q_m. \qquad (3.4.16)$$

Critical values of parameter $\lambda_{кр\,m}$ are determined from conditions at the edge of the plate $r = R$. These conditions form a system of two homogeneous equations, the determinant of which in the case of nontrivial solution must be equal to zero (see also § 2.5). Thus, for free plate $\lambda_{кр\,m}$ is determined from equation

$$\Psi_z(\lambda R) = 0. \qquad (3.4.17)$$

and in the case of restraint ($w = \frac{dw}{dr} = 0$ when $r = R$) - from equation

$$J_{\alpha}(\lambda R) \quad 0. \qquad\qquad (3.4.18)$$

When $\kappa \to 0$ $N_{кр} \to N^{*}_{кр\ m}$, where $N^{*}_{кр\ m}$ is the critical force determined without taking into account transverse shears [96].

The effect of transverse shears on $N_{кр\ m}$ is determined by multiplier ϕ_{m}, which is the monotonically decreasing function of parameter $\kappa_{m} = \lambda_{кр\ m}\beta H$. Consequently, the effect of shears is greater for restrained plates and for materials with large α (in these cases larger than $\lambda_{кр\ m}$). Figure 3.4.5 illustrates this phenomenon, on which there is shown the change of critical force for free (solid lines) and restrained (dotted lines) plates at different values of parameter α depending on the parameter $\beta\frac{H}{R}$. As is evident, transverse shears substantially decrease the critical force. With an increase of parameter $\beta\frac{H}{R}$ the effect of the method of restraint of the plate and parameter α fades away. This indicates that the stability of plates weakly resisting shear cannot be radically raised only due to more rigid fixing of edges and increase of Young's modulus of material. In the limiting case, when E_{r} or E_{θ} become infinite or $\frac{R}{H} \to 0$, i.e., when $\kappa_{m} \to 0$, as for a rod (§ 2.5), $N_{кр} \to 2HG_{rz}$. Consequently, the

Fig. 3.4.5. The effect of shears on the critical force of round plates. --- restrained plate; $-\ -\ -$ free plate.

160
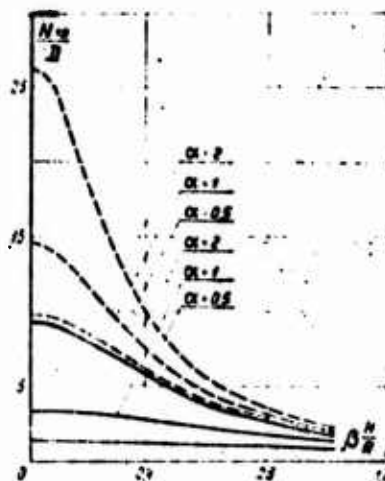
compressive stress, which the plate can perceive, not having lost
stability, is equal to the shear modulus of the material:

$$\sigma_{1,p} = \frac{N_{1,p}}{2H} \cdot G_u.$$

(3.4.19)

3.4.4. **The stability of annular plates.** During compression
by outside and internal pressure q and p (Fig. 3.4.6) in a round
annular plate there appear radial and peripheral normal stresses
[123]

$$\sigma_r = g_a - h_a, \quad \sigma_\theta = a(g_a + h_a),$$

(3.4.20)

where

$$g_a(r) = \frac{pc^{a+1} - q}{1 - c^{2a}} x^{a-1};$$

$$h_a(r) = \frac{p - qc^{a-1}}{1 - c^{2a}} c^{a+1} x^{a-1};$$

$$c = \frac{a}{b}; \quad x = \frac{r}{b}.$$

With axisymmetric buckling the equations of stability can be
obtained from system of equations (3.3.4), (3.3.5), after placing
in it ficticious transverse load [75]:

$$q = \sigma \cdot \frac{d^2 w}{dr^2} + c_\theta \frac{1}{r} \cdot \frac{dw}{dr}.$$

(3.4.21)

If the initial subcritical stressed state can be considered
uniform (this condition is satisfied exactly when $\alpha = 1$, $p = q =$
$= \frac{N}{2H}$), then the equations of stability have the form (3.4.13),
(3.4.14). Using solution (3.3.6), equation (3.4.13), equation
(3.4.15) can be given the form

$$\lambda_m^2 \beta \, \mathrm{ch} \, \varkappa_m (N - \varphi_n \lambda_m^2 D)[A J_0(\lambda_m r) + A_2 Y_0(\lambda_m r)] + 2BN = 0.$$

(3.4.22)

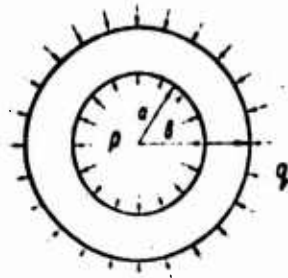This equation is fulfilled if B = 0 and

161

Fig. 3.4.6. Annular plate loaded by evenly distributed pressure.

$$N = N_{\kappa p\,m} = \varphi_m \lambda_{\kappa p\,m}^2 D. \tag{3.4.23}$$

Constant $\lambda_{\kappa p\,m}$ is determined by the conditions of restraint of the edges of plate $r = a$ and $r = b$. These conditions form the system of homogeneous equations, the equating of the determinant of which to zero gives the equation for finding $\lambda_{\kappa p\,m}$. These equations for a number of versions are given in Table 3.4.1 [189]. It is easy to check that when $\kappa_m \to 0$ they all change to the appropriate expressions obtained without taking into account shears [181].

Solutions of equations (Table 3.4.1), obtained on BESM-2 [189], make it possible to investigate the effect of shears (with respect to parameter $\beta \frac{2H}{R}$) and the relationship of radii $c = \frac{a}{b}$ on the magnitude of critical force. Results for the plate, supported when $r = a$, $r = b$, are given on Figs. 3.4.7, 3.4.8 (for $\nu_{r\theta} = 0.3$).

As computations showed, the effect of change of Poisson ratio $\nu_{r\theta}$ within from 0 to 0.5 can be disregarded. As can be seen from Fig. 3.4.7, the effect of shears on the amount of critical forces is decreased with decrease of the inside radius of the plate a, i.e., relationship $c = \frac{a}{b}$. In the case of both restrained edges (Table 3.4.1) parameter $\lambda_{\kappa p\,m}$ does not depend on shears. In other cases (see, for example, Fig. 3.4.8) the effect of shears on parameter $\lambda_{\kappa p\,m}$ is small, consequently, the basic correction from them is contained in parameter ϕ_m (see expression (3.4.23)). This makes it possible to use the values

162

$N^*_{\text{кр}}$ obtained not taking into account shears [181] with correction only for parameter ϕ_m.

Table 3.4.1. Dependences for determining $\lambda_{\text{кр}}$.

Diagram of support	$r = a$	$r = b$	Equations
	$\omega = M_r = 0$	$\omega = M_r = 0$	$\Lambda J(\bar{Y}_a - \bar{Y}_b) + \Lambda Y(\bar{J}_b - \bar{J}_a) +$ $+ (J_a Y_b - J_b Y_a)\ln c = 0$
	$\omega = \frac{d\omega}{dr} = 0$	$\omega = \frac{d\omega}{dr} = 0$	$\Lambda J(Y_a - \bar{Y}_b) + \Lambda Y(J_b - J_a) +$ $+ (J_a Y_b - J_b Y_a)\ln c = 0$
	$\omega = M_r = 0$	$\omega = \frac{d\omega}{dr} = 0$	$\Lambda J(\bar{Y}_a - Y_b) + \Lambda Y(J_b - \bar{J}_a) +$ $+ (J_a Y_b - J_b \bar{Y}_a)\ln c = 0$
	$\omega = \frac{d\omega}{dr} = 0$	$\omega = M_r = 0$	$\Lambda J(Y_a - \bar{Y}_b) + \Lambda Y(\bar{J}_b - J_a) +$ $+ (J_a \bar{Y}_b - \bar{J}_b Y_a)\ln c = 0$
	$Q_{rz} = M_r = 0$	$\omega = M_r = 0$	$J_a(Y_a - Y_b) + Y_a(J_b - J_a) = 0$
	$Q_{rz} = M_r = 0$	$\omega = \frac{d\omega}{dr} = 0$	$J_a(\bar{Y}_a - Y_b) + Y_a(J_b - \bar{J}_a) = 0$

In Table 3.4.1 $\bar{T}_a = \frac{\gamma a^2}{\nu - 1}\left[J_0(\lambda a) + \frac{\nu - 1}{a}J_1(\lambda a)\right];$

$J_a = J_1(\lambda a); \ M = J_0(\lambda b) - J_0(a);$ remaining functions can be obtained after substituting J for Y and a for b.
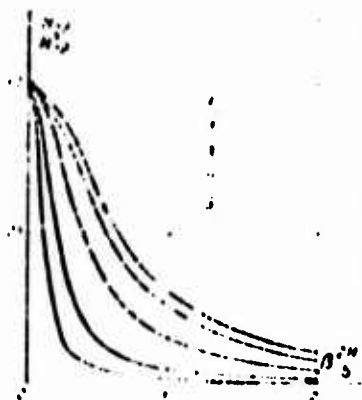

Fig. 3.4.7. The effect of shears on critical force for annular plates with different relationship of outside and inside diameters. KEY: (1) Curve.

(1) · · | / | · | · · , | ·

a/b 0.2   0.4   0.6   0.8   0.9

With increase of relationship $c = \frac{a}{b}$ the conditions in which
the annular plate is located approach conditions of elongated
rectangular plate with distance between the long sides $l = b - a$.
The critical load for such a plate

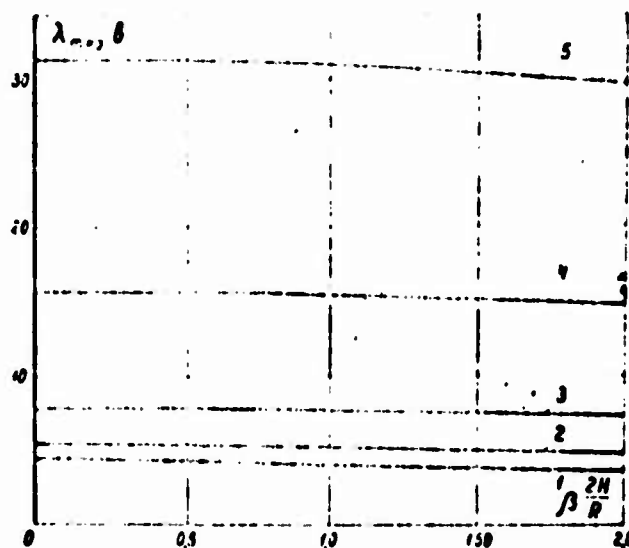$$N_{\text{кр}} = \overline{\lambda}_{\text{кр}} \, D\varphi_m.$$ (3.4.24)

where $\varphi_m = \dfrac{(\varkappa_m - \text{th}\,\overline{\varkappa}_n)}{\varkappa_m}; \quad \overline{\varkappa}_m = \lambda_{m; m|i/l}$

Parameter $\overline{\lambda}_{\text{кр}\,m}$ is determined by formula:

$$\overline{\lambda}_{\text{кр}\,m} = \frac{\lambda'_{\text{кр}\,m}}{1 - c}$$

($\lambda'_{\text{кр}\,m}$ - Eulerian values of the critical parameter of longitudinally
compressed rod with the appropriate boundary conditions).

Fig. 3.4.8. The effect of
shears on the magnitude of
critical parameter $\lambda_{m\,\text{кр}}$
for free annular plate
(when $r = a$, $r = b$).
Designations are the same
as on Fig. 3.4.7.

The comparison of the critical loads, calculated by
formula (3.4.23) and simplified formula (3.4.24), showed [189]
that even with relatively small c the approximate replacement of
$\overline{\Pi}_{\text{кр}\,i} \sim \overline{\Pi}_{\text{кр}\,i}$ was permissible. This gets rid of the need for the
solution of the transcendental equations given in Table 3.4.1.

164

FOURTH CHAPTER

RINGS OF TRANSVERSALLY WEAK MATERIALS

§ 4.1. THE TECHNICAL THEORY OF WINDING

4.1.1. The anisotropy of material in the state of treatment.
Winding with filament or fabric is one of the most rational methods
of the manufacture of parts, which have the shape of solids of
revolution, from materials reinforced by fibers. The possibility
of change of the winding angle makes it possible to easily control
the anisotropy of the strength and deformation properties of the
part being made. For this very reason winding is the basic method
of treatment of glass fiber-reinforced plastics, reinforced by
continuous filaments. The treatment by the winding method is
developed faster than other methods of forming articles from
composite materials. According to Rosato [312], in the USA in
1966 by this method 45,000 t of parts were produced from glass
fiber-reinforced plastics.

The most investigated is the geometric side of winding -
optimization in terms of the angle of winding (see, for example,
[113, 262, 311]. A survey of the works of scientists of the
USA on the geometric optimization of winding is given in [289]).
In the works dedicated to the investigation of the winding of
glass fiber-reinforced plastics, the nonuniformity of the distri-
bution of tension in the turns of wound articles is at best only

mentioned (for example [295, 316]). In works on the calculation
of constructions made by this method [258, 272, 285], the power
side of the process of winding and the effects determined by it
are not examined at all. However, this question has great
practical interest during the development of the mechanics of
winding parts from materials reinforced by fibers (as a result
of the strong anisotropy of the latter in the state of treatment).

The anisotropy of materials when winding can be characterized
by the relationship of Young's modulus in the direction of winding
E_θ and in transversal (radial) direction E_r. It is natural that
the examination of the mechanics of winding in an elastic setting
is only the first approximation, however, such an approach makes
it possible to determine and investigate the basic features of
this process. The materials in question, especially reinforced
plastics, in the state of treatment combine comparatively high
rigidity in the direction of winding with large pliability in
perpendicular direction. This is explained by the fact that in
the direction of winding the deformating properties are virtually
completely determined by the reinforcing fibers, and in trans-
versal - by pliable matrix (for example, by polymer binder).

The properties of material in transversal direction are
absolutely insufficiently studied. However the experimental
data appearing recently [167, 296] make it possible, at least
qualitatively, on an example of glass fiber-reinforced plastics
to evaluate relation $\alpha_H^2 = E_\theta/E_r$.[1] In the practically used
range of compacting pressure $\tilde{p}_0$ dependence $E_r = f(\tilde{p}_0)$ for glass
fiber-reinforced plastics, reinforced by rove and fabric, is
represented on Figs. 4.1.1. and 4.1.2. These data are obtained
with compression of a pile, collected from layers of rove or

---

[1]Subsequently for the sake of simplicity of recording index H
with α_H is dropped in formulas; it is retained on the graphs.

cloth pre-impregnated with polymer binder by uniform pressure $\tilde{p}_0$ in a closed mold. As is evident, dependence $E_r = f(\tilde{p}_0)$ is virtually linear both for unidirectional glass fiber-reinforced plastics and for glass laminates, however, the rigidity of the latter is considerably higher, which is explained by the presence of cross-links.
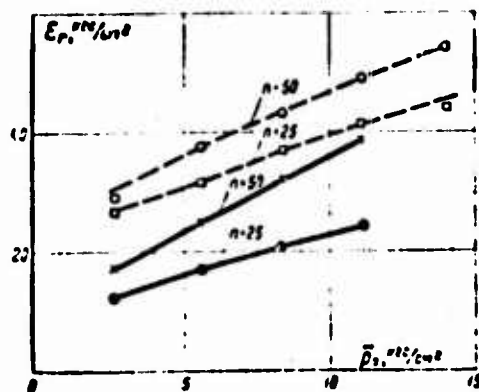

Fig. 4.1.1. The dependence of transversal modulus E_r of uni-directional glass fiber-reinforced plastics in the state of treatment on the compacting pressure $\tilde{p}_0$ during compression of a pile of n layers [60]. ——— LSB-F; ---- AG-4S.
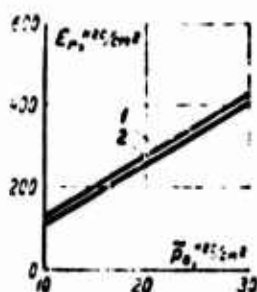
Designation: ĸгc/cм^2 = kgf/cm^2.

Fig. 4.1.2. The effect of compacting pressure $\tilde{p}_0$ on transversal modulus E_r on woven glass fiber-reinforced plastics in the state of treatment [167]: 1 - reinforcing fabric of satin weave, impregnated with polyester bonding agent; 2 - reinforcing fabric of linen weave, impregnated with polyester bonding agent.

The given experimental data make it possible to evaluate the boundaries of change of the parameter of the anisotropy of material in the state of treatment $\alpha = \sqrt{E_\theta/E_r}$. For oriented glass fiber-reinforced plastics E_r can be changed within from 20 to 800 kgf/cm^2, and the elastic modulus in the direction of fibers E_θ - within $(0.25-0.80) \cdot 10^6$ kgf/cm^2. Consequently, E_r and E_θ in the state of treatment can differ by three orders. Precisely this forces us to turn the most serious attention to the force optimization of the process of winding.

167

Pressure between layers when winding depends on the force of winding, the geometric dimensions of the part being wound and the properties of material. The enumerated parameters can be changed within rather wide limits, which leads to change of value E_r (Figs. 4.1.1, 4.1.2) and, consequently, the parameter of anisotropy α. Therefore all the numerical results are given for a rather wide range of values of $α(30 \leq α \leq 70)$, which encompasses the majority of practically real cases. When winding one particular part the pressure between turns (regardless of their arrangement) is comparatively constant. This makes it possible to disregard the change of parameter α over the height of the part being wound.

4.1.2. The force features of winding. High pliability in the transverse direction of materials reinforced with fibers leads to the fact that under the action of tensioning force each subsequent turn strongly deforms the layers lying below in radial direction. In spite of the insignificance of radial stresses ($\sigma_r \sim \frac{H_0}{R} \sigma_\theta$ where H_0 and R – the thickness and radius of the part being wound), they can cause large deformations:

$$\varepsilon_r \sim \frac{H_0}{R} \cdot \frac{E_\theta}{E_r} \varepsilon_\theta. \qquad (4.1.1.)$$

For isotropic materials $E_r = E_\theta$, consequently, $\varepsilon_r \ll \varepsilon_\theta$. This makes it possible to use the hypothesis of noncompressible standards, accepting in the practical calculations of thin-walled rings $E_r = \infty$. During the calculation of isotropic rings for the action of external or internal pressure these parts are calculated as thin-walled to the ratio of radii equal to 1.4 [247]. For rings of materials reinforced by fibers as a result of large values of parameter α in the state of treatment it is necessary to consider the compressibility of standards even for very thin rings (with ratio of radii less than 1.01).

The most visual illustration of the differences between the winding of isotropic and anisotropic materials can be pressure

168

on the part being wound. Figure 4.1.3 shows change of pressure
p on the force-measuring mandrel depending on number of turns n
during winding of isotropic (nickel strip, curve 1) and essentially
anisotropic (strip of glass fiber-reinforced plastic, curve 2)
materials. When winding isotropic materials the drop of initial
tensioning force in turns, assigned by the winding device,
virtually does not occur, therefore the pressure on the mandrel
increases in proportion to the number of layers. When winding
materials reinforced by fibers, dependence $p = f(n)$ becomes
nonlinear already at small n. For these materials it is necessary
to get rid of the hypothesis about the incompressibility of the
standard even with comparatively small thicknesses of the parts
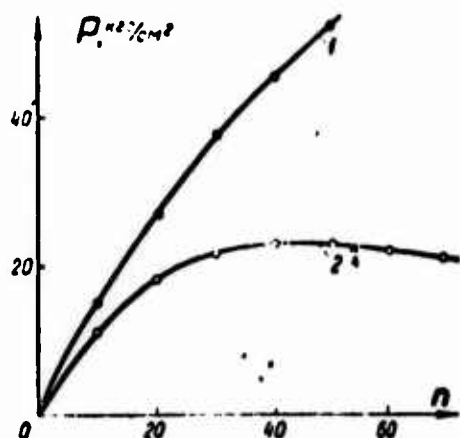being wound.

Fig. 4.1.3. Pressure change on
mandrel p with winding of strip:
1 - isotropic material (nickel
strip); 2 - essentially aniso-
tropic material (glass fiber-
reinforced plastic LSB-F).

4.1.3. Calculated dependences.[1]

The small thickness of the strip being wound makes it
possible to disregard the spiral arrangement of turns and to
represent the process of winding in the form of the successive

---

[1]The problem, similar to the examined, appears during the
determination of pressure on a drum with multi-layer winding of
rope [105, 111]. However, the proposed method of solution is
simpler than that given in the indicated works.

application of thin annular anisotropic layers on each other with thickness $h = h' + h''$ (Fig. 4.1.4). The original tensioning in each layer T_0 is created by the winding device and it can be changed according to a certain law. With the application of i-th layer on radius r_i pressure appears on the layers lying below $q_0 = \dfrac{T_0}{r_i}$. If the mandrel is absolutely rigid it is possible to consider that the layers lying below form a uniform anisotropic ring with inside radius R_B and outside radius r_i, then application of the next layer, which creates pressure $q_0 = T_0/r_i$, causes radial displacement at radius r [123]:

$$\Delta u(r_i) = - \frac{T_0(\varrho^\alpha - \varrho^{-\alpha})}{E_\theta \left(\frac{\varrho_i^\alpha}{\alpha - \nu_{\theta r}} + \frac{\varrho_i^{-\alpha}}{\alpha + \nu_{\theta r}} \right)}, \qquad (4.1.2)$$

where

$$\varrho_i = \frac{r_i}{R_B}; \quad \varrho = \frac{r}{R_B}.$$

The importance of anisotropy makes it possible to disregard the Poisson effect if a change of tensioning in turns occurs only because of the settling of underlayers. This assumption is equipollent to the disregarding of $\nu_{\theta r}$ in comparison with α, since $\nu_{\theta r} \ll \alpha$. Consequently, expression (4.1.2) assumes the form

$$\Delta u(r_i) = - \frac{T_0 \alpha (\varrho^\alpha - \varrho^{-\alpha})}{E_\theta (\varrho_i^\alpha - \varrho_i^{-\alpha})}. \qquad (4.1.3)$$

The total radial displacement $u(r)$ in the ring being wound on radius r is equal to the settling from the application of all the subsequent rings from $r_i = r$ to $r_i = R_H$ (r is the fixed radius, on which the displacements are determined; R_H is the outside radius of the prepared ring):

$$u(r) = \Delta u(r_i) + \Delta u(r_i + h) + \ldots + \Delta u(R_H - h). \qquad (4.1.4)$$

170

As a result of the thinness of elementary layer h with a sufficiently smooth change of tensioning force T_0 the sum of (4.1.4) can be approximately replaced by integral

$$u = \frac{1}{h} \int_r^{R_\text{\tiny M}} \Delta u(r_i) \, dr_i.$$

(4.1.5)

One ought to consider that such a replacement gives considerable error when determining the displacements near the inside surface of the ring being wound, where the number of terms of sum (4.1.4) is small.
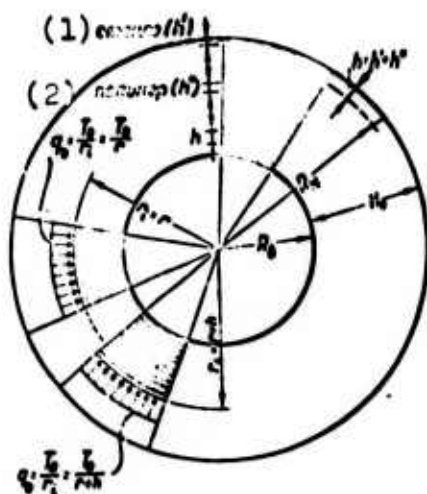

Fig. 4.1.4. Model of winding.
KEY: (1) glass (h');
(2) polymer (h").

The computation of integral (4.1.5), as a rule, is cumbersome. In the case of constant tensioning force of the strip T_0 for the practical calculations of the constructions, which have $1.02 \leq \frac{R_\text{H}}{R_\text{B}} \leq 1.10$ and $10 \leq \alpha \leq 80$, it is possible to recommend the approximation formula

$$u = -\frac{nT_0}{x_\text{\tiny H}E_0}\left[(1+x)^\text{\tiny H} - (1+x)^{-\text{\tiny H}}\right]\left[\operatorname{arc tg}(1+x_\text{\tiny H})^\text{\tiny H} - \operatorname{arc tg}(1+x)^\text{\tiny H}\right].$$

(4.1.6)

where $x = \frac{r}{R_\text{B}} - 1$, $x_\text{\tiny H} = \frac{R_\text{H}}{R_\text{B}} - 1$.

171

The difference between the results calculated by formula (4.1.5) (on BESM-2) and by approximation formula (4.1.6) does not exceed 5% with $\frac{R_H}{R_B} \leq 1.05$ and 10% - with $\frac{R_H}{R_B} \leq 1.1$.

If we consider the pliability of the mandrel, then the radial displacement

$$\Delta u(r_i) = -\frac{T_0 a (\eta^2 \varrho^a - \varrho^{-a})}{E_\Theta (\eta^2 \varrho_i^a + \varrho_i^{-a})} \, . \qquad (4.1.7)$$

where

$$\eta = \frac{a + \gamma_{on}}{a - \gamma_{on}} \, .$$

The mandrel and rings have identical width.[1] The outside radius of the mandrel $R_1 = R_B$, inside radius R_2. It is made of isotropic material with Young's modulus E_{on} and Poisson ratio γ_{on}.

$$\gamma_{on} = \frac{E_\Theta}{E_{on}} \left(\frac{R_1^2 + R_2^2}{R_1^2 - R_2^2} - \nu_{on} \right)$$

- the parameter which characterizes the rigidity of the mandrel. When the mandrel is absolutely rigid, $\gamma_{on} = 0$ and formula (4.1.7) changes into (4.1.3).

Table 4.1.1 depicts the value of parameter γ_{on}, which characterizes the pliability of steel mandrels in the form of rings with different thickness during winding of glass fiber-reinforced plastics on them (it is accepted that $\nu_{on} = 0.3$, $E_{on} = 2.1 \cdot 10^6$ kgf/cm^2, $E_\theta = 0.4 \cdot 10^6$ kgf/cm^2).

_____

[1] Change of the tensioning force as a result of bending of generatrix, when the width of the mandrel is greater than the width of the wound strip of noncompressible material, is examined by V. L. Biderman [28].

Table 4.1.1. The radial pliability of thin-walled steel mandrels.

R_1/R_2	1.01	1.02	1.03	1.04	1.05	1.06	1.07	1.08	1.09	1.10
γ_{max}	19.0	9.6	6.5	4.9	3.9	3.3	2.8	2.4	2.1	1.9

§ 4.2. FORCE EFFECTS WHEN WINDING WITH CONSTANT TENSIONING FORCE

4.2.1. A drop in original tensioning. As a result of the high pliability of the material being wound in radial direction there appear large radial displacements (settling) u of the turns of the strip. As can be seen from Fig. 4.2.1, the amount of these displacements rapidly grows with increase of the parameter of anisotropy α (initial section of curves is marked by dotted line, since (4.1.6) gives too rough an approximation in the area of small thicknesses, when the thickness of the ring is commensurable with the amount of displacements).

As a result of the large settling of turns the original tensioning T_0 created in them by the force of winding considerably decreases. Lowering of tensioning T^- is directly proportional to settling u:

$$T^- = E_\theta \frac{u}{r}.\qquad(4.2.1)$$

consequently, residual tensioning

$$T = T_0 - T^-.\qquad(4.2.2)$$

The total drop of tensioning in all turns, i.e., drop of tensioning along the section of the rings,

$$\Sigma T^- = E_\theta \int_{R_0}^{R_n} \frac{u}{r}\,dr.\qquad(4.2.3)$$

173

In this case the total residual tensioning

$$\Sigma T = \Sigma T_0 - \Sigma T^-. \qquad (4.2.4)$$

In the case of thin-walled rings, when it is possible to disregard the change of radius along its thickness,

$$\Sigma T^- = E_\theta \int_0^{r_0} u \, dx. \qquad (4.2.5)$$

With accuracy to 5% in the range of change of parameters $1.01 \leq \dfrac{R_H}{R_B} \leq 1.1$; $10 \leq \alpha \leq 80$ integrand (4.1.6) of integral (4.2.5) can be replaced by expression

$$u = -\frac{2nT_0}{x_H E_\theta} \operatorname{sh} x (\operatorname{arc \, tg} e^{\alpha x_H} - \operatorname{arc \, tg} e^{\alpha x}). \qquad (4.2.6)$$

which leads to

$$\Sigma T = -T_0 \left[n + \frac{1}{x_H} \left(\frac{\pi}{2} - 2 \operatorname{arc \, tg} e^{-nx_H} \right) \right]. \qquad (4.2.7)$$
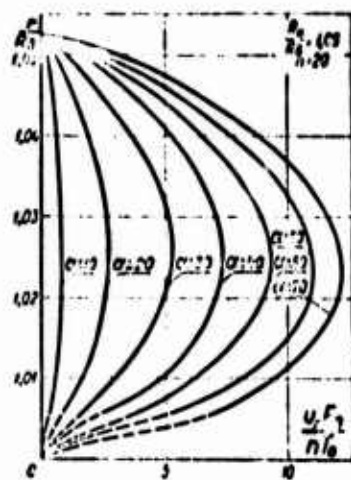

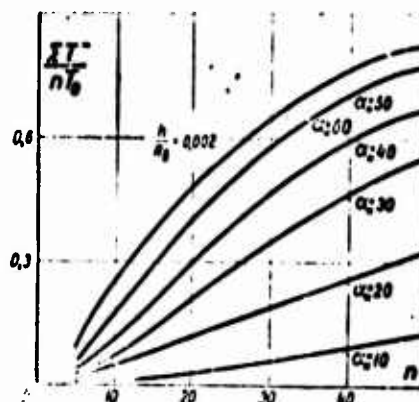Fig. 4.2.1. The effect of the degree of anisotropy on the amount of radial displacements in the turns of the rings.

Fig. 4.2.2. The effect of the degree of anisotropy on the total drop of tensioning force, $h = H_0$ – thickness of the rings.

174

In formula (4.2.7) parameter $\kappa_H = \alpha \dfrac{h}{R_B}$ characterizes the anisotropy of the deformating properties of the material being wound and the relationship of the geometric dimensions of the turn of material and the investigated construction.

As can be seen from Fig. 4.2.2, the total drop of tensioning grows faster with an increase in the number of turns, the larger the parameter of anisotropy α. During winding of radially incompressible turns on absolutely rigid mandrel the total tensioning ΣT increases in proportion to the number of turns:

$$\Sigma T = n T_0. \qquad (4.2.8)$$

As can be seen from Fig. 4.2.3, dependence $\Sigma T = f(n)$ for isotropic materials is also virtually linear. However, for the materials reinforced by fibers, for which in the state of winding $\alpha > 30$ (see § 4.1.1), the nonlinearity of dependence $\Sigma T = f(n)$ is manifested with $n < 10$, which attests to intense lowering of initially created tensioning T_0.
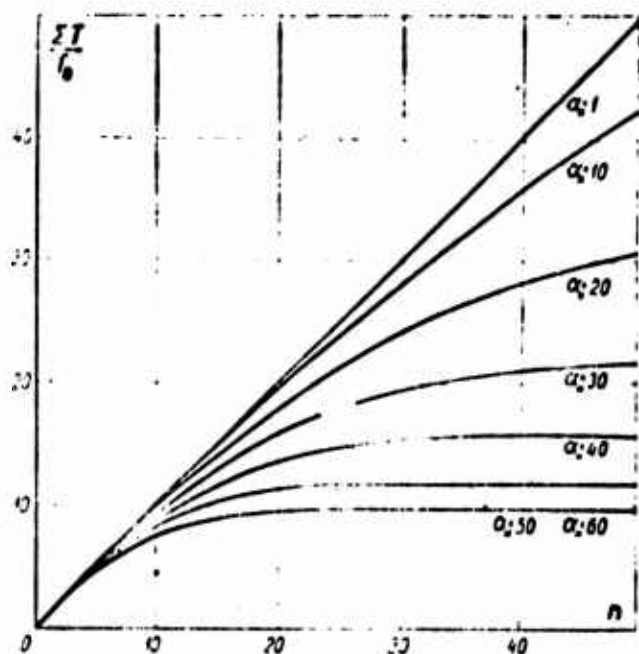

Fig. 4.2.3. The effect of the degree of anisotropy on the value of total tensioning force in the section of rings.

175

4.2.2. Pressure on absolutely rigid mandrel. For a series of problems, especially during the manufacture of different types of constructions with guaranteed tightness,[1] the total pressure p, transmitted to the working mandrel or the part being wound, is of the greatest interest. It is determined by the preserved tensioning in turns ΣT.

$$p = \int_{R_s}^{R_e} \frac{T}{r}\, dr. \qquad (4.2.9)$$

If the ring is thin-walled and it is possible to disregard the change of radius along its thickness, then p is directly proportional to the total preserved tensioning ΣT. Consequently, the growth of pressure on the mandrel with an increase in the number of turns n can be judged by Fig. 4.2.3. The character of the calculated curves (Fig. 4.2.3) for isotropic material ($\alpha \approx 1$) and glass fiber-reinforced plastic ($\alpha \approx 50$) agrees well with experimental curves Fig. 4.1.3.

When winding thin-walled rings with mean radius R from radially incompressible turns ($E_r = \infty$) to absolutely rigid mandrel the pressure transmitted by it is equal to

$$p^{*}_{_{H}} = \frac{n T_{_0}}{R}. \qquad (4.2.10)$$

With the winding of radially compressible turns

$$p_{_{H}} = \frac{T_{_0}}{\varkappa_{_0} R}\, \text{arctg sh } n\varkappa_{_0}. \qquad (4.2.11)$$

Ratio $\dfrac{p_{_{H}}}{p^{*}_{_{H}}}$ depending on the thickness of the article being wound and anisotropy is shown on Fig. 4.2.4. The given data visually illustrate the need for not using the hypothesis of

---

[1] For example the shrouds of electric motors [62, 265], high pressure cylinders and others.

176

incompressible standards for the predominant majority of practical problems about winding of materials reinforced by fibers.
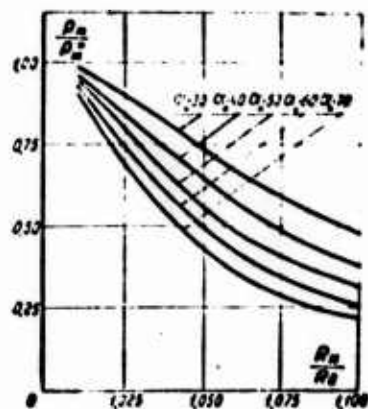

Fig. 4.2.4. The effect of the degree of anisotropy and thickness of the article being wound on the pressure transmitted to absolutely rigid mandrel.

4.2.3. Limiting number of turns when winding on absolutely rigid mandrel.

The consideration of the compressibility of materials when winding makes it possible to establish the existence of limiting number of turns $n_{\text{кр}}$, above which pressure on the mandrel or the part being wound virtually ceases to grow. This fact was established experimentally when winding on mandrels, which it is possible to consider absolutely rigid (see, for example, Fig. 4.1.3). The same conclusion follows from the given theory. Actually, from expression (4.2.4) taking into account (4.2.7) it is evident that the total residual tensioning in turns, which determines the pressure created by the wound rings on the mandrel, is limited value - when $n \to \infty$ $\Sigma T \to \dfrac{\pi T_0}{2\varkappa_{\text{н}}}$. Limiting value $\lim\limits_{n \to \infty} \Sigma T$ is determined by the tensioning force and by parameter $\varkappa_{\text{н}}$, characterizing anisotropy and geometry. It is obvious that such increase in the number of turns for obtaining maximum pressure p_{max} on the part being wound is senseless. Therefore, for obtaining the calculated dependence it is advantageous to pause on a certain part of the maximum force, created by finite number of turns. The number of turns $n_{\text{пр}}$, which corresponds to prescribed fraction $\omega = (1 - \dfrac{p}{p_{max}})$ of maximally possible pressure on the mandrel, is determined from the following expression:

177

$$\operatorname{arctg} e^{x_n n_{\text{пр}}} = \frac{\pi}{4}\left(1 - \frac{p}{p_{\text{max}}}\right). \tag{4.2.12}$$

If we examine the area of pressures p, close to p_{max}, then the limiting number of turns can be determined by formula

$$n_{\text{пр}} = -\frac{\ln\left[\left(1 - \frac{p}{p_{\text{max}}}\right)\frac{\pi}{4}\right]}{x_n}. \tag{4.2.13}$$

The dependences of limiting number $n_{\text{пр}}$ of turns on the anisotropy of material with assigned magnitude ω are given on Fig. 4.2.5, which illustrates the effect of the degree of anisotropy and the required pressure on the mandrel with fixed ratio of the thickness of strip to the radius of the ring being wound. Figure 4.2.6 shows the connection between the parameters of winding κ_{H}, assigned by ratio p/p_{max} and limiting number of turns.
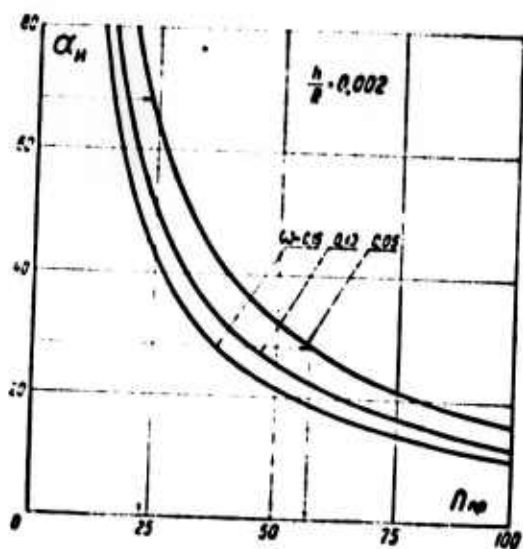

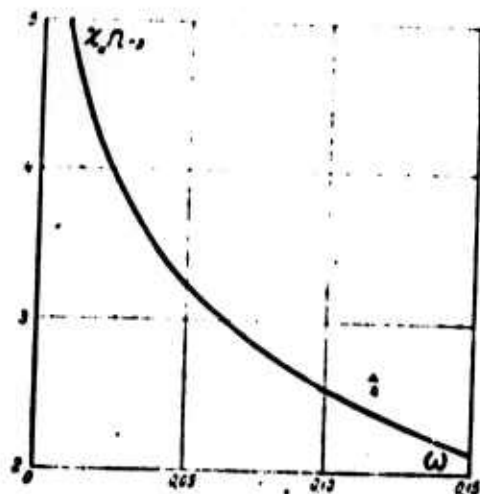Fig. 4.2.5. Limiting number of turns with fixed ratio of the thickness of the strip being wound to radius, ω = 1 - p/p_{max}.

Fig. 4.2.6. Limiting number of turns with prescribed ratio p/p_{max}.

178

As can be seen from the presented data, as a result of the transversal weakness of wound materials the pressure on rigid mandrel rapidly ceases to rise. For oriented glass fiber-reinforced plastics ($30 \geq \alpha \geq 70$) this is already observed with number of turns 25-50, which, specifically, indicates the uselessness of the tendency to attain a substantial increase of pressure on the part being wound by means of a further increase of the number of wound turns.

4.2.4. The account of pliability of the mandrel.

The winding of the investigated materials is performed on the working mandrels, which reproduce the configuration of the article being made. During the manufacture of biconstructions or when using reinforced materials for banding parts being wound serve as the mandrel. Depending on the relationships of the pliabilities of the wound constructions and wound parts the rigid and pliable mandrels can be separated. When winding thin-walled constructions of large diameter made of glass fiber-reinforced plastics to thick-walled metal mandrels of high rigidity the pliability of the mandrel can naturally be disregarded. During the manufacture of a number of other articles (winding on investment patterns [290], the winding of thin-walled metal shells [184, 301], the winding of engine block on solid-propellant grain, the winding of thick-walled constructions of glass fiber-reinforced plastic to thin-walled metal mandrels [310] and others) the pliability of the wound article in radial direction can be commensurable with the pliability of the working mandrel or the wound construction. In this case the account of deformation of the mandrel is necessary.

The effect of the pliability of the mandrel on a change of the tensioning force is investigated in [310]. Typical results are given on Fig. 4.2.7, on which there is shown change of pressure transmitted to thin-walled metal mandrel with winding of comparatively thick-walled shells of glass fiber-reinforced plastics with

179

ratio of outside and inside radius up to 1.5. When winding on steel mandrels the pliability of the mandrel can be disregarded, whereas for aluminum mandrels of the same thickness a pressure drop can reach 50%. The given results are obtained on the assumption that the properties of the wound material are close to isotropic. With such an approach the basic reason for change of the tension along the section of the wound part is missed - the compressibility of material in radial direction. This feature can be taken into account on the basis of the theory given in § 4.1 and 4.2. On the basis of (4.2.9), (4.2.2), (4.2.3), (4.1.5) and (4.1.7) the pressure transmitted to the mandrel (for the case where $\gamma_{on} < \alpha$; see Table 4.1.1),

$$p = \frac{2p_{\text{ж}}}{x_{\text{н}}) a^2 - \gamma_{\text{он}}^2} [\text{arctg}\, \eta\,(1 + x_{\text{н}})^a - \text{arctg}\, \eta]. \qquad (4.2.14)$$

When the rigidity of the mandrel becomes infinite $\gamma_{on} \to 0$, the obtained expression changes into dependence (4.2.11), which determines the pressure on absolutely rigid mandrel.
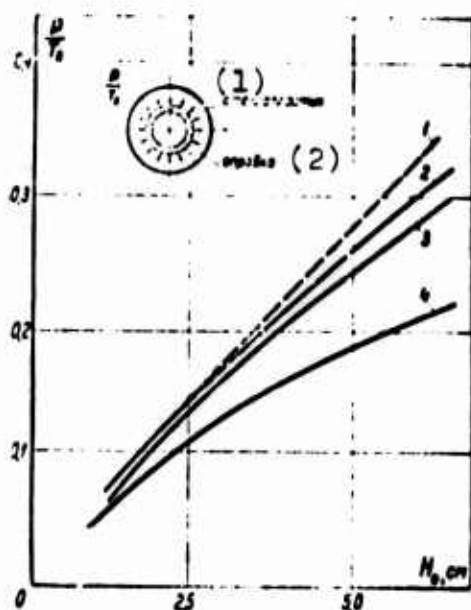

Fig. 4.2.7. The effect of pliability of the mandrel and thickness of rings H_0 on the pressure transmitted to the mandrel (diameter of mandrel 152 cm) [310]: 1 - winding on absolutely rigid mandrel; 2 - winding on steel mandrel; 3 - winding on aluminum mandrel; 4 - winding on gypsum mandrel (P/T_0 - the contact pressure on the mandrel, pertaining to tensioning force when winding).
KEY: (1) Glass fiber-reinforced plastic; (2) Mandrel.

The effect of the pliability of the mandrel on the value of contact pressure is characterized by Fig. 4.2.8. From the presented data it is evident that the pliability of the mandrel substantially affects the drop of contact pressure; however, with an increase in the degree of anisotropy of the wound strip the effect of the pliability of mandrel on the value of the pressure transmitted to it weakens. Thus, neglecting the compressibility of material when winding (as this is done in [310]) when evaluating the pliability of mandrel can lead to incorrect results, where the error grows with an increase of the thickness of the part being wound.
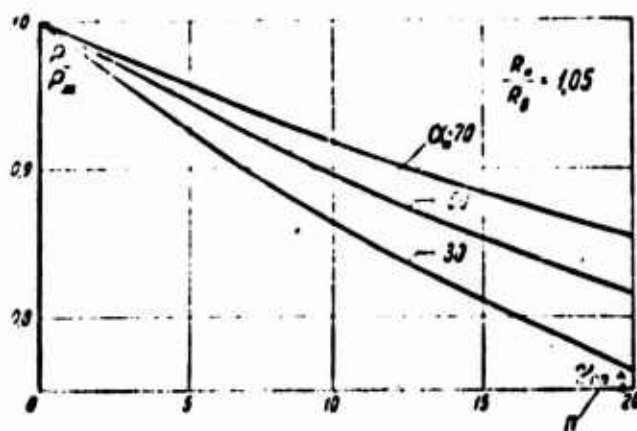

Fig. 4.2.8. The effect of pliability of the mandrel on the magnitude of contact pressure.

4.2.5. Experimental data. Pressure on the mandrel in the process of winding and limiting number of turns are most easily amenable to experimental check. The measurement of these values has independent interest, especially for calculating so-called constructions with guaranteed negative allowance. The typical experimental data, obtained when winding unidirectional glass fiber-reinforced plastic, are given on Fig. 4.2.9. In this figure the pressure is shown at the end of winding p on a force-measuring mandrel depending on the number of turns with different tensioning forces T_0 = const (solid line marks the mean value of the value being determined; broken line shows the boundaries of

181

confidence intervals with the confidence probability equal to
0.8). Relative pressure on the mandrel at the end of the stage
of winding $p/p_{_{\text{H}}}^{*}$ is presented on Fig. 4.2.10.

Detailed description of the experiment, carried out on an
arrangement, the general view of which is shown on Fig. 1.2.6,
is given in [60]. As a mandrel thin-walled steel rings are used.
The thickness of the rings is selected by dependence (4.2.14) so
that the pliability of the mandrel would not have a substantial
effect on the magnitude of the pressure acting on it. Thus,
although the mandrel was the force-measuring part, it was possible
to consider it absolutely rigid in comparison with the ring being
wound and to disseminate the conclusions obtained as a result
of experiments to absolutely rigid mandrels. Pressure on the
mandrel is changed after the process of imposition of turns on
the remaining stages of winding. The diagrams of pressure during
the entire technological cycle when winding glass fiber-reinforced
plastics are given in [59, 60]. The analysis of these diagrams
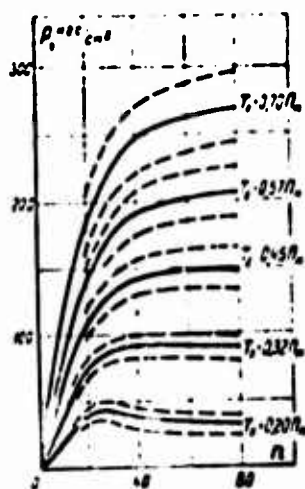falls outside the scope of this work.

Fig. 4.2.9. Pressure on force-
measuring mandrel at the end of
winding [60]. The outside diameter
of the mandrel 295 mm, thickness
4 mm, width 100 mm (mandrel is
shown on Fig. 1.2.7). The material
is LSB-F (α = 70, width of strip
16 mm, thickness 0.2 mm, strength
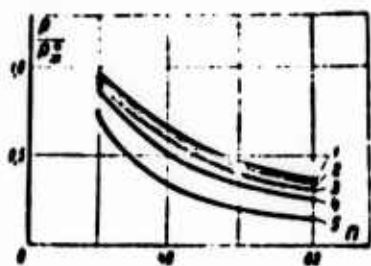in the state of winding 125 kgf).

182

Fig. 4.2.10. Relative drop of the tensioning force when winding on rigid mandrel. Material LSB-F, curves are constructed with $T_0 =$ = const for different relations T_0/Π_M: 1 - 0.7; 2 - 0.57; 3 - - 0.45; 4 - 0.32; 5 - 0.20.

The comparison of the experimental data on determining the value of $p/p^*_{нн}$, given on Fig. 4.2.10, with theoretical (Fig. 4.2.4) reveals good qualitative coincidence. The data presented in Fig. 4.2.9 attest to the existence of limiting number of turns. During the solution of the problem in linear elastic statement the relative drop of the tensioning force ΣT - and limiting number of turns do not depend on the tensioning force T_0. The dependence of $n_{пр}$ on T_0 (Fig. 4.2.9) revealed in experiments can be given simple qualitative explanation, if one considers that the degree of anisotropy of the material being wound α is connected with $\tilde{p}_0$ (see § 4.1). The growth of tensioning force caused seemingly ruggedizing of the material in radial direction, therefore $n_{пр}$ is increased with increase of α. Thus, the results obtained during the solution of the problem of winding of elastic anisotropic strip, at least qualitatively, describe the available experimental data. This opens the possibility of utilization of the obtained dependences during the development of the mechanics of the winding of the materials reinforced by fibers.

§ 4.3. THE OPTIMIZATION OF THE LAW
OF CHANGE OF THE FORCE OF WINDING

4.3.1. The possibility of bending of the reinforcing layers. As a result of severe drop of tensioning during winding there appears the danger of local bending of reinforcing fibers. Tensioning force T, which is retained in the turns of the reinforced plastics after winding, can be insufficient in order to avoid the danger of bending of the reinforcing fibers in the polymerization process of the bonding agent. When winding woven materials,

183

whose fibers are already initially bent, the danger of increase
in the bending appears. (For the negative consequences, caused
by the bending of fibers, see Chap. I.) For elimination of the
danger of the bending of fibers the minimum tensioning force T_{min}
before polymerization in any turn along the height of the part
must be more than a certain value of $T_{кр}$. Critical tensioning
$T_{кр}$ depends on the material used and forming conditions. For
example, for material AG-4S it must be more than (0.1-0.2) Π_M
[72, 215] (Π_M – the strength of material in the state of treat-
ment). For the materials, the bonding agents of which possess
large shrinkage (for example, polyester glass fiber-reinforced
plastics), $T_{кр}$ is considerably higher [293].

The greatest radial displacements when winding with constant
force T_0 are obtained by the middle turns (see Fig. 4.2.1), there-
fore the drop of tensioning in them is the greatest. The rein-
forcing fibers precisely in these turns are most prone to bending
during polymerization (Fig. 4.3.1). The residual tensioning T is
determined by the formulas given in § 4.1 and 4.2. As can be
seen from Fig. 4.3.2, it decreases with an increase of the parameter
of anisotropy α. With an increase of relative thickness R_H/R_B
a decrease of the minimum tensioning force virtually does not occur,
but the number of turns, encompassed by it, is considerably
increased. The physical sense of this phenomenon becomes clear,
if one considers that there is a limiting number of turns $n_{пр}$
(see § 4.2), upon reaching which the pressure virtually ceases
to grow. Obviously, with an increase in the number of turns
above $n_{пр}$ there appears a zone of turns in which interlayer pressure
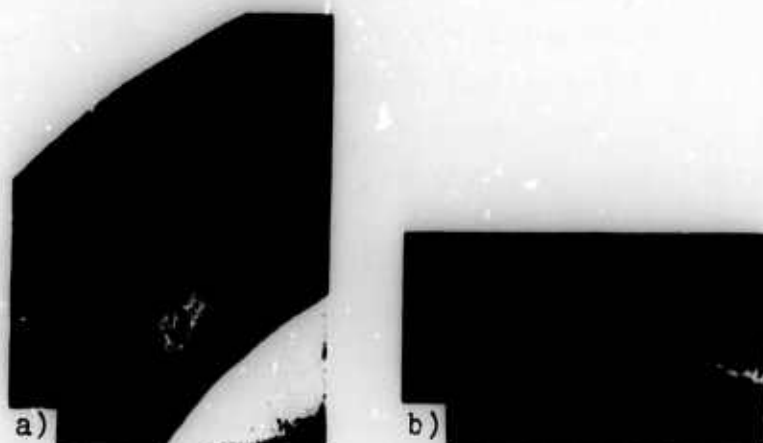barely changes. This leads to the invariability of tensioning
force in this zone.

Fig. 4.3.1. The diagram of cutout (a) and macrosection of part of a ring (b), wound from woven fiberglass strip with tensioning force $T_0 \leq T_{\text{кр}}$.
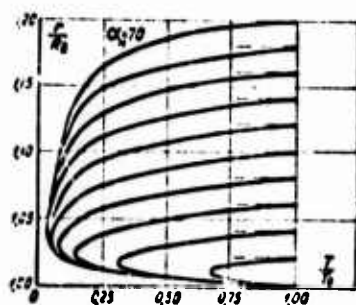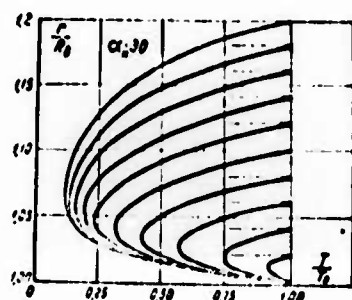
Fig. 4.3.2. The diagrams of retained tensions T after winding with T_0 = const to an absolutely rigid mandrel.

In order to evaluate the possibilities of the bending of reinforcing fibers, it is necessary to know the minimum value of T_{min}, to which the tensioning force drops in turns with real parameters of winding ($30 \leq \alpha \leq 70$; $1.01 \leq R_H/R_B \leq 1.2$). Dependence $T_{min}/T_0 = f(R_H/R_B)$, calculated on BESM-2, with different degree of anisotropy of the wound strip α is shown on Fig. 4.3.3. The curves presented in the figure attest to the fact that T_{min} asymptotically approaches zero. The noted effect follows from simple formula

$$\frac{T_{min}}{T_0} = e^{-0.5\alpha r_s}, \qquad (4.3.1)$$

185

which is obtained taking into account that values T_{min} approximately correspond to coordinate $x = 0.5\ x_H$, i.e., are found in the middle of the height of thin-walled rings. It is natural that the force of winding $T_0 \leq \Pi_M$, and since $T_{min} > 0.1\ \Pi_M$, for the materials in question, which have $30 \leq \alpha \leq 70$, the danger of the bending of fibers appears already during the winding of thin-walled rings with $R_H/R_B \leq 1.2$ (see Fig. 4.3.3).
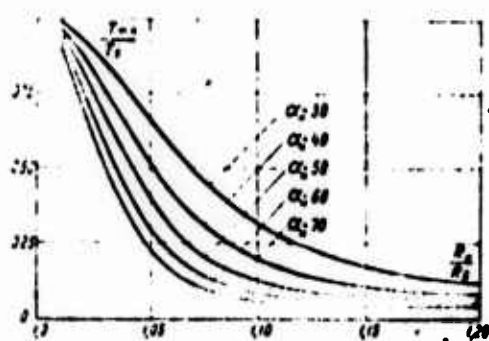

Fig. 4.3.3. Minimum tensioning T_{min} in the section of the ring, wound with T_0 = const on absolutely rigid mandrel.

4.3.2. The programming of winding. For the elimination of the danger of the bending of fibers it is necessary to perform winding in such a way that a certain minimum, preassigned tensioning force $T_{min} > T_{\kappa p}$ would be retained after finishing winding in all turns. The program, according to which the tensioning force of fibers must be changed in the tightener $T_0(r)$, in order to obtain the assigned diagram of tensioning $T(r)$ in the wound ring,[1] is determined by expression (4.2.2) (diagram of residual forces can be any). The simplest program consists of providing constant tensioning force T = const in all turns after the completion of winding. It is natural that this minimum force must be greater than $T_{\kappa p}$. Subsequently by programmed winding there is meant winding with $T_0 \neq$ const in all turns, then winding should be conducted according to the program

---

[1]The program investigated further does not consider the change of the parameter of anisotropy in the polymerization process of the bonding agent. This effect when winding reinforced plastics can be taken into account with the aid of the method proposed by V. L. Biderman [31].

$$T_0(r) = T\left[1 + a(\varrho^{-1} - 1)\frac{\varrho^{2a} - \eta^2}{\varrho^{2a} + \eta^2}\right]. \tag{4.3.2}$$

In the range of relative thicknesses $1.05 \leq R_H/R_B \leq 1.10$ when winding on absolutely rigid mandrel expression (4.3.2) can be simplified:

$$T_0(x) = T\left(1 + a\frac{x_H - x}{1 + x}\right). \tag{4.3.3}$$
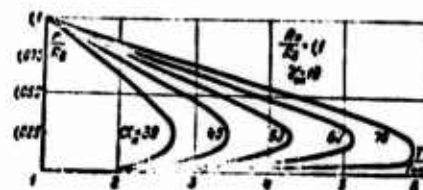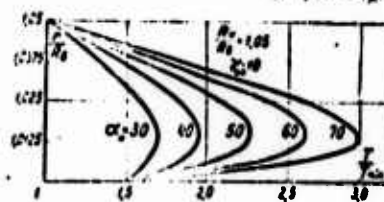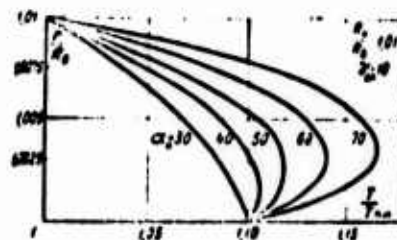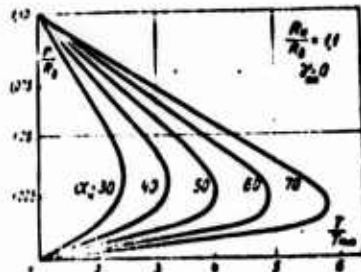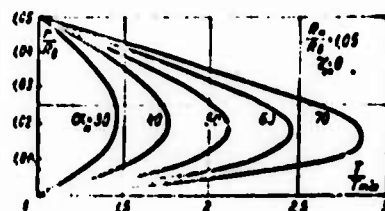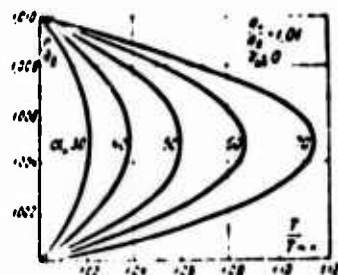
Fig. 4.3.4. Programs of change of the force of winding $T_0(r)$ for the creation of constant tension T = const in all turns (mandrel is absolutely rigid).

Fig. 4.3.5. Programs of the change of the tensioning force $T_0(r)$ for creation of T = const in all turns when winding on pliable mandrel (γ_{on} = 10).

Figure 4.3.4 gives the programs, according to which the tensioning force should be changed during the winding of rings of three different thicknesses on a rigid mandrel (with γ_{on} = 0), on Fig. 4.3.5 – when winding on pliable mandrel (γ_{on} = 10, which

187

corresponds to the winding of fiberglass strip with $E_\theta = 0.4 \cdot 10^6$ kgf/cm^2 to a steel ring with ratio of radii 1.02). The presented data attest to the fact that to provide for uniform tensioning T_{min} = const on the entire height of the ring the winding of the middle turns must be accomplished with tensioning force T_{0max}, considerably exceeding T_{min}. Taking into account that maximum value T_{0max} is reached when x $\approx$ 0.5 x_π, from (4.3.3) follows the simple formula:

$$T_{0\,max} = T_{min}(1 + 0.5\alpha x_{\text{H}}).$$
  (4.3.4)

Relation T_{0max}/T_{min} depending on the thickness of the wound ring and the degree of anisotropy for case $\gamma_{0\pi}$ = 0 is presented on Fig. 4.3.6. As is evident, in certain cases with large α and R_H/R_B it is impossible to wind the ring in order to create $T > T_{\text{кр}}$ in all turns. This pertains to materials for which $T_{\text{кр}}$ composes a significant portion of the strength of material Π_M. In this case $T_{0max} > \Pi_M$, which, of course, is unattainable.
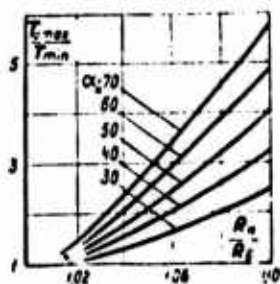
Fig. 4.3.6. Change of the maximum force with programmed winding T_{0max} with increase of the thickness of the wound ring.

4.3.3. Experimental data. Experimental determination of the diagram of residual tensions T along the height of the ring is very difficult. The total residual tensioning with different programs of winding (investigated programs are shown on Fig. 4.3.7) can be experimentally evaluated by the pressure on force-measuring mandrel. During winding depending on the predetermined program there is changed the pressure, transmitted to the mandrel. This change is characterized by the coefficient of transmission of

188

pressure $k_{H} = p/p_{H}$ (p – pressure on mandrel when winding according to the predetermined program, p_{H}^{*} – pressure when winding with constant tensioning force, equal to maximum with programmed winding) on the assumption that the turns of material are noncompressible.
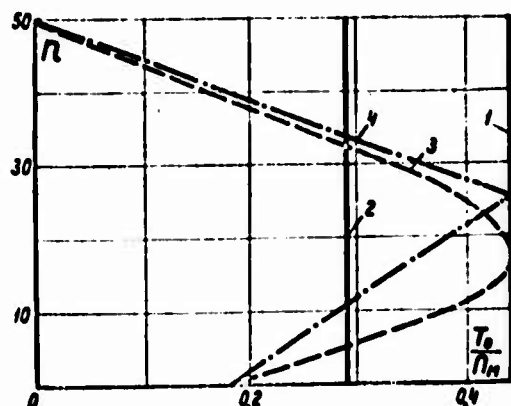
Fig. 4.3.7. Programs of the change of tensioning force in the process of winding.

The programmed winding is completely insufficiently studied. In [60] an attempt is made at the estimation of pressure on the mandrel during the preparation of rings according to different programs; four programs are experimentally realized (Fig. 4.3.7). They are selected in such a way that it would be possible to compare the programmed winding, optimized according to the assigned tensioning force along the height of the ring (program 3), and program close to it (program 4), which is technically more easily realized when winding with constant tensioning force: maximum T_0 (program 1) and given – T_0 (program 2). Program 3 is constructed according to expression (4.3.3) when $T_{max}(r) = T_0$. For program 2 $\tilde{T}_0$ is calculated from the condition of equality of the total forces when winding according to programs 2 and 3, $\Sigma T_1(r) = n\tilde{T}_0$, i.e., in such a way that the areas limited by lines 2 and 3 would be equal. When winding according to program 4 the force in the tightener is changed along the broken line. And in this case the total forces (according to programs 3 and 4) are virtually equal to each other.

189

In the process of winding according to the indicated programs on the device described earlier the pressure was measured on a force-measuring mandrel at the end of the winding stage. By each program not less than five rings are wound (material LSB-F, number of turns n = 50). The obtained experimental data (Fig. 4.3.8) were used to evaluate the pressure transmission factor and ratio of the total pressure on the mandrel, measured with programmed winding $\Delta_{\kappa p}$, to pressure on the mandrel when winding with constant tensioning force $\Delta_{\tilde{T}}$ along the height. In this case the total force, applied in the process of programmed winding $\Sigma T_1(r_1)$, is equal to total force nT_0 for the case where tensioning in all turns is identical and is equal to T_0 = const.
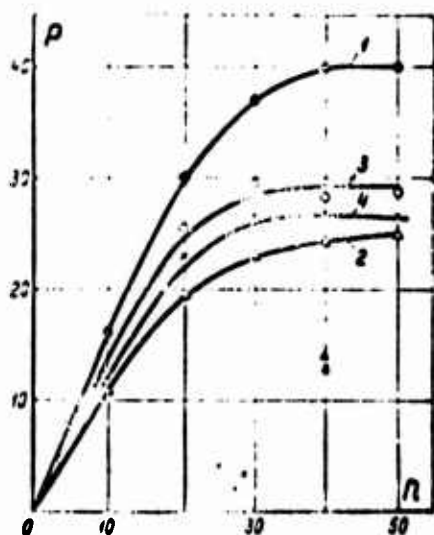
Fig. 4.3.8. Pressure on the mandrel p* (kgf/cm^2) in the process of winding with increase of number of turns. Every point in the figure is constructed according to the results of tests of five samples on the average: ● – program 1; Δ – program 2; ○ – program 3; x – program 4.

Experiments confirmed that a drop of pressure, transmitted to the mandrel, is considerably less with programmed winding, providing the retaining of T = const in all turns, than when winding according to the law T_0 = const. The transmission factor of pressure k_H when winding according to these programs proves to be higher than when winding for case T_0 = const. Winding according to the optimal program provides considerably better utilization of the total force applied in the process of winding.

Under experimental conditions it turned out that for programs 2 and 3 relations $\Delta_3/\Delta_{\tilde{T}_0}$ and $\Delta_4/\Delta_{\tilde{T}_0}$ comprise ≈ 1.20. The realization of programs 3 and 4 gives approximately the same contact pressure on the mandrel (points which correspond to $n = 50$ on Fig. 4.3.8) as program 2, providing in this case a more uniform diagram of the initial stresses along the section of the ring. It is especially important that with programmed winding there is no overstress of outer layers, which, as will be shown further, provides reduction of the danger of "unwinding" under pressure.

The given data characterize only the process of winding itself. It is necessary to note that for constructions of reinforced plastics the diagram of residual stresses is changed in the process of heating, polymerization, cooling and removal from the mandrel. For these materials the proposed program provides only the elimination of the danger of the bending of fibers in the process of winding. Creation of the assigned diagram of residual stresses in articles of glass fiber-reinforced plastics requires the consideration of a change of the assigned stress force at all remaining stages of the production process.

§ 4.4.   THE LIMITING THICKNESS OF RINGS
WHICH WORK UNDER PRESSURE

4.4.1. Thick walls. It is necessary to consider the anisotropy of the properties of materials reinforced by fibers not only during the development of the mechanics of winding (as is shown in § 4.1-4.3), but also when designing the winding articles. In a number of cases it limits the useful thickness of these constructions.

The accumulated experience of calculation, construction and the testing of articles made of reinforced plastics, in particular glass fiber-reinforced plastics, by the method of winding is obtained on comparatively thin-walled constructions – with the

ratio of thickness H_0 to radius R equal to 1/50 and less.
Recently in a number of branches there was outlined the transition
to comparatively large relative thicknesses, there are developed
the constructions of shells which work under external or internal
pressure with $H_0/R = 0.1$, there are tested rings with $H_0/R = 0.5$
[310]. The growth of the relative thickness of articles which
work under pressure does not only lead to the need for the account
of the features of the mechanics of winding noted in the preceding
paragraphs, the effect of which sharply rises with increase of
H_0/R. It is established that the failure of rings made of the
investigated materials occurs earlier than the strength is
exhausted in the direction of fibers. The supporting power of
isotropic rings (in the range of thicknesses in question) increases
virtually in proportion to thickness.

The macrostructure and the weak compressive strength deter-
mined by it when loading perpendicular to the fibers place a
limitation on the useful thickness of rings of materials reinforced
by fibers (Fig. 4.4.1). The graph presented in the figure describes
the dependence of the value of the destructive internal pressure p_B
on the structure and the relative thickness of the tested ring
H_0/R. In this figure is given the loading diagram; tests were
conducted with the aid of a rubber ring and on half-disks.[1]
Data presented in the figure are obtained when testing rings of
materials which have fibrous structure (LSB-F, $\frac{E_\theta}{E_r} \leqslant 5$, $\frac{\Pi_\theta^+}{\Pi_r} \sim 12$) and
laminated (reinforced by glass cloth of satin weave - VPS-7,
$\frac{E_\theta}{E_r} \approx 3$, $\frac{\Pi_\theta^+}{\Pi_r^-} \approx 3$). These materials are close in elastic properties, but
sharply differ in compressive strength perpendicular to the fibers.

---

[1] Comparison of the curves given on Fig. 4.4.1 attests to the
inadequacy of half-disks (NOL-ring method) for testing thick-
walled rings of reinforced plastics. With an increase of the
thickness of the tested rings the effect of the bending stresses
at the joint places of half-disks is intensified [148]. The
consideration of these stresses during the examination of the
results of tests presents considerable difficulty.
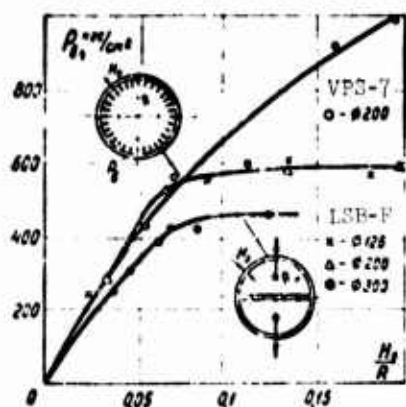
Fig. 4.4.1. The dependence of bursting pressure on the relative thickness of the rings and structure of material. Unidirectional material: x - rings 126 mm in diameter, material LSB-F; Δ - rings 200 mm in diameter, material LSB-F; ● - rings 300 mm in diameter, material LSB-F. Laminated material: o - rings 200 mm in diameter, material VPS-7.
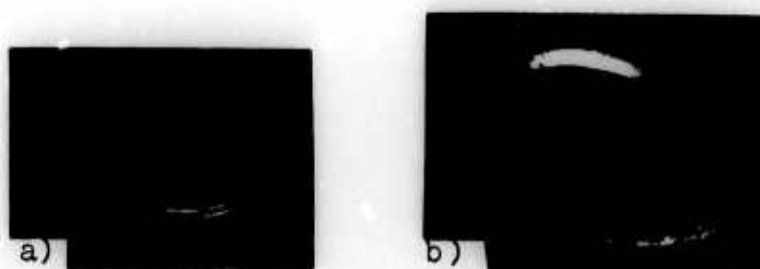
Fig. 4.4.2. The types of failure of rings with internal pressure: a) thin-walled rings H_0/R = 0.05, material VPS-7; b) thick-walled rings H_0/R = 0.15, material LSB-F.

The presented data attest to the fact that the supporting power of rings made of unidirectional materials rapidly ceases to increase with an increase in the number of turns. This phenomenon is accompanied also by a change in the character of the fracture. With the small thickness of the sample the character of fracture is analogous to that observed with the stretching of thin flat samples (Fig. 4.4.2a). The failure of thick samples occurs in the direction of the action of the maximum tangential stresses (Fig. 4.4.2b).[1] When testing rings of woven materials in the investigated range of thicknesses no limitation of supporting power is observed, although the dependence of bursting pressure on the number of turns becomes more gently sloping.

_____

[1]Detailed data on this question are presented in [61].

193

The macrostructure of articles made by winding is such that the reinforcing fibers in the plane perpendicular to the axis of the article are placed on a spiral with very small spacing. The weak shear strength of polymer bonding agent combined with the spiral arrangement of fibers leads to the danger of a special type of failure of the winding constructions, which work under pressure, by means of "unwinding" [166]. Overstresses at places of attachment of fibers and tangential stresses, which appear under the action of internal or external pressure near cracks on the surfaces of the article, can serve as the reason for spontaneous structural failure. The appearing fracture will be continuously propagated along the spiral, formed by the reinforcing fibers. Failure by "unwinding" can also limit the useful thickness of articles of reinforced plastics and prevent the complete utilization of potential possibilities of the material in the direction of fibers.

Thus, when evaluating the supporting power of the constructions made by the method of winding it is necessary to estimate the effect of the anisotropy of properties $\alpha^2 = E_\theta/E_r$ (one ought to emphasize that it is substantially less than in the state of winding: see Table 1.1.1), the weak compressive strength when loading perpendicular to fibers $\underset{II}{\overset{II\#^+}{\cdots}}$ and the danger of "unwinding" on the limiting thickness of rings of the investigated materials, which work under pressure. Let us note that during the testing of thin rings (NOL-ring type) further effects in question simply could not be revealed, since they are developed only with an increase of the thickness of articles.

4.4.2. **Anisotropy of deformating properties.** It is known [123, 315] that the anisotropy of elastic properties along and across the fibers leads to an increase in the nonuniformity of the distribution of circumferential stresses σ_θ along the thickness of the rings. With an increase of parameter α part of the load received by layers near the surface, on which the pressure acts, is increased. For isotropic thick-walled rings (see,

194

for example [247]) with the ratio of outside and inside radii $R_H/R_B \geq 4$ further increase of the outside radius virtually does not decrease the value of the maximum circumferential stresses $\sigma_{\theta max}$ near the internal surface of the ring, which works under pressure. Substantial elastic anisotropy α can transfer the noted effect into the area of much less thicknesses.

The effect of relation E_θ/E_r on the value of the maximum stresses $\sigma_{\theta max}$, and consequently also on the limiting thickness of the ring can be evaluated with the aid of the expression given in S. G. Lekhnitskiy's book [123]:

$$\sigma_{\theta max} = \alpha p_B \frac{1 + \left(\dfrac{R_H}{R_B}\right)^{2\alpha}}{1 + \left(\dfrac{R_H}{R_B}\right)^{2\alpha}} .$$

where p_B is internal pressure.
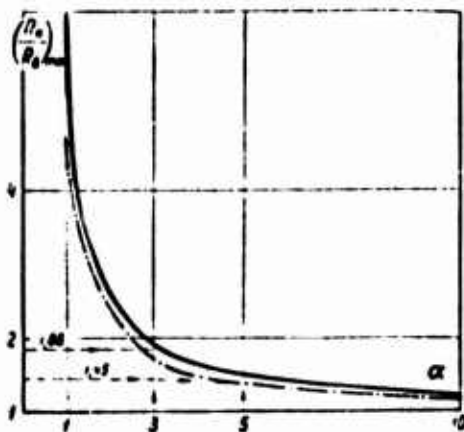
Fig. 4.4.3. The effect of the degree of anisotropy on the limiting thickness of ring. ——— is decrease of $\sigma_{\theta max}$ as a result of the growth of thickness of ring 5%; —·—·—·— is decrease of $\sigma_{\theta max}$ 10%. Pointers show limiting thicknesses with assigned anisotropy.

The effect of the degree of anisotropy on the limiting relative thickness of rings $(R_H/R_B)_{Hp}$ is shown on Fig. 4.4.3; curves are constructed when a further increase of the thickness of rings virtually does not lead to decrease of $\sigma_{\theta max}$ when $p_B =$ = const. In the area of weak anisotropy, i.e., with $\alpha^2 \leq 5$, which is characteristic for the majority of the existing reinforced plastics after polymerization, the limiting thickness lies

within $(R_H/R_B)_{HP} = 1.4-1.8$. However the growth of parameter α for new materials with increased elastic modulus in the direction of fibers E_θ, made on the same bonding agents, can lead to further decrease of the limiting thickness of ring.

4.4.3. Low strength during compression perpendicular to fibers. Condition of strength.

The weak compressive strength when loading perpendicular to the reinforcing fibers for materials with fibrous structure leads to the fact that with an increase of the relative thickness of the rings, loaded by internal pressure, in the interior layers the compressive strength is exhausted earlier than the ultimate strength in the direction of the grain. For these materials Π_{μ}' and Π, sharply differ, $\dfrac{\Pi_{\mu}^{+}}{\Pi_{.}} \approx 10$ (see diagram 1 and Fig. 1.1.3), this relation increases with an increase of strength and the percentage of fibers [280]. The weak compressive strength is the reason which limits the supporting power of rings made of materials with fibrous structure. The fact that the bursting pressure is identical when testing sufficiently thick rings with identical relative thickness H_0/R, but different diameter (Fig. 4.4.1), attests to this. In this case the maximum compressive stresses $\sigma_{\theta max}$ are equal to each other, and the maximum circumferential stresses are inversely proportional to the radius of rings. Under conditions of the experiment $\sigma_{\theta max}$ differed 1.6 times, and the value of bursting pressure was virtually identical.

For the problem in question, taking into account the importance of the anisotropy of strength properties, it is natural to assume that the stresses which act in the direction of reinforcement do not affect the strength in perpendicular direction. V. L. Biderman [29] came to such a conclusion as a result of the processing of the data of tensile tests of samples cut out at different angles from material reinforced by braided

glass cloth.   In this case the condition of strength[1] is written
in the following form:

$$\sigma_{\theta\,max} \leqslant \Pi_{\theta}{}^{+}, \quad \sigma_{r\,max} \leqslant \Pi_{r}{}^{-}.$$

For the establishment of the boundary of transition from one
type of failure to another it is possible to use the method applied
during the study of the bending strength (see § 2.4).   For this
the obtained experimental data are presented in coordinates
$\sigma_{\theta max}$ and σ_{rmax}.   In these axes the course of loading is described
by a ray proceeding from the origin of coordinates, the inclina-
tion of the ray depends on relation H_0/R and parameter α.   On
Fig. 4.4.4 the rays are constructed for $H_0/R = 1/40-1/5$, investi-
gated experimentally, and two values of parameter α: $\alpha^2 = 1$
(isotropic material) and $\alpha^2 = 5$ (the extreme value of the parameter
of anisotropy for LSB-F).   In the area of the investigated rela-
tions H_0/R in the case $\alpha^2 \leq 5$ the parameter of anisotropy α
virtually does not affect the transition from one type of failure
to another.   For these relative thicknesses the rays for $\alpha = 1$
and $\alpha^2 = 5$ virtually flow into one line.

The plotting of limiting straight lines $\Pi_{\theta}{}^{+}$ and $\Pi_{r}{}^{-}$, obtained
during independent tensile and compression tests along and across
the reinforcing fibers, makes it possible to judge the expected
character of fracture.   The presented data attest to the fact that
the transversal weakness of the materials reinforced by fibers
considerably "lowers" the boundary of the failure of unidirectional
materials from compression under the action of internal pressure

---

[1]Survey of the existing strength criterion for anisotropic
materials is given in book [23] and in the review papers of
I. I. Goldenblat and V. A. Kopnov [85] and A. K. Malmeyster [131].
The use of the existing strength conditions to evaluate the
supporting power of parts from glass fiber-reinforced plastics is
given in book [227].   Let us note that the experimental evaluation
of these criterion is realized on thin pipes of glass fiber-
reinforced plastics, i.e., under conditions when radial stresses
could be disregarded.

in the area of comparatively small thicknesses (for isotropic materials the boundary of failure is moved far upward along the axis σ_{rmax}).
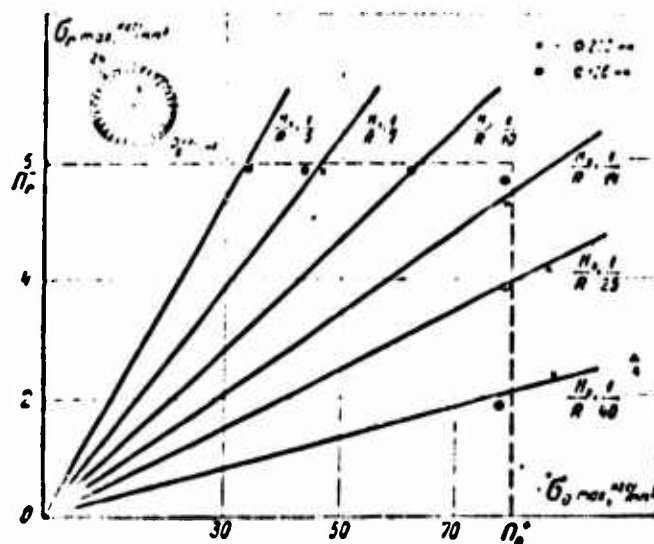
Fig. 4.4.4. The character of fracture of rings of different thickness under the action of internal pressure. x is diameter 200 mm; ● is diameter 126 mm (material LSB-F).

For the class of materials in question the limitation of the relative thickness of rings, which work under pressure, can be obtained when the bursting pressure must not exceed the strength of material during compression perpendicular to the reinforcing fibers. Hence $H_0/R = \Pi_\theta^+/\Pi_r^-$. For the investigated materials this is approximately 0.08-0.10. If one considers that an increase of the strength reinforcing fibers and their percentage barely affects the transversal properties of the reinforced plastics (see, for example, Fig. 1.1.3), since the properties of polymer matrix remain without changes, the creation on the basis of existing bonding agents of unidirectional fibrous material with increasingly higher tensile strength will be connected with decrease of the maximum possible thicknesses of winding articles, which work under pressure. In a number of cases an increase in Π_r^- to the detriment of Π_θ^+, i.e., the use in thick-walled constructions of

198

less strong woven materials in the direction of the grain, for which strength Π_r is greater.

4.4.4. Failure by "unwinding."

The low pitch of the spiral, formed by fibers during winding, makes it possible to replace the turns with concentrically arranged rings. The large number of rings and their insignificant relative thickness make it possible to complete the limiting change to quasi-homogeneous medium. Such an approach, valid when determining the appearing stresses and deformations, is not exhausting, since it eliminates from examination the possibility of the special type of failure - "unwinding." The feature of the problem consists of the fact that the limiting transition must not be propagated to the boundary (internal or outside) layer of the ring.

To evaluate the danger of "unwinding" under pressure it is necessary to investigate the stressed state in the area which includes the end of the strip, which forms the ring (or shell). Analogous stressed state appears at places of breaks of fibers or notches on the surface of the article. The calculation diagram is shown on Fig. 4.4.5. The end of the reinforcement strip is a long strip with thickness h' (elastic modulus E'), fixed by a layer of polymer with thickness h". The elastic modulus of composite material in circumferential direction is E_θ. The pliable matrix is considered ideally elastoplastic (Fig. 4.4.6). For the problem in question the overall height of the ring considerably exceeds the thickness of the strip being wound, i.e., $H_0 \gg h' + h"$. Therefore it is possible to consider that the normal stresses in the glued reinforcing layer σ'_θ and the tangential stresses in the interlayer of polymer $\tau''_{\theta r}$ are constant along the thickness of the layers. The equation of equilibrium for the reinforcing layer, attached to the ring, with outside radius R is written in the following form (Fig. 4.4.5):

$$\tau''_{\theta r} R d\theta - H_\omega d\sigma'_\theta = 0. \tag{4.4.1}$$
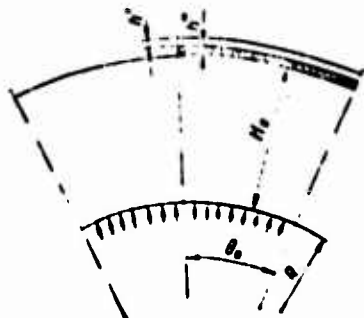
Fig. 4.4.5. The calculation diagram.
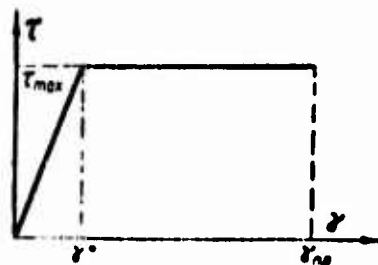
Fig. 4.4.6. The accepted diagram of deformation of bonding agent.

Both stresses can be expressed by displacement of the layer of reinforcement in circumferential v and radial u directions:

$$\tau''_{\theta r} = \frac{v}{h''} G''; \quad \sigma'_\theta = \frac{E_\theta}{r}\left(\frac{dv}{d\theta} + u\right). \tag{4.4.2}$$

Having substituted (4.4.2) in (4.4.1), we obtain the equation of equilibrium in displacements:

$$\frac{d^2 u}{d\theta^2} - \chi^2 v = 0; \tag{4.4.3}$$

$$\chi^2 = \frac{R^2 G''_{\theta r}}{h' h'' E_\theta}.$$

Boundary conditions of equation (4.4.3):

$$\text{when } \theta = 0 \quad \sigma_\theta = 0; \quad \frac{1}{r}\left(\frac{dv}{d\theta} + u\right) = 0;$$

$$\text{when } \theta = \theta_0 \quad \tau_{\theta r} = 0; \quad v = 0. \tag{4.4.4}$$

With sufficient distance from the end of the strip the normal stresses in it are equal to the stresses in the ring σ_θ, since according to conditions of the problem $H_0 \gg h' + h''$. The solution of equation (4.4.3) in boundary conditions (4.4.4) has the form

$$v = \frac{\sigma_0}{E_\theta}\sqrt{\frac{h' h'' E'}{G''}} \, (\text{th}\,\chi\theta_0\,\text{ch}\,\chi\theta - \text{sh}\,\chi\theta). \tag{4.4.5}$$

200

Since χ is great, th $\chi\theta_0 \approx 1$ and the expression for tangential stresses in polymer interlayer is equal to:

$$\tau = \frac{\sigma_0}{E_\theta} \sqrt{\frac{h'E'\bar{G}''}{h''}} e^{-\chi\theta}.$$ (4.4.6)

As can be seen from (4.4.6), as a result of large value of χ the tangential stresses are rapidly damped in proportion to the distance from the end of the strip.

The maximum tangential stress

$$\tau_{max} = \frac{\sigma_0}{E_\theta} \sqrt{\frac{h'E'\bar{G}''}{h''}}.$$ (4.4.7)

which corresponds to the value of internal pressure p_{1ynp}, at which (in elastic setting) the failure of thin-walled ring of radius R begins:

$$p_{1\,ynp} = \frac{\tau_{max}H_0E_\theta}{R\sqrt{\frac{h'E'G}{h''}}}.$$ (4.4.8)

If the thickness of the reinforcing layers and interlayers of polymer bonding agent is constant on the entire height of the shell and near the end of the wound strip, then, by accepting on the basis of the method of summation $E_\theta = \frac{h'}{h'+h''}E'$ and $G_{r\theta} = \frac{h'+h''}{h''} G''$, expression (4.4.8) can be rewritten in the following form:

$$p_{1\,ynp} = \tau_{max} \frac{H_0}{R} \sqrt{\frac{E_\theta}{G_{r\theta}}}.$$ (4.4.9)

The value of $\frac{H_0}{R}\sqrt{\frac{E_\theta}{G_{r\theta}}}$ characterizes the geometry of the part and anisotropy of its elastic properties. It is analogous to the criterion used earlier (Second and Third Chapters) in the examination of problems of the calculation of parts from essentially anisotropic materials.

For a thick-walled ring the value of internal pressure at the moment of the beginning of the failure of polymer interlayer will comprise

$$p_{2\,\text{упр}} = \frac{\tau_{\max}\left[\left(\frac{R_{\text{н}}}{R_{\text{в}}}\right)^{2\alpha} - 1\right]E_{\Theta}R_{\text{в}}^{\alpha-1}}{2\alpha R_{\text{н}}^{\alpha-1}\sqrt{\dfrac{h'E'G''}{h''}}}. \tag{4.4.10}$$

The solution of the same problem on the assumption that the polymer layer behaves as an ideal elastoplastic body with elastic shear deformations γ^* and limiting deformations $\gamma_{\text{пл}}$ (Fig. 4.4.6), makes it possible to establish that with the same value of $\tau_{\max}$ the failure of polymer interlayer will occur for thin-walled shell with internal pressure $p_{1\text{пл}}$ equal to

$$p_{1\,\text{пл}} = \frac{H_0\tau_{\max}E_{\Theta}}{R\sqrt{\dfrac{h'E'G''}{h''}}}\left[1 + \frac{E'}{E_{\Theta}}\sqrt{2\left(\frac{\gamma_{\text{пл}}}{\gamma^*} - 1\right)}\right]. \tag{4.4.11}$$

For thick-walled ring

$$p_{2\,\text{пл}} = \frac{\tau_{\max}E_{\Theta}R_{\text{в}}^{\alpha-1}\left[\left(\frac{R_{\text{н}}}{R_{\text{в}}}\right)^{2\alpha} - 1\right]}{2\alpha R_{\text{н}}^{\alpha-1}\sqrt{\dfrac{h'E'G''}{h''}}}. \tag{4.4.12}$$

The dependence of critical pressure $p_{1\text{пл}}$ on the properties of polymer matrix is shown on Fig. 4.4.7. During calculation there are used typical parameters of epoxy glass fiber-reinforced plastics. Numerical values of these parameters are given in the caption under the figure.

The failure of the interlayer, which began in a small section near the notch or the end of the strip, will be continuously propagated along the spiral formed by the strip. Such a failure – "unwinding" – will be continued until the shell will be destroyed by normal stresses increasing in view of decrease in its thickness. As an example Fig. 4.4.7 shows the failure of rings of glass fiber-reinforced plastic VPS-7 by "unwinding" when loading by internal pressure. It was observed for a number of rings during

202
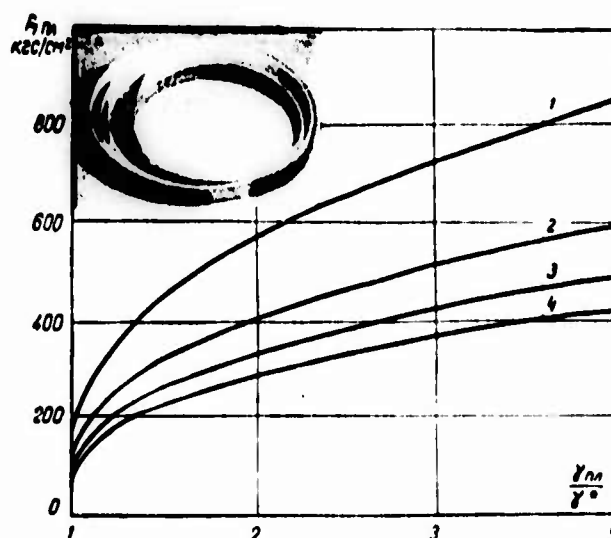
Fig. 4.4.7. The dependence of critical pressure on the plasticity and shear rigidity of the polymer bonding agent: 1 – $G'' = 0.01 \cdot 10^6$ kgf/cm^2; 2 – $G'' = 0.02 \cdot 10^6$ kgf/cm^2; 3 – $G'' = 0.03 \cdot 10^6$ kgf/cm^2; 4 – $G'' = 0.04 \cdot 10^6$ kgf/cm^2. During calculation there is accepted: $H_0/R = 0.1$; $E' = 0.6 \cdot 10^6$ kgf/cm^2, $h'/h'' = 2$, $\tau_{max} = 500$ kgf/cm^2, $E_\theta = 0.4 \cdot 10^6$ kgf/cm^2. In the upper corner is shown the failure of rings of material VPS-7 by "unwinding ."

the study of the effect of tensioning on strength (the installation and the results were examined in § 1.3). The reason for the failure can also be any discontinuities of reinforcement (for example, cracks on the outside or internal surface of ring or shell, parallel to their axis, notches, etc.). "Unwinding" can begin not only on the outside, but also from the inside both with external and internal pressure. Let us note that the appearance of a crack on the surface, on which pressure does not act, is more dangerous, since in this case there are no forces which would press the wound layer to the shell and contribute to the appearance of frictional forces, preventing unwinding. For reinforced plastics as a result of the fact that the pliable matrix is a viscoelastic material, the danger of "unwinding" increases with an increase in the rate of loading – with increase of the rate G'' is increased. As can be seen from the given formulas, this leads to decrease of the pressure at which "unwinding" begins.

The analysis carried out above makes it possible to establish the reasons and to give the explanation of the experimentally observed cases of "unwinding" of articles, described in [276, 277], to indicate the ways which make it possible to avoid the failures of this type. These ways include, for example, decrease of the rigidity and increase of the limiting deformation of polymer matrix, increase of the thickness of polymer layer in the last turn, the creation of favorable diagram of residual stresses.[1] The described type of failure is possible not only in articles of oriented glass fiber-reinforced plastics, but also in wound articles from other materials reinforced by fibers.

Naturally the application of materials for constructions, which work under pressure, that are stronger in the direction of reinforcing (for example boron plastics) without an increase in the shear strength of the polymer layer, increases the danger of the appearance of the described type of failure. "Unwinding" can be the reason, which prevents the complete utilization of the potential possibilities of material in the direction of winding.

§ 4.5. THE INITIAL STRESSES IN RINGS
OF GLASS FIBER-REINFORCED PLASTICS,
MANUFACTURED WITH NEGATIVE ALLOWANCE

4.5.1. The reasons for the appearance of initial stresses. In the preceding paragraph when evaluating the supporting power of rings, which work under pressure, the initial stresses were not taken into account. The process of manufacture of articles from reinforced plastics by the method of winding is accompanied

---

[1]For shells of glass fiber-reinforced plastics the winding of the last layers of strip without tensioning makes it possible after polymerization of bonding agent and removal from the mandrel to create compressive stresses in the outer layers. In this case in the layer of polymer near the end of the strip there will appear tangential stresses reverse in sign to the internal pressure appearing with the loading of the shell. This makes it possible to raise the supporting power of polymer interlayer.

by the appearance of initial (they are still called residual) stresses - circumferential σ_θ^0 and radial σ_r^0. As an example

Fig. 4.5.1 shows characteristic diagrams σ_θ^0 and σ_r^0 acting in the section of thick-walled ring (Fig. 4.5.2). The ring is equipped with strain gauges on the end and internal surfaces. The gauges, stuck on the inside radius, are necessary for determining the diagrams of initial stresses. Gauges on the butt end serve to evaluate a change in the elastic properties along the height of the ring[1] (as a result of a change in the tensioning force; see § 1.4). The ring is made from glass laminate on bonding agent EDT-10 with small negative allowance of strip, equal to 1-3 kgf/cm. As can be seen from the given experimental data, the initial stresses can be very considerable. So, $\sigma_{\theta max}^0$ comprises approximately a third of the tensile strength of material in the direction of base.

Of special danger are radial stresses. The tensile strength of reinforced plastics perpendicular to the reinforcing fibers Π_r^+ is small, therefore the initial stresses σ_r^0 in spite of their relative smallness, can be the reason for the failure. For example, they are the reason for the appearance of thermal cracks (Fig. 4.5.8) in the process of heating of the ring, made with large negative allowance. Such cracks are frequently encountered in the practice of manufacture of shells of glass fiber-reinforced plastics, especially in thick-walled articles. In this case there is manifested transversal weakness of the materials reinforced by fibers. The danger of residual stresses is aggravated by the large scattering of strength Π_r^+, especially for thick-walled articles. For conditions in the described

---

[1]Under conditions of the described experiment the gauges, stuck on the butt surface, revealed a change of the elastic properties through the thickness of rings. This required during the examination of the results of experiments the consideration of change E_θ along the radius.

experiment (Figs. 4.5.1 and 4.5.2) it turned out that the value of residual stresses is covered by the scattering of strength (Table 4.5.1).

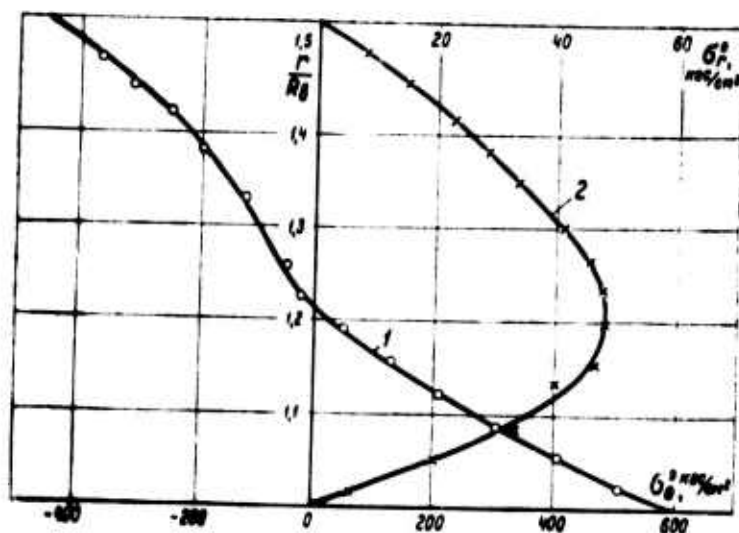
Fig. 4.5.1. The diagram of the initial stresses in thick-walled ring of glass fiber-reinforced plastic ($R_H/R_B = 1.5$,

$R_B \simeq 300$ mm): $1 - \sigma_\theta^0$; $2 - \sigma_r^0$.
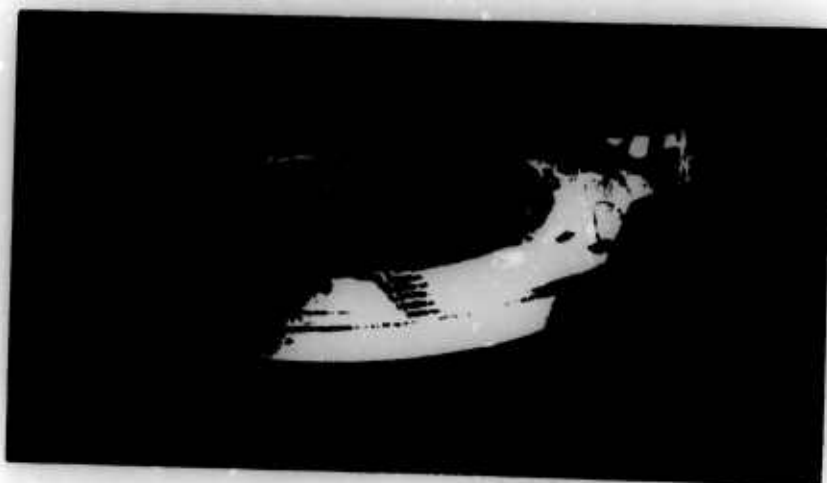
Fig. 4.5.2. The ring equipped with strain gauges on inside and side surfaces. $2R_B$ = = 595 mm, $2R$ = 906 mm, thickness 50 mm. The removal of layers along the outside diameter.

Table 4.5.1. The tensile strength of thick-walled ring perpendicular to fibers.

Radius on which the middle of the sample falls,[1] cm	Π_r^+, kgf/cm^2	$\dfrac{\Pi_{r\ min}^+}{\Pi_{r\ max}^+}$	Quantity of samples	Coefficient of variation v, %
41.0	178	$\dfrac{28.3}{262}$	12	41.6
33.5	312	$\dfrac{265}{347}$	10	8.94

[1]Samples had the shape of a blade 80 mm long and 5 mm thick, were cut from a thick-walled ring (Fig. 4.5.2) with inside diameter 595 mm and outside 906 mm.

The reasons for the appearance of the initial stresses consist of the nonuniformity of tensioning force along the height of the part, the difference of coefficients of thermal expansion for the wound material and mandrel, the shrinkage processes, which accompany the polymerization of bonding agent.[1] All these reasons are examined in detail in [168]. One additional reason for the appearance of initial stresses is the nonhomogeneity of elastic and thermophysical properties over the section of thick-walled parts (for example, for articles of reinforced plastics due to the different conditions of polymerization along the thickness, different content of reinforcement, etc.). As shown in [51], already the very anisotropy of elastic and thermophysical properties can be the reason for the appearance of initial stresses even during uniform heating or cooling of the article.

The effect of initial stresses much depends on the tensioning force, relative thickness of part (number of turns) and shop

[1]Shrinkage stresses play a significant role on the boundary of reinforcement and polymer matrix [114, 283].

characteristics. For the winding of reinforced plastics the difficulty of the analytical determination of initial stresses consists of the account of processes which proceed during the heating and subsequent hardening of bonding agent. During the initial period of heat treatment the bonding agent is softened. This leads to change of E_r, and consequently also the diagram of tensioning force in the turns of the ring, preset when winding. After the solidification of bonding agent the rigidity of the material in radial direction sharply rises and with subsequent cooling (heating) of the article together with the mandrel the further redistribution of circumferential and radial stresses occurs in it. As a result the diagrams of residual forces after the preparation of the article differ significantly from those initially predetermined when winding. After removal from the mandrel the obtained diagram is summarized with the stresses which act due to contact pressure. For comparatively thin-walled rings it is possible to consider that these stresses are not changed along the height. The process of change of the diagram of forces in the sections of the ring for two principally differing programs of winding is shown schematically on Figs. 4.5.3 and 4.5.4. Let us note that V. L. Biderman [31] proposed the method of solution of the problem which makes it possible to consider the change of the elastic properties in the process of softening of the bonding agent.

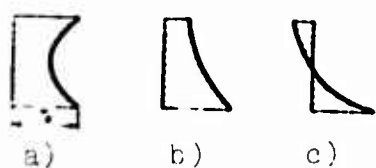Fig. 4.5.3. The diagram of circumferential stresses in the sections of ring when winding with T_0 = const: a) after winding; b) after polymerization; c) after removal from the mandrel.
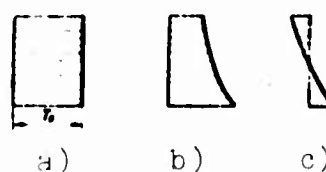
Fig. 4.5.4. The diagram of circumferential stresses in the sections of ring when winding according to the program calculated by (4.3.3): a) after winding; b) after polymerization; c) after removal from the mandrel.

208

4.5.2. The methods of determination of initial stresses.

The initial stresses in rings are determined with the aid of two most widespread methods: cuts along the radius with measurement of the convergence or divergence of ends (sides of cut) [236] and the laminar boring or turning of the ring with measurement of deformations on the opposite side (Sachse method) [33, 110]. The last method is the most convenient during the study of initial stresses in rings of materials reinforced by fibers, especially for laminar structure [167]. In this case boring or turning can be replaced with laminar unwinding of the layers of strip or cloth with measuring of deformations on the opposite side of the ring through a certain quantity of removed turns. This sharply decreases the labor expense of the "Sachse method" and raises the accuracy of determination of the stresses; however, high accuracy can be obtained only during the investigation of sufficiently thick rings.

When using the cut method for determining the absolute value of initial stresses there is necessary the hypothesis about the character of their distribution over the section of the ring (see, for example, [236]). Assuming that the stress distribution is linear, then the initial stresses in the rings, whose thickness is small in comparison with the radius, are equal to

$$\sigma_\theta{}^0 = \frac{E_\theta\,(r-R)}{2\pi R}\,\Delta h, \qquad (4.5.1)$$

where R is the mean radius of the ring; Δh - convergence (or divergence) of the ends of the ring with its cutting. Figure 4.5.5 for illustration shows the dependence of Δh on tensioning force (rings of material VPS-7, diameter 200 mm, thickness 5.5 mm, wound with different tensioning force, but constant along the height, are tested. Straight line is drawn by the least squares method. Recalculation of the shown diagram into stresses gave $\sigma_{\theta max}^0$ on the order of 1000 kgf/cm^2.
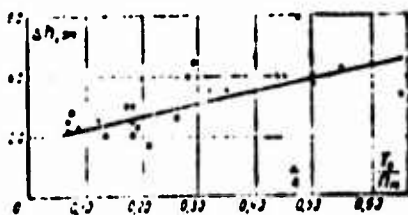
Fig. 4.5.5. The dependence of convergence of ends after cutting of ring on the tensioning force when winding.

The method of laminar unwinding, unfortunately, is much more work consuming; however, it makes it possible to determine not only the value, but also the character of distribution of the initial stresses. For thick-walled rings of materials with cylindrical orthotropy with the utilization of the idea of 'the Sachse method the expressions for circumferential and radial stresses are obtained in [168].

With unwinding along the outside diameter (i.e., with "turning"):

$$\sigma_\theta{}^0 = -\frac{E_\theta}{2aR_{\text{в}}{}^{a-1}}\left[\frac{a(r^{2a}+R_{\text{в}}{}^{2a})}{r^{a+1}}\varepsilon_\theta(r) + \frac{r^{2a}-R_{\text{в}}{}^{2a}}{r^a}\cdot\frac{d\varepsilon_\theta(r)}{dr}\right]; \qquad (4.5.2)$$

$$\sigma_r{}^0 = \frac{E_\theta}{2a}\cdot\frac{R_{\text{в}}{}^{2a}-r^{2a}}{R_{\text{в}}{}^{a-1}r^{a+1}}\varepsilon_\theta(r). \qquad (4.5.3)$$

where r is the current radius, at which the removal of the layer occurs; $\varepsilon_\theta(r)$ - circumferential deformation on inside radius during the removal of layers to radius r. With unwinding along the inside diameter (i.e., with "boring")

$$\sigma_\theta{}^0 = \frac{E_\theta}{2aR_{\text{н}}{}^{a-1}}\left[\frac{R_{\text{н}}{}^{2a}-r^{2a}}{r^a}\cdot\frac{d\overline{\varepsilon}_\theta(r)}{dr} - a\frac{R_{\text{н}}{}^{2a}+r^{2a}}{r^{a+1}}\overline{\varepsilon}_\theta(r)\right]; \qquad (4.5.4)$$

$$\sigma_r{}^0 = -\frac{E_\theta}{R}\cdot\frac{r^{2a}-R_{\text{н}}{}^{2a}}{R_{\text{н}}{}^{a-1}r^{a+1}}\overline{\varepsilon}_\theta(r); \qquad (4.5.5)$$

$\overline{\varepsilon}_\theta(r)$ - circumferential deformation on outside radius during the removal of layers to radius r.

210
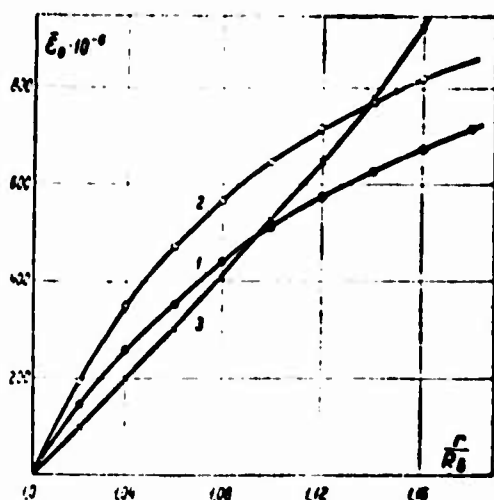
Fig. 4.5.6. Deformation curves with "bcring" (R_B = 100 mm, n = = 80 turns: 1 - T_0 = 0; 2 - T_0 = = 30 kgf/cm = const; 3 - $T_0(r)$ according to the program shown on Fig. 4.5.9a.

With laminar "unwinding" of deformation on the inside or outside surface the rings are measured with the aid of resistance strain gauges. From the readings of gauges are constructed the deformation curves ε_θ = f(r). The typical curves, obtained with the "unwinding" of thick-walled rings, are shown on Fig. 4.5.6. They are constructed with "unwinding" from the internal surface of rings manufactured according to different programs. Deformations were measured on the outside surface; along the axis of abscissas there is plotted an increase in the inside diameter of the ring in the process of removing the layers. The graphic differentiation of deformation curves makes it possible to determine the derivatives of corresponding deformation along the radius. By knowing $\varepsilon_\theta(r)$ and $\dot{\varepsilon}_\theta(r)$, putting to use dependences (4.5.2)-(4.5.5), it is possible to construct diagrams $\sigma_\theta^0(r)$ and $\sigma_r^0(r)$. The results obtained by the method of laminar unwinding are represented on Fig. 4.5.7, on which there are shown the diagrams of initial stresses $\sigma_\theta(r)$ in the section of thick-walled rings of glass-reinforced plastics (material VPS-7, inside diameter 200 mm, number of turns 70 and 90, T_0/Π_M - 0.625). As is evident, the character of the diagram differs significantly from linear, which places in doubt the possibility of applying the method of cutting for investigation of the initial stresses in rings made of materials reinforced with fibers. The assumption about the linear law of distribution of stresses along the

211

section turned out to be unjustified, the deviation from linearity
can be very substantial.
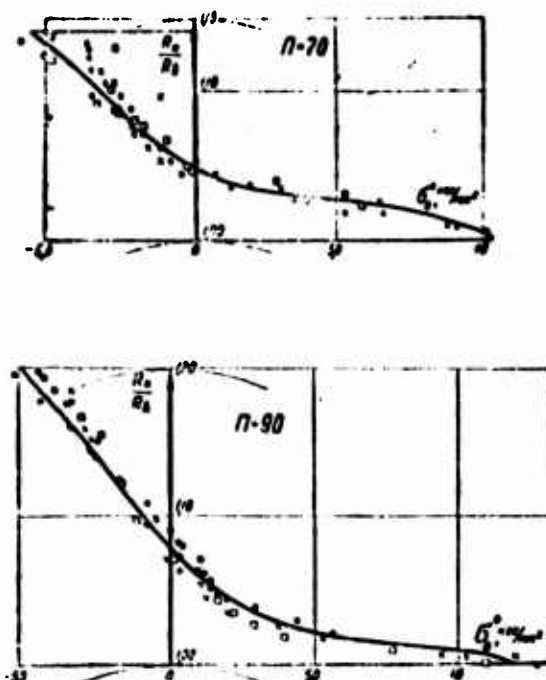
Fig. 4.5.7. The diagram of
initial stresses in rings of
different relative thickness.
$\bigcirc$, $\square$, x - different samples.
Designation: кгс/мм^2 = kgf/mm^2.

4.5.3. The effect of tensioning force.

The cutting of
glass fiber-reinforced plastics, manufactured with different,
but constant tensioning force, attests to the fact that with an
increase of tensioning force the value of initial stresses
sharply rises. The dependence of initial stresses σ_θ^0 and σ_r^0 on
the value and the law of change of tensioning force when winding
is studied in [168]. The investigation is performed on rings of
material VPS-7, manufactured with T_0 = const and according to
the program shown on Fig. 4.5.9. When winding with constant
tensioning force T_0 was changed from 0 to 0.62 H_H. Diagrams
σ_θ^0 and σ_r^0 for these tensions are presented on Fig. 4.5.8. They
attest to the systematic growth of $\sigma_{\theta max}^0$ and $\sigma_{r max}^0$ depending
on tensioning force when winding. The values of the maximum

212

stresses $\sigma^0_{\theta max}$ as a function of tensioning force are given in Table 4.5.2. The maximum tensile stresses act on the inside surfaces, and compressive act on the outside surfaces of the ring.
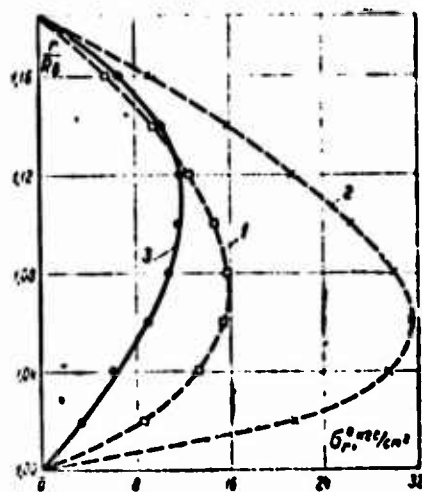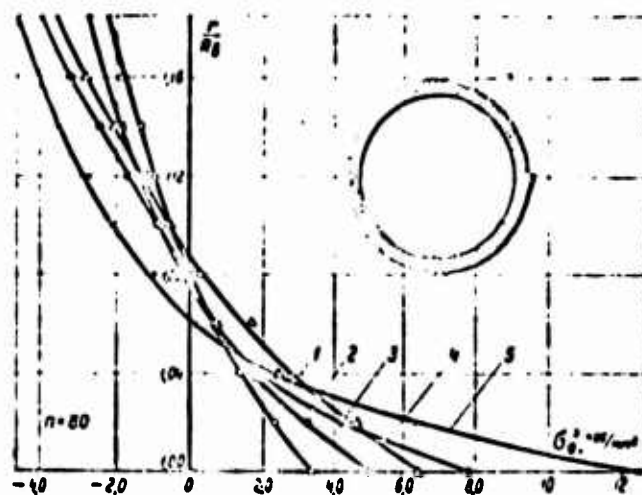
Fig. 4.5.8. The dependence of initial stresses on tensioning force. Relative tensioning force when winding T_0/Π_M: 1 - 0; 2 - 0.1; 3 - 0.2; 4 - 0.4; 5 - 0.62. In the figure are visible thermal cracks (ring of glass fiber-reinforced plastic VPS-7, $R_H/R_B = 1.2$; $T_0/\Pi_M = 0.62$, crack appeared during heating to $120°C$).

213
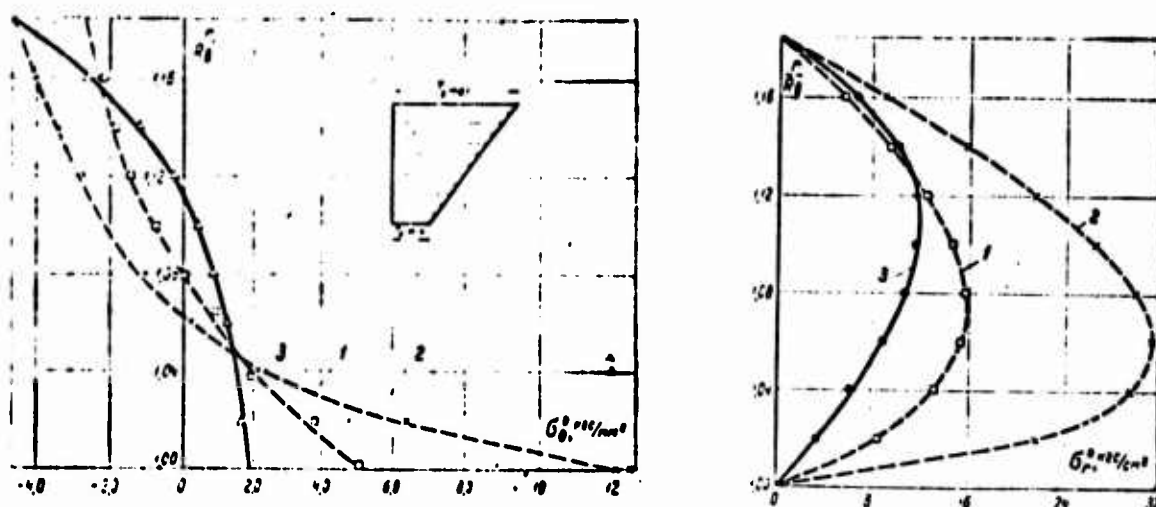
Fig. 4.5.9. Comparison of diagrams of initial stresses when winding with T_0 = const and programmed winding. 1 - T_0/Π_M = 0.1; 2 - T_0/Π_M = 0.62; 3 - $T_0(r)$ is changed according to the program given above.

Table 4.5.2. Change of the value of maximum and minimum initial stresses with a change in the tensioning force (n = 80).

Tensioning T_0, kgf/cm	$\dfrac{T_0}{\Pi_M}$	Initial stresses, kgf/cm^2			Quantity of samples
		$\sigma^{0(+)}_{\theta\ max}$	$\sigma^{0(-)}_{\theta\ max}$	$\sigma^0_{r\ max}$	
0	0	318	—235	11,0	7
10	0,1	500	—290	15,0	5
20	0,2	640	—315	16,5	5
40	0,4	775	—380	20,7	4
62,5	0,6	1260	—450	31,0	4

The transition to programmed winding leads to a change of the diagram of initial stresses in the finished product. On Fig. 4.5.9 there are compared σ^0_θ and σ^0_r, obtained in rings when winding with T_0 = const, and the investigated case, where force in the tightener is changed according to linear law (Fig. 4.5.9). Curves 1 and 2 are obtained with tensioning force equal to 0.1 and 0.62 Π_M respectively; curve 3 - when winding with tensioning force, which was changed according to linear law from T_{0min} = 0.1 Π_M to T_{0max} = 0.62 Π_M. The presented data attest to the fact that even with transition to such a simple program it is possible

214

to considerably decrease the value of the initial stresses in
the sections of the ring. The dependence of the initial stresses
on tensioning force makes it possible to raise the question
concerning the optimization of this force when winding with respect
to the diagram of residual stresses. Selection of $T_0(r)$ can
be realized in such a way that taking into account the process
of polymerization σ_θ^0 and σ_r^0 would be minimum or subordinate to
preassigned law, providing the optimization of the properties of
the articles being wound.

Table 4.5.3. Change of the value of maximum
and minimum initial stresses with an increase
of number of turns (tensioning $T_0/\Pi_M = 0.62$).[1]

Number of turns	$\dfrac{R_в}{R_в}$	Initial stresses, kgf/cm^2			Quantity of samples
		$\sigma_{\theta\,max}^{0(+)}$	$\sigma_{\theta\,max}^{0(-)}$	$\sigma_{r\,max}^{0}$	
40	1.09	510	110	12.3	3
60	1.14	710	275	22.7	3
80	1.18	1260	450	31.0	4

[1]Material VPS-7, $R_в$ = 100 mm.

The change of diagrams of residual forces depending on the
relative thickness of ring is insufficiently studied. It is
possible to assume that when winding with T_0 = const with an
increase of the thickness of ring the initial stresses are increased.
This can be explained by an increase in the nonuniformity of the
tension of the top and bottom layers. The experimental data,
presented in Table 4.5.3, attest to growth of $\sigma_{\theta max}^0$ and σ_{rmax}^0
with increase of the relative thickness of the ring (with constant
T_0 = const for all rings).

Thus, the tensioning of fibers is one of the basic sources
of initial stresses when winding. Winding with constant tensioning
force increases the initial stresses. By a change in the tensioning

force it is possible to a considerable degree to regulate the value and the character of the distribution of these stresses.[1]

---

[1]Program $T_0(r)$ taking into account a change of the deformative properties of material in the process of polymerization is given in the work of Yu. M. Tarnopol'skiy, G. G. Portnov "Programmed winding of glass fiber-reinforced plastics." - Mechanics of polymers, 1970, No. 1.

BIBLIOGRAPHY

1.   Agalovyan, L. A.   Boundary conditions for the bending of anisotropic plates. - Bulletin of the Academy of Sciences Armenian SSR, Mechanics, 1966, No. 4.

2.   Aynola, L., Nigul, U.   The wave processes of the deformation of elastic plates and shells. - Bulletin of the Academy of Sciences Estonian SSR, 1965, No. 1.

3.   Alfutov, N. A., Balabukh, L. I.   The possibility of the solution of problems of stability of plates without the preliminary determination of initial stressed state. - PMM, 1967, No. 4.

4.   Alfutov, N. A., Trofimov, V. V.   Stability of cylindrical orthotropic shell with small shear rigidity, loaded by external pressure - Bulletin of schools of higher learning, Machine-building, 1967, No. 5.

5.   Ambartsumyan, S. A.   The theory of anisotropic shells. M., Fizmatgiz, 1961.

6.   Ambartsumyan, S. A.   The theory of anisotropic plates. M., Fizmatgiz, 1967.

7.   Ambartsumyan, S. A.   Long anisotropic shells of revolution. - Bulletin of the Academy of Sciences Armenian, SSR, FME and T of science, 1951, No. 6.

8.   Ambartsumyan, S. A.   For the general theory of anisotropic shells. - PMM, 1958, No. 2.

9.   Ambartsumyan, S. A.   For the theory of bending of anisotropic plates. - Bulletin of the Academy of Sciences of USSR, DTS, 1958, No. 5.

10.   Ambartsumyan, S. A.   For the theory of bending of anisotropic plates and slightly curved shells - PMM, 1960, No. 2.

11.   Ambartsumyan, S. A.   Some questions of the development of the theory of anisotropic shells. - Bulletin of the Academy of Sciences Armenian, SSR, ser. of physico-mathematical sciences, 1964, No. 3.

12.   Ambartsumyan, S. A.   The question of two-dimensional problem of the differently resisting or variable modulus theory of elasticity. - Bulletin of the Academy of Sciences Armenian SSR, Mechanics, 1966, No. 2.

13.   Ambartsumyan, S. A., Peshtmaldzhyan, D. V.   The theory of orthotropic shells and plates. - Bulletin of the Academy of Sciences Armenian SSR, ser. of physico-mathematical sciences, 1959, No. 1.

14.   Ambartsumyan, S. A., Khachatryan, A. A.   About stability and vibrations of anisotropic plates. - Bulletin of the Academy of Sciences of the USSR, DTS, mechanics and machine-building, 1960, No. 1.

15.   Ambartsumyan, S. A., Khachatryan, A. A.   About the stability and the ibrations of mildly sloping orthotropic cylindrical panel. - Reports of Academy of Sciences of Armenian SSR, 30, 1960.

16.   Ambartsumyan, S. A., Khachatryan, A. A.   The basic questions of elasticity theory for materials differently resisting tension and compression. - Engineering journal, Mechanics of solids, 1966, No. 2.

17.   Ambartsumyan, S. A., Khachatryan, A. A.   The variable modulus theory of elasticity. - Engineering journal, Mechanics of solids, 1966, No. 6.

18.   Ambartsumyan, S. A., Khachatryan, A. A.   Some problems of the variable modulus theory of elasticity. - The theses of reports to IV All-Union conference on strength and plasticity. M., 1967.

19.   Andriyevskaya, G. D.   High-strength oriented glass fiber-reinforced plastics.   M., "Science", 1966.

20.   Arutyunyan, N. Kh., Abramyan, B. L.   The twisting of elastic bodies., M., Fizmatgiz, 1963.

21.   Ashkenazi, Ye. K.   Strength of anisotropic wood and synthetic materials.   M., "Wood industry", 1966.

218

22.   Ashmarin, Yu. A.   The effect of the value of shear modulus on the stress concentration. - Applied mechanics, 3, 1967, No. 2.

23.   Bazhanov, V. L., Gol'denblat, I. I., Kopnov, V. A., Pospelov, A. D., Sinyukov, A. M.   The resistance of glass fiber-reinforced plastics (ed. by I. I. Gol'denblat).   M., "Machine-building", 1968.

24.   Bazhant, Z. P.   The effect of the bending of the reinforcing filaments on elastic and strength moduli of composite materials. - Mechanics of polymers, 1968, No. 2.

25.   Balabukh, L. I.   The stability of plywood plates. - Air fleet technology, 1937, No. 9.

26.   Bezukhov, N. I.   Fundamentals of the theory of elasticity, plasticity and creep.   M., "Higher school", 1961.

27.   Bezukhov, N. I.   Examples and problems in the theory of elasticity, plasticity and creep.   M., "Higher school", 1965.

28.   Biderman, V. L.   The determination of the tensioning of steel-strand rope, reeled on the drum of load-lifting device. - In the coll.:   Strength calculations, 2. M., Mashgiz, 1958.

29.   Biderman, V. L. Elasticity and strength of glass-fiber reinforced anisotropic plastics. - In the coll.:   Strength calculations, 11. M., "Machine-building", 1965.

30.   Biderman, V. L.   Plates and shells of glass fiber-reinforced plastics. - In the book: Strength, stability, vibrations, Vol. 2.   M., "Machine-building", 1968.

31.   Biderman, V. L., Dmitriyenko, I. P., Polyakov, V. I., Sukhova, N. A.   The determination of the residual stresses during the manufacture of rings from glass fiber-reinforced plastics. - Mechanics of polymers, 1969, No. 4.

32.   Birger, I. A.   Circular plates and shells of revolution. M., Oborongiz, 1961.

33.   Birger, I. A.   Residual stresses.   M., Mashgiz, 1963.

4.   Birman, S. Ye.   The problem of the bending of flat cantilever. - Engineering journal, Mechanics of solids, 1966, No. 2.

35.   Blagonadezhin, V. L., Sinitzyn Ye. N.   The behavior of viscoelastic compressively bent rods from glass fiber-reinforced plastic. - Reports of the scientific and technical conference of MPI on the results of research works for 1964-1965, section of electric machine-building, subsection of dynamics and strength of machines.   M., 1965

36.   Bolotin, V. V.   The theory of laminated plates. –
Bulletin of the Academy of Sciences of the USSR, Mechanics and
machine-building, 1963, No. 3.

37.   Bolotin, V. V.   About the bending of plates, which consist
of a large number of layers. – Bulletin of the Academy of
Sciences of the USSR, Mechanics and machine-building, 1964, No. 1.

38.   Bolotin, V. V.   The vibrations of laminated curvilinear
rods. – Engineering journal, 1964, No. 4.

39.   Bolotin, V. V.   About the reducing of three-dimensional
problems of the theory of elastic stability to one-dimensional
and two-dimensional problems. – In the coll.: Stability problems
in structural mechanics. M., Stroyizdat, 1965.

40.   Bolotin, V. V.   About the theory of reinforced bodies. –
Bulletin of the Academy of Sciences of the USSR, Mechanics, 1965,
No. 1.

41.   Bolotin, V. V.   The fundamental equations of the theory
of reinforced media. – Mechanics of polymers, 1965, No. 2.

42.   Bolotin, V. V.   The problems of the mechanics of reinforced
media. – Reports of the scientific and technical conference of
MPI on the results of research works for 1964-1965, the section
of power equipment construction, subsection of dynamics and
strength. M., 1965.

43.   Bolotin, V. V.   Strength, stability and vibrations of
laminated plates. – In the coll.: strength calculations, issue
11. M., "Machine-building", 1965.

44.   Bolotin, V. V.   The theory of reinforced laminated
medium with random initial inaccuracies. – Mechanics of
polymers, 1966, No. 1.

45.   Bolotin, V. V.   The two-dimensional problem of
elasticity theory for parts of reinforced materials. – In the
coll.: strength calculations, issue 12, M., "Machine-building",
1966.

46.   Bolotin, V. V.   The estimation of error of equations
in the applied theory of elasticity. – In the coll.: Structural
mechanics. M., Publishing house of literature on building. 1966.

47.   Bolotin, V. V.   Laminated elastic and viscoelastic media
with small initial inaccuracies. – Engineering journal, Mechanics
of solids, 1966, No. 3.

48. Bolotin, V. V. The density of eigenvalues in problems of the vibrations of elastic plates and shells. - Transactions of VI All-Union conference on the theory of shells and plates. Baku, 1966.

49. Bolotin, V. V. The equations of stability theory of thin elastic shells. - Engineering journal, Mechanics of solids, 1967, No. 4.

50. Bolotin, V. V. The equations of neutral equilibrium for thin elastic shells. - The reports of scientific and technical conference of MPI on the results of research works for 1966-1967, section of electric machine-building, subsection of dynamics and strength. M., 1967.

51. Bolotin, V. V., Bolotina, K. S. The thermoelastic problem for a circular cylinder of reinforced laminated material. - Mechanics of polymers, 1967, No. 1.

52. Bolotin, V. V., Kuranov, B. A., Makarov, B. P. The vibrations of circular transformer windings. - Bulletin of the Academy of Sciences of the USSR, Power engineering and transport, 1965, No. 4.

53. Bolotin, V. V., Makarov, B. P., Kuranov, B. A. Strength and rigidity of the internal windings of transformers. - Electricity, 1964, No. 4.

54. Bolotin, V. V., Moskalenko, V. N. Plates and shells of reinforced materials - the fundamental equations, quantitative results. - Reports of the scientific and technical conference of MPI on the results of research works for 1966-1967, section of power equipment construction, subsection of dynamics and strength. M., 1967.

55. Bolotin, V. V., Sinitzyn, Ye. N. The effect of random inaccuracies on creep of reinforced laminated plastics. - Mechanics of polymers, 1966, No. 5.

56. Bolotin, V. V., Sinitzyn, Ye. N. The surface bulge of viscoelastic reinforced medium. - Reports of the scientific and technical conference on MPI on the results of research works for 1966-1967, section of power equipment construction, subsection of dynamics and strength, M., 1967.

57. Bolotina, K. S. The mechanical and thermophysical characteristics of laminated material. - Bulletin of schools of higher learning. Machine-building, 1966, No. 12.

58. Bolotina, K. S. The coefficients of thermal expansion of unidirectional glass fiber-reinforced plastics. - Mechanics of polymers, 1968, No. 3.

59. Brivmanis, R. E. The experimental determination of the residual stresses when winding unidirectional glass fiber-reinforced plastics. - Mechanics of polymers, 1966, No. 1.

60. Brivmanis, R. E., Gaganov, A. K. The winding construction of electrical machines and apparatuses. M., "Energy", 1969.

61. Brivmanis, R. E., Portnov, G. G. Strength of rings from glass fiber-reinforced plastics loaded by internal pressure. - Mechanics of polymers, 1968, No. 1.

62. Brivmanis, R. E., Portnov, G. G. The study of the process of winding of binding band from unidirectional fiberglass tape. - Electrical engineering, 1968, No. 3.

63. Bryzgalin, G. I. The calculation for creep of plates of glass fiber-reinforced plastics. - ZhPMTF, 1963, No. 4.

64. Van Fo Fy G. A. State of stress and strain of synthetic materials with shear. - Applied mechanics, 1965, No. 5.

65. Van Fo Fy G. A. The fundamental principles of the theory of oriented glass fiber-reinforced plastics with hollow filaments. - Mechanics of polymers, 1966, No. 5.

66. Van Fo Fy G. A. The fundamentals of the theory of polymer bodies with oriented structure. Dr. diss. Kiev, 1965.

67. Van Fo Fy G. A., Savin, G. N. The fundamental principles of the theory of nonfabric glass fiber-reinforced plastics. - Mechanics of polymers, 1965, No. 1.

68. Vasiliev, V. V. The investigation of edge effect in a cylindrical shell of glass fiber-reinforced plastic. - Engineering journal, 1965, No. 1.

69. Vasiliev, V. V. The theory of orthotropic laminated cylindrical shells. - Mechanics of polymers, 1968, No. 1.

70. Vishnevskiy, G. G., Shlenskiy O. F. The effect of the properties of components and dimensional characteristics of the structure on the values of the coefficients of the thermal conductivity of glass fiber-reinforced plastics. - Mechanics of polymers, 1968, No. 1.

71. Vlasov, B. F. One case of bending of a thick plate. - Herald of MGU (Moscow State Univ.), Mechanics, 1957, No. 2.

72. The effect of bending and tension of filaments on the elastic and strength characteristics of glass fiber-reinforced

plastics (ed. by Tarnopol'skiy, Yu. M., Perov, B. V). M., 1968.

73. Volkov, S. D., Dolgikh, V. Ya. The statistical theory of elasticity of reinforced plastics. - Mechanics of polymers, 1968, No. 3.

74. Volkov, S. D., Dolgikh V. Ya., Stavrov, V. P. The dependability of constructions from reinforced plastics - In the coll.: polymers in machines. M., 1968.

75. Vol'mir, A. S. The actual problems of stability theory of shells. - Transactions of II All-Union congress on theoretical and applied mechanics, issue 3. M., "Science", 1966.

76. Vol'mir, A. S. The stability of deformable systems. M., "Science", 1967.

77. Vorovich, I. I. Some mathematical questions of the theory of plates and shells. - transactions of II All-Union congress on theoretical and applied mechanics, reports, issue 3. M., "Science", 1966.

78. Vorovich, I. I. The general problems of the theory of plates and shells. - Transactions of VI All-Union conference on the theory of shells and plates. Baku, 1966.

79. Vorovich, I. I., Prokorov, V. K. Some questions of the three-dimensional theory of elasticity. - III All-Union congress on theoretical and applied mechanics, Abstracts of reports. M., "Science", 1968.

80. Vorovich, I. I., Shlenev, M. A. Plates and shells. - results of science, Mechanics. M., 1965.

81. Galin'sh, A. K. The calculation of plates and shells according to refined theories. - Investigations in the theory of plates and shells, 5. Kazan', 1967.

82. Glazyrin, V. S. The application of the Reissner theory on the calculation of unrestricted plates, lying on elastic support. - structural mechanics and calculation of constructions, 1964, No. 2.

83. Gradshteyn, I. S., Ryzhik, I. M. Tables of the integrals of sums, series and products. M., Fizmatgiz, 1963.

84. Gol'denblat, I. I. Some questions of the mechanics of deformable media. M., GITTL, 1955.

85. Gol'denblat, I. I., Kopnov, V. A. The criterion of strength of anisotropic materials. - Bulletin of the Academy of sciences of USSR, Mechanics, 1965, No. 6.

86. Gol'denveyzer, A. L. The theory of elastic films.
M. GITTL, 1953.

87. Gol'denveyzer, A. L. The theory of bending of Reissner
plates. - Bulletin of the Academy of Sciences of the USSR, DTS,
1958, No. 4.

88. Gol'denveyzer, A. L. The construction of the approximate
theory of bending of a plate by the method of asymptotic
integration of the equation of elasticity theory. - PMM, 1962,
No. 4.

89. Gol'denveyzer, A. L. The development of the theory of
elastic films. - transactions of I All-Union congress of theoretical
and applied mechanics. M.-L., 1962.

90. Gol'din, R. Kh. Glass shroud strip for the armature
of traction motors and the experience of its application at the
REZ plant. - In the coll.: Production and treatment of plastics,
synthetic resins and glass fibers, issue 6. M., 1964.

91. Gordon, J. Some considerations about the development
of technical materials on the basis of brittle solids. - In the
coll.: Mechanical properties of new materials (translation from
English ed. by G. I. Barenblatt). M., "World", 1966.

92. Grezin, V. M., Kagan, M. Ye. Testing of glass fiber-
reinforced plastics AG-4S for static bending. - Standardization,
1964, No. 2.

93. Guz', A. N. The stability of orthotropic bodies. -
applied mechanics, 1967, No. 5.

94. Dedyukhin, V. G., Stavrov, V. P. Technology of pressure
forging and strength of articles made of glass fiber-reinforced
plastics. M., "Chemistry", 1968.

95. Deyev, V. M., Kolod'ko, V. M. The axisymmetric problem
of elasticity theory for transversally isotropic thick plate. -
Applied mechanics, 1966, No. 4.

96. Dinnik, A. N. The stability of compressed circular
plates. - In the book: Selected transactions, vol. 2. Kiev, 1955.

97. Domanskaya, Z. B. The question of the bending computation
of laminated plywood rods. - Scientific transactions of Leningrad
forestry academy, issue 103. L., 1966.

98. Dubinkin, M. V. The vibrations of plates taking into
account the inertia of rotation and shear. - Bulletin of the
Academy of Sciences of the USSR, DTS, 1958, No. 12.

99. Yegorov, N. G., Roginskiy, S. L. The investigation of unidirectional glass fiber-reinforced plastics in circular samples. - In the coll.: physical chemistry and mechanics of oriented glass fiber-reinforced plastics. M., "Science", 1967.

100. Zhigun, I. G. The bending of prestressed rods of oriented glass fiber-reinforced plastics. - Mechanics of polymers, 1967, No. 5.

101. Zhigun, I. G. The experimental estimation of the effect of pretensioning of filaments in two directions on some elastic characteristics of fabric glass fiber-reinforced plastics. - Mechanics of polymers, 1968, No. 5.

102. Zhigun, I. G. The effect of the bending of reinforcing filaments on rigidity and the strength of composite materials. Masters diss. Riga, 1968.

103. Ilyushin, A. A., Ogibalov, P. M. Some basic questions of the mechanics of polymers. - Mechanics of polymers, 1965, No. 3.

104. Ilyushin, A. A., Ogibalov, P. M. Some questions of the mechanics of polymers. - Mechanics of polymers, 1966, No. 2.

105. Koval'skiy, V. S. The theory of laminated winding of cable. - Reports of Academy of Sciences of the USSR, 24, 1950, No. 3.

106. Kalinin, V. S. The instability of elongated rod, caused by shearing strain. - Theses of the reports of All-Union conference on stability problems in structural mechanics. Vilnius, 1967.

107. Kargin, V. A. The problems of the science of polymers. MGU, 1962.

108. Kil'chevskiy, N. A. The analysis of different methods of reduction of three-dimensional problems of the elasticity theory to two-dimensional and the investigation of the setting of the boundary value problems of the theory of shells. - In the coll.: Theory of plates and shells. Kiev, 1962.

109. Kil'chevskiy, M. Fundamentals of analytical mechanics of shells. Kiev, 1963.

110. Kobrin, M. M., Dekhtyar', L. I. The determination of the internal stresses in cylindrical parts. M., "Machine-building", 1965.

111. Kozhin, S. V. The loading of a drum with multilayer winding on cable. - Transactions of VNIIPTMASh, issue 8 (30), 1962.

112. Korolev, V. I. Laminated anisotropic plates and shells of reinforced plastics. M., Machine-building, 1965.

113. Korolev, V. I. Some problems on the selection of optimum structure of glass fiber-reinforced plastics. - Engineering journal, 1965, No. 2.

114. Korten, Kh. The failure of reinforced plastics. M., "Chemistry", 1967.

115. Kosmodamianskiy, A. S. The estimation of St. Venant principle with elongation of anisotropic band. - Bulletin of the Academy of Sciences of the USSR, DTS, 1958, No. 9.

116. Kottrel, A. Strength of materials. - In the coll.: The mechanical properties of new materials (translation from Engl. ed. by G. I. Barenblatt). M., "World", 1966.

117. Kritsuk, A. A. The solution of two-dimensional problem for wood as anisotropic material during the action of load at an angle to the principal axes of elasticity. - Informational materials of the institute of structural mechanics of the Academy of Sciences of Ukrainian SSR, 1957, No. 9.

118. Kuranov, B. A., Makarov, B. P. The stability of laminated elastic rings under the action of uniform pressure. - Bulletin of schools of higher learning, Machine-building, 1964, No. 8.

119. Kurshin, L. M. Review of the calculation of sandwich plates and shells. - In the coll.: Calculation of three-dimensional constructions, issue 7. M., Gosstroyizdat, 1962.

120. Levi, S. Shear and bending of short cylindrical shells. - construction and mechanical engineering (USA, translation from Engl.), 1965, No. 3.

121. Lekhnitskiy, S. G. The stability of anisotropic plates, Guide for aircraft designers. M.-L., Gostekhizdat, 1943.

122. Lekhnitskiy, S. G. Elasticity theory of anisotropic body. M., Gostekhizdat, 1950.

123. Lekhnitskiy, S. G. Anisotropic plates, M., GITTL, 1957.

124. Lekhnitskiy, S. G. The theory of anisotropic thick plates. - Bulletin of the Academy of Sciences of the USSR, DTS, Mechanics and machine-building, 1959, No. 2.

125.   Lokshin, A. Z.   The stability of shipboard plates and covers from glass fiber-reinforced plastics.   L., "Shipbuilding", 1964.

126.   Lomakin, V. A.   Koltunov, M. A.   The action of reinforcing elements during elongation on the deformation and strength of glass fiber-reinforced plastics. - Mechanics of polymers, 1965, No. 2.

127.   Lomakin, V. A., Ogibalov, P. M.   The calculation of glass fiber-reinforced plastics in plane stressed state. - Herald of MGU, Mathematics and Mechanics, 1961, No. 4.

128.   Lur'ye, A. I.   The three-dimensional problems of elasticity.   M., Fizmatgiz, 1961.

129.   Lyav, A.   The mathematical theory of elasticity.   M., ONTI, 1935.

130.   Malinin, N. I.   The investigation of the questions of creep and strength of plastics. Dr. diss. M., 1965.

131.   Malmeyster, A. K.   The geometry of the theories of strength. - Mechanics of polymers, 1966, No. 4.

132.   Malmeyster, A. K., Tamuzh, V. P., Teters, G. A.   The resistance of rigid polymer materials (ed. by A. K. Malmeyster). Riga, "Knowledge", 1967.

133.   Medovikov, A. I.   The question concerning the account of shearing strain with bending of plates. - Transactions of VI All-Union conference on the theory of shells and plates.   Baku, 1966.

134.   Melkonyan, A. P.   The bending of transversally isotropic plates lying on elastic support. - Bulletin of the Academy of Sciences Armenian SSR, Mechanics, 1967, No. 1.

135.   Melkonyan, A. P., Khachatryan, A. A.   The bending of transversally isotropic plates. - Bulletin of the Academy of Sciences Armenian SSR, ser. of physico-mathematical sciences, 1965, No. 1.

136.   Melkonyan, A. P., Khachatryan, A. A.   The stability of rectangular transversally isotropic plates. - Applied mechanics, 1966, No. 2.

137.   Melkonyan, A. P., Khachatryan, A. A.   The stability of transversally isotropic circular plates. - Bulletin of the Academy of Sciences Armenian SSR, Mechanics, 1966, No. 2.

138.   Melkonyan, A. P., Khachatryan, A. A.   The vibrations of transversälly isotropic plates. - Bulletin of the Academy of sciences Armenian SSR, Mechanics, 1966, No. 3.

139.   The mechanics of polymers and reinforced materials (ed. by V. V. Bolotin), section 1. - Reports of scientific and technical conference of MPI for 1964-1965 and 1966-1967, M., 1965, 1967.

140.   Meshcheryakov, V. B.   The effect of shears on the work of thin-walled rods. - Engineering journal, 1965, No. 1.

141.   Meshcheryakov, V. B.   The stability and vibrations of thin-walled rods of open profile taking into account shears. - All-Union conference on the problem of stability in structural mechanics. Theses of reports. Vilnius, 1967.

142.   Moskolenko, V. N.   The application of the refined theories of bending of plates in the problem of natural oscillations. - Engineering journal, 1961, No. 3.

143.   Morgan, F.   Glass fiber-reinforced plastics. M., IL, 1961

144.   Mushtari, Kh. M.   The theory of bending of plates of average thickness. - Bulletin of the Academy of Sciences of the USSR, DTS, Mechanics and machine-building, 1959, No. 2.

145.   Mushtari, Kh. M., Teregulov, I. G.   The theory of shells of average thickness. - Reports of Academy of Sciences of USSR, 128, 1959, No. 6.

146.   Mushtari, Kh. M., Teregulov, I. G.   The theory of mildly sloping orthotropic shells of average thickness. - Bulletin of the Academy of Sciences of USSR, DTS. Mechanics and machine-building, 1959, No. 6.

147   Nazarov, G. I., Mironov, Yu. M., Kalashkov, V. M. The mechanical properties of glass fiber-reinforced plastics at elevated and low temperatures. - Polymers in machines. Transactions of II All-Union conference on the application of polymer materials in machine-building. M., 1966.

148.   Nikolayev, V. P.   Some problems connected with tests of anisotropic materials for strength and rigidity. Masters diss. M., 1968.

149.   Nikolayev, V. P., Partsevskiy V. V.   The bending of rods from unidirectional glass fiber-reinforced plastics. - Reports of scientific and technical conference of MPI on the results of scientific research works for 1964-1965, section of power equipment construction, subsection of dynamics and strength. M., 1965.

150. Novozhilov, V. V. The fundamentals of nonlinear theory of elasticity. M., Gostekhizdat, 1948.

151. Ogibalov, P. M. Bending, stability and oscillations of plates. M., 1958.

152. Ogibalov, P. M., Gribanov, V. F. The thermal stability of plates and shells. M., 1968.

153. Ogibalov, P. M., Suvorova, Yu. V. The mechanics of reinforced plastics. M., 1965.

154. Report on agreement No. 66044 of the technical laboratory of the central research institute of the energy industry. Tokyo, June 1966 (in the Japanese language).

155. Panovko, Ya. G. The fundamentals of applied theory of elastic vibrations. M., "Machine-building", 1967.

156. Panovko, Ya. G., Gubanova, I. I. The stability and vibrations of elastic systems. M., "Science", 1967.

157. Pankovich, P. F. Elasticity theory. 1939.

158. Pankovich, P. F. Structural mechanics of a ship, vol. 2. M.-L., "Sea transport", 1947.

159. Partsevskiy, V. V. The mechanism of transmission of forces in laminated media. Masters diss. M., 1968.

160. Pelekh, B. L., Teters, G. A. The dynamic bending of plates, which weakly resist shear. - Mechanics of polymers, 1968, No. 4.

161. Petoyan, A. Sh. The theory of bending of transversally isotropic plate. - Collection of scientific works of Yerevan polytechnic institute, 1964, No. 24.

162. Petoyan, A. Sh. The stability and vibrations of transversally isotropic rectangular plate. - Bulletin of the Academy of Sciences Armenian SSR. Mechanics, 1966, No. 4.

163. Petoyan, A. Sh. The stability of circular transversally isotropic plate during its compression by radial load evenly distributed along the contour. - Bulletin of the Academy of Sciences Armenian SSR. Mechanics, 1966, No. 3.

164. Polyakov, V. A. The analysis of the stress-strain state in circular plates of glass fiber-reinforced plastic. - Mechanics of polymers, 1969, No. 6.

165. Popugayev, V. S., Levin, L. I. Bending of circular thick transversally isotropic plate. - Collection of works of Leningrad engineering and structural institute, 49, 1966.

166. Portnov, G. G. The effect of low shear strength of polymer layer on the supporting power of pipes of glass fiber-reinforced plastics. - Mechanics of polymers, 1967, No. 3.

167. Portnov, G. G. The features of the mechanics of winding of glass fiber-reinforced plastics. Masters diss. Riga, 1967.

168. Portnov, G. G., Goryushkin, V. V., Tilyuk, A. G. The initial stresses in rings of glass fiber-reinforced plastics manufactured by winding. - Mechanics of polymers, 1969, No. 3.

169. Protasov, V. D., Kopnov, V. A. The investigation of the strength of glass fiber-reinforced plastics in plane stressed state. - Mechanics of polymers, 1966, No. 5.

170. Strength, stability, vibrations (edited by I. A. Birger and Ya. G. Panovko), vol I-III. M.-L., "Machine-building", 1968, 1969.

171. Rabinovich, A. L. Some basic questions of the mechanics of reinforced polymers. Dr. diss. M., 1965.

172. Rabinovich, A. L., Bilik, Sh. I. The strength test of pipes of glass fiber-reinforced plastics with compression. - Herald of machine-building. 1960, No. 4.

173. Rabinovich, A. K., Verkhovskiy I. A. Elastic constants of oriented glass fiber-reinforced plastics. - Engineering journal. 1964, No. 1.

174. Rabotnov, Yu. N. The mechanics of solids and paths of its development. - Bulletin of the Academy of Sciences of the USSR, Mechanics and machine-building, 1962, No. 2.

175. Rabotnov, Yu. N. Strength of materials. M., Fizmatgiz, 1963.

176. Rabotnov, Yu. N. The mechanics of solids and polymer materials. - Herald of the Academy of Sciences of the USSR, 1965, No. 7.

177. Rappoport, R. M. General equations of the plane strain of laminated two-component elastic medium of the correct structure. L., 1960.

178. Rappoport, R. M. The bending of thick plate as a problem of the applied theory of elasticity. - Bulletin of VNIIGidrotekhnika, 1962, No. 2.

179. Rappoport, R. M. Some problems of the theory of bending of thick laminated plates. - Transactions of VNIIGidrotekhnika, 80, 1966.

180. Rappoport, R. M., Braginskaya, N. I., Katranova, L. A., Yuzefovich, G. I. Some questions of the calculation of thick arches. - Transactions of the Leningrad Institute of rail transport, issue 230, 1965.

181. Strength calculations in machine-building, vol. 3 (edited by S. D. Ponomarev). M., Mashgiz, 1959.

182. Rzhanitsyn, A. R. The theory of composite rods of structures. M., Stroyizdat, 1948.

183. Rzhanitsyn, A. R. The stability of the equilibrium of elastic systems. M., GITTL, 1955.

184. Roginskiy, S. L., Yegorov, N. G. The effect of the tensioning of filler on the strength of metal shells, reinforced by glass fiber-reinforced plastic. - Mechanics of polymers, 1966, No. 2.

185. Roze, A. V. The bending of plates from oriented glass fiber-reinforced plastics. - Mechanics of polymers, 1965, No. 3.

186. Roze, A. V. The features of calculation of parts from materials with low shear rigidity and strength. Masters diss. Riga, 1966.

187. Roze, A. V. Longitudinal-transverse bending of circular cylindrically orthotropic plates, which weakly resist shear. - Mechanics of polymers, 1968, No. 1.

188. Roze, A. V., Kintsis, T. Ya. The stability of rods from materials reinforced by filaments. - Mechanics of polymers, 1968, No. 5.

189. Roze, A. V., Khitrov, V. V. The stability of circular transversally isotropic plates, which weakly resist shear. - Mechanics of polymers, 1969, No. 5.

190. Rozen, B. The mechanics of strengthening of compositions. - In the coll.: Fibrous composite materials. M., "World", 1967.

191. Rotsens, K. A. The deformative characteristics of oriented reinforced plastics. Masters diss. Riga, 1967.

192. Sborovskiy, A. K., Nikol'skiy, Yu. A., Popov, V. D. The vibration of ships with hulls of glass fiber-reinforced plastics. M., "Ship-building", 1967.

193. Senitskiy, Yu. E. The account of shearing strains during the analysis of stability and vibrations of composite rods. - Bulletin of schools of higher learning, Building and architecture, 1966, No. 6.

194. Sidorin, Ya. S. The experimental research of anisotropy of glass fiber-reinforced plastics. - Bulletin of the Academy of Sciences of the USSR, Mechanics and machine-building, 1964, No. 3.

195. Sidorin, Ya. S. The experimental research of anisotropy of glass fiber-reinforced plastics with shear. - Plant laboratory, 1966, No. 5.

196. Sidorin, Ya. S. The possibility of determination of the shear modulus of glass fiber-reinforced plastics with the aid of four-bar hinge. - Mechanics of polymers, 1968, No. 5.

197. Sinitsyn, Ye. N. Buckling of plate of laminated glass fiber-reinforced plastics under the action of longitudinal forces. - Bulletin of schools of higher learning, Machine-building, 1966, No. 10.

198. Sinitsyn, Ye. N. The calculation of flattened elements of viscoelastic reinforced materials. Masters diss. Saratov, 1966.

199. Scala, Ye. The characteristic of filaments and the construction of compositions. - In the coll.: fibrous composite materials. M., "World", 1967.

200. Skudra, A. M. The deformation and static fatigue of reinforced plastics with simple plane loading. Dr. diss. M., 1967.

201. Skudra, A. M., Rotsens, K. A. The technical deformative characteristics of dispersed-reinforced viscoelastic materials. - Materials of VI All-Union Conference on concrete and reinforced concrete. Riga. 1966.

202. Smirnov, V. I., Meshcheryakov, V. V. Testing and check of ship-building glass fiber-reinforced plastics. M., "Ship-building", 1965.

203. Smirnova, M. K., Sokolov, V. P., Sidorin, Ya. S., Ivanov, A. P. Strength of a ship's hull of glass fiber-reinforced plastic (edited by M. K. Smirnova). L., 1965.

204. Solomenko, N. S., Abramyan, K. G., Sorokin, V. V. Strength and stability of plates and shells of ship hull. M., "Ship-building", 1967.

205. Stavrov, V. P., Volkov, S. D. The moments of functions which describe the properties of glass fiber-reinforced plastics. - Mechanics of polymers, 1968, No. 1.

206. Stavrov, V. P., Dedyukhin, V. G. The utilization of the technological anisotropy of glass fiber-reinforced plastics with press forging of load-bearing components. - Herald of machine-building, 1966, No. 2.

207. Stavrov, V. P., Fomina, G. S. The elastic constants of glass fiber-reinforced plastics of anisotropic structure. - Mechanics of polymers, 1968, No. 4.

208. Strelyaev, V. S., Tarnopol'skiy, Yu. M., Timofeyev, A. F., Shlitsa, R. P. The effect of the parameters of shaping on the strength of parts from glass fiber-reinforced plastics. - In the coll.: The questions of dynamics and strength, II. Riga, Publishing house of the Academy of Sciences Latvian SSR, 1964.

209. Tamuzh, V. P., Pranch, A. S. About the dependence between the structural and strength characteristics of fiberglass laminate. - Mechanics of polymers, 1967, No. 2.

210. Tarnopol'skiy, Yu. M. The effect of shears during the bending of a beam on elastic support. - The questions of dynamics and strength, 4. Riga, Publishing house of the Academy of Sciences Latvian SSR, 1959.

211. Tarnopol'skiy, Yu. M. The applied problems of the theory of elasticity of structurally anisotropic materials. Dr. diss. M., 1967.

212. Tarnopol'skiy, Yu. M., Kintsis, T. Ya. The mechanism of the transmission of forces with the deformation of oriented glass fiber-reinforced plastics. - Mechanics of polymers, 1965, No. 1.

213. Tarnopol'skiy, Yu. M., Portnov, G. G. Change in the tensioning force when winding articles made of glass fiber-reinforced plastics. - Mechanics of polymers, 1966, No. 2.

214. Tarnopol'skiy, Yu. M., Portnov, G. G. The features of the mechanics of winding of reinforced plastics. - Theses of IV All-Union conference on strength and plasticity. M., "Science", 1967.

215. Tarnopol'skiy, Yu. M., Portnov, G. G., Zhigun, I. G. The effect of the bending of filaments on the elastic characteristics of oriented glass fiber-reinforced plastics. - Mechanics of polymers, 1967, No. 1.

216. Tarnopol'skiy, Yu. M., Roze, A. V. The bending of cross sections with deformation of oriented glass fiber-reinforced plastics. - Mechanics of polymers, 1965, No. 5.

217. Tarnopol'skiy, Yu. M., Roze, A. V. The strength of oriented glass fiber-reinforced plastics with bending. - Mechanics of polymers, 1966, No. 4.

218. Tarnopol'skiy, Yu. M., Roze, A. V. The experimental estimation of the effect of transverse shear during the bending of plates on the oriented glass fiber-reinforced plastics. - Mechanics of polymers, 1967, No. 1.

219. Tarnopol'skiy, Yu. M., Roze, A. V. The account of weak shear strength during the calculation of parts made of reinforced plastics. - Herald of machine-building, 1968, No. 4.

220. Tarnopol'skiy, Yu. M., Roze, A. V., Kintsis, T. Ya. The bending of restrained beams of materials which weakly resist shear. - Mechanics of polymers, 1967, No. 4.

221. Tarnopol'skiy, Yu. M., Roze. A.V., Polyakov, V. A. The application of the theory of laminated media to research on oriented glass fiber-reinforced plastics. - Bulletin of the Academy of Sciences of the USSR, Mechanics, 1965, No. 2.

222. Tarnopol'skiy, Yu. M., Roze, A. V., Polyakov, V. A. The account of shears during the bending of oriented glass fiber-reinforced plastics. - Mechanics of polymers, 1965, No. 2.

223. Tarnopol'skiy, Yu. M., Roze, A. V., Polyakov, V. A. Edge effect during the twisting of cylinders from essentially anisotropic materials. - Mechanics of polymers, 1966, No. 4.

224. Tarnopol'skiy, Yu. M., Roze, A. V., Portnov, G. G. The negative features of materials reinforced by filaments. - Mechanics of polymers, 1969, No. 1.

225. Tarnopol'skiy, Yu. M., Roze, A. V., Shlitsa, R. P. The bending of beams from materials which weakly resist shear on an elastic support. - Mechanics of polymers, 1967, No. 5.

226. Tarnopol'skiy, Yu. M., Roze, A. V., Shlitsa, R. P. The testing of rings, manufactured by winding by concentrated forces. - Mechanics of polymers, 1969, No. 4.

227. Tarnopol'skiy, Yu. M., Skudra, A. M. Structural strength and deformation of glass fiber-reinforced plastics. Riga, "Knowledge", 1966.

228. Tarnopol'skiy, Yu. M., Shlitsa, R. P., Smirnov, G. S. The account of shears when evaluating the edge effect for axisymmetric loaded shells of oriented glass fiber-reinforced plastics. - Questions of dynamics and strength, 16, Riga, "Knowledge", 1968.

229. Teregulov, A. G. The calculation of plates from oriented glass fiber-reinforced plastic. - Transactions of VI All-Union conference on the theory of shells and plates. Baku, 1966.

230. Teregulov, A. G. The bending of thin rectangular plate of oriented glass fiber-reinforced plastics. - In the coll.: Investigations in the theory of plates and shells, 4, Kazan', 1966.

231. Teters, G. A. The effect of orthotropy on the stability of inelastic plates taking into account the deformation of transverse shears. - Mechanics of polymers, 1965, No. 2.

232. Teters, G. A. The combined loading and stability of shells of polymer materials. Riga, "Knowledge", 1969.

233. Teters, G. A., Pelekh, B. L. The stability of anisotropic plates during creep taking into account the strain of transverse shears. - Mechanics of polymers, 1965, No. 5.

234. Tilyuk, A. G. The experimental determination of residual technological tensioning in glass fiber-reinforced plastics. - In the coll.: Filled and modified polymers. Riga, 1969.

235. Timofeyev, Ye. I. The calculation of structural parts of glass fiber-reinforced plastics. - PNTPO, No. 13-63-235/12, GOSINTI, 1963.

236. Timoshenko, S. P. Elasticity theory. M.-L., ONTI, 1934.

237. Timoshenko, S. P. The stability of elastic systems. M., GITTL, 1955.

238. Timoshenko, S. P. The history of the science of strength of materials, M., 1957.

239. Timoshenko, S. P. The strength of materials, vol. 1, 2. M., Fizmatgiz, 1965.

240. Timoshenko, S. P. Vibrations in engineering. M., Fizmatgiz, 1967.

241. Timoshenko, S. P., Voynovskiy-Kriger, S. Plates and shells. M., Fizmatgiz, 1963.

242. Tomashevskiy, V. T. The effect of transverse shears and stressed state on the stability of cylinder. - Applied mechanics, 2, 1966, No. 6.

243. Tomashevskiy, V. T. The axisymmetric deformation of a thick circular cylinder of glass fiber-reinforced plastics reinforced by stiffening ribs. - Mechanics of polymers, 1966, No. 1.

244. Tomashevskiy, V. T. The method of stability analysis of anisotropic circular cylinders under arbitrary boundary conditions. - Applied mechanics, 1967, No. 1.

245. Whitney, J., Riley, M. The elastic properties of composite materials reinforced by filaments. - Rocket technology and astronautics, 1966, No. 9.

246. Fabrikant, V. I. Some problems of the theory of viscoelastic reinforced media. Masters diss. M., 1966.

247. Feodos'yev, V. I. Strength of materials. M., "Science", 1964.

248. Feodos'yev, V. I. The selected problems and questions concerning strength of materials. M., Fizmatgiz, 1967.

249. Filonenko-Borodich, M. M. One system of functions and its applications in elasticity theory. - PMM, 1946, No. 1.

250. Fish, A. Ya., Tarnopol'skiy, Yu. M., Akunts, K. A., Petrov, A. V. The commutators of electrical machines on plastic. M., "Energy", 1963.

251. Flavianov, V. P., The analysis of the stressed state of a bar with shear (splitting). - In the coll.: Theory of structures and constructions, 10, VISI, 1964, issue 1.

252. Khashin, Z. The viscoelastic behavior of nonhomogeneous media. - Applied mechanics (USA, translation from Eng.), 1965, No. 3.

253. Khashin, Z., Rozen, B. The elastic moduli of materials reinforced by filaments. - Applied mechanics (USA, translation from Eng.), 1964, No. 2.

254. Khachaturyan, T. T. The account of the effect of tangential stresses in the theory of bending of plates. - Bulletin of the Academy of Sciences Armenian SSR, ser. of physico-mathematical sciences, 1961, No. 1.

255. Khachatryan, A. A. Some problems of bending of transversally isotropic circular plates. - Engineering journal, Mechanics of solids, 1966, No. 3.

256. Khishchenko, Yu. M. The effect of shear on the elastic modulus of fiberglass laminated samples with lateral bending. - Plant laboratory, 1964, No. 6.

257. Tsyplakov, O. G. The production of large ship articles of glass fiber-reinforced plastic. L., "Ship-building", 1967.

258. Tsyplakov, O. G. Ship pipelines made of glass fiber-reinforced plastics. L., "Ship-building", 1967.

259. Shafer, B. The relationships between the stress and deformations for reinforced plastics during the action of external forces parallel and normal to their internal filaments. - Rocket technology and astronautics, 1964, No. 2.

260. Schwarz, R., Schwarz, G. The properties of filaments of boron and those reinforced by plastics. - Rocket technology and astronautics, 1967, No. 2.

261. Sheremet'yev, M. P., Pelekh, B. L. The construction of the refined theory of plates. - Engineering journal, 1964, No. 3.

262. Sherch, Ah., Berggraf, O. Analytical investigation of the optimum shape of pressure containers wound from filaments. - Rocket technology and astronautics, 1964, No. 5.

263. Shlitsa, R. P. The features of deformation of glass fiber-reinforced plastics with tension. - Mechanics of polymers, 1966, No. 2.

264. Yanke, Ye., Emde, F. Tables of functions. M., Fizmatgiz, 1959.

265. Appleby E. C. Paper of American Society of Mechanical Engineers, No. 58-A-173.

266. Algra E. A. H. & van den Beek M. H. B. Standards and Test Methods for Filament-Wound Reinforced Plastics. Conference of Filament Winding, Paper 12, London, 1967.

267. Azzi V. D., Tsai, S. W. Elastic Moduli of Laminated Anisotropic Composites. - Exptl Mech., 5, 1965, No. 6.

268. Bayer E. Engineering Design for Plastics. N. Y., 1964.

269. Biblis E. I. Shear Deflection of Wood Beams. - Forest Prod. J., 15, 1965, No. 11.

270. Bolotin V. V. Vibration of Layered Elastic Plates. - Proceedings of Vibration Problems, 4, 1963, No. 4.

271. Book of ASTM Standards, 1964, Part 26, 27.

272. Brown R. I. Analisi semplificate di serbatoi a pressione in PRFV realizzati mediante afvolgi mento di filamenti uniderizionati. - Poliplasti, 12, 1964, No. 1.

273. Carley T. G. A Theoretical and Experimental Investigation of the Transverse Shearing Stress Distribution in Simply Supported Thin Rectangular Plates. Doct. diss., Univ. Ill., 1965.

274. Case J. W., Robinson I. D. Parallel Glass-Fiber-Reinforced Plastics. - Modern Plast., 32, 1955, No. 7.

275. Chambers R. E., McGarry F. J. Shear Effects in Glass-Fiber-Reinforced Plastics Laminates. 14th Annual Meeting of Reinforced Plastics Division, 1959. - ASTM Bulletin, May, 1959.

276. Cies J. A., Bernstein H. Recent Advances in Glass-Fiber-Reinforced Plastic Rocket Motors. - Proc. SPJ, 17th Annual Conference, Sect. 6B, February, 1962.

277. Cies J. A., Bernstein H. Progressive Failure Mechanisms in Glass-Reinforced Plastic Rocket Cases. - Proc. of 5th Internat. Sympos. of Space Technol. and Sci., Tokyo, 1963, Tokyo, ACNE Corp., 1964.

278. Cowper G. R. The Shear Coefficient in Timoshenko's Beam Theory. - Trans. ASME, Ser. E., 33, June, 1966, No. 2.

279. Davis I. W., Modig G. R. Properties of Epoxy Pre-Pregs. - SPE Journal, 1963, No. 11.

280. Davis I. W. Preimpregnated Epoxy of Nonwoven Materials. - SPE Journal, 1966, No. 6.

281. Dietz A. G. H., Sonnborn R. H. Fiberglass-Reinforced Plastics, N. Y., 1954.

282. Engesser F. Die Knickfestigkeit gerader Stäbe. - Zentralblatt der Bauverwaltung, 1891, Nr. 49.

283.   Epstein G., Bandaruk W.   Grazing of Filament-Wound Composites. - Plastics Techn. 9, 1963, No. 8.

284.   Erikson W.   NOL-Ring Method for Control of Filament Winding. Second International Reinforced Plastics   Conference, Paper 18.

285.   Foerster A. P., Boller T. I.   Structural Characteristics and Optimization of Filament-Wound Cylindrical Rocket Cases. - SPE Trans., 4, 1964, 2.

286.   Girkmann K., Beer R.   Anwendung der verschärften Plattentheorie nach Erich Reissner auf orthotrope Platten. - Osterreichisches Ingenieur-Archiv, 1958, Nr. 12.

287.   Goldfein S.   Prestressed Reinforced Plastics. - Modern Plast., August 1956.

288.   Grashof F.   Theorie der Elastizität und Festigkeit. Berlin, 1878.

289.   Habip L. M.   A Review of Recent Work on Filamentary Structures. - Int. J. Mech. Sci., 7, 1965, 297-299.

290.   Hankins N. K., Predaux P. G. Wash-Away Mandrels for Filament Winding. - Modern Plast., 41, 1963, No. 3, 115.

291.   Hashin Z., Rosen B. W.   The Elastic Moduli of Fiber-Reinforced Materials. - J. Appl. Mech., 29, 1964, No. 2.

292.   Hearmon R. F. S.   An Introduction to Applied Anisotropic Plasticity. Oxford University Press, 1961.

293.   Hediard M.   Influence de la preantraine sur la résistance des stratifies unidiretionnels. - Rech. aérospat., 1966, No. 113.

294.   Hugo J. Konstrukéni plasticke hmoty. Praha, 1965.

295.   Kinne M. A., Prosen B. P., Erickson P. W.   Influence of Process Variables in NOL-Ring Properties. - Western Pl., 1963, No. 4.

296.   Kiyohisa T., Tsuneo H.   The Compressional Behavior of Glass-Fiber Sheets and Forming Pressure of RP. - J. Textile Machinery Soc. Japan, 10, 1964, 1.

297.   Kromm A. Verallgemeinerte Theorie der Plattenstatik. - Ingenieur-Archiv, 21, 1953.

298.   Marine Design Manual for Fiberglass Reinforced Plastics, 1960 (Boats of glass fiber-reinforced plastic.   Abbrev. translation, ed. by. G. F. Tkachenko.   M., "Ship-building", 1964).

299. Matting A., Haferkamp H. Spannungsoptische Grenzflächenuntersuchungen an glasfaserverstärkten Kunststoffen. - Glastechn. Ber., 37, 1964, No. 1.

300. Niederstadt G. Probenauswahl bei der Prüfung glaserverstärkter Kunststoffe. - Kunststoffe, 51, 1961, Nr. 4.

301. Adell C. N., Albert W. E. Glass Reinforced Motor Cases. - Aerospace Eng., 21, 1962, No. 4.

302. Olegsky S., Mohr G. Handbook of Reinforced Plastics of the SPJ, N. Y., 1964.

303. Panc V. Verschärfte Theorie der elastischen Platte. - Ingenieur-Archiv, 33, 1964.

304. Pnac V. Verallgemeinerte Theorie der schubweichen orthotropen Platte konstanter Stärke. - Acta technica CSAV, 10, 1965, Nr. 5.

305. Pflüger A. Stabilitätsprobleme der Elastostatik. Berlin, 1964.

306. Rankine W. Applied Mechanics. London, 1958.

307. Reissner E. On the Theory of Bending of Elastic Plates. - J. Math. Phys., 31, 1944, No. 1.

308. Reissner E. The Effect of Transverse Shear Deformation on the Bending of Elastic Plates. - J. Appl. Mech., 12, 1945, No. 1.

309. Reissner E. On Bending of Elastic Plates. - Quart. J. Appl. Math., 5, 1947, No. 1.

310. Residual Stresses in Filament-Wound Laminates and Optimum Programmed Winding Tension (by C. Y. Lois and C. C. Chamis). 20th Annual Meeting of Reinforced Plastics Division, 1965.

311. Rosato D. V. Filament Winding. Interscience Publ., 1964.

312. Rosata D. V. Reinforced Plastics, What They Can Do for You in the Next 10 Years. - SAE Preprints, s. a. No. 660643.

313. Roskos T. G., Pflenderer E. R., Prosen S. P. The Compressive Testing of Filament-Wound Ring Specimens. 18th Annual Conf. Reinforced Plastics Div. - Proc. SPJ, Sect. 9D, February, 1963.

314. Russel G. M. Elastic Deflection of Thick Plates Uniformly Loaded. - Engineering, 123, 1928, 343.

315. Shaffer B. W. Generalized Plane Strain of Pressurized Orthotropic Tubes. - Trans. ASME, B, 1965, No. 3.

316. Sheppard H. R., Sampson R. H. Maximizing Design Stress of Filament-Wound Structures. - SPE Journal, 1964, No. 4.

317. Timoshenko S., Gere J. Theory of Elastic Stability, N. Y., 1961.

318. Timpe A. Die Torsion von Umdrehungskörpern. - Math. Ann., 71, 1911.

319. Wende A., Moebes W., Marten H. Glasfaserverstärkte Plaste. Leipzig, 1963.

320. Woinovsky-Krieger S. Öber die Beulsicherheit von Kreisplatten mit kreiszylindrischer Aelotropie. - Ingenieur-Archiv, 1958, Nr. 2.

321. Zimmer K. Ein Beitrag zur verbesserten Plattentheorie. - Wissenschaftliche Zeitschrift der Technischen Universität Dresden, 12, 1963, Nr. 5.